



THESIS

3  
2010



This is to certify that the  
dissertation entitled

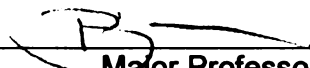
SYNERGISTIC USE OF MILLED WASTE GLASS AND RECYCLED  
AGGREGATE TOWARDS A SUSTAINABLE CONCRETE-BASED  
INFRASTRUCTURE

presented by

Roz-Ud-Din Nassar

has been accepted towards fulfillment  
of the requirements for the

Ph.D. degree in Civil Engineering

  
Major Professor's Signature

5/19/2012

Date

**PLACE IN RETURN BOX** to remove this checkout from your record.  
**TO AVOID FINES** return on or before date due.  
**MAY BE RECALLED** with earlier due date if requested.

DATE DUE	DATE DUE	DATE DUE

**SYNERGISTIC USE OF MILLED WASTE GLASS AND RECYCLED AGGREGATE  
TOWARDS A SUSTAINABLE CONCRETE-BASED INFRASTRUCTURE**

**By**

**Roz-Ud-Din Nassar**

**A DISSERTATION**

**Submitted to  
Michigan State University  
in partial fulfillment of the requirements  
for the degree of**

**DOCTOR OF PHILOSOPHY**

**Civil Engineering**

**2010**

## **ABSTRACT**

### **SYNERGISTIC USE OF MILLED WASTE GLASS AND RECYCLED AGGREGATE TOWARDS A SUSTAINABLE CONCRETE-BASED INFRASTRUCTURE**

By

Roz-Ud-Din Nassar

A novel concept of using milled waste glass, as partial replacement for cement, to overcome the drawbacks of recycled aggregate concrete was investigated. Based on experimental investigations of the structure and properties of concrete materials, it was found that waste glass, when milled to micro-scale particle size, undergoes pozzolanic reactions with cement hydrates, forming secondary calcium silicate hydrate (C-S-H). These reactions bring about favorable changes in the structure (including pore system characteristics of the hydrated cement paste and the interfacial transition zones in normal and recycled aggregate concrete.

Use of milled waste glass, as partial replacement of cement, produced significant gains in the resistance to moisture sorption and chloride permeation, durability under freeze-thaw and abrasive effects, dimensional stability and mechanical properties of normal and particularly recycled aggregate concrete. Milled waste glass was also found to suppress alkali-silica reactions. Unlike normal pozzolanic reactions, those involving glass do not reduce the alkalinity of cement paste; this is favorable to the chemical stability of concrete and its protection of reinforcing steel against corrosion. Field investigations confirmed the compatibility of recycled glass concrete with conventional concrete production and construction techniques, and verified the excellent performance

of pavement sections made with recycled glass concrete after two years of natural weathering.

Numerical studies were conducted in order to predict the service lives of concrete pavements and bridge decks exposed to sulfate or freeze-thaw attack in different climatic conditions. Partial replacement of cement with milled waste glass in normal and recycled aggregate concrete produced significant gains in service life due to the improved resistance of concrete to the transport of moisture and deleterious ions.

Recycling of waste glass in concrete can divert large quantities of the market-limited (mixed-color) waste glass from landfills for value-added use as partial replacement for cement, enable effective use of recycled aggregates in concrete, yield major cost and energy savings, and enhance the long-term performance, the life-cycle economy and the sustainability of concrete-based infrastructure systems.

## DEDICATION

I dedicate this dissertation to my mother; *Bhabai*, my late father; *Muhammad Din*, my wife, and my children; *Farhan, Sufyan, Shumayal, Nauman*, and little *Zeeshan*.

## **ACKNOWLEDGEMENT**

My sincere and deep gratitude goes to my advisor Professor Parviz Soroushian whose enduring support and enlightening guidance made this research possible. I am also grateful to my guidance committee members for their valuable guidance. Part of this research was funded by Michigan State University Physical Plant Division, their support is gratefully acknowledged.

## TABLE OF CONTENTS

LIST OF TABLE .....	ix
LIST OF FIGURES .....	xii
KEY TO SYMBOLS AND ABBREVIATIONS .....	xix
INTRODUCTION .....	1
CHAPTER 1 .....	3
The Rationale and Challenges of Using Recycled Glass and Aggregate in Concrete....	3
1.1 The Need for a Sustainable Concrete-Based Infrastructure.....	3
1.2 Concrete Demolition Waste.....	5
1.3 Waste Glass.....	6
1.4 Glass Recycling in Normal concrete.....	8
1.5 Energy and Environmental Benefits of Partially Replacing Cement with Milled Waste Glass.....	15
1.6 Drawbacks of Recycled Aggregate.....	17
1.7 Recycled Aggregate Concrete.....	20
1.8 Objectives of the Project.....	23
REFERENCES .....	25
CHAPTER 2 .....	33
Moisture Transport in Concrete: Basic Principles, and Effects of Milled Waste Glass and Recycled Aggregate .....	33
2.1 Moisture Transport in Porous Materials .....	33
2.1.1 Sorption .....	36
2.1.2 Diffusion.....	42
2.2 Effects of Concrete Microstructure on Moisture Transport.....	48
2.2.1 Effect of Aggregate Porosity .....	49
2.2.2 Effect of Cement Paste .....	50
2.2.3 Effects of the Mortar and Concrete Microstructure .....	52
2.2.4 Interfacial Transition Zone (ITZ) .....	53
2.3 Microstructure of Recycled Aggregate Concrete.....	56
2.4 Improvement of the Moisture Barrier Attributes of Recycled and Normal Glass Concretes.....	58
2.5 Materials and Experimental Methods .....	61
2.6 Experimental Results and Discussion.....	67
2.6.1 1-D Sorptivity of Normal and Recycled Aggregate Concretes with and without Milled Waste Glass .....	68
2.6.2 2-D Sorptivity of Normal and Recycled Aggregate Concretes with and without Milled Waste Glass .....	78
2.6.3 SEM and EDX Analyses of Hydrated Cementitious Paste, Mortar and Concrete with and without Milled Waste Glass .....	83
REFERENCES .....	94

CHAPTER 3 .....	99
Effects of Partially Replacing Cement with Milled Waste Glass on the Fresh Mix Properties, and the Physical and Mechanical Performance of Normal and Recycled Aggregate Concrete .....	99
3.1 Background Investigations of the Fresh Mix Properties and Mechanical Performance of Recycled Aggregate Concrete.....	99
3.2 Background Information on the Effects of Milled Waste Glass on the Mechanical Performance of Normal Concrete.....	101
3.3 The Innovative Aspect of Our Approach.....	103
3.4 Materials and Concrete Mix Designs.....	103
3.5 Experimental Methods, Test Results and Discussion .....	104
3.5.1 Fresh Mix Properties .....	104
3.5.2 Hardened Concrete Properties.....	106
REFERENCES .....	138
 CHAPTER 4 .....	 142
Effects of Milled Waste Glass As Partial Replacement for Cement on the Durability Characteristics of Normal and Recycled Aggregate Concrete .....	142
4.1 Durability of Recycled Aggregate Concrete.....	143
4.2 Effects of Milled Waste Glass on Durability of Normal and Recycled Aggregate Concrete.....	146
4.2.1 Chloride Permeability.....	147
4.2.2 Freeze-Thaw Durability .....	151
4.2.3 Abrasion Resistance .....	155
4.2.4 Alkali-Silica Reactions.....	159
REFERENCES .....	178
 CHAPTER 5 .....	 182
Prediction of the Recycled Aggregate and / or Milled Waste Glass Effects on Concrete Performance .....	182
5.1 Introduction and Background .....	182
5.2 Freeze-Thaw Attack.....	183
5.2.1 Service Life of Concrete under Frost Attack.....	186
5.3 Sulfate Attack.....	189
5.3.1 Sulfate Attack and Service Life of Concrete.....	192
5.4 Prediction of Concrete Pavement and Bridge Deck Service Life: Effects of Milled Waste Glass and/or Recycled Aggregate .....	194
5.4.1 Surface Temperature and Time-of-Wetness Prediction Model.....	195
5.4.2 Freeze-Thaw Attack Model.....	200
5.4.3 Sulfate Attack Model.....	201
5.5 Input Material Properties and Pavement / Bridge Deck Section Characteristics.. .....	202
5.6 Meteorological Regions Considered for Analyses .....	203
5.7 Results of Numerical Analysis.....	206
REFERENCES .....	219

CHAPTER 6 .....	221
Field Projects .....	221
6.1 Introduction.....	221
6.2 Materials, Mix Designs and Construction Methods .....	222
6.2.1 Construction of Sidewalk / Maintenance Vehicle Pavement Sections.	225
6.2.2 Construction of the Recycling Center External Concrete Pavements and Curbs .....	225
6.3 Test Results and Discussion.....	226
6.3.1 Compressive and Flexural Strength of Concrete Specimens .....	227
6.3.2 Compressive Strength of Concrete Cores.....	230
6.3.3 Water Sorption of Concrete Cores .....	232
6.3.4 Chloride permeability of concrete cores .....	234
6.3.5 Abrasion resistance.....	235
REFERENCES .....	237
 CHAPTER 7 .....	 238
Conclusions and Recommendations .....	238
7.1 Summary and Conclusions .....	238
7.2 Practical Implications of the Findings .....	244
7.3 Recommendations for Future Research .....	245

## LIST OF TABLES

Table 1. 1	Chemical composition of glass versus the ASTM requirements for supplementary cementitious materials (pozzolans).....	11
Table 1. 2	Typical chemical compositions of glass versus cement.....	12
Table 1. 3	Typical mechanical properties of waste glass [43].....	12
Table 1. 4	Thermal conductivity test results [52].....	13
Table 1. 5	Typical properties of recycled aggregate [56, 83, 86].....	19
Table 1. 6	Comparison of properties of recycled aggregate concrete and normal concrete [11, 63, 86, 91-92].....	20
Table 2. 1	Physical properties of milled waste glass.....	62
Table 2. 2	Physical properties of aggregates .....	62
Table 2. 3	Mix Designs .....	63
Table 2. 4	Fly Ash Concrete Mix Designs .....	64
Table 2. 5	Initial and final rates of absorption of oven dried low-water-content, oven-dried mixes with and without milled waste glass.....	70
Table 2. 6	Initial and final rate of absorption of oven dried high water content mixes .....	71
Table 2. 7	Percent reduction in the initial rate of absorption due to glass inclusion for the oven-dried specimens of the three different coarse aggregate concrete mixes.....	71
Table 2. 8	Percent reduction in secondary rate of absorption due to glass inclusion for the oven-dried specimens of the three different coarse aggregate concrete mixes.....	71
Table 2. 9	Percent reduction in cumulative sorption due to milled waste glass inclusion for the three different coarse aggregate concrete mixes (oven-dried) .....	73
Table 2. 10	Initial and final rates of absorption of low-water-content, air-dried mixes with and without milled waste glass.....	75

Table 2. 11	Initial and final rates of absorption of high-water-content, air-dried mixes with and without milled waste glass.....	76
Table 2. 12	Percent reduction in the initial rate of absorption due to introduction of milled waste glass for air-dried specimens of the three different coarse aggregate concrete mixes .....	76
Table 2. 13	Percent reduction in the secondary rate of absorption due to glass inclusion for the air-dried specimens of the three different coarse aggregate concrete mixes .....	76
Table 2. 14	Percent reduction in cumulative sorption due to milled waste glass inclusion for the three different coarse aggregate concrete mixes (air-dried specimens).....	78
Table 3. 1	Fresh concrete properties for mixtures with and without milled waste glass .....	105
Table 3. 2	Fresh mix properties for fly ash concrete mixtures.....	106
Table 3. 3	Density, water absorption, and volume of voids for concrete materials with and without milled waste glass at 56 days of age .....	108
Table 3. 4	Density, water absorption, and volume of voids for fly ash concrete materials at 56 days of age .....	108
Table 4. 1	Cumulative percent weight gains for concrete materials with and without glass after 310 freeze-thaw cycles .....	153
Table 4. 2	Damage index values for concrete materials with and without milled waste .....	154
Table 4. 3	Cement paste and mortar mixes with normal sand.....	162
Table 4. 4	Mortar mixes with reactive sand.....	163
Table 5. 1	Some material properties used in numerical analyses .....	203
Table 5. 2	Weather information of different geographical locations of the U.S. considered for analysis .....	205
Table 5. 3	Predicted service life of concrete pavement and bridge deck based on freeze-thaw deterioration for recycled aggregate .....	207
Table 5. 4	Predicted service life of concrete pavement and bridge deck based on sulfate attack deterioration for recycled aggregate.....	209

Table 5. 5	Predicted service life of concrete pavement and bridge deck based on freeze-thaw deterioration for normal concrete.....	211
Table 5. 6	Predicted service life of concrete pavement and bridge deck based on sulfate attack deterioration for normal concrete .....	213
Table 6. 1	Typical chemical compositions of waste glass and Portland cement .....	222
Table 6. 2	Physical properties of milled glass .....	223
Table 6. 3	Concrete Mix Designs and fresh concrete properties .....	224

## LIST OF FIGURES

Figure 1. 1	Schematics of the glass cycle in the United States [43] .....	8
Figure 1. 2	Scanning electron microscope image of milled waste glass .....	11
Figure 1. 3	Recycled Aggregate.....	18
Figure 1. 4	SEM micrographs of recycled aggregate: (a) clinging mortar on the surface of recycled aggregate; (b) enlarged image of the clinging (porous) old mortar.....	19
Figure 2. 1	Different modes of one-dimensional water absorption [14].....	41
Figure 2. 2	Schematics of moisture transport phenomena within pores .....	44
Figure 2. 3	Molecular diffusion in macropores at low humidity .....	45
Figure 2. 4	Evaporation and condensation phenomena inside a pore at high humidity.. .....	46
Figure 2. 5	The process of surface diffusion inside pore .....	47
Figure 2. 6	Diffusivity dependence on humidity.....	48
Figure 2. 7	Diagrammatic representation of ITZ [26].....	54
Figure 2. 8	SEM micrographs of calcium hydroxide [26] .....	55
Figure 2. 9	Two interfacial transition zones (ITZ) in recycled aggregate concrete ....	57
Figure 2. 10	Model of hydrated cement	Figure 2. 11 Model of hydrated cement / ..... 60
Figure 2. 12	Pictures of 1-D and 2-D sorption test specimens.....	66
Figure 2. 13	1-D and 2-D sorption test specimens inside the test pan .....	66
Figure 2. 14	Sorption plot of low-water-content, oven-dried low water content mixes with and without milled waste glass .....	69
Figure 2. 15	Sorption plot of oven dried high-water-content, oven-dried mixes with and without milled waste glass.....	70
Figure 2. 16	Sorption plots of concrete mixes incorporating class-F and C fly.....	72

Figure 2. 17	Comparison of the milled waste glass, class-F fly ash, and class-C fly ash contributions towards reduction of the 8-day cumulative sorption of oven dried specimens (means and standard errors).....	72
Figure 2. 18	Sorption plot of low-water-content, air-dried mixes with and without milled waste glass .....	74
Figure 2. 19	Sorption plot of high-water-content, air-dried mixes with and .....	75
Figure 2. 20	Sorption plots of air-dried specimens of concrete mixes incorporating Class-F and Class-C fly ashes.....	77
Figure 2. 21	Comparison of milled waste glass, class-F and class-C fly ash towards reduction of 8 days cumulative sorption of air dried specimens (means and standard errors) .....	77
Figure 2. 22	2-D sorption plot of oven-dried, low-water-content mixtures with and without milled glass .....	79
Figure 2. 23	2-D sorption plot of oven-dried, high-water-content mixtures with and without milled glass .....	80
Figure 2. 24	Comparison of the effects of milled waste glass, Class-F fly ash and Class-C fly on 2-D cumulative sorption of oven-dried concrete specimens (means and standard errors).....	80
Figure 2. 25	2-D sorption plot of air-dried, low-water-content mixtures with and.....	81
Figure 2. 26	2-D sorption plot of air-dried, high-water-content mixtures with and without milled glass .....	82
Figure 2. 27	2-D cumulative (8-day) sorptions of air-dried milled waste glass, Class-F fly ash and Class-C fly concrete materials (means and standard errors)..	82
Figure 2. 28	SEM image of the fractured surface of pure cement paste .....	85
Figure 2. 29	EDX spectrum of the of the pure cement paste at the location of Figure 2.28 .....	85
Figure 2. 30	SEM image of the fractured surface of cementitious paste incorporating milled waste glass as replacement for 20% of cement .....	86
Figure 2. 31	SEM image of the fractured surface of cementitious paste incorporating milled waste glass as replacement for 40% of cement .....	86
Figure 2. 32	EDX spectrum of the of the cement paste containing milled waste glass as replacement for 20% of cement at the location of Figure 2.30.....	87

Figure 2. 33	SEM image showing heterogeneous microstructure of the cement paste constituent in mortar made without milled waste glass .....	88
Figure 2. 34	SEM image showing homogeneous structure of the cementitious paste constituent in mortar made with milled waste glass as replacement for 20% of cement .....	89
Figure 2. 35	SEM image of the cement paste constituent of mortar made without milled waste glass .....	89
Figure 2. 36	EDX spectrum at the location of Figure 2.35 for the cement paste in mortar made without milled waste glass.....	90
Figure 2. 37	SEM image of the cementitious paste constituent of mortar made with milled waste glass replacing 40% of cement .....	91
Figure 2. 38	EDX spectrum at the location of Figure 2.37 for the cementitious paste in mortar made with milled waste glass replacing 40% of cement.....	91
Figure 2. 39	SEM image of the ITZ region of a fractured surface of a recycled aggregate concrete specimen without milled waste glass.....	92
Figure 3. 1	Compressive strengths at different ages of low w/c ratio concrete materials with and without milled waste glass (means & standard errors) .....	112
Figure 3. 2	Compressive strengths at different ages of high w/c ratio concrete materials with and without milled waste glass (means & standard errors) .....	113
Figure 3. 3	Compressive strengths at different ages of fly ash concrete materials (means & standard errors).....	114
Figure 3. 4	Compressive strengths at different ages of milled waste glass and class-F fly ash concrete materials (means & standard errors).....	115
Figure 3. 5	Flexural strengths at different ages of low w/c ratio concrete materials with and without milled waste glass (means & standard errors) .....	118
Figure 3. 6	Flexural strengths at different ages of high w/c ratio concrete materials with and without milled waste glass (means & standard errors) .....	119
Figure 3. 7	Flexural strengths at different ages of fly ash concrete materials (means & standard errors) .....	120
Figure 3. 8	Flexural strengths at different ages of milled waste glass and Class-F fly ash concrete materials (means & standard errors) .....	121

Figure 3. 9	Split tensile strengths at different ages of low w/c ratio concrete materials with and without milled waste glass (means & standard errors) .....	123
Figure 3. 10	Split tensile strengths at different ages of high w/c ratio concrete materials with and without milled waste glass (means & standard errors) .....	124
Figure 3. 11	Split tensile strengths at different ages of fly ash concrete materials (means & standard errors).....	125
Figure 3. 12	Split tensile strengths at different ages of milled waste glass and Class-F fly ash concrete materials (means & standard errors).....	126
Figure 3. 13	Elastic moduli of low w/c ratio concrete materials with and without milled waste at 90 days of age (means & standard errors) .....	128
Figure 3. 14	Elastic moduli of high w/c ratio concrete materials with and without milled waste glass at 90 days of age (means & standard errors) .....	129
Figure 3. 15	Elastic moduli of fly ash concrete materials at 90 days of age (means & standard errors) .....	130
Figure 3. 16	Elastic moduli of milled waste glass versus Class-F fly ash concrete materials at 90 days of age (means & standard errors).....	131
Figure 3. 17	Drying shrinkage versus time of low w/c ratio concrete materials with and without milled waste and Class-F fly ash .....	134
Figure 3. 18	Drying shrinkage versus time of high w/c ratio concrete materials with and without milled waste glass.....	135
Figure 3. 19	Cumulative 20-week drying shrinkage of low w/c ratio concrete materials with and without milled waste glass (means & standard errors) .....	136
Figure 3. 20	Cumulative 20-week drying shrinkage of high w/c ratio concrete materials with and without milled waste glass (means & standard errors) .....	136
Figure 3. 21	Cumulative 20-week drying shrinkage of milled waste glass and class-F fly ash concrete materials (means & standard errors).....	137
Figure 4. 1	The rapid chloride permeability test setup.....	149
Figure 4. 2	Rapid chloride permeability test results for low w/c ratio concrete materials with and without milled waste glass (means & standard errors) .....	150

Figure 4. 3	Rapid chloride permeability test results for high w/c ratio concrete materials with and without milled waste glass (means & standard errors) .....	150
Figure 4. 4	Rapid chloride permeability test results for Class-F and class-C fly ash concrete materials (means & standard errors) .....	151
Figure 4. 5	The time-temperature plot of a freeze-thaw cycle .....	152
Figure 4. 6	Flexural strength of aged and unaged concrete materials with and without milled waste glass (means & standard errors) .....	154
Figure 4. 7	Abrasion weight losses of low w/c ratio concrete materials with and without milled waste glass (means & standard errors) .....	157
Figure 4. 8	Abrasion weight losses of high w/c ratio concrete materials with and without milled waste glass (means & standard errors) .....	158
Figure 4. 9	Abrasion weight losses of fly ash concrete materials (means & standard errors) .....	159
Figure 4. 10	Compressive strength test results at different ages for cement pastes with and without milled waste glass (means & standard errors) .....	164
Figure 4. 11	Compressive strength test results at different ages for normal sand mortar mixes with and without milled waste glass (means & standard errors)..	165
Figure 4. 12	Compressive strength test results at different ages for reactive sand mortar mixes with and without milled waste glass (means & standard errors)..	166
Figure 4. 13	ASR test results for normal sand mortars with and without milled waste glass .....	168
Figure 4. 14	ASR test results for reactive sand mortars with and without milled waste glass .....	169
Figure 4. 15	ASR test results for low w/c ratio concrete materials with and without milled waste glass .....	170
Figure 4. 16	ASR test results for high w/c ratio concrete materials with and without milled waste glass .....	171
Figure 4. 17	Results of pH tests on cement paste mixes with and without milled waste glass (means & standard errors).....	173
Figure 4. 18	Plot of pH vs. % replacement level of cement with milled waste glass in normal sand mortar .....	174

Figure 4. 19	Plot of pH vs. % replacement level of cement with milled waste glass in reactive sand mortar.....	175
Figure 4. 20	SEM micrograph of fractured surface of mortar without milled waste glass after 20 days after exposure to ASR environment.....	176
Figure 4. 21	SEM micrograph of fractured surface of mortar with 40% milled waste glass after 20 days after exposure to ASR environment.....	177
Figure 5. 1	(a) Schematic diagram of ice formation in capillary voids; (b) Ice formation in an air void; and (c) SEM micrograph of ice formation inside an air void [3].....	185
Figure 5. 2	Ettringite lining rims around aggregates.....	191
Figure 5. 3	SEM micrograph showing 20 $\mu\text{m}$ wide ettringite rim resulting in about 2.8% expansion.....	191
Figure 5. 4	Cross-section of concrete pavement .....	197
Figure 5. 5	Cross-section of bridge deck.....	197
Figure 5. 6	Time-of-wetness plot for Alpena, MI (from ConcLife) .....	198
Figure 5. 7	A typical ConcLife plot for prediction of concrete service life under freeze-thaw attack .....	201
Figure 5. 8	A typical ConcLife plot for prediction of concrete service life under sulfate attack .....	202
Figure 5. 9	Predicted service lives of recycled aggregate concrete pavement and bridge deck with and without milled waste glass when damage is due to freeze-thaw attack .....	208
Figure 5. 10	Predicted service lives of recycled aggregate concrete pavement and bridge deck with and without milled waste glass when damage is due to sulfate attack .....	210
Figure 5. 11	Predicted service lives of normal concrete pavement and bridge deck with and without milled waste glass when damage is due to freeze-thaw attack .....	212
Figure 5. 12	Predicted service lives of normal concrete pavement and bridge deck with and without milled waste glass when damage is due to sulfate attack ...	214

Figure 5. 13	Percent gain in service life of concrete pavement and bridge deck due to recycled glass exposed to freeze-thaw or sulfate attack and made with recycled aggregate concrete.....	216
Figure 5. 14	Percent gain in service life of concrete pavement and bridge deck due to recycled glass exposed to freeze-thaw or sulfate attack and made with normal concrete.....	217
Figure 6. 1	SEM micrograph of milled waste glass .....	222
Figure 6. 2	Construction of the sidewalk/maintenance vehicle pavement with recycled .....	226
Figure 6. 3	Construction with recycled glass concrete at the MSU Recycling Center (a) concrete driveway (b) concrete curb .....	226
Figure 6. 4	Compressive strength test results at different ages for concrete specimens prepared using the field concrete materials (means and standard errors)	229
Figure 6. 5	Flexural strength test results at different ages for concrete specimens prepared using the field concrete materials (means and standard errors)	230
Figure 6. 6	Compressive strength of concrete cores at different ages (means and standard errors) .....	231
Figure 6. 7	Water sorption versus time of concrete cores .....	233
Figure 6. 8	Cumulative water sorption of concrete cores after 9 days of exposure to water (means and standard errors).....	233
Figure 6. 9	Chloride permeability of concrete cores.....	234
Figure 6. 10	Abrasion resistance of recycled glass and control concretes (means and standard errors) .....	236

## KEY TO SYMBOLS AND ABBREVIATIONS

$a$	=	cross-sectional area
$ACI$	=	American concrete institute
$a_{CR}$	=	critical air content
$ANOVA$	=	analysis of variance
$a_r$	=	residual air content
$A_r$	=	surface area of air-filled pores
$ASR$	=	alkali silica reaction
$ASTM$	=	American society for testing and materials
$BCSJ$	=	building contractor society of Japan
$BREEAM$	=	building research establishment environmental assessment
$BTU$	=	British thermal unit
$C$	=	concentration
$C\&D$	=	construction and demolition
$C_3S$	=	tricalcium silicate
$C_E$	=	concentration of reacted sulfate as ettringite
$CH$	=	calcium hydroxide
$c_o$	=	external sulfate concentration
$C-S-H$	=	calcium silicate hydrate
$d$	=	diameter of pore
$D$	=	diffusivity

$D_i$	=	intrinsic diffusion coefficient
$EDX$	=	energy dispersive X-ray spectroscopy
$g$	=	gravitational constant
$GBI$	=	green building institute
$H$	=	water
$h_{conv}$	=	convection coefficient
$i$	=	sorption
$IPCC$	=	intergovernmental panel on climate change
$ITZ$	=	interfacial transition zone
$IUPAC$	=	international union of pure and applied chemistry
$K$	=	hydraulic conductivity
$k_{conc}$	=	thermal conductivity of concrete
$L_{CR}$	=	critical distance
$LEED$	=	leadership in energy and environmental design
$MDOT$	=	Michigan department of transportation
$MRF$	=	material recovery facility
$NREL$	=	national renewal energy laboratory
$PCA$	=	Portland cement association
$ppm$	=	parts per million
$Q_{cond}$	=	heat flow due to conduction
$Q_{conv}$	=	heat transfer due to convection

$Q_{inc}$	=	incident solar radiation ( $W/m^2$ )
$Q_{sun}$	=	radiation absorbed from incoming sunlight
$r$	=	mean radius of curvature
$S$	=	sorptivity
$S_{CAP}$	=	capillary degree of saturation
$SCM$	=	secondary cementitious material
$SCR$	=	critical moisture content
$SEM$	=	scanning electron microscopy
$T^{\circ}K$	=	concrete surface temperature ( $^{\circ}K$ )
$T_{sky}$	=	calculated sky temp ( $^{\circ}K$ )
$w/c$	=	water to cement ratio
$X$	=	thickness of reaction zone
$a_r$	=	specific surface of pore
$\beta$	=	linear strain caused by one mole of sulfate
$\gamma$	=	fracture surface energy
$\gamma_{abs}$	=	solar absorptivity of concrete
$\Delta m$	=	change in mass
$\varepsilon$	=	emissivity of concrete
$\theta$	=	water content
$\rho$	=	density of water
$\rho_{\sigma}$	=	bulk density of medium

- $\sigma$  = surface tension
- $v$  = volume flux of moisture
- $\Psi$  = capillary potential
- $\Phi$  = moisture potential

## **INTRODUCTION**

Concrete, a primary building construction material, is the world's most consumed man-made material. About 800 million tons of concrete was consumed in the U.S. in 2007, and the world consumption was estimated at 11 billion tons, or approximately 1.7 ton for every living human being [1-3]. Production of cement (the binder in concrete) is an energy-intensive and highly polluting process, which contributes about 5 to 8% to global CO<sub>2</sub> emissions, and accounts for 3% of total (5% of industrial) energy consumption worldwide. Production of each ton of cement results in the emission of one ton of carbon dioxide (CO<sub>2</sub>) to the atmosphere [4-7].

The growing environmental concerns and the increasing scarcity of landfills encourage the recycling of construction waste, including concrete, and the landfill-bound constituents of the municipal waste stream, including glass which occurs largely as mixed-color waste glass with limited market value. Out of the over 2 billion tons of aggregate consumed each year in the U.S, only 5 percent comes from recycled sources such as demolished concrete [8]. The use of recycled aggregate in concrete is hindered by its higher water absorption (two to three times that of normal aggregate) and the increased shrinkage of the resulting recycled aggregate concrete. These drawbacks result largely from the cement hydrates (from old concrete) that adhere to the surface of recycled aggregates. It should be noted that most aggregates offer engineering properties that are superior to those of cement hydrates.

The waste glass generated in the U.S. in 2008 was about 12.2 million tons, 77% of which was disposed of in landfills [9]. The bulk of waste glass can be collected in mixed colors, and has limited markets. Mixed-color waste glass, however, offers desired

chemical composition and reactivity for use as a supplementary cementitious material (SCM) for enhancing the chemical stability, pore system characteristics, moisture resistance and durability of concrete. To realize this potential, waste glass needs to be milled to micro-scale particle size for accelerating its beneficial chemical reactions in concrete. These beneficial effects of milled waste glass can enhance the residual cement occurring on the surface of recycled aggregates, thus improving the performance characteristics of recycled aggregate concrete.

This research investigated the novel concept of using recycled glass as a partial replacement for cement to enhance the resistance to moisture sorption, durability and dimensional stability of recycled aggregate concrete, and to reduce the adverse environmental and energy impacts of concrete production. The high recycled content and the improved engineering properties of the concrete materials developed in this research can make major contributions towards development of sustainable concrete-based infrastructure systems.

## **CHAPTER 1**

### **The Rationale and Challenges of Using Recycled Glass and Aggregate in Concrete**

#### **1.1 The Need for a Sustainable Concrete-Based Infrastructure**

For more than two centuries mankind has accepted concrete as a dependable construction material because of its durability, strength, local availability of raw material, low cost, and architectural moldability to form aesthetically pleasing shapes and forms [10] . Concrete as a building construction material has good moisture and weathering resistance, fire resistance, and desirable energy impacts which make it a construction material of choice [3, 11]. The thermal mass of concrete lowers the temperature fluctuations within buildings, thus lowering the energy demand for heating and cooling by about 5% [12] . Globally, concrete is the most widely used manufactured product. In 2007, about 800 million tons concrete was consumed in the U.S., with the global consumption estimated at 11 billion tons [11]. With the continued increase in global industrialization and urbanization, and the high demand for repair and replacement of existing structures, the consumption of concrete is on the rise. It is estimated that, by the year 2050, the US and world annual consumption of concrete will grow to one billion and eighteen billion tons, respectively [13-14]. The 2005 consumption of concrete was about five times that of steel.

Manufacturing of cement, a key ingredient used for the production of concrete, is an energy-intensive process which is also a major source of greenhouse gas emissions. Fabrication of a ton of cement results in emission of one ton of carbon dioxide (CO<sub>2</sub>) to

the atmosphere [3-5, 15-20]. Carbon dioxide is a by-product of the chemical reactions involved in production of cement (chiefly decarbonation of limestone); the energy consumed in the course of cement production is another source of CO<sub>2</sub> emissions. Globally, cement production contributes 5-8% of anthropogenic CO<sub>2</sub> emissions [3-5, 18-19, 21-23]. The estimated total carbon emissions from cement production plants were 1.35 billion tons in 2002, which rose to 2 billion tons in 2004 (compared to total worldwide CO<sub>2</sub> emissions of 28 billion tons in 2004) [24]. In 2007, the total cement production in the United States was close to 100 million tons, which contributed about 100 million tons of CO<sub>2</sub> to the atmosphere [25]. The 1995 CO<sub>2</sub> emission from cement industry was equivalent to the emission from 300 million automobiles [26]. In 2007, the global cement consumption by the concrete industry was 3.05 billion tons, with the U.S. cement consumption estimated at 95 million tons; this shows the large carbon footprint of the industry [27]. The atmospheric concentration of CO<sub>2</sub> has reached 390 ppm which is the highest ever recorded. Recognizing this fact, the U.N. Intergovernmental Panel on Climate Change (IPCC) has recommended that the global CO<sub>2</sub> emission must be brought down to the 1990 level in the next 20 years [27]. Cement production also involves emission of moderate quantities of NO<sub>x</sub>, SO<sub>x</sub> and particulates [5].

Manufacturing of cement is an energy-intensive process, which ranks 3<sup>rd</sup> after aluminum and steel manufacture in terms of energy consumption. Close to 5.5 million BTU of energy is consumed in production of a ton of cement [28]. The cement industry accounts for about 3% of the global primary energy consumption (or ~5% of the total global industrial energy consumption) [29]. The energy used for production of cement accounts for more than 90% of the total energy required for production of concrete [30].

In spite of major efforts in recent decades, significant gains in fuel-efficiency of cement production plants has not been realized [17]. This situation warrants decisive measures to be taken to reduce the carbon contribution of the cement and concrete industry.

## **1.2 Concrete Demolition Waste**

About 300 million tons of construction and demolition (C&D) waste is generated in the U.S. each year. About 50% of this is recovered for recycling, and the rest is landfilled [31-33]. According to Mehta [14], the global concrete industry consumes close to 10 billion tons of sand and rocks (2002 data), and produces over 1 billion tons of C&D waste annually. Recycled aggregates constitute only 5% of the total aggregate used in concrete [14, 34-35]. The disposal of C&D waste is becoming increasingly difficult and expensive. Environmental concerns are increasingly limiting the option of landfilling such waste. Planners, engineers and public authorities are therefore looking for ways of making reuse of the C&D waste. Since aggregates constitute approximately 70% of concrete volume, the utilization of waste concrete as recycled aggregate can yield significant environmental impact. This encourages urgent steps towards increasing the recycling rate of demolished concrete as aggregate in new concrete construction. The ever growing scarcity of quality (virgin) aggregates in some regions coupled with the increasing haulage and growing landfill costs are additional driving forces promoting the recycling of concrete demolition waste. Many consider the use of recycled aggregate in concrete as an inevitable practice to for conserving the rock resources which are currently depleting rapidly in urban areas due to the excess use for production of virgin aggregates. Although a considerable proportion of recycled aggregate is used as roadfill, which is a

better practice than landfilling, experts term it as “down cycling”, because virgin aggregate continues to be used in higher-value applications for production of concrete [18]. Recycling of concrete offers additional environmental and energy benefits, such as reduction of fuel consumption for production of virgin aggregates and their hauling over increasingly long distances, and reduced consumption of non-renewable resources. The growing availability of cost-effective technologies for recycling the C&D waste, particularly demolished concrete, is an enabling factor in broader use of recycled aggregates in concrete.

### **1.3 Waste Glass**

Glass is obtained by supercooling of a melted liquid mixture of sand (silicon dioxide) and soda ash (sodium carbonate) to a rigid condition. The supercooling does not allow crystallization of glass, but rather retains the organization and internal structure of the melted liquid. This amorphous structure of glass makes it reactive when it is pulverized to different size fractions.

Although the bottle bill legislation, which is promulgated in some states and provides for return of glass bottles at retail outlets, glass recovery often occurs through collection of waste glass at Material Recovery Facilities (MRFs) [36]. The waste glass collected at MRFs is crushed for size reduction to less 51 mm (2 in.) in planar dimension. About 41 billion glass containers are manufactured annually in the United States. Additionally, 2 to 4 billion glass containers are imported annually to the U.S., mostly as containers for alcoholic beverages. The domestic waste glass stream comprises: 33% food containers, 31% beer bottles, 9% wine and liquor bottles, 22% other beverage

bottles, and 5% containers for cosmetic, pharmaceuticals, etc. By color, 65% of the domestic glass waste stream is clear, 25% is brown or amber, and 10% occurs in different shades of green, blue and other colors [37].

It is estimated that globally, each year, 2.02 billion tons of municipal solid waste is generated, about 100 million tons (5%) of this comprises of glass [38]. The glass content of the municipal solid waste stream in the U.S. was estimated at 12.2 million tons in 2008, which is about 6% of the municipal solid waste (by weight); 77% of this waste glass was landfilled [39]. The predominantly mixed-color post-consumer waste glass has limited market value. Recycling of the waste glass occurring in the municipal solid waste stream for use as raw material towards production of new glass products is limited due the high cost of processing (hand sorting by color), and also because of specifications that limit the presence of impurities (e.g. ferrous metal, paper, plastics and mixed-color glass) in the glass production process. The high percentages (up to 60%) of waste glass breakage during collection and handling is an additional factor limiting the recovery of glass through hand-sorting (by color) [40].

Landfilling of waste glass is not only an expensive way of disposal, with a tipping fee of \$65 per ton (2001 data), it also occupies increasingly scarce landfill space available in urban areas [37]. Since glass is not biodegradable, its disposal in landfills is not an environmentally friendly solution. There is a strong need to utilize the waste glass in an environmentally friendly way. One option is to recycle waste glass in construction materials, including concrete, where the chemistry of glass can make contributions towards the end product quality [36, 41-46]. So far, the construction industry has made low-value use of waste glass (cullet) as replacement for aggregate (e.g., as filter layer in

storm water drainage systems). Figure 1.1 shows this recycling option within the schematics of the glass cycle in the United States.

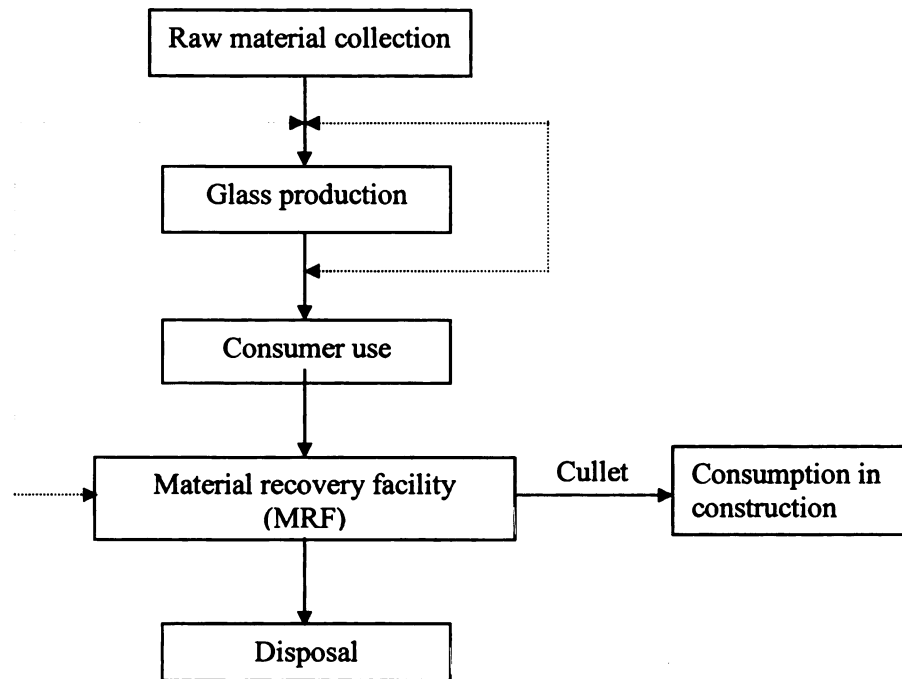


Figure 1.1 Schematics of the glass cycle in the United States [43]

#### 1.4 Glass Recycling in Normal concrete

Rapid depletion of resources and concerns over degradation of the environment have led to a growing emphasis on sustainable development [47]. As a result, the construction industry is required to adopt environmentally friendly practices and make judicious use of natural resources. Major contributions to sustainable development can be made by reducing the consumption of Portland cement through partially replacing it with supplementary cementitious materials (SCMs). While coal fly ash has been the primary SCM used so far, new constraints on coal combustion (prompted by environmental concerns) are limiting the availability of coal ashes which qualify as SCM. Waste glass

(including mixed-color waste glass) offers a highly desirable chemistry for use as a SCM. Size reduction of glass to enhance its chemical reactivity is the key enabling step for converting the landfill-bound mixed-color waste glass into a valuable produce capable of partially replacing cement in concrete. This highly promising concept has not, however, been picked up by the cement and concrete industry. The reason is that earlier efforts to recycle waste glass in concrete viewed crushed glass with dimensions of few millimeters (a fraction of an inch) as replacement for sand in concrete. The prolonged reactions of these relatively coarse glass particles in concrete, however, produced adverse effects on concrete structure [48-50]. This negative experience stopped any evaluation of other options for recycling of glass in concrete where the chemical reactivity of glass could be a virtue. Our view of milled waste glass as a SCM seeks to make value-added use of the (mixed-color) waste glass chemistry to realize major environmental, energy, performance and cost benefits by partially replacing cement with milled waste glass in concrete production.

An important factor that determines the ease with which a material can be recycled is the extent to which its composition varies. Traditional SCMs such as coal fly ash are subject to wide variations of material composition. Glass, however, has a minor variation in chemical composition. An in-depth study of the waste glass occurring in the solid waste stream has shown that the waste glass composition is highly consistent [49].

Waste glass (including mixed-color waste glass) has a highly favorable chemical composition for use as a SCM. Table 1.1 compares the chemical composition of glass with different colors versus the American Society of Testing and Materials (ASTM) requirements for SCMs [51]. When compared with alternative SCMs (with diminishing

supplies), mixed-color waste glass actually offers a more favorable chemistry for effective use as an SCM in concrete. Glass, which is rich in amorphous silica (see Table 1.2 for a comparison of typical glass and cement chemical compositions) has the proper chemistry and reactivity for pozzolanic reactions with the lime released during hydration of cement to produce highly stable end products with desired binding qualities. Table 1.3 shows typical mechanical properties while Table 1.4 shows the thermal conductivity test results of mixed-color waste glass. The lower thermal conductivity of glass has several benefits when it is used in concrete.

Our exploratory laboratory work indicated that the pozzolanic reactions of waste glass occur within a viable time frame (when the bulk of cement hydration occurs) as far as glass is milled to about 14  $\mu\text{m}$  particle size. Figure 1.2 shows a typical SEM micrograph of milled waste glass. Glass has a desired chemistry to act (after milling) as a pozzolan which partially replaces cement in concrete (see Table 1.1). The term pozzolan is derived from the name of the Italian village Pozzouli. During the time of the Roman Empire, volcanic ash from this area was mixed with water and lime to make a cement mortar. The mortar was used for construction of many buildings in Rome, the ruins of which still remain. Today, we define pozzolans as silicon- and aluminum-based materials that can react with lime (e.g., the lime generated during hydration of cement) to form rock-hard solids (i.e., cement hydration products) when mixed with water in suitable proportions.

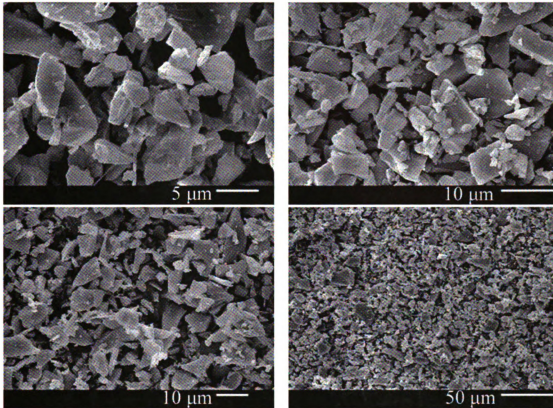


Figure 1. 2 Scanning electron microscope image of milled waste glass

Table 1. 1 Chemical composition of glass versus the ASTM requirements for supplementary cementitious materials (pozzolans)

Constituents	ASTM C618	GLASS		
		Green	Amber	Flint
$\text{SiO}_2 + \text{Al}_2\text{O}_3 + \text{Fe}_2\text{O}_3$	$\geq 70\%$	74.1%	74.2%	74.9%
$\text{SO}_3$	$\leq 5\%$	0.053%	0.13%	0.22%
Loss on Ignition	$\leq 6\%$	0%	0%	0%

**Table 1.2 Typical chemical compositions of glass versus cement**

Chemical	Glass	Cement
SiO <sub>2</sub>	73.5%	20.2%
Al <sub>2</sub> O <sub>3</sub>	0.4%	4.7%
CaO	9.2%	61.9%
Fe <sub>2</sub> O <sub>3</sub>	0.2%	3.0%
MgO	3.3%	2.6%
Na <sub>2</sub> O	13.2%	0.19%
K <sub>2</sub> O	0.1%	0.82%
SO <sub>3</sub>	-	3.9%
Loss on ignition	-	1.9%

**Table 1.3 Typical mechanical properties of waste glass [43]**

Property	Value	Test Method
Loss Angeles abrasion (%)	3042	ASTM C131
Maximum dry density (kg/m <sup>3</sup> )	1800 – 1900	ASTM D1557
Optimum moisture (%)	5.7 – 7.5	ASTM D1557
Angle of internal friction (deg)	51 - 53	ASTM D3080
California bearing ratio (%)		
15% Glass	132	ASTM D1883
50% Glass	42 – 125	
Hardness (Moh's scale)	5.5	

Table 1. 4 Thermal conductivity test results [52]

Material	Apparent thermal conductivity (watts/meter-°K)	
	Sample 1	Sample 2
Crushed Glass	0.315	0.260
Gravelly Sand	0.463	0.638

Pozzolanic reactions occur in concrete incorporating milled waste glass (as partial replacement for cement); these reactions take place between the lime released by hydration of cement and glass, and fall into three categories:



The end products of above reactions are calcium silicate hydrate, calcium aluminate hydrate, and calcium aluminosilicate hydrate, which are also present among the products of cement hydration, and offer desired moisture resistance and chemical stability (far surpassing those offered by lime). These stable end products of pozzolanic reactions tend to block and fill the capillary pore system of concrete which greatly enhances the resistance of concrete to penetration of moisture and aggressive chemicals. Major gains in concrete impermeability, durability, dimensional stability and mechanical performance can thus be realized through partial replacement of cement with milled (mixed-color) waste glass.

Past efforts to recycle waste glass in concrete focused on the use of crushed glass as replacement for sand in concrete. These efforts neglected the reactive nature of glass in concrete, which was slowed down due to the relatively large (millimeter-scale) size of glass particles [48-49]. Such long-term reactions proved to be detrimental to the long-term stability of concrete incorporating large glass particles. It is interesting to note that the accelerated reactions of finer (micrometer-scale) glass particles would produce a favorable chemical environment for mitigating detrimental chemical reactions in the presence of unstable aggregates such as coarse glass particles.

The recycling of glass in concrete as partial replacement of cement offers three major benefits. First, waste glass has negative value when disposed of in landfills, requiring tipping fees; it assumes a considerable positive value as partial replacement for cement in concrete. Second, as partial replacement of cement, waste glass reduces the significant polluting effects, energy consumption and cost of producing Portland cement. Third, the use of waste glass in concrete as partial replacement of cement yields enhanced physical, mechanical and durability characteristics through pozzolanic reactions with cement hydrates. These technical contributions enable effective use of demolished concrete as recycled aggregates in new concrete construction, adding to the environmental benefits of the practice. It can thus be stated that the use of waste glass as partial replacement for cement in concrete transforms an abundantly available and market-limited waste material into a high-value product with significant environmental, energy, economic and technical benefits.

The proposed practice of replacing about 15% to 20% of cement in concrete with milled waste glass would benefit from the fact that cement consumption and waste glass

generation levels are of comparable orders of magnitude (the waste glass generated in the U.S. is about 15% to 20% of the cement consumed in the nation). The proposed practice can thus be implemented at large scale to render important environmental, energy, economic and technical benefits. The economical benefits of the practice result from the favorable economics of milled waste glass versus cement; the improved moisture resistance and durability of concrete containing recycled glass would yield further life-cycle cost savings.

### **1.5 Energy and Environmental Benefits of Partially Replacing Cement with Milled Waste Glass**

Concrete, compared to other construction materials, is an environmentally friendly material. However, the concrete industry is faced with the tremendous challenges of reducing the environmental pollution and the high energy demand of cement production. Cement accounts for more than 90% of the embodied energy per ton of concrete production [53]. The concrete industry can address such growing environmental and energy concerns by minimizing the cement content in concrete required to meet the required performance levels; this goal can be accomplished by replacing as much of Portland cement as possible with pozzolanic (supplementary cementitious) materials [54]. This practice would be most successful if the pozzolanic materials are abundantly available waste products with minimal impurities and consistent quality.

Annually, cement production in the U.S. consumes about 0.6 quadrillion Btus or quads (1 quad =  $10^{15}$  Btus) of energy. This accounts for about 0.6% of the total energy use in the United States, which is a remarkable amount given that, in dollar value, cement

represents only about 0.06% of the gross national product. This means that cement production is approximately ten times more energy intensive when compared with the U.S. economy in general [53]. Replacement of 20% of cement with milled waste glass in concrete will result in annual energy savings of about 95 trillion Btus [53]. According to the World Watch Institute, cement production in some developing nations accounts for up to two-thirds of the total energy use. The rate of growth in cement consumption is high in developed nations due to the growing repair/rehabilitation needs of an aging infrastructure; it is also high in developing nations where a vast infrastructure system is under construction. This trend is not favorable as far as the position of concrete as a major contributor to global warming is concerned. In order to reduce the carbon footprint and the consumption of energy in production of concrete, one can reduce the consumption of concrete, reduce the cement content of concrete, or reduce less clinker for cement production. [27] The consumption of concrete can be reduced through implementation of innovative architectural concepts and structural designs for new construction and for rehabilitations of old structures. The cement content in concrete can be reduced through changes in concrete mix designs (e.g., use of high-range water reducers and aggregate size optimization), partial replacement of cement with pozzolans (e.g., milled waste glass), and specifying 56- or 90-day target compressive strength in structural elements instead of 28-day strength (which helps maximize the consumption of pozzolans while requiring adjustment of construction and use scheduling). Pozzolans such as milled waste glass can also partially replace clinker; milling of clinker together with waste glass can yield blended cement with desired particle size distribution for use in concrete. This practice eliminates the need for separate milling of waste glass.

The building rating systems of the Building Research Establishment Environmental Assessment (BREEAM) in UK and Europe, the Green Building Initiative (GBI), and the Green Building Council's Leadership in Energy and Environmental Design (LEED) in North America have emerged as popular tools encouraging "sustainable" design and construction practices which are favorable to the environment. These systems are designed to ensure efficient use of energy and natural resources. They rank building materials based on their carbon emissions potential, embodied primary energy, pollution to air and water, and weighted resource use [55]. Use of milled waste glass in concrete as partial replacement for cement, or its utilization towards production of blended cement efficiently fulfills such requirements for sustainable construction systems. Concrete mixtures produced using milled waste glass as partial replacement for cement can be less vulnerable to cracking and more durable and sustainable, increasing the service life of the concrete-based infrastructure and reducing maintenance requirements; these benefits make further contributions towards the sustainability of infrastructure systems.

### **1.6 Drawbacks of Recycled Aggregate**

There is a wealth of literature available on the quality of recycled aggregates produced by concrete demolition, and the mechanical properties and durability of recycled aggregate concrete [11, 35, 56-82]. When old concrete is crushed, a certain amount of mortar from original concrete remains attached to the stone particles in recycled aggregate (Figure 1.3). According to Hansen and Narud [83], the volume percentage of the attached mortar varies between 25% and 35% when concrete with natural gravel is reduced to 16-32 mm

particle size, about 40% in the case of recycled aggregate with 8-16 mm particle size, and near 60% in recycled aggregate with 4-8 mm particle size. Hasaba et al. [84] reported that 35.5% of old mortar is attached to natural gravel in recycled aggregate with 5-25 mm particle size produced from concrete with 24 MPa compressive strength. For the same size of recycled aggregate, the attached mortar fraction increased to 36.7% and 38.4% when the recycled aggregate was produced by crushing concretes with compressive strengths of 41 MPa and 51 MPa, respectively. According to Japanese studies [85], approximately 20% of cement paste is attached to the recycled aggregate with 20-30 mm particle size. Figure 1.4 shows a scanning electron microscope image illustrating the attached old mortar to the original aggregate surface in recycled aggregate. The old cement paste and mortar attached to the recycled aggregate tends to unfavorably impact the properties of recycled aggregate and thus recycled aggregate concrete. Table 1.5 presents typical properties of recycled aggregate, where some properties are compared against those of virgin/natural aggregate.

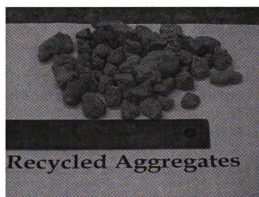


Figure 1.3 Recycled Aggregate

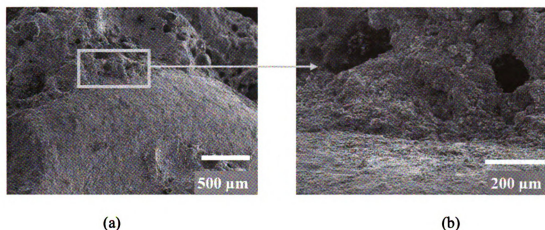


Figure 1.4 SEM micrographs of recycled aggregate: (a) clinging mortar on the surface of recycled aggregate; (b) enlarged image of the clinging (porous) old mortar

Table 1.5 Typical properties of recycled aggregate [56, 83, 86]

Property	Description
Water Absorption	5 - 10%
Loss Angles Abrasion	Satisfies ASTM C 33 requirements
Density	5 to 10% lower than virgin aggregate
Sulfate Soundness	Comparable to virgin aggregate

A marked difference between recycled aggregate and virgin aggregate is the much higher water absorption of recycled aggregate, which is due to the higher water absorption capacity of the old, porous cement mortar attached to the recycled aggregate particles [62, 85, 87]. Nixon [88] has also concluded that the most significant difference between recycled aggregate and virgin aggregate is the markedly higher water absorption of the recycled aggregate.

## 1.7 Recycled Aggregate Concrete

Concrete produced with coarse recycled aggregate and natural sand differs from normal concrete produced with virgin aggregates in terms of some mechanical properties and durability characteristics. Some of these differences depend upon the quality of the original concrete from which the recycled aggregate is obtained for use in recycled aggregate concrete [77, 83, 87]. Original concrete of relatively low strength tends to produce lower-quality aggregates when compared with higher-strength original concrete as far as the effects on the strength and durability of recycled aggregate concrete are concerned. It has been reported that recycled aggregate concrete with properties in fresh and hardened states that are comparable to those of normal concrete can be produced using coarse recycled aggregate of desired quality and natural sand [86-87]. Past research points at the suitability of using recycled aggregate concrete towards production of high-strength concrete materials and prestressed concrete structures [87, 89-90]. Depending on the quality of recycled aggregate, different properties of recycled aggregate concrete can reach various percentages of the normal concrete properties, as shown in Table 1.6.

Table 1. 6 Comparison of properties of recycled aggregate concrete and normal concrete [11, 63, 86, 91-92]

Recycled Aggregate Concrete Property	Values / Comparison
Compressive Strength	64 – 100% of normal concrete
Modulus of Elasticity	60 – 100% of normal concrete
Flexural Strength	80 – 100% of normal concrete
Linear Coefficient of Thermal Expansion	Comparable to that of normal concrete
Freeze-thaw Resistance	Comparable to that of normal concrete
Drying Shrinkage	Up to 160% of normal concrete

Table 1.6 continued

Moisture Absorption	200% - 300% of normal concrete
Creep	130 – 160% of normal concrete
Permeability	200% - 500% of normal concrete

As can [93] be seen in Table 1.6, moisture absorption (and related properties such as drying shrinkage and creep) are the attributes of recycled aggregate concrete that distinguish them from normal concrete. Limbachiya et al. [90] has reported that increased recycled aggregate content led to increased water absorption and drying shrinkage of the resulting concrete due to the increased proportion of the cementitious material clinging to the surface of recycled aggregates. Tavakoli and Soroushian [76] found that the water absorption capacity of recycled aggregate reflects on the amount of cement paste adhering to the surface of the aggregate particles. With increased quantity of the clinging paste, the drying shrinkage of the resulting concrete increased accordingly. They further reported that recycled aggregate concrete shows higher drying shrinkage than normal concrete, and the magnitude of the increase in drying shrinkage depends on the properties of the parent concrete from which the recycled aggregate was obtained. RYU [72] has reported that the quality of the adhering mortar and the interfacial transition zone (ITZ) of the original concrete significantly affects the quality of recycled aggregate concrete, specially when it is produced with relatively low water/cement ratio. Similar findings have been reported by Shayan and Aimin [87]. They concluded that the improvement of the weak zone of the surface layer can improve the durability of the resulting recycled aggregate concrete. Gomez-Soberon [94] observed that an increase in the volume of pores having size fraction of  $< 30$  nm when the virgin aggregate was replaced with

recycled aggregate. This size fraction of pores has been reported to play an important role in the drying shrinkage of concrete [11]. Katz [95] has shown that the difference between the quality of new cement paste and that of the old paste clinging to the surface of recycled aggregate is the major parameter that determines the quality of recycled aggregate concrete. Buyle-Bodin and Hadjieva-Zaharieva, Salem et al., and Ravindrarajah [75, 96-97] have also found increased water absorption, drying shrinkage and particularly air permeability of the recycled aggregate concrete when compared with normal. An initial absorption that is nearly four times that of normal concrete has been measured with recycled aggregate concrete [96].

Increased moisture absorption and drying shrinkage of recycled aggregate concrete adversely influence its long-term performance and durability [11, 98-100]. Moisture movement in hydrated cement paste influence the drying shrinkage of concrete. Concrete is generally restrained against dimensional movements (e.g., by friction against subgrade or by adjacent structural elements). Restrained drying shrinkage stresses are thus induced which may exceed the tensile strength of concrete and produce shrinkage cracks.

Recycled aggregate is a valuable resource; value-added consumption of recycled aggregate, as replacement for virgin aggregate in concrete, can yield significant energy and environmental benefits. Large-volume use of recycled aggregate concrete requires resolution of the problems with increased water absorption drying shrinkage of the resulting concrete.

## **1.8 Objectives of the Project**

Waste glass has limited market value. Recycling of post-consumer glass for use as raw material in production of new glass is very limited, mainly due to the mixed-color nature of waste glass. Waste glass (including mixed-color waste glass) has a highly favorable chemical composition for use as a SCM in concrete. It can thus be used as partial replacement for cement in concrete. The favorable chemistry of glass would make timely contributions to development of a high-quality cementitious paste need as far as the waste glass is milled to a particle size that is comparable to that of cement for enhanced reactivity with cement hydrates.

The scarcity of virgin aggregates and the increasing cost of landfilling the construction and demolition (C&D) waste are encouraging more value-added use of recycled aggregate (demolished concrete). Production and transport of virgin aggregates generate emissions representing 0.0046 million tons of carbon equivalent for each ton of virgin aggregate, compared to only 0.0024 million tons of carbon equivalent per ton of recycled aggregates [34]. Considering the global consumption of 10 billion tons/yr of aggregate for concrete production, the net emission reductions resulting from the replacement of virgin aggregates with recycled aggregates can yield major environmental benefits. These benefits are bound to get more pronounced over time as the depletion of the sources of virgin aggregates force shipments over longer distances, while recycled aggregates is generally available locally. The limitations of recycled aggregate concrete noted above (higher water absorption and drying shrinkage of resulting concrete) need to be overcome before recycled aggregate can replace virgin aggregate in large volumes. The old mortar / paste clinging to the surface of recycled aggregate is porous in nature

due to the presence of large oriented crystals of calcium hydroxide (a product of cement hydration) at the aggregate-remnant interface. When milled waste glass is used in recycled aggregate concrete as partial replacement of cement, it interacts with calcium hydroxide to form calcium silicate hydrate (C-S-H) which is the key binder among cement hydrates. This reaction can enhance the quality of the remnant cement paste on recycled aggregates, thus benefiting the impermeability and dimensional stability of recycled aggregate concrete.

## REFERENCES

1. Mehta, K.P., ed. *Concrete: Microstructure, Properties, and Materials*. 3rd ed. 2006, McGraw-Hill Professional.
2. Naik, T.R., *Sustainability of cement and concrete industries*. Proceedings of the International Conference on Achieving Sustainability in Construction, 2005: p. 141-150.
3. Naik, T.R., *Sustainability of concrete construction*. Practice Periodical on Structural Design and Construction, 2008. **13**(2): p. 98-103.
4. Worrell, E., et al., *Carbon dioxide emissions from the global cement industry*. Annual Review of Energy and the Environment, 2001. **26**: p. 303-329.
5. Van Oss, H.G. and A.C. Padovani, *Cement manufacture and the environment, Part II: Environmental challenges and opportunities*. Journal of Industrial Ecology, 2003. **7**(1): p. 93-126.
6. Guimaraes, C.P.a.M., *The CO<sub>2</sub> uptake of concrete in 100 year perspective*. Cement and Concrete Research, 2007. **37**: p. 1348-1356.
7. Gartner, E., *Industrially interesting approaches to "low CO<sub>2</sub>" cements*. Cement and Concrete Research, 2004. **34**: p. 1489-1498.
8. FS-181-99, U.F.S., *Recycled Aggregates - Profitable Resource Conservation* U.S.G. Survey, Editor. 2000.
9. E.P.A., U.S. *Wastes - Resources Conservation - Common Wastes and Materials*. November 23rd, 2009 January 2010]; Available from: <http://www.epa.gov/waste/conserves/materials/glass.htm>.
10. Naik, T.R. *Sustainability of cement and Concrete Industries*. in *Global Construction: Ultimate Concrete Opportunities*. 2005. Dundee, Scotland.
11. Mehta P. K., M.P.J.M., *Concrete: Microstructure, Properties and Materials*. 2006: McGraw-Hill New York.
12. *Guide to energy efficiency in masonry and concrete buildings*. Masonry Council of Canada, 1982.
13. Low, M.-S., *Materials Flow analysis of Concrete in the United States*. 2005, Massachusetts Institute of Technology.
14. Mehta, P.K., *Greening of concrete industry for sustainable development*. Concrete International, 2002: p. 23-28.

15. Bremner, T.W., *Environmental aspects of concrete: Problems and solutions*, in *All-Russian Conference on Concrete and Reinforced Concrete* 2001.
16. Oss, A.C.P.a.H.G.v., *Cement manufacture and the environment, Part 1: chemistry and technology*. *Industrial Ecology*, 2002. 6(1).
17. Gartner, E., *Industrially interesting approaches to "low-CO2" cements*. *Cement and Concrete Research*, 2004. 34(9): p. 1489-1498.
18. Mehta, P.K., *Reducing the environmental impact of concrete*. *Concrete International*, 2001.
19. Scrivener, K.L. and R.J. Kirkpatrick, *Innovation in use and research on cementitious material*. *Cement and Concrete Research*, 2008. 38(2): p. 128-136.
20. Uchikawa, H., *Approaches to ecologically benign system in cement and concrete industry*. 2000, Reston, VA, ETATS-UNIS: American Society of Civil Engineers. 57.
21. Hendriks C. A., E.W., D. de. Jager, K. Blok, and P. Riemer *Emission reduction of greenhouse gases from the cement industry* Greenhouse gas control technologies conference paper - cement 2004 [cited 2010 January 21]; Available from: <http://www.wbcasd.org/web/projects/cement/tfl/prghgt42.pdf>.
22. Malhotra, V.M., *Sustainable development and concrete technology*. *Concrete International*, 2002.
23. Malhotra, V.M., *Making concrete 'greener' with flyash*. *Indian Concrete Journal*, 1999. 73(10): p. 609-614.
24. *Environmental Indicators: Greenhouse gas emissions*. United Nations Report 2009 [cited 2010 January 28]; Available from: [http://unstats.un.org/unsd/environment/air\\_co2\\_emissions.htm](http://unstats.un.org/unsd/environment/air_co2_emissions.htm).
25. *Mineral commodity summaries*, USGS, Editor. 2008.
26. Malhotra, V.M., *Role of Supplementary Cementing Materials in Reducing Greenhouse Gas Emissions in Concrete Technology for a Sustainable Development in 21st Century* O.E.G.a.K. Sakai, Editor. 2000, E&FN Spon: London.
27. Mehta, P.K., *Global Concrete Industry Sustainability*. *Concrete International*, February 2009: p. 45-48.

28. Naik, R.N.K.T.R., *The role of flowable slurry in sustainable developments in civil engineering*, in *Materials and Construction: Exploring the Connection*. 1999, American Society of Civil Engineers: Reston, Va. p. 826-834.
29. *Efficient use of energy utilizing high technology: An assessment of energy use in industry and building* 1995, World Energy Council: London.
30. *Cement and concrete: Environmental Considerations*. 2004 [cited 2010 Jan 30th ]; Available from: <http://www.wbcscement.org/pdf/tf2/cementconc.pdf>.
31. *Wastes - Resources Conservation - Reduce, Reuse, Recycle - Construction and Demolition Materials*, U.S. E.P.A., Editor. 2009.
32. *Background Document for Life-Cycle Greenhouse Gas Emission Factors for Clay Brick Reuse and Concrete Recycling*. 2003, EPA.
33. Damtoft, J.S., et al., *Sustainable development and climate change initiatives*. Cement and Concrete Research, 2008. **38**(2): p. 115-127.
34. EPA530-R-03-017, *Background document for life-cycle greenhouse emission factors for clay brick reuse and concrete recycling*, EPA, Editor. 2003.
35. *Recycled Aggregates – Profitable Resource Conservation*, USGS, Editor. 2000.
36. *User Guidelines for Waste and By-Product Materials in Pavement Construction*, F.H.A. U.S. Department of Transportation, Editor. 1998.
37. Meyer, C. *Recycled Glass - from waste Material to Valuable Resource*. in *Recycling and Reuse of Glass Cullet* 2001. Dundee, Scotland.
38. *Global Waste Management - Market Assesment*. 2007; Available from: [www.bharatbook.com](http://www.bharatbook.com).
39. *Wastes - Resource Conservation - Common Wastes & Materials*. 2009, U.S. EPA.
40. Egosi, N.G. *Utilization of Waste Materials in Civil Engineering Construction*. in *Mixed Broken Glass Processing Solutions*. 1992: ASCE.
41. Topçu, I.B. and M. Canbaz, *Properties of concrete containing waste glass*. Cement and Concrete Research, 2004. **34**(2): p. 267-274.
42. *Recycling and Reuse of Glass Cullet*. 2001. Dundee, Scotland: Thomas Telford.
43. Siddique, R., *Waste Materials and By-Products in Concrete*. 2008: Springer.
44. Xie, Z. and Y. Xi, *Use of recycled glass as a raw material in the manufacture of Portland cement*. Materials and Structures, 2002. **35**(8): p. 510-515.

45. Shayan, A. and A. Xu, *Value-added utilisation of waste glass in concrete*. Cement and Concrete Research, 2004. 34(Compendex): p. 81-89.
46. Shao, P.L.a.Y., *Feasibility of using ground waste glass as cementitious material*, in *Recycling and Reuse of Glass Cullet*. 2001, Thomas Telford: Dundee, Scotland.
47. Meyer, C., *Concrete and sustainable development in Concrete Materials Science to Application*. 2002, American Concrete Institute: Michigan.
48. Johnston, C.D., *Waste Glass as Coarse Aggregate for Concrete* Journal of Testing and Evaluation 1974. 2(5): p. 344-350.
49. Dhir, R.K.a.D., T. D. , *Maximising Opportunities for Recycling Glass*, in *Sustainable Waste Management and Recycling: Glass Waste*, M.C.L.a.J.J. Roberts, Editor. 2004, Thomas Telford: London.
50. Jin, W., C. Meyer, and S. Baxter, *"Glascrete"-concrete with class aggregate*. ACI Materials Journal, 2000. 97(Compendex): p. 208-213.
51. ASTM, *Standard Specification for Coal Fly Ash and raw or Calcined natural Pozzolan for Use in Concrete*, in C 618-05. 2005, ASTM International: PA, United States.
52. WSDTED, *Washington State Department of Trade and Economic Development Glass Feed-stock Evaluation Project*. 1993.
53. *Cement and Concrete: Environmental Considerations*. EBN 1993 [cited 2; Available from: <http://www.buildinggreen.com/features/cem/cementconc.cfm>].
54. Meyer, C., *The greening of the concrete industry*. Cement and Concrete Composites, 2009. 31(8): p. 601-605.
55. Sakai, K.a.S., Douglas. *Planning for the effects of green building and international standards*. in *ACI St. Louis Workshop on Sustainability*. 2009.
56. 555R-01, A., *Removal and reuse of hardened concrete*, in *Manual of Concrete Practice*. 2006, American Concrete Institute.
57. Cuttell, G.D., et al., *Performance of rigid pavements containing recycled concrete aggregates*. Transportation Research Record, 1996(Compendex): p. 89-98.
58. Dhir, R.K., K.A. Paine, and S. O'Leary. *Use of recycled concrete aggregate in concrete pavement construction: A case study*. in *Sustainable Waste Management, Proceedings of the International Symposium, September 9, 2003 - September 11, 2003*. 2003. Dundee, United kingdom: Thomas Telford Services Ltd.

59. Etxeberria, M., A.R. Mari, and E. Vazquez, *Recycled aggregate concrete as structural material*. Materials and Structures/Materiaux et Constructions, 2007. **40**(Compendex): p. 529-541.
60. Etxeberria, M., E. Vazquez, and A. Mari, *Microstructure analysis of hardened recycled aggregate concrete*. Magazine of Concrete Research, 2006. **58**(Compendex): p. 683-690.
61. Gokce, A., et al., *Freezing and thawing resistance of air-entrained concrete incorporating recycled coarse aggregate: The role of air content in demolished concrete*. Cement and Concrete Research, 2004. **34**(Compendex): p. 799-806.
62. Hansen, T.C., *RECYCLED AGGREGATES AND RECYCLED AGGREGATE CONCRETE SECOND STATE-OF-THE-ART REPORT DEVELOPMENTS 1945-1985*. Materials and Structures/Materiaux et Constructions, 1986(Compendex): p. 201-246.
63. Hansen, T.C. and E. Boegh, *ELASTICITY AND DRYING SHRINKAGE OF RECYCLED-AGGREGATE CONCRETE*. Journal of the American Concrete Institute, 1985. **82**(Compendex): p. 648-652.
64. Kasai, Y. *Development and subjects of recycled aggregate concrete in Japan*. in *Environmental Ecology and Technology of Concrete*. 2006: Trans Tech Publications Ltd.
65. Khatib, J.M., *Properties of concrete incorporating fine recycled aggregate*. Cement and Concrete Research, 2005. **35**(Compendex): p. 763-769.
66. Limbachiya, M.C., T. Leelawat, and R.K. Dhir, *Use of recycled concrete aggregate in high-strength concrete*. Materials and Structures/Materiaux et Constructions, 2000. **33**(Compendex): p. 574-580.
67. Poon, C.S., Z.H. Shui, and L. Lam, *Effect of microstructure of ITZ on compressive strength of concrete prepared with recycled aggregates*. Construction and Building Materials, 2004. **18**(Compendex): p. 461-468.
68. Rahal, K., *Mechanical properties of concrete with recycled coarse aggregate*. Building and Environment, 2007. **42**(Compendex): p. 407-415.
69. Ravindraji Sri, R., Y.H. Loo, and C.T. Tam, *STRENGTH EVALUATION OF RECYCLED-AGGREGATE CONCRETE BY IN-SITU TESTS*. Materials and Structures/Materiaux et Constructions, 1988. **21**(Compendex): p. 289-295.
70. Ridzuan, A.R.M., et al. *Durability performance of recycled aggregate concrete*. in *2005 International Congress - Global Construction: Ultimate Concrete*

*Opportunities, July 5, 2005 - July 7, 2005.* 2005. Dundee, Scotland, United Kingdom: Thomas Telford Services Ltd.

71. Ryu, J.S., *An experimental study on the effect of recycled aggregate on concrete properties.* Magazine of Concrete Research, 2002. **54**(Compendex): p. 7-12.
72. Ryu, J.S., *Improvement on strength and impermeability of recycled concrete made from crushed concrete coarse aggregate.* Journal of Materials Science Letters, 2002. **21**(20): p. 1565-1567.
73. Sagoe-Crentsil, K.K., T. Brown, and A.H. Taylor, *Performance of concrete made with commercially produced coarse recycled concrete aggregate.* Cement and Concrete Research, 2001. **31**(Compendex): p. 707-712.
74. Salem, R.M. and E.G. Burdette, *Role of chemical and mineral admixtures on physical properties and frost-resistance of recycled aggregate concrete.* ACI Materials Journal, 1998. **95**(Compendex): p. 558-563.
75. Salem, R.M., E.G. Burdette, and N.M. Jackson, *Resistance to freezing and thawing of recycled aggregate concrete.* ACI Materials Journal, 2003. **100**(Compendex): p. 216-221.
76. Tavakoli, M. and P. Soroushian, *Drying shrinkage behavior of recycled aggregate concrete.* Concrete International, 1996. **18**(Compendex): p. 58-61.
77. Tavakoli, M. and P. Soroushian, *Strengths of recycled aggregate concrete made using field-demolished concrete as aggregate.* ACI Materials Journal, 1996. **93**(Compendex): p. 182-190.
78. Xiao, J., J. Li, and C. Zhang, *On statistical characteristics of the compressive strength of recycled aggregate concrete.* Structural Concrete, 2005. **6**(Compendex): p. 149-153.
79. Xiao, J., J. Li, and C. Zhang, *Mechanical properties of recycled aggregate concrete under uniaxial loading.* Cement and Concrete Research, 2005. **35**(Compendex): p. 1187-1194.
80. Yamasaki, J. and K. Tatematsu, *Strength and freeze-thaw resistance properties of concrete using high-quality recycled aggregate.* Transactions of the Japan Concrete Institute, 1998. **20**(Compendex): p. 45-52.
81. Zaharieva, R., et al., *Assessment of the surface permeation properties of recycled aggregate concrete.* Cement and Concrete Composites, 2003. **25**(Compendex): p. 223-232.

82. Zaharieva, R., F. Buyle-Bodin, and E. Wirquin, *Frost resistance of recycled aggregate concrete*. Cement and Concrete Research, 2004. **34**(Compendex): p. 1927-1932.
83. Hansen, T.C. and H. Narud, *STRENGTH OF RECYCLED CONCRETE MADE FROM CRUSHED CONCRETE COARSE AGGREGATE*. Concrete International, 1983. **5**(Compendex): p. 79-83.
84. Hasaba, S., Kawamura, M., and Toriik, K. et al *Drying shrinkage and durability of concrete made of recycled concrete aggregates*. Japan Concrete Institute, 1981. **3**: p. 55-60.
85. B.C.S.J, *Study on recycled aggregate and recycled aggregate concrete*. Concrete Journal, Japan, 1978. **16**(7): p. 18-31.
86. Hansen, T.C., ed. *Recycling of demolished concrete and masonry 1992*, Taylor & Francis. 336.
87. Shayan, A. and A. Xu, *Performance and Properties of Structural Concrete made with Recycled Concrete Aggregate*. ACI Materials Journal, 2003. **100**(Compendex): p. 371-380.
88. Nixon, P., *Recycled concrete as an aggregate for concrete—a review*. Materials and Structures, 1978. **11**(5): p. 371-378.
89. Dolara, E.D.N., G.; and Carins, R. , *RAC Prestressed Beams. Sustainable Construction: Use of Recycled Concrete Aggregate 1998*, London: Thomas Telford.
90. Limbachiya, M., T. Leelawat, and R. Dhir, *Use of recycled concrete aggregate in high-strength concrete*. Materials and Structures, 2000. **33**(9): p. 574-580.
91. Topçu, I.B., *Physical and mechanical properties of concretes produced with waste concrete*. Cement and Concrete Research, 1997. **27**(12): p. 1817-1823.
92. Rasheeduzzafar and Khan, A., *Recycled Concrete- A source of new aggregate*. Journal of Cement, Concrete and Aggregates 1984. **6**(1): p. 17-27.
93. Arioz, O., A. Ozsoy, and G. Yilmaz. *Concrete with recycled aggregate. in Proceedings of the 8th Conference and Exhibition of the European Ceramic Society, June 29, 2003 - July 3, 2003*. 2004. Istanbul, Turkey: Trans Tech Publications Ltd.
94. Gómez-Soberón, J.M.V., *Porosity of recycled concrete with substitution of recycled concrete aggregate: An experimental study*. Cement and Concrete Research, 2002. **32**(8): p. 1301-1311.

95. Katz, A., *Properties of concrete made with recycled aggregate from partially hydrated old concrete*. Cement and Concrete Research, 2003. **33**(5): p. 703-711.
96. Buyle-Bodin, F. and R. Hadjieva-Zaharieva, *Influence of industrially produced recycled aggregates on flow properties of concrete*. Materials and Structures/Materiaux et Constructions, 2002. **35**(Compendex): p. 504-509.
97. Ravindrarajah Sri, R., *Properties of concrete made with crushed concrete as coarse aggregate*. Magazine of Concrete Research, 1985. **37**(130).
98. Mindess S., Y.J.F., and Darwin D., *Concrete*. Second ed. 2003: Prentice Hall.
99. Neville, A.M., *Properties of Concrete*. 4th ed. 2000: Pearson Education.
100. Basheer, L., J. Kropp, and D.J. Cleland, *Assessment of the durability of concrete from its permeation properties: A review*. Construction and Building Materials, 2001. **15**(Compendex): p. 93-103.

## **CHAPTER 2**

### **Moisture Transport in Concrete: Basic Principles, and Effects of Milled Waste Glass and Recycled Aggregate**

#### **2.1 Moisture Transport in Porous Materials**

The entry of moisture into porous materials is one of the most common physical phenomena encountered in everyday life. This phenomenon is of great interest in many scientific fields. A great deal of fundamental work concerning the flow of water in unsaturated porous materials has been conducted in the field of soil physics [1-4]. Modes of transport governing moisture infiltration into soils have been identified as: capillary uptake (sorption) and vapor diffusion. Material characteristics such as hydraulic conductivity ( $K$ ), capillary potential ( $\psi$ ), and diffusivity ( $D$ ) have been identified as factors that significantly influencing moisture transport in porous materials; these factors are functions of moisture content. The earlier work of Philips [3] highlighted the dominance of liquid-phase moisture movement in soil; this work has also shown that the total potential for unsaturated hydraulic conductivity comprises the negative pressure potential (capillary) component and the gravitational component.

Most common inorganic construction materials, including concrete, have open porosity (i.e., a pore system that is partly continuous and connected to the boundaries or surfaces). Once exposed to moisture sources such as rain, groundwater, humid air and condensation, these construction materials take up water. Similarly, drying would occur upon exposure to dry atmosphere. In porous materials such as concrete, the unsaturated flow at varying moisture contents generally occupies the central place between the

extremes of water vapor movement in the relatively dry state and the pressure-driven liquid water transport in the saturated state [5]. With the exception of concrete water-retaining structures, concrete in above-ground structures is rarely saturated. Hence, saturation in concrete is an exception rather than the rule. Consequently, unsaturated flow is the main mode of water transport in concrete throughout its life. Even if concrete gets locally saturated from time to time, e.g. in the event of driving rain on a concrete pavement surface or concrete facade, water will migrate from saturated to unsaturated regions and ultimately to the surrounding environment.

Water transport in concrete and other porous materials has a thermodynamically explained energy basis. It is the nature of most liquids and solids to be in the state of minimum energy. Wetting of a solid porous material by water results in the replacement of solid/air interfaces with solid/liquid interfaces; this change results in reducing the energy of the system [6]. All liquids and solids have characteristic surface energies since surface atoms and molecules are in a less stable state than the ones in the interior. Water tends to migrate in porous solids in order to lower its potential energy. Similarly, the spontaneous redistribution of water in porous solids occurs to achieve an equilibrium distribution in the lowest energy state [7]. A liquid droplet forms the shape of a sphere which is the state of minimum surface energy. Its surface is in tension and acts like a stretched skin. If the work done in changing the size of the droplet (work done =  $\Delta P \cdot dV = \Delta P \cdot 4\pi r^2 dr$ ) is equated to the energy required ( $\sigma \cdot dA$ ) to create extra surface area ( $dA = 8\pi r dr$ ), one gets the equilibrium excess pressure inside the droplet, given by;  $\Delta P = 2\sigma/r$ . This is referred as the Young-Laplace equation, according to which the excess pressure depends on the radius of the sphere and the surface tension of water [5]. For a

sphere having a radius of curvature equal to 100  $\mu\text{m}$ , the pressure drop is equal to 0.0142 atm (assuming that the surface tension of water is equal to 72.14 mN/m); it increases to 1.42 atm for a radius of 1  $\mu\text{m}$ .

Moisture transport in concrete can occur in three modes: (i) capillary absorption; (ii) diffusion; and (iii) permeation [5, 8-10]. The pressure-driven mode of transport (i.e., permeation) is specific to either water-retaining or underground structures [11]. Diffusion, which is a slow process of moisture transport, accounts for the long-term moisture movement driven by concentration gradient or vapor pressure gradient [5, 12]. Upon exposure to an atmosphere which has higher vapor pressure than the salt-concentrated solution in the material, the vapor pressure gradient leads to moisture diffusion into concrete. Condensation of water occurs on the film of saturated salt solution. The processes of moisture diffusion and water condensation continue until the concentration of salt solution has dropped to a level where its vapor pressure is in equilibrium with the external atmospheric vapor pressure [5]. The dominant mode of moisture transport in concrete is sorption for which the driving force is the capillary suction [5, 11, 13-17]. The moisture content of concrete is generally less than saturated condition; hence, moisture transport in concrete is governed by unsaturated flow, at the heart of which lies the capillary suction. Capillary force is a function of the pore structure, but it is modified by the local water content. It is strongest when concrete is dry, and reduces with increase in saturation level; it almost vanishes at complete saturation [18].

### 2.1.1 Sorption

The concept of sorptivity / sorption was first introduced by Philips [19] in 1957 in the context of hydrology and soil physics. He defined sorptivity as the most important single quantity governing the unsaturated flow in porous media. In the modern context, sorption has been defined as the absorption of water by capillary pores, and its transport by the capillary action [14, 17]. If an initially dry specimen of a porous material is placed in contact with a water source, capillary sorption sets in and water transportation into concrete starts. Capillarity, referred to the action of liquids in fine tubes [1], forms a basis for sorption in porous materials.

Capillarity deals with liquid interactions with porous solids where the driving force is determined by the surface tension and curvature of a gas-liquid interface. The most common case of capillary action occurs when one surface of a liquid is in contact with air. Because of the free energy possessed by the molecules of liquid lying on such a surface, there is a tendency for the surface to assume a configuration which minimizes the area. Mathematically, a uniform surface density of free energy is equivalent to a uniform tension in the surface and, for some purposes, it is convenient to express the physical properties of an air-liquid interface in terms of surface tension. As stated in Section 2.1, the pressure difference caused by a curved liquid surface is expressed as:

$$pW - pA = \frac{T}{\left(\frac{1}{R1}\right) + \left(\frac{1}{R2}\right)} \quad (2.1)$$

where,  $pW$  and  $pA$  are the pressures on water and liquid sides of the surface, respectively,  $T$  is the surface tension, and  $(1/R1+1/R2)$  represents the total curvature of the surface. Because of the inequality between cohesive and adhesive forces at the liquid-solid

interface, these surfaces also have a free energy which is important in determining the capillary behavior of liquids. Because of their effect on the angle of contact, adhesive forces are directly involved in an initial wetting process such as the spreading of a liquid in a dry porous medium; once the medium is wetted, the adhesive forces are no longer effective in producing a motion of the liquid, and influence capillary action only to the extent that they hold a thin film firmly in contact with the solid surface. The liquid lying outside the adsorbed films is free to move under the action of unbalanced forces.

The pore space region in a porous medium typically forms a complicated geometry, and the configuration arising when only part of this space is filled with the liquid is even more difficult to picture [1]. Because of the action of surface tension, liquid tends to collect in small wedge and disk-shaped bodies in sharp corners of the pores or where the particles of the medium are closer together. The size of these bodies and the thickness of the films connecting them depend upon the amount of liquid present in the medium. It is through this connected configuration, bounded on one side by the adsorbed films in contact with the solid, and on the other by the curved air-liquid interface, that capillary flow takes place.

Applying the equation of continuity and Darcy's law it is possible to derive an equation for the flow of water in an unsaturated porous medium. The equation of continuity, which is a statement of the principle of conservation of matter, may be written (for an unsaturated porous medium) as [2]:

$$\frac{\partial}{\partial t}(\rho_{\sigma}\theta) = -\nabla \cdot V \quad (2.2)$$

Where,  $\rho_{\sigma}$  is the bulk density of the medium,  $\theta$  is its moisture content on a dry weight basis, and  $V$  is the mass flux of moisture, that is, the mass of fluid flowing through a unit cross-sectional area normal to the line of flow in unit time. Extended Darcy's law for the transport of moisture in an unsaturated porous medium may be written as:

$$v = -K(\theta)\nabla\Phi \quad (2.3)$$

Where is  $\nabla$  vector differential operator,  $\Phi$  is the moisture potential tending to produce motion,  $v$  is the volume flux of moisture, and  $K(\theta)$  is variously known as hydraulic conductivity, capillary conductivity, coefficient of aqueous conductivity, transmission constant, and the coefficient of permeability; it depends on the number and kind of pore spaces of the porous medium. In the above equation,

$$\Phi = \psi + z \quad (2.4)$$

where,  $\Psi$  (capillary potential) can be calculated from the famous Young-Laplace equation:

$$\psi = \frac{2\sigma}{r} \quad (2.5)$$

Where,  $\sigma$  is the surface tension of invading liquid, and  $r$  is the mean radius of curvature of the liquid meniscus within the pore.

Combination of Equations (2.2) and (2.3) will yield the following equation for flow of water in an unsaturated system:

$$\frac{\partial}{\partial t}(\rho_{\sigma}\theta) = \nabla(\rho K\nabla\Phi) \quad (2.6)$$

Assuming that the liquid density is constant, Equation (2.6) reduces to [3]:

$$\frac{\partial\theta}{\partial t} = \nabla(K\nabla\Phi) \quad (2.7)$$

Equation (2.7) is known as the Richard's equation.

If the total moisture potential is considered as the sum of the pressure and gravitational potentials; for a system in which flow is only in vertical direction, the equation can be expressed as:

$$\frac{\partial \theta}{\partial t} = \frac{\partial}{\partial z} \left( K \frac{\partial \psi}{\partial z} \right) + \frac{\partial}{\partial z} (Kg) \quad (2.8)$$

where,  $\psi$  is capillary potential,  $g$  is gravitational constant, and  $z$  is the vertical ordinate.

Equation (2.6) is a fundamental equation of unsaturated moisture flow in porous media. If  $\theta$  and  $\psi$  are considered to be related, then equation (2.6) may be written as:

$$\frac{\partial \theta}{\partial t} = \frac{\partial}{\partial z} \left( D \frac{\partial \theta}{\partial z} \right) + g \frac{\partial K}{\partial z} \quad (2.9)$$

where,  $D$  (capillary diffusivity) is expressed as follows:

$$D = K \frac{\partial \psi}{\partial \theta} \quad (2.10)$$

In above equations, both,  $K$  and  $\psi$  are strongly dependent upon the moisture content ( $\theta$ ) of the medium, and so is  $D$ . In case of moisture movement in porous materials, the capillary forces are much stronger than the gravitational forces [3, 5, 7, 11, 14-15, 17]; hence, the gravity part of Equation (2.7) may be ignored. For a one-dimensional horizontal flow, Equation (2.7) may be written as:

$$\frac{\partial \theta}{\partial t} = \frac{\partial}{\partial x} \left( D \frac{\partial \theta}{\partial x} \right) \quad (2.11)$$

where,  $x$  is the horizontal ordinate. When the column is semi-infinite, the governing boundary conditions for Equation (2.9) are [3]:

$$\left. \begin{array}{lll} \theta = \theta_n, & t = 0, & x > 0 \\ \theta = \theta_o, & x = 0, & t \geq 0 \end{array} \right\} \quad (2.12)$$

For many building materials, different modes of one-dimensional water absorption into an initially dry porous solid have been found to be indistinguishable due to the dominance of capillary forces when compared with other forces such as gravity. This is shown in Figure 2.1, where in the horizontal case (Figure 2.1a) flow is independent of gravitational effects, in the infiltration case (Figure 2.1b) total flow is the sum of capillary-driven and gravity-driven flows, and in the capillary rise (Figure 2.1c) the of capillarity and gravity effects oppose each other.

The numerical solution of Equation (2.9) subject to Equation (2.10) has been derived using the procedure of Boltzmann transformation;

$$\varphi = xt^{-1/2} \quad (2.13)$$

This reduces Equation (2.9) to an ordinary differential equation:

$$-\frac{\varphi}{2} \frac{d\theta}{d\varphi} = \frac{d}{d\varphi} \left( D \frac{d\theta}{d\varphi} \right) \quad (2.14)$$

where,  $\theta$  is made the independent variable by multiplying both sides of equation by  $d\theta/d\varphi$ , yielding:

$$-\frac{\varphi}{2} = \frac{d}{d\varphi} \left( D \frac{d\theta}{d\varphi} \right) \quad (2.15)$$

Detailed descriptions of the numerical solution are given elsewhere [2-3]. Once  $\varphi$  is known, the cumulative volume of water absorbed through a unit area of surface,  $i$ , is given as:

$$i = St^{1/2} \quad (2.16)$$

where,  $S$  is called Sorptivity. The predicted  $t^{1/2}$  dependence has been confirmed for many inorganic building materials [7, 14]. It should be noted that the  $t^{1/2}$  scaling holds good for one-dimensional imbibitions into a semi-infinite material with a constant-concentration boundary condition. In 2-D or 3-D cases, the flow may be divergent or convergent, and this scaling is not expected. Using experimental water absorption data,  $S$  can be calculated from the plot of  $i$  vs.  $t^{1/2}$  as the slope of the curve.

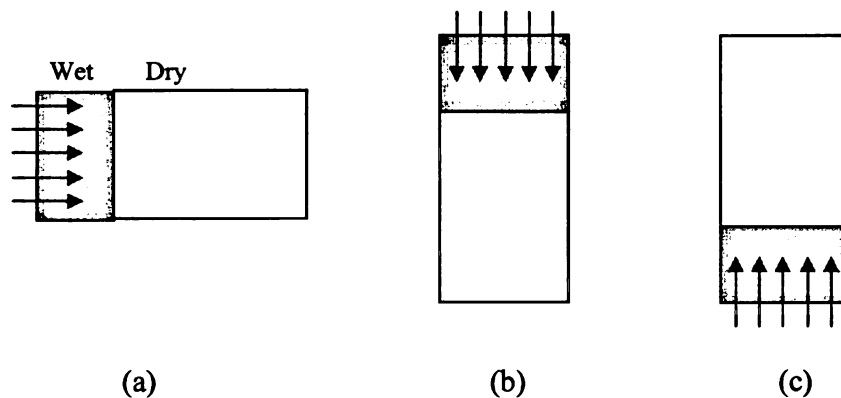


Figure 2. 1 Different modes of one-dimensional water absorption [14]

The porous materials and water within them are characterized by macroscopic parameters such as hydraulic conductivity  $K$  and total hydraulic potential  $\Phi$ , which must be determined experimentally. The complementary microscopic approach has to relate permeability and associated properties to pore size distribution and pore structure [7]. As discussed in Section 2.1, according to the unsaturated flow theory, water flows within a porous material under the action of a capillary force. The strength of capillary force is determined by the pore size distribution, the pore structure and the material type, but is

modified by the local water content. Hence, the capillary force is strongest when the material is dry, and reduces with increase in moisture content until it almost vanishes at complete saturation [18]. The flow velocity produced by the capillary force likewise depends upon the pore structure which determines the hydraulic conductivity of the porous material. The flow velocity is, however, affected by the local water content as well. The permeability (known strictly as the unsaturated hydraulic conductivity) is itself a strong function of the water content, being vanishingly small in completely dry materials and reaching its maximum value in fully saturated materials (where it is conventionally the saturated Darcy permeability). In concrete, water absorption and subsequent movement of water within the material by the action of capillary forces depends primarily on the geometry of the pore system.

### 2.1.2 Diffusion

Moisture diffusion is an important mode of moisture transport from the standpoint of long-term moisture transport through cementitious materials [20-21]. The moisture diffusion can be described by the diffusion equations. Fick's first law states:

$$J_D = D\nabla C \quad (2.17)$$

where,  $J_D$  is the diffusive flux density,  $D$  is the diffusion constant ( $\text{mm}^2/\text{t}$  ( $\text{in}^2/\text{t}$ )), and  $C$  is the concentration ( $\text{gm}/\text{ltr}$  ( $\text{lb}/\text{ltr}$ )). The time evolution of the concentration is obtained from the divergence of the flux density [21]:

$$\frac{\partial C}{\partial t} = D\nabla^2 C \quad (2.18)$$

Equation (2.18) is known as the diffusion equation or Fick's second law, and can alternatively be written as:

$$\frac{\partial C}{\partial t} = D \frac{\partial^2 C}{\partial x^2} \quad (2.19)$$

In one-dimensional moisture movement, Equation (2.19) reduces to Equation (2.20) shown below:

$$\frac{dC}{dt} = D \frac{dC}{dx} \quad (2.20)$$

The diffusion constant  $D$  depends on the microstructure in which the material is diffusing.

Moisture diffusion has been reported to occur through three distinct transport mechanisms that may operate singularly or simultaneously: molecular diffusion which is commonly known as ordinary diffusion or vapor diffusion, Knudsen diffusion, and surface diffusion [16, 20, 22]. The total diffusion is a complex property that contains contributions from multiple mechanisms. The basic criterion for the assessment, whether water in a given pore is in the form of water vapor or only as isolated molecules, is the Knudsen number  $Kn$ :

$$Kn = \frac{\lambda}{d} \quad (2.21)$$

where,  $\lambda$  is the mean free path of molecules of water vapor, and  $d$  is the diameter of the pore. For  $Kn \gg 1$ , Knudsen diffusion will occur, and for  $Kn < 1$ , molecular diffusion will occur [22]. Like sorption, diffusion of moisture inside cementitious material is controlled by the microstructure of the material, and especially by the pore size distribution [20]. This fact highlights the importance of the pore size distribution, which lies at the heart of moisture transport in cementitious materials. Figure 2.2 shows the combined effects of different diffusion mechanisms assuming a cylindrical capillary pore within concrete. On

both sides of the pore, the boundary conditions considered assume that the vapor pressure is greater on the interior side and relative humidity is greater on the exterior side. If the material is sufficiently dry or not hygroscopic, then water vapor will diffuse from inside to outside (higher to lower vapor pressure). If the material contains enough moisture to cause mobility of a sorbate film on pore walls, then surface diffusion will occur due to the sorbed water on the surface of pore walls. As the example shows, the transport directions of vapor diffusion and surface diffusion might not be the same under given ambient conditions. It is therefore difficult to treat each mechanism individually and derive a general expression for diffusivity. It is more realistic to try to predict a general combined trend [20].

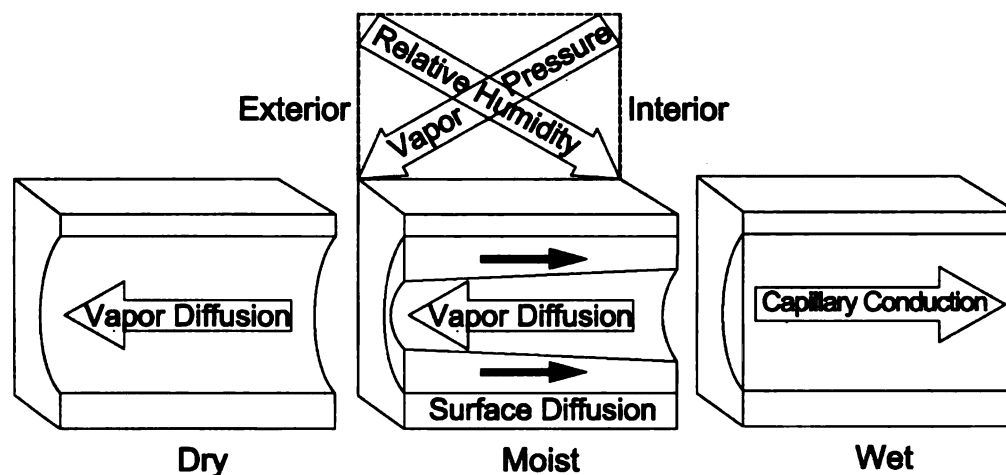


Figure 2.2 Schematics of moisture transport phenomena within pores

As stated earlier, diffusion mechanisms are influenced by the pore structure of concrete. Figure 2.3 shows the molecular diffusion process inside the macropores (capillary pores) of concrete. At a low relative humidity, the field force of the pore wall (van der Waals bonding) captures water molecules to form the first attached layer. Other water molecules

continue to move ahead and, with increase in humidity, more layers of water molecules cover the pore walls. This results in a decrease of the free space available to vapor inside macropores. The force field of the wall thus weakens and, at the same time, the mean free path of the water molecules decreases. These trends have opposite effects on the resistance to diffusion.

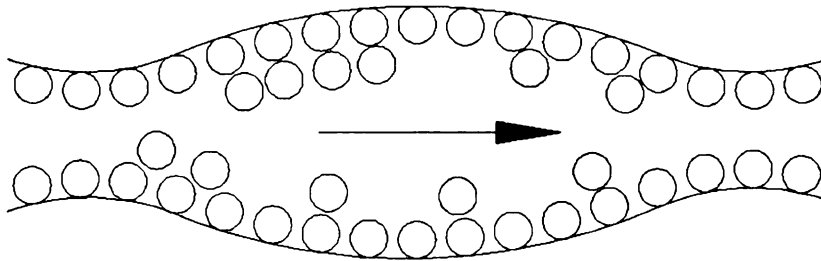


Figure 2.3 Molecular diffusion in macropores at low humidity

When the pore humidity is high enough, the adsorbed water will form a meniscus at a neck (a narrow connection between larger pores). At high humidity, menisci form on both ends of the neck, and the neck is completely filled. At this point, water molecules condense at one end of the neck, while at the other they evaporate, as shown in Figure 2.4. Since part of the transport is through gas, this condensation and evaporation process strongly accelerates the diffusion process.

The foregoing diffusion process will dominate whenever the mean free path of water vapor (which is  $800 \text{ \AA}$  at  $25^\circ\text{C}$ ) is small relative to the diameter of macropore (generally considered to be about  $50 \text{ nm}$  to  $10 \text{ }\mu\text{m}$ ) [20]. Pores of this size constitute only a small portion of the pores in concrete. Therefore, molecular diffusion (or ordinary diffusion) occurs only occasionally in concrete, and is not a dominant mechanism.

Mesopores and micropores comprise the largest portion of concrete pores. In these pores, collisions between molecules as well as against pore walls provide the main resistance against diffusion. In such conditions, diffusion is called Knudsen diffusion (defined earlier). Similar phenomena occur at various humidity levels, but a difference exists between molecular diffusion and Knudsen diffusion. For Knudsen diffusion, the resistance against diffusion is related to the pore size. For smaller pores, the resistance is larger and thus the diffusivity is smaller.

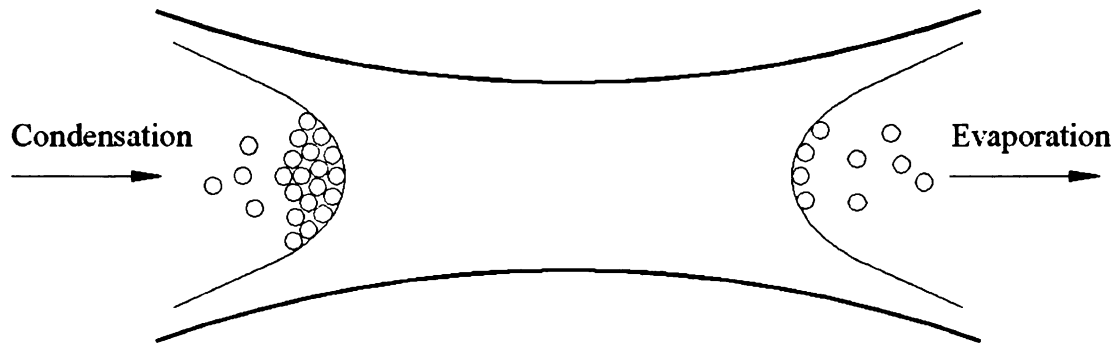


Figure 2. 4 Evaporation and condensation phenomena inside a pore at high humidity

Figure 2.5 shows the process of surface diffusion that occurs in certain Mesopores and micropores, such as the pore of parallel walls. The water molecules never escape the force field of the pore surface. Moisture transport in this case is a thermally activated process with jumps between the adsorption sites. In such a surface diffusion process, pores with typical sizes occurring in concrete offer greater resistance to transport than in the case of Knudsen diffusion. Hence, surface diffusion tends to be insignificant in concrete unless most of the water is adsorbed water. This implies that surface diffusion is significant in concrete only at very low humidity. To formulate a realistic approach to simulation of moisture diffusion in concrete, factors such as pore connectivity and

tortuosity, and changes in the pore structure at different water/cement ratios need to be considered. Furthermore, the formation process of fine micropores depends strongly on time and humidity level, which need to be accounted for. As stated earlier, these factors make it difficult to derive a general expression for diffusivity.

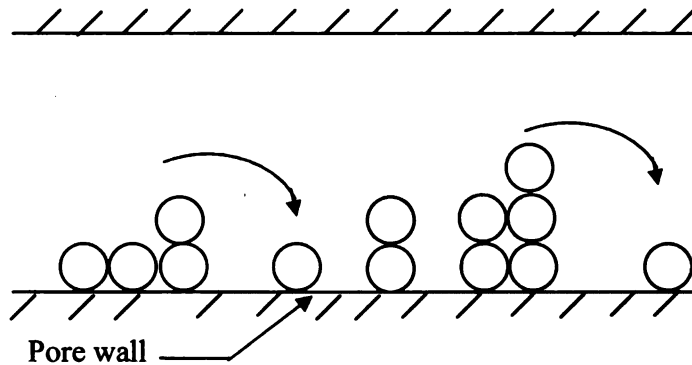


Figure 2. 5 The process of surface diffusion inside pore

After evaluation and comparison of all three diffusion mechanisms, it is clear that they share similarities. At low humidity, the pore volume decreases, the surface force field weakens, and the mean free path decreases. These behaviors may just offset each other such that the effective diffusivity for all mechanisms becomes constant at low humidity. At high humidity, capillary condensation occurs and the resistance to diffusion decreases. The effective diffusivity of the system may be assumed to follow the simple empirical curve shown in Figure 2.6.

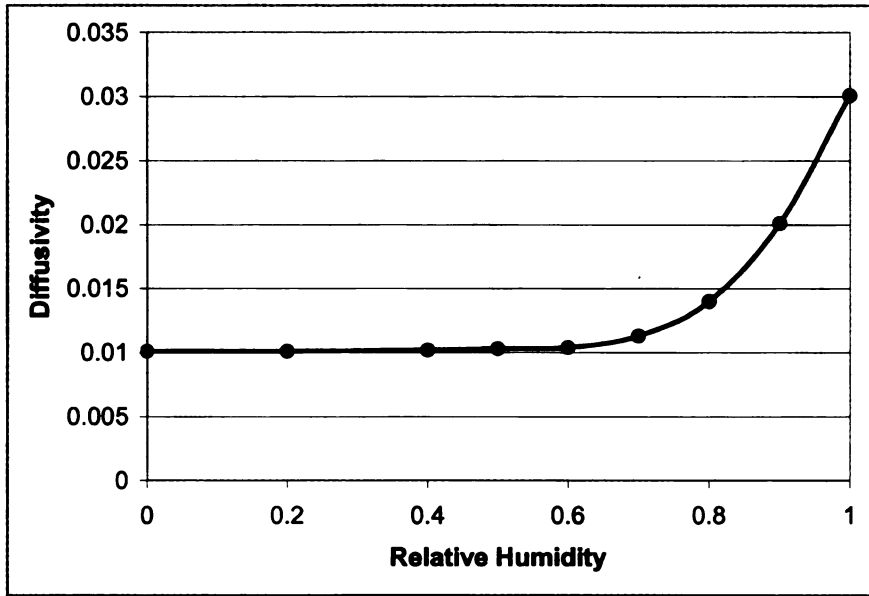


Figure 2.6 Diffusivity dependence on humidity

## 2.2 Effects of Concrete Microstructure on Moisture Transport

Concrete is a composite material with random microstructure over a wide range of length scales. On a scale-down approach; concrete is a mortar/rock composite, where the randomness in its structure is of the order of centimeters (fraction of an inch), that is the size of a coarse aggregate. Mortar itself is a composite of cement paste and sand. In this case, the randomness is of the order of millimeters (tenths of an inch). Cement paste can also be viewed as a random composite material. It has unreacted cement, calcium silicate hydrate (C-S-H), calcium hydroxide (CH), capillary pores, and other chemical phases in its structure [23]. At the lowest scale, C-S-H is itself a complex material having a random structure over a scale of nanometers (observed by neutron scattering) [24]. Concrete has, therefore, a wide range of random structures with a scale bracket of nanometers to centimeters covering seven orders of magnitude [23]. Therefore, relating the microstructure of concrete to its properties is a difficult task.

In its simplest form, the concept of “tube theory” has been applied to moisture transport in concrete [23]. According to which, the larger-diameter tubes have higher transport rates than smaller-diameter tubes, and the tubes that are blocked have zero transport rates. This translates into the idea of ‘pore size’ and ‘pore connectivity’ forming the basis for evaluating the role of concrete microstructure in moisture transport. Considering the wide range of randomness in concrete, it is required to describe the role of various constituent phases such as ‘cement paste’ and ‘mortar as well as the concrete microstructure’ and flaws in deciding its moisture transport characteristics. Accordingly, efforts have been undertaken to relate the transport characteristic of concrete to the porosities of the following three phases: aggregate, cement-based matrix, and interfacial transition zone (ITZ).

### **2.2.1 Effect of Aggregate Porosity**

Aggregates are far less porous in comparison to the cement-based paste and mortar. Their porosity ranges from less than 1% to about 5% by volume [25]. Some researchers [26] have reported the porosity of aggregate is generally less than 3%. The transport characteristic of concrete, however, could vary widely due to differences in pore size distribution and connectivity [27].

The transport properties aggregates are measurable and usually constant in time. Some of the aggregate pores are wholly within the solid (i.e., discontinuous), whereas others open onto the surface of the particle. Aggregates constitute about three-quarters of the volume of concrete, and their porosity contributes to the overall porosity of the concrete [28].

### **2.2.2 Effect of Cement Paste**

Cement paste is considered to comprise: unreacted cement, surface products such as C-S-H, pore products like CH, and capillary pores [23, 26, 29-30]. Surface products grow out from the unreacted cement particles and contain continuous gel pores; they are dense, and lack connected pores. Capillary pores are the remnant spaces that were once occupied by water and could not be filled by the hydration products. Immediately after mixing, the solid phases are discontinuous, and thus the freshly mixed paste is a viscous liquid. With random growth of the reaction products, the solid phase starts to build up. The formation of C-S-H as a surface product gradually makes the solid phase continuous. From the percolation threshold's standpoint, what is important for the transport processes is the point at which the solid phase grows enough to produce a discontinuous capillary pore system [23]. At this point, the capillary pores are trapped and cut off from the main pore network, thus reducing the fraction of pores that form a connected pathway for transport. This process is influenced by various factors, including water/cement ratio, degree of hydration, curing, and the use of SCM. An important consideration from the pore size standpoint is the existence of a critical pore size in the hydrated cement paste. It has been recognized that pores with a diameter above a certain size contribute significantly to moisture transport within the paste. This critical pore diameter has been observed to occur near the inflection point on the cumulative pore size distribution curve [25, 31]. Another characteristic that is important to moisture transport is the mean square diameter. In some studies [31], the transport coefficients has been related to the mean square pore diameter. Some have divided the capillary porosity into large and small components [32]. The reason for this division is the influence of the SCMs on the two types of porosities.

The formation of additional surface products, to improve the discontinuity of capillary pores, through the use of SCMs has been described to be very effective in improving the moisture impermeability of the paste [30].

Apart from capillary porosity, cement paste also contains smaller pores, called 'gel pores'. The size of gel pores is, however, fixed within a range by the structure of C-S-H, which remains constant. The diameter of a stable gel pore is assumed to be about 2 nm [33]. The reason is that cement hydration products can not precipitate in pores with diameters smaller than this size. Gel pores reside in hydration products that accumulate between the liquid phase and the anhydrous cement grains; they have major effect on the rate of hydration, but minor effects on transport processes involving the liquid phase. On the contrary, capillary porosity has major effects on transport processes but minor effects on the rate of hydration. If the capillary porosity drops below a critical value (percolation threshold), then the gel porosity starts to contribute towards moisture transport (in the form of diffusion) within the cementitious paste. In such a case, hybrid paths comprising isolated capillary pockets linked by gel pores dominate the transport process [23]. Moisture transport through this mechanism is quite slow when compared with the liquid phase transport through capillary pores.

In concrete, the unsaturated flow under isothermal conditions is macroscopically characterized by parameters such as 'hydraulic conductivity' ( $K$ ), and the 'total hydraulic potential' ( $\Phi$ ). At microscopic level, these parameters are dependent on the pore size distribution, pore structure, and pore connectivity and tortuosity [7-8, 17-18, 21, 34]. The large pores connected to the surface provide the easiest path for moisture transport into concrete. Their lower hydraulic potential (capillary suction) is

more than compensated for by their markedly lower resistance to flow when compared with smaller pores. However, the redistribution of water in concrete matrix is dominated by the smaller pores since their higher hydraulic potential draws water out of the larger pores. According to the classification of the International Union of Pure and Applied Chemistry (IUPAC), pores with size exceeding  $0.05\ \mu\text{m}$  or  $50\ \text{nm}$  ( $500\ \text{Å}$ ) are called macropores (capillary pores); those with size not exceeding  $2.0\ \text{nm}$  ( $20\ \text{Å}$ ) are called micropores; and the pores of intermediate size ( $20\ \text{nm} < \text{width} < 50\ \text{nm}$ ) are called mesopores [35]. Capillary pores have particularly significant detrimental effects on the strength and impermeability of concrete, whereas pores smaller than  $50\ \text{nm}$  tend to have significant effects on the dimensional movements (drying shrinkage and creep) of concrete [26]. It has been suggested that the pore size distribution rather than the total porosity is a more consequential measure of pore system characteristics in Portland cement concrete. Improvements in pore size distribution can bring about major gains in moisture resistance beside superior strength, durability, and dimensional stability of hydrated cement paste and concrete.

### **2.2.3 Effects of the Mortar and Concrete Microstructure**

Mortar and concrete are both considered composites comprising coarse or fine aggregates as inclusions in the cementitious matrix. Compared to paste which might have a porosity well in excess of 25% (depending on water/cement ratio), the effect of aggregate in concrete is such that it reduces the porosity of paste used for production of concrete [25]. For example, aggregate and paste with the above-mentioned range of porosities, when mixed to produce concrete, produce an end product with about 7% to 15% porosity by

volume. In spite of this, the permeability of mortar and concrete tends to be higher than that of a cementitious paste with similar water content and age [26-27]. The greater the size of aggregate, the greater is the permeability of concrete. While aggregates provide for longer and more tortuous transport paths in concrete, they also introduce the interfacial transition zone which, as described in the following section, facilitates moisture transport through concrete [28].

#### **2.2.4 Interfacial Transition Zone (ITZ)**

The microstructure of hydrated cement paste in the immediate vicinity of coarse aggregate particles differs from that of the bulk of cement paste. This zone, which has a thickness of about 50  $\mu\text{m}$ , is referred to as the interfacial transition zone (Figure 2.7). The main reason for the difference in the microstructure of ITZ and bulk phase is that, dry cement particles cannot pack closely against the large aggregate particles during mixing. This phenomena is referred to as the 'wall effect' [28, 36-37]. As a result, much less cement is present to hydrate in the ITZ to fill up the voids. Consequently, ITZ develops a higher porosity than the bulk of hydrated cement paste.

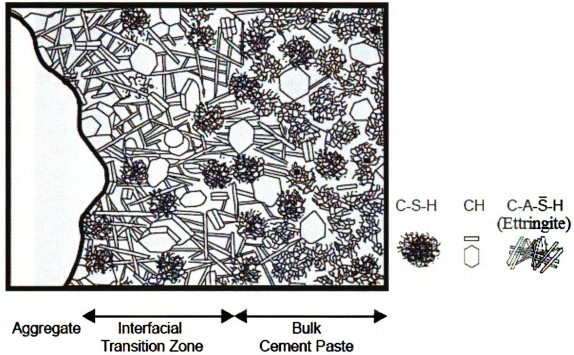


Figure 2. 7 Diagrammatic representation of ITZ [26]

In the microstructure of ITZ, the surface of aggregate is covered with a  $0.5\ \mu\text{m}$  thick layer of oriented CH; behind this layer is a layer of C-S-H of about same thickness. This composition is referred to as the duplex film. Further away from the aggregate is the main interface zone which is about  $50\ \mu\text{m}$  thick. This zone contains large crystals of CH but no unhydrated cement (Figure 2.8).

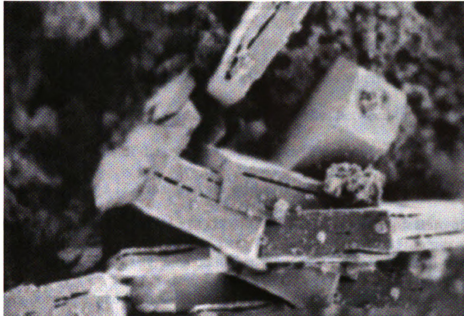


Figure 2. 8 SEM micrographs of calcium hydroxide [26]

The microstructure of the interfacial transition zone (ITZ) differs from that of the bulk cement paste partly due to the higher water/cement ratio of the ITZ. Some distinguishing features of ITZ are the higher content of large CH crystals and a relatively high porosity. In general, the larger the aggregate size, the higher would be the local water/cement ration of ITZ [26, 28]. ITZ reportedly forms an important fraction of the cement paste volume. About 20% of the paste is estimated to lie within the 20  $\mu\text{m}$  distance form the aggregate surfaces, and about 50% within the 50  $\mu\text{m}$  distance near the aggregate surfaces [23].

The porous nature of ITZ has also been attributed to the ‘one-sided growth effect’ [23]. In a capillary region located in the bulk paste, on average, the reactive growth occurs in all directions, since cement particles are originally located randomly and isotropically. In a similar region of capillary pore space located very near an aggregate surface, the reactive growth occurs only on the cement side and not on the aggregate side.

This effect results in a higher capillary porosity at the ITZ than the bulk of hydrated cement paste.

ITZ also experiences microcracking which develops when concrete is subjected to drying or thermal shrinkage as a result of the differences between the elastic moduli and dimensional movements of the paste and aggregates [26]. In the microstructure of mortar and concrete, it is the ITZ that plays a critical role in determining the bulk transport properties of concrete [23-24, 26, 28, 37-38]. Some distinguishing feature of ITZ, when compared with the bulk paste, include higher porosity, more pronounced microcracking, and larger pore size, and higher CH content. These features result in a significant rise in moisture transport within concrete [39]. It is due to the effect of ITZ that concrete, even when dense aggregates are used, offers far greater transport coefficients than corresponding cement pastes [26]. It has been reported that concrete can have up to 100 times the water permeability of the cement paste it is made of [24]. This can be rationalized by the presence of ITZ in concrete [23].

### **2.3 Microstructure of Recycled Aggregate Concrete**

The microstructure of recycled aggregate concrete differs from that of normal concrete because it has two interfacial transition zones (ITZs) in comparison with the one ITZ found in normal concrete [40-41]. The first ITZ in recycled aggregate concrete is between the original aggregate and the adhering (residual) mortar, and the second one occurs between the adhering (residual) mortar and the new mortar in the recycled aggregate concrete (Figure 2.9). It has been shown that the average residual mortar content (defined as the weight of residual mortar divided by the total weight of the recycled aggregate) is

between 23% and 41%. In one investigation [42], the weight of the residual mortar was found to exceed 50%. The porosity of recycled aggregate increases increasing percentage of the adhered mortar. As noted in Section 2.2.3, the old clinging mortar (with a strong presence of the old ITZ) plays a significant role in increasing the moisture absorption capacity of recycled aggregate concrete. Improvements in the clinging (residual) mortar constituent of recycled aggregate (including the old ITZ included in it) can bring about important gains in the moisture resistance and thus the dimensional stability and durability of recycled aggregate concrete [41].

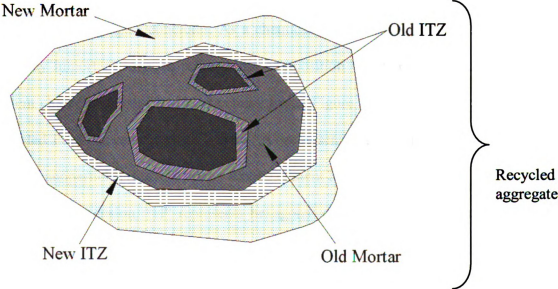


Figure 2.9 Two interfacial transition zones (ITZ) in recycled aggregate concrete

## **2.4 Improvement of the Moisture Barrier Attributes of Recycled and Normal Glass Concretes**

Traditional pozzolans such as coal fly ash, silica fume, and ground granulated blast furnace slag have been used to improve the strength and durability of normal and recycled aggregate concretes [26, 28, 36, 43-50]. The primary effect of the pozzolans on moisture transport characteristics is through refinement of the capillary pore size distribution, and increasing the discontinuity and partial filling of capillary pores. Several earlier studies [51-52] have shown that pastes containing mineral admixtures provide reduced total porosity and a finer pore structure due to pozzolanic reactions

This research employs milled waste glass to bring about improvements in normal and recycled aggregate concretes. As a chemically active ingredient, milled waste glass can play important roles in refining the composition of cement hydrates and the pore system characteristics of hydrated cement paste. Figure 2.10 shows the model of a well-hydrated Portland cement paste, where “A” represents aggregation of poorly crystalline C-S-H nanoparticles (the key binder among cement hydrates) with at least one nano-scale (<100 nm) dimension, “H” represents hexagonal crystalline products such as CH with inferior binding qualities, chemical stability and moisture resistance, and “C” represents capillary pores which form when the space originally occupied with water does not get completely filled with the hydration products of cement. These capillary pores range in size from 10 nm to 1  $\mu\text{m}$ ; in well-hydrated cement pastes with relatively low water/cement ratios, capillary pores tend to be less than 100 nm in size. Different phases in cement hydrates are not uniformly distributed, and are not uniform in size and morphology. These microstructural inhomogeneities can have considerable effects on

some key engineering characteristics which are governed by microstructural extremes and not the average microstructure.

Milled waste glass enters reactions with cement hydrates which can benefit the chemical composition and the pore size distribution of the hydrated cement paste in concrete. A key chemical reaction defining the hydration of Portland cement is between tricalcium silicate ( $C_3S$ ) and water (H), yielding calcium silicate hydrate (C-S-H) and calcium hydroxide (CH):



The chemical constituents of recycled glass (e.g., amorphous silica) would enter reactions involving the calcium hydroxide generated in normal hydration of cement to produce additional calcium silicate hydrate:



The chemical reactions of milled waste glass in concrete are lime-consuming; the conversion of CH to C-S-H benefits the moisture resistance and chemical stability of concrete. The C-S-H resulting from hydration of cement would partially fill the capillary pores (Figure 2.11), thereby refining the pore size distribution and lowering the interconnectivity of capillary pores (compare Figures 2.10 & 2.11), which greatly improve the moisture resistance, chemical stability and durability of concrete. It is important to note that reduction of glass size to micrometer scale increases the surface area and reactivity of glass; the chemical reaction potential of glass would thus be largely exhausted during the active period of cement hydration. A micro-scale manifestation of the conversion of CH to C-S-H as a result of the pozzolanic reaction of glass can be observed through the comparison of the Scanning Electron Microscope (SEM) imaged

presented in Section 2.6. These images point at the conversion of large crystals of CH to C-S-H, and production of a denser microstructure. These observations confirm the occurrence of the pozzolanic reaction of milled waste glass with cement hydration products.

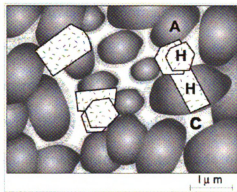


Figure 2.10 Model of hydrated cement

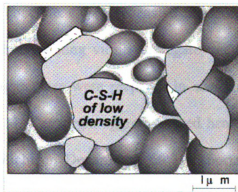


Figure 2.11 Model of hydrated cement / milled waste glass

Milled waste glass can have a particularly beneficial effect on the microstructure of recycled aggregate concrete. This is due to the strong presence of the old ITZ within cement hydrates clinging to recycled aggregates, which is highly porous and includes a relatively large concentration of calcium hydroxide. These conditions provide for pronounced pozzolanic reactions of milled waste glass, yielding beneficial effects by refining the capillary pores and converting CH to C-S-H. One can thus expect important gains in the structure and performance of the clinging mortar in recycled aggregates (which is key to improvement of the recycled aggregate quality for use in new concrete). These effects, confirmed in our experimental investigations presented in Chapter 3, point

at the enabling role of milled waste glass (as partial replacement for cement) towards value-added use of recycled aggregates in new concrete construction.

## **2.5 Materials and Experimental Methods**

In order to make a detailed investigation of the effects of milled waste glass on the microstructure of normal and recycled aggregate concrete, a comprehensive experimental work was carried out. Concrete mix designs incorporating virgin aggregate, recycled aggregate, and blends of virgin and recycled aggregates were prepared in accordance with the procedure outlined in ACI 211.1-91 [53]. The virgin aggregate used here was limestone conforming to Grade 6AA of the Michigan Department of Transportation (MDOT) standard specifications. Recycled aggregate was obtained from a local construction and demolition (C&D) waste recycling facility. Two different water/cementitious (w/cm) ratios were considered. Each mix design was produced with either 100% ordinary Portland cement or with ordinary Portland cement: milled waste glass at 80: 20 weight ratio. Normal sand satisfying the '2NS' grade of the MDOT standard specification was used in all concrete materials. Water-reducing and air-entraining admixtures were also used in all mixtures. The air entraining agent (surfactant based admixture with brand name of CATEXOL™ A.E. 260, manufactured by Axim) was used at a rate of 2.43 ml/kg (1.1 ml/lb) of the cementitious material in all mixes. The water reducing agent (non-ionic surfactant based admixture known by brand name CATEXOL™ A.E. 260, manufactured by Axim) was used at a rate of 2.43 ml/kg (1.1 ml/lb) in low w/cm mixes, and at a rate of 1.98 ml/kg (0.90 ml/lb) in high w/cm mixes. Table 2.1 shows the physical properties of the milled waste glass used in all mix designs,

and Table 2.2 shows the physical properties of the virgin and recycled coarse aggregates and well as the sand used in our experimental work. Table 2.3 introduces all the mix designs used in our investigation. For comparison purposes, six mixtures, three with Class-F and three with Class-C fly as replacement for 20% by weight of cement, were also prepared with virgin aggregate, recycled aggregate, and the blend of the two (as shown in Table 2.4).

Table 2. 1 Physical properties of milled waste glass

% Passing # 325 mesh	97%
Specific gravity	2.46 gm/cc (153.57 lb/ft <sup>3</sup> )
Median particle size	13 μm
Moisture content	0.1%
Brightness	80%
Specific surface area	4,925 cm <sup>2</sup> /gm (70.33 in <sup>2</sup> / lb)
Loss on ignition	0.4%

Table 2. 2 Physical properties of aggregates

Aggregate Type	Dry Density kg/m <sup>3</sup> (lb/ft <sup>3</sup> )	Bulk specific gravity	Bulk specific gravity (SSD)	Absorption (%)	Loss on abrasion (%)
Virgin	1743 (108.84)	2.57	2.65	2.28	22.8
Recycled	1446 (90.28)	2.30	2.40	4.35	31.6
Sand	2.86 (F.M.)	2.65	-	0.97	-

**Table 2.3 Mix Designs**

S/No.	Mix Designation	Virgin Coarse Aggregate kg/m <sup>3</sup> (lb/ft <sup>3</sup> )	Recycled Coarse Aggregate kg/m <sup>3</sup> (lb/ft <sup>3</sup> )	Fine Aggregate kg/m <sup>3</sup> (lb/ft <sup>3</sup> )	W / Cm ratio	Cement Content kg/m <sup>3</sup> (lb/ft <sup>3</sup> )	Water Content kg/m <sup>3</sup> (lb/ft <sup>3</sup> )	Milled Waste Glass* kg/m <sup>3</sup> (lb/ft <sup>3</sup> )
1	CIW	951.49 (59.4)	-	650.83 (40.63)	0.36	468.38 (29.24)	168.83 (10.54)	-
2	RIW	-	797.34 (49.78)	650.83 (40.63)	0.36	468.38 (29.24)	168.83 (10.54)	-
3	BIW	475.75 (29.7)	398.54 (24.88)	650.83 (40.63)	0.36	468.38 (29.24)	168.83 (10.54)	-
4	CGIW	951.49 (59.4)	-	650.83 (40.63)	0.36	374.67 (23.39)	168.83 (10.54)	93.71 (5.85)
5	RGIW	-	797.34 (49.78)	650.83 (40.63)	0.36	374.67 (23.39)	168.83 (10.54)	93.71 (5.85)
6	BGIW	475.75 (29.7)	398.54 (24.88)	650.83 (40.63)	0.36	374.67 (23.39)	168.83 (10.54)	93.71 (5.85)
7	ChW	951.49 (59.4)	-	650.83 (40.63)	0.45	468.38 (29.24)	211.44 (13.20)	-
8	RhW	-	797.34 (49.78)	650.83 (40.63)	0.45	468.38 (29.24)	211.44 (13.20)	-
9	BhW	475.75 (29.7)	398.54 (24.88)	650.83 (40.63)	0.45	468.38 (29.24)	211.44 (13.20)	-
10	CGhW	951.49 (59.4)	-	650.83 (40.63)	0.45	374.67 (23.39)	211.44 (13.20)	93.71 (5.85)
11	RghW	-	797.34 (49.78)	650.83 (40.63)	0.45	374.67 (23.39)	211.44 (13.20)	93.71 (5.85)
12	BGhW	475.75 (29.7)	398.54 (24.88)	650.83 (40.63)	0.45	374.67 (23.39)	211.44 (13.20)	93.71 (5.85)

C = Normal (control); R = Recycled aggregate; B = Blended aggregate; l = low water; h = high water; G = glass; \* = 20% of cement by weight

Table 2.4 Fly Ash Concrete Mix Designs

S/No.	Mix Designation	Virgin Coarse Aggregate kg/m <sup>3</sup> (lb/ft <sup>3</sup> )	Recycled Coarse Aggregate kg/m <sup>3</sup> (lb/ft <sup>3</sup> )	Fine Aggregate kg/m <sup>3</sup> (lb/ft <sup>3</sup> )	W / Cm ratio	Cement Content kg/m <sup>3</sup> (lb/ft <sup>3</sup> )	Water Content kg/m <sup>3</sup> (lb/ft <sup>3</sup> )	Fly Ash* kg/m <sup>3</sup> (lb/ft <sup>3</sup> )
1	CFIW	951.49 (59.4)	-	650.83 (40.63)	0.36	468.38 (29.24)	168.83 (10.54)	-
2	RFIW	-	797.34 (49.78)	650.83 (40.63)	0.36	468.38 (29.24)	168.83 (10.54)	-
3	BFIW	475.75 (29.7)	398.54 (24.88)	650.83 (40.63)	0.36	468.38 (29.24)	168.83 (10.54)	-
4	CSIW	951.49 (59.4)	-	650.83 (40.63)	0.36	374.67 (23.39)	168.83 (10.54)	93.71 (5.85)
5	RSIW	-	797.34 (49.78)	650.83 (40.63)	0.36	374.67 (23.39)	168.83 (10.54)	93.71 (5.85)
6	BSIW	475.75 (29.7)	398.54 (24.88)	650.83 (40.63)	0.36	374.67 (23.39)	168.83 (10.54)	93.71 (5.85)

C = Normal (control); R = Recycled aggregate; B = Blended aggregate; l = low water; h = high water; G = glass; F = class-F fly ash  
 S = Class-C fly ash; \* = 20% of cement by weight

Samples were cast in 200 mm (8 in.) x 100 mm (4 in.) cylindrical molds in accordance with ASTM C 192 [53] for each mix design, and were subjected to limewater curing over 28 days. Concrete disc specimens with thickness (height) of 50 mm (2 in.) were prepared from the inside of the cylinders to avoid any peculiarities of the top and bottom surfaces [54]. Sorption tests were carried out in accordance with ASTM C 1585 -04 [55]. Specimens were subjected to two different conditioning methods, referred to as oven drying and air drying. In oven drying, the disc specimens were dried in oven at 50° C (122° F) until a constant mass was achieved. This required 23 days of continuous oven drying. In air drying, specimens were dried in the laboratory environment at 20°C (68°F) and 28% RH over a period of 7 months until constant mass was achieved. Specimens were sealed on sides and top with epoxy to produce one-dimensional sorption during the test. Each mix design had three replicate specimens. In order to carry out two-dimensional sorption tests, 100 mm (4 in.) x 100 mm (4 in.) square specimens with 50 mm (2 in.) thickness were used. Two sides and top of the specimens were sealed with epoxy to cause two dimensional sorption upon exposure to water. Figures 2.12 and 2.13 show views of some of the 1-D and 2-D sorption test specimens before epoxy coating and inside the test setup, respectively.



Figure 2. 12 Pictures of 1-D and 2-D sorption test specimens



Figure 2. 13 1-D and 2-D sorption test specimens inside the test pan

## 2.6 Experimental Results and Discussion

Sorption is measured as the change in mass divided by the product of the cross-sectional area of the test specimens and the density of water which is taken equal to  $0.001 \text{ gm} / \text{mm}^3$  ( $62.4 \text{ lb/ft}^3$ ) [55]. Neglecting the temperature dependence of the water density, the unit of the sorption reduces to that of length (mm, inch).

$$i = \frac{\Delta m}{a \times \rho} \quad (2.24)$$

where:

$i$  = sorption in mm (in.)

$\Delta m$  = change in mass of specimen in gm (lb)

$a$  = cross-sectional area of the specimen exposed to water in  $\text{m}^2$  ( $\text{in.}^2$ )

$\rho$  = density of water in  $\text{g/mm}^3$  ( $\text{lb/ft}^3$ )

The value of “ $i$ ” within the initial six hours is termed the “initial sorption” with corresponding value of “ $S$ ” in the units of  $\text{mm/sec}^{1/2}$  ( $\text{inch/sec}^{1/2}$ ) in equation 2.16 called the “initial sorptivity” or the “initial rate of absorption”. Similarly, the value of “ $i$ ” after the initial six hours of exposure of specimen to water is called “secondary sorption” with the corresponding “ $S$ ” referred to as “secondary sorptivity” or “secondary rate of sorptivity”. The initial sorptivity and the secondary sorptivity are the slopes of “ $i$ ” vs.  $\text{time}^{1/2}$  plot during the corresponding times of exposure.

## **2.6.1 1-D Sorptivity of Normal and Recycled Aggregate Concretes with and without Milled Waste Glass**

### **2.6.1.1 Oven Dried Specimens**

Figure 2.14 shows the,  $i$  vs. time<sup>1/2</sup> plots, which are herein referred to as sorption plot of oven-dried, low-water-content concrete mixes for 1-d sorption. Figure 2.15 shows the corresponding sorption plot of the high-water-content, oven-dried specimens. As can be seen in these plots, partial replacement of cement with milled waste glass results in significant reduction of water sorption of the concretes produced with the three types of aggregates (virgin, recycled, and blended). Tables 2.5 and 2.6 show the initial and secondary rates of water absorption for low-water and high-water concrete mixtures, respectively. Tables 2.7 and 2.8 show the percent reduction in the initial and final rates of absorption, respectively, as a result of incorporating milled waste glass as partial replacement of cement. Analysis of variance (ANOVA) of the test results showed statistically significant effects (at 95% confidence level) of glass of the (initial and final) rates of absorption for the low- and high-water-concrete mixtures.

Figure 2.16 shows the sorption plots of Class-F and Class-C fly ash concrete materials made with the three types of aggregate. As can be seen in Figure 2.17, milled waste glass has a better effect on the 8-day cumulative water sorption than that of Class-F and class-C fly ashes. As shown in Table 2.9, the cumulative sorption of low-water-content concrete mixtures is reduced by up to 27% with introduction of glass; for the high-water-content mixes, the corresponding reduction in sorption is as much as 33%. The effects of milled waste glass on 8-day cumulative water sorption was found to be statistically significant at 95% level of confidence.

While partial replacement of cement with milled waste glass results in reduction of the rate of absorption and cumulative sorption of concrete mixes of made with the three categories of aggregate (virgin, recycled, and blend), concrete specimens with recycled aggregate appear to benefit the most from introduction of milled waste glass. They experience the highest reduction in cumulative sorption and the rate absorption of water. This could be attributed to the availability of more CH at the old ITZ of recycled aggregate to undergo pozzolanic reaction, producing more C-S-H and hence greater pore refinement effects.

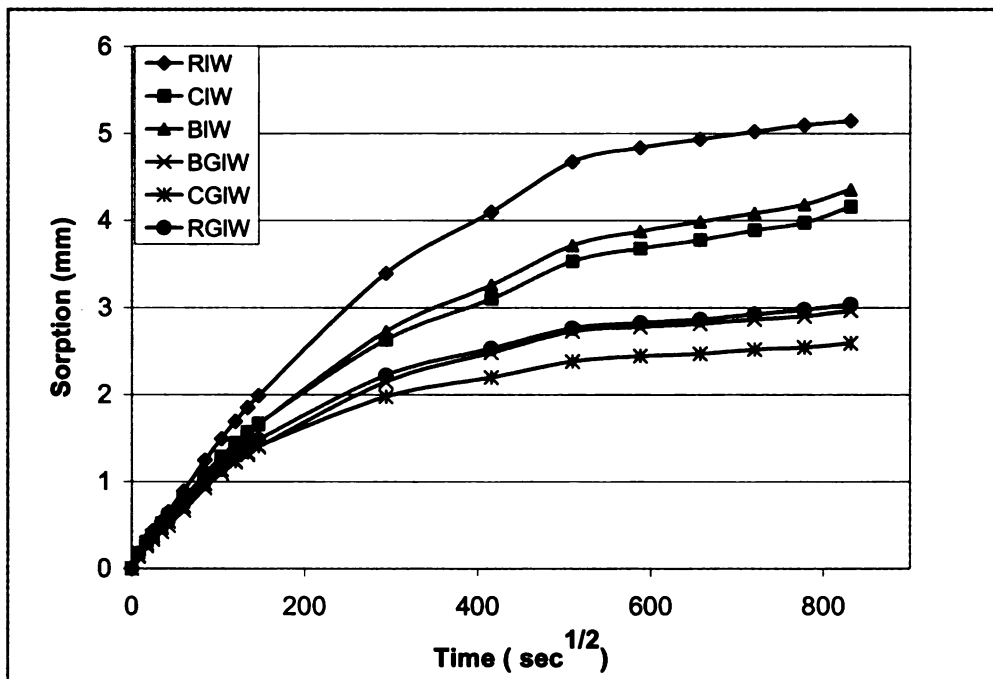


Figure 2. 14 Sorption plot of low-water-content, oven-dried mixes with and without milled waste glass

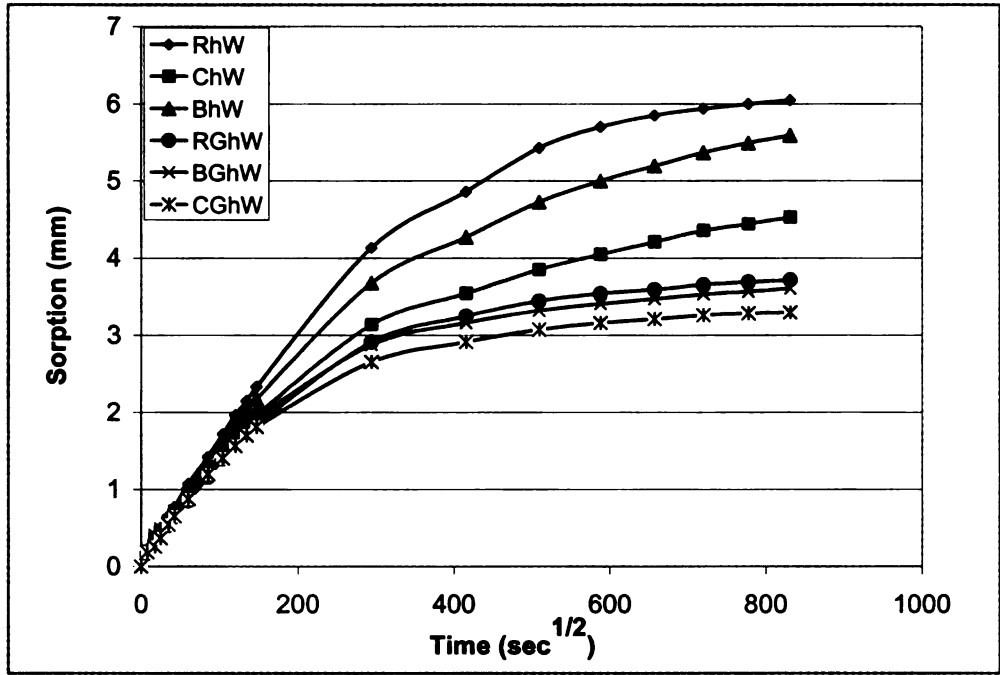


Figure 2. 15 Sorption plot of oven dried high-water-content, mixes with and without milled waste glass

Table 2. 5 Initial and final rates of absorption of oven dried low-water-content, mixes with and without milled waste glass

Mix Design	Initial rate of absorption	Secondary rate of absorption
	(mm / $\sqrt{\text{sec}}$ ) $\times 10^{-3}$ (inch / $\sqrt{\text{sec}}$ ) $\times 10^{-4}$	(mm / $\sqrt{\text{sec}}$ ) $\times 10^{-3}$ (inch / $\sqrt{\text{sec}}$ ) $\times 10^{-4}$
CIW	10.5 (4.13)	2.75 (1.08)
RIW	13.1 (5.16)	3.10 (1.22)
BIW	10.7 (4.21)	2.90 (1.14)
CGIW	8.8 (3.46)	1.33 (0.52)
RGIW	9.1 (3.58)	1.45 (0.57)
BGIW	9.0 (3.54)	1.40 (0.55)

**Table 2. 6 Initial and final rate of absorption of oven dried high water content mixes with and without glass**

Mix Design	Initial rate of absorption	Secondary rate of absorption
	(mm / $\sqrt{\text{sec}}$ ) $\times 10^{-3}$ (inch / $\sqrt{\text{sec}}$ ) $\times 10^{-4}$	(mm / $\sqrt{\text{sec}}$ ) $\times 10^{-3}$ (inch / $\sqrt{\text{sec}}$ ) $\times 10^{-4}$
ChW	12.4 (4.88)	2.6 (1.02)
RhW	15.0 (5.90)	3.5 (1.37)
BhW	14.2 (5.59)	3.0 (1.18)
CGhW	11.4 (4.48)	1.3 (0.51)
RGhW	12.0 (4.72)	1.5 (0.59)
BGhW	11.7 (4.60)	1.4 (0.55)

**Table 2. 7 Percent reduction in the initial rate of absorption due to glass inclusion for the oven-dried specimens of the three different coarse aggregate concrete mixes**

Mix Design	% Reduction in initial sorption due to waste glass inclusion	
	Low-Water Mixes	High-Water Mixes
Virgin Aggregate Mixes	16	8
Recycled Aggregate Mixes	31	20
Blended Aggregate Mixes	16	17

**Table 2. 8 Percent reduction in secondary rate of absorption due to glass inclusion for the oven-dried specimens of the three different coarse aggregate concrete mixes**

Mix Design	% Reduction in secondary sorption due to waste glass inclusion	
	Low Water Mixes	High Water Mixes
Virgin Aggregate Mixes	52	50
Recycled Aggregate Mixes	54	57
Blended Aggregate Mixes	52	53

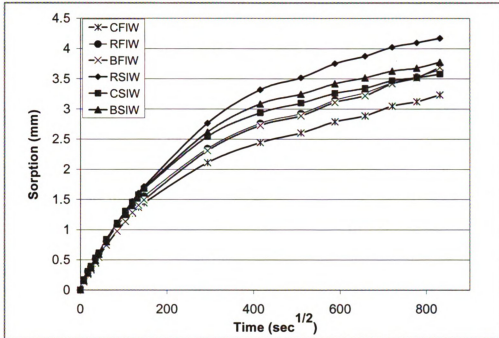


Figure 2.16 Sorption plots of concrete mixes incorporating class-F and C fly ashes

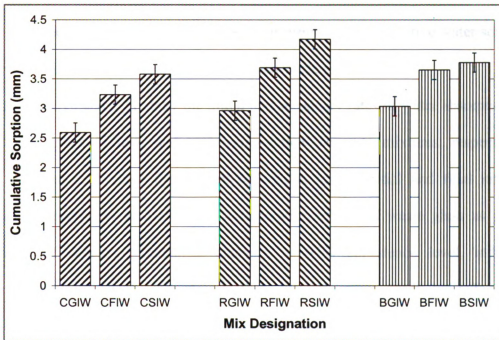


Figure 2.17 Comparison of the milled waste glass, class-F fly ash, and class-C fly ash contributions towards reduction of the 8-day cumulative sorption of oven dried specimens (means and standard errors)

**Table 2. 9** Percent reduction in cumulative sorption due to milled waste glass inclusion for the three different coarse aggregate concrete mixes (oven-dried)

Mix Design	% Reduction in cumulative sorption due to glass inclusion	
	Low Water	High Water
Virgin Aggregate Mixes	26	31
Recycled Aggregate Mixes	27	33
Blended Aggregate Mixes	26	33

### **2.6.1.2 Air-Dried Specimens**

Results of the 1-D sorption tests on air-dried specimens of low- and high-water-content concrete mixes are shown in Figures 2.18 and 2.19, respectively. The test results on air-dried specimens exhibit similar trends as those on oven-dried specimens; that is, concrete mixes with milled waste glass as partial replacement of cement show significant reductions in the initial and secondary rates of absorption and cumulative water sorption when compared with similar mixes without milled waste glass.

Tables 2.10 and 2.11 show the initial and secondary rates of water absorption for air-dried specimens of low- and high-water-content concrete mixtures, respectively. Tables 2.12 and 2.13 show the percent reductions in the initial and final rates of absorption, respectively, as a result of incorporation of milled waste glass as partial replacement of cement. Statistical analysis, at 95% confidence level, indicated significant effects of milled waste glass on these concrete mixes, producing reduced the (initial and final) rates of for the low- and high-water-content concrete mix designs.

Figure 2.20 shows the sorption plots of concretes incorporating Class-F and Class-C fly ashes, made with three different aggregate types, and tested in air-dried

condition. Figure 2.21 shows the strong effect of the milled waste glass on the 8-day cumulative water sorption of air-dried specimens, by comparing sorption performance of concrete mixes with milled waste glass, Class-F fly ash, and Class-C fly ashes. Similar to the oven-dried specimens, milled waste glass performs better than class-F and class-C fly ash. As shown in Table 2.14, the most significant reduction in cumulative sorption with introduction of milled waste glass in low-water-content mixes is for recycled aggregate concrete at 43%. Similarly, among the high-water-content mixes the highest sorption reduction with introduction of milled waste glass is 39%, again recorded for the recycled aggregate concrete mix. Statistical analysis, at 95% confidence level, confirmed the statistically significant effect of milled waste glass on the 8-day cumulative water sorption. As was the case with oven-dried specimens, the air-dried specimens of recycled aggregate concrete experienced the most significant effect of milled waste glass as far as the reduction of absorption rate and cumulative sorption are concerned.

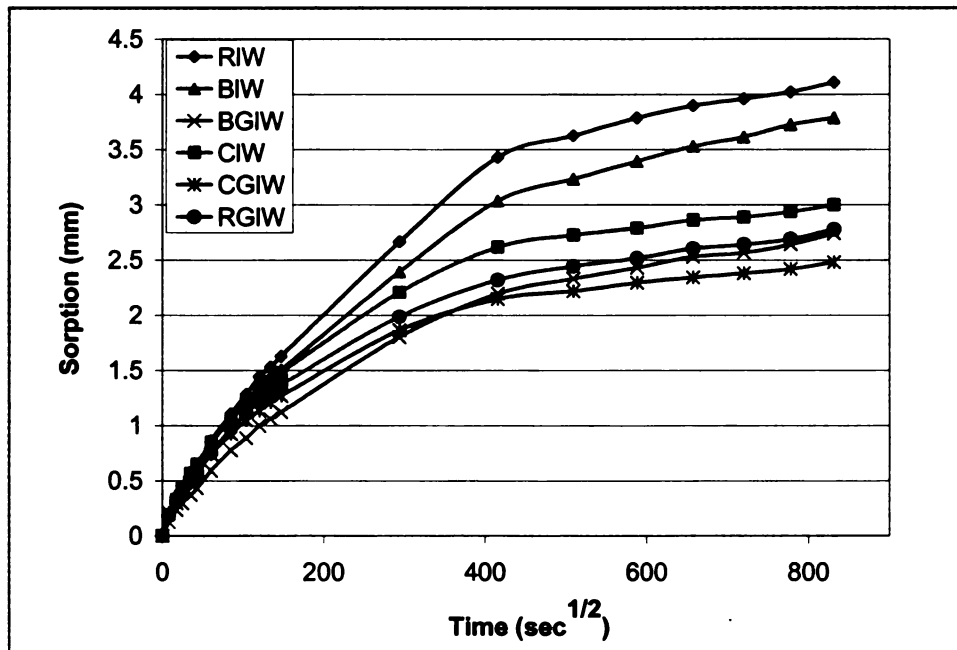
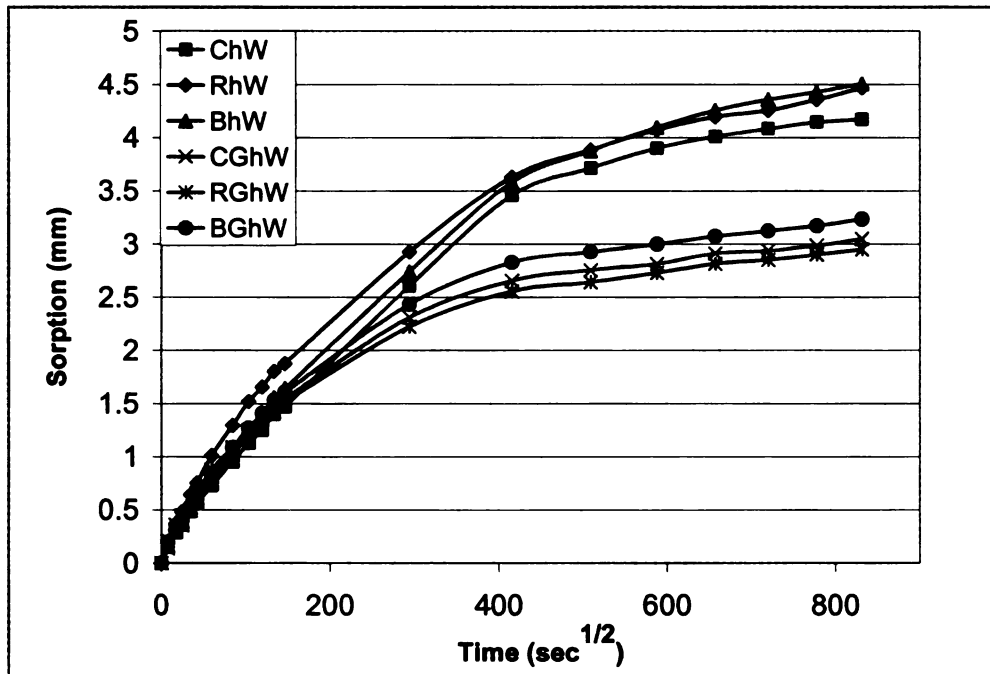


Figure 2. 18 Sorption plot of low-water-content, air-dried mixes with and without milled waste glass



**Figure 2. 19** Sorption plot of high-water-content, air-dried mixes with and without milled waste glass

**Table 2. 10** Initial and final rates of absorption of low-water-content, air-dried mixes with and without milled waste glass

Mix Design	Initial rate of absorption		Secondary rate of absorption	
	(mm / $\sqrt{\text{sec}}$ ) $\times 10^{-3}$	(inch / $\sqrt{\text{sec}}$ ) $\times 10^{-4}$	(mm / $\sqrt{\text{sec}}$ ) $\times 10^{-3}$	(inch / $\sqrt{\text{sec}}$ ) $\times 10^{-4}$
CIW	9.0	(3.54)	2.1	(0.83)
RIW	10.1	(3.98)	2.4	(0.94)
BIW	9.5	(3.74)	2.1	(0.83)
CGIW	7.6	(2.99)	1.30	(0.51)
RGIW	8.4	(3.30)	1.35	(0.53)
BGIW	8.2	(3.23)	1.32	(0.52)

**Table 2. 11 Initial and final rates of absorption of high-water-content, air-dried mixes with and without milled waste glass**

Mix Design	Initial rate of absorption	Secondary rate of absorption
	(mm / $\sqrt{\text{sec}}$ ) $\times 10^{-3}$ (inch / $\sqrt{\text{sec}}$ ) $\times 10^{-4}$	(mm / $\sqrt{\text{sec}}$ ) $\times 10^{-3}$ (inch / $\sqrt{\text{sec}}$ ) $\times 10^{-4}$
ChW	9.80 (3.86)	2.6 (1.02)
RhW	11.8 (4.65)	3.0 (1.18)
BhW	10.4 (4.09)	2.7 (1.06)
CGhW	9.20 (3.62)	1.26 (0.49)
RGhW	10.1 (3.98)	1.37 (0.54)
BGhW	9.10 (3.58)	1.33 (0.52)

**Table 2. 12 Percent reduction in the initial rate of absorption due to introduction of milled waste glass for air-dried specimens of the three different coarse aggregate concrete mixes**

Mix Design	% Reduction in initial sorption due to waste glass inclusion	
	Low Water Mixes	High Water Mixes
Control	15	6
Recycled	17	14
Blended	13	12

**Table 2. 13 Percent reduction in the secondary rate of absorption due to glass inclusion for the air-dried specimens of the three different coarse aggregate concrete mixes**

Mix Design	% Reduction in secondary sorption due to glass inclusion	
	Low Water Mixes	High Water Mixes
Control	38	51
Recycled	44	54
Blended	37	51

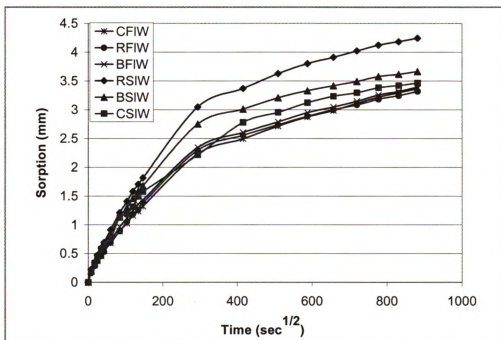


Figure 2.20 Sorption plots of air-dried specimens of concrete mixes incorporating Class-F and Class-C fly ashes

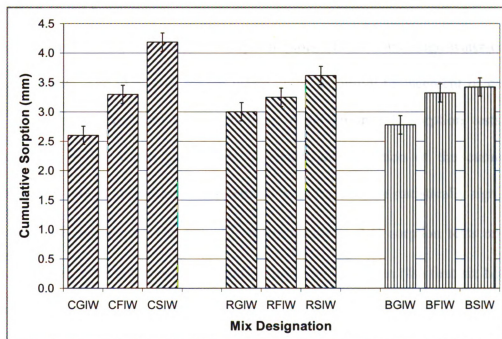


Figure 2.21 Comparison of milled waste glass, class-F and class-C fly ash towards reduction of 8 days cumulative sorption of air dried specimens (means and standard errors)

Table 2. 14 Percent reduction in cumulative sorption due to milled waste glass inclusion for the three different coarse aggregate concrete mixes (air-dried specimens)

Mix Design	% Reduction in cumulative sorption due to waste glass inclusion	
	Low Water	High Water
Virgin Aggregate Mixes	38	27
Recycled Aggregate Mixes	43	39
Blended Aggregate Mixes	30	36

## 2.6.2 2-D Sorptivity of Normal and Recycled Aggregate Concretes with and without Milled Waste Glass

### 2.6.2.1 Oven Dried Specimens

Figures 2.22 and 2.23 show the 2-D sorption plots of low- and high-water-content concrete mixtures. The effects of milled waste glass, as partial replacement of cement, follow general trends that are similar to those observed in 1-D sorption tests. The introduction of milled waste glass leads to significant reduction of the cumulative sorption and the rate of absorption. These effects were found to be statistically significant at 95% level of confidence. The  $i$  vs.  $t^{1/2}$  relationships in 2-D sorption tests on most concrete mixtures were not linear in the initial sorptivity time span (the first six hours of exposure). Figure 2.24 compares the 8-days cumulative sorptions of concrete mixtures with milled glass and fly ash used as partial replacement for cement (with the three aggregate categories of virgin, recycled, and blend). Again, the trends are very similar to those in 1-D sorption tests; milled waste glass produces superior results when compared

with Class-F and Class-C fly ash (as partial replacement for cement). When compared with the (Class-C) fly ash concrete mix (with recycled aggregate), the milled waste glass concrete mix (with recycled aggregate) showed 25% reduction in 8-day cumulative sorption. The corresponding reduction in the case of mixes with virgin aggregate was 24%. When compared with the (Class-F) fly ash concrete mix (with recycled aggregate), the milled waste glass concrete mix (with recycled aggregate) showed 8% reduction in 8-day cumulative sorption.

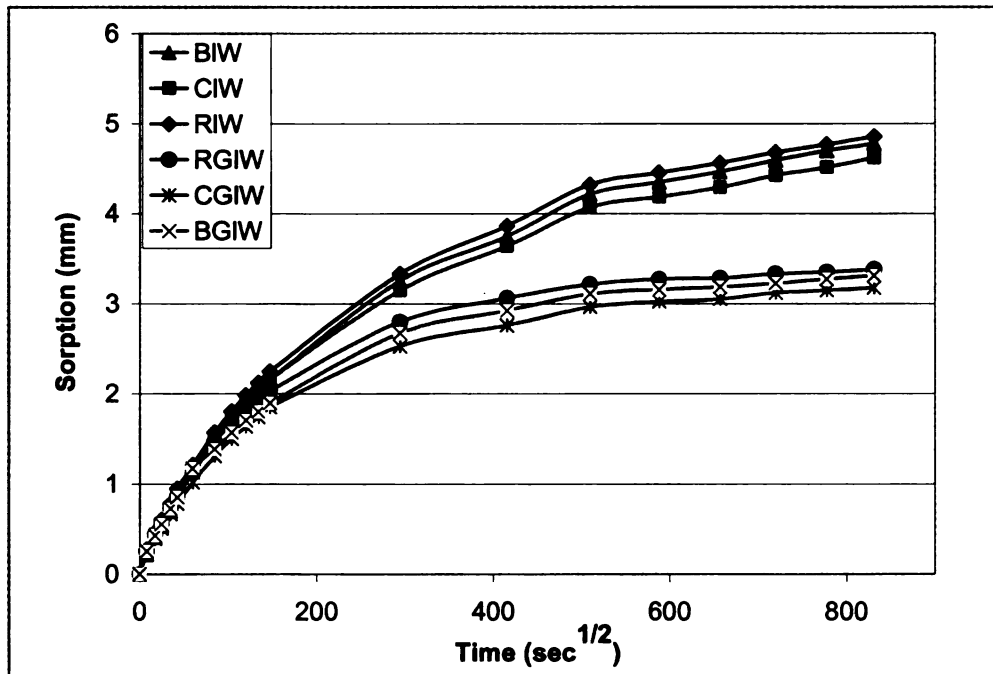


Figure 2. 22 2-D sorption plot of oven-dried, low-water-content mixtures with and without milled glass

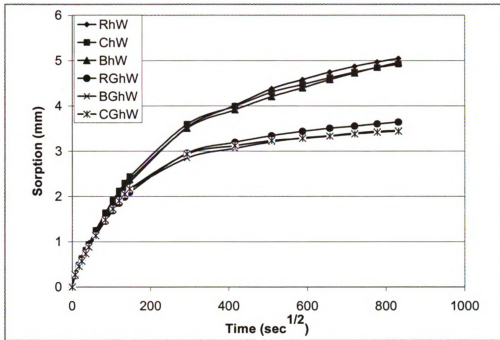


Figure 2.23 2-D sorption plot of oven-dried, high-water-content mixtures with and without milled glass

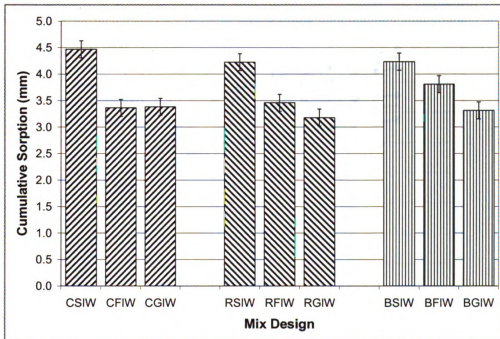


Figure 2.24 Comparison of the effects of milled waste glass, Class-F fly ash and Class-C fly on 2-D cumulative sorption of oven-dried concrete specimens (means and standard errors)

### 2.6.2.2 Air Dried Specimens

Figures 2.25 and 2.26 show the sorption plots of low- and high-water-content concrete mixtures, respectively, for the concrete materials considered in the previous section. Again, concrete mixtures with milled waste glass used as partial replacement for cement are observed to exhibit the best sorption resistance. Figure 2.27 compares the 8-day cumulative sorption of concrete materials with milled waste glass, class-F fly ash and Class-C fly ash used as partial replacement for cement. When compared with the (Class-C) fly ash concrete mix (with virgin aggregate), the milled waste glass concrete mix (with virgin aggregate) showed 22% reduction in 8-day cumulative sorption. When compared with the (Class-F) fly ash concrete mix (with virgin aggregate), the milled waste glass concrete mix (with virgin aggregate) showed 8% reduction in 8-day cumulative sorption.

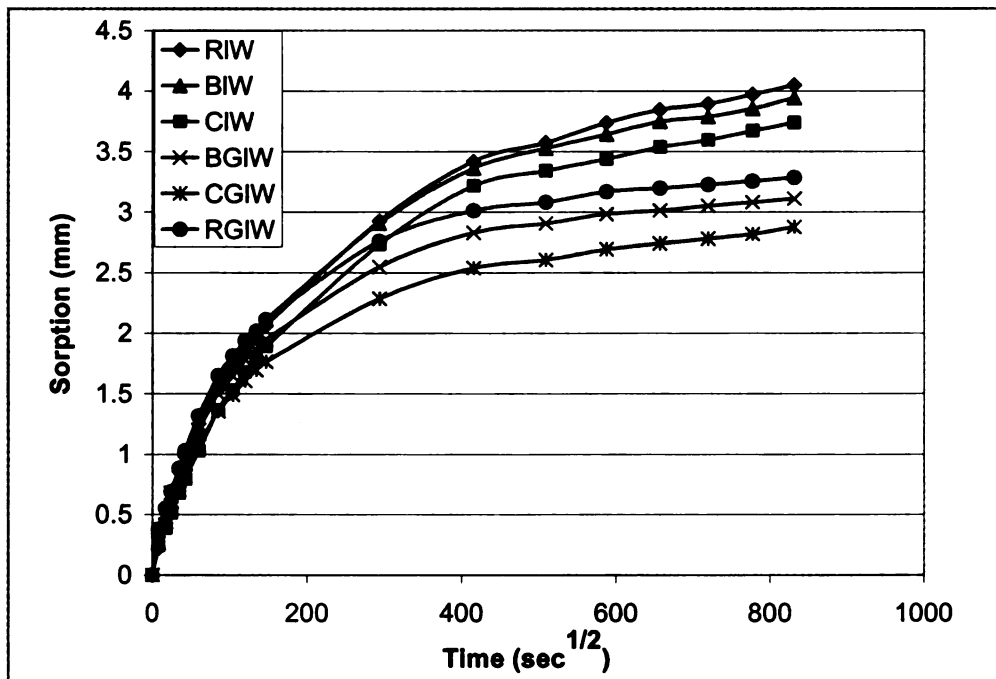


Figure 2. 25 2-D sorption plot of air-dried, low-water-content mixtures with and without milled waste glass

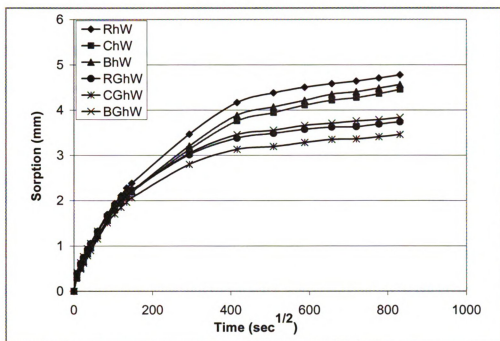


Figure 2.26 2-D sorption plot of air-dried, high-water-content mixtures with and without milled glass

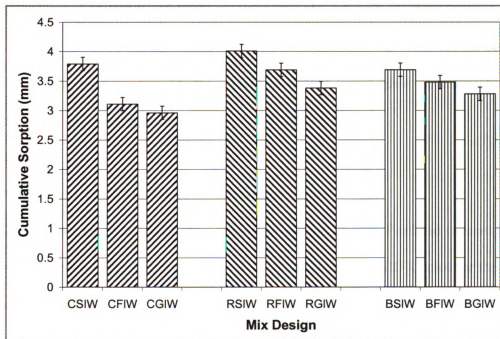


Figure 2.27 2-D cumulative (8-day) sorptions of air-dried milled waste glass, Class-F fly ash and Class-C fly concrete materials (means and standard errors)

### **2.6.3 SEM and EDX Analyses of Hydrated Cementitious Paste, Mortar and Concrete with and without Milled Waste Glass**

Scanning electron microscopy (SEM) and energy dispersive X-ray spectroscopy (EDX) are powerful tools for investigating the structure and composition of cement-based materials [56]. These techniques have been successfully applied to cement powders, hydrated cement pastes and concrete [57-59]. SEM and EDX analyses can provide insight into the pore structure, ITZ, microcracking, and composition of concrete.

SEM and EDX analyses were conducted on cement paste and mortar mixtures introduced in Chapter 4 (Tables 4.3 and 4.4) with and without the addition of milled waste glass as partial replacement for cement. Concrete materials introduced in Table 2.3 were also subjected to SEM and EDX analyses in order to evaluate the microstructural changes brought about by incorporation of milled glass as partial replacement for cement. The focus of this analysis was on the effects of milled waste glass on microstructure densification, reduction in porosity, and the ITZ structure.

#### **2.6.3.1 SEM and EDX Analyses of Cementitious Pastes**

Figure 2.28 shows an SEM image of a fractured surface of pure Portland cement paste, and Figure 2.29 shows the energy dispersive X-ray spectroscopy (EDX) plot for the same location. SEM images of the fractured surface of the cementitious paste with milled waste glass replacing 20% and 40% of are shown in Figures 2.30 and 2.31, respectively. Figure 2.32 shows the EDX plot of the cement paste with milled waste glass used as replacement for 20% of cement taken at the location of Figure of 2.30.

The SEM micrograph of pure cement paste (Figure 2.28) points at a strong presence of C-S-H fibrillar structures. Some ettringite needles can also be detected. The SEM micrograph of cement paste with milled waste glass used as replacement for cement 20% of cement (Figure 2.30) shows a uniform, dense microstructure. The SEM micrograph of Figure 2.31 points at a porous structure developed when 40% of cement is replaced with milled waste glass. The C-S-H globules are somewhat localized (probably around the glass micro-particles); the relatively high porosity of this system indicates that 40% cement replacement with milled waste glass is excessive. The structure of C-S-H formed by pozzolanic reaction (Figure 2.30) seems to be different from that formed by normal hydration of cement paste (Figure 2.28).

A comparison of the EDX plots of pure cement paste (Figure 2.29) and that of the cementitious paste containing milled waste glass as replacement for 20% of cement (Figure 2.32) points at a significant difference in silica (Si) peaks. While the 'Si' peak has about 1300 compositional counts in pure cement paste, the corresponding peak in cementitious paste with milled waste glass has about 3500 compositional counts which is indicative of a silica-rich microstructure resulting from the addition of milled waste glass. The Ca/Si ratio (C/S ratio) of 3.54 observed in pure cement paste dropped to 1.5 in the cementitious paste incorporating milled waste glass as replacement for 20% of cement. The drop in C/S ratio provides support for the occurrence of pozzolanic reactions in the presence of milled waste glass.

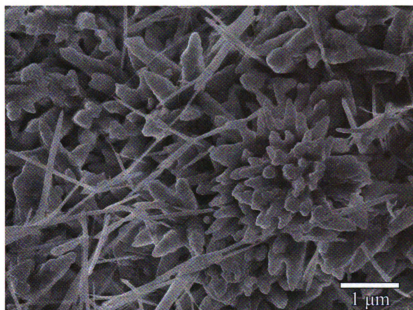


Figure 2. 28 SEM image of the fractured surface of pure cement paste

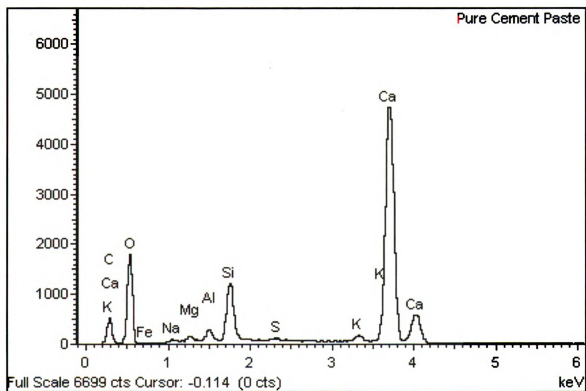


Figure 2. 29 EDX spectrum of the of the pure cement paste at the location of Figure 2.28

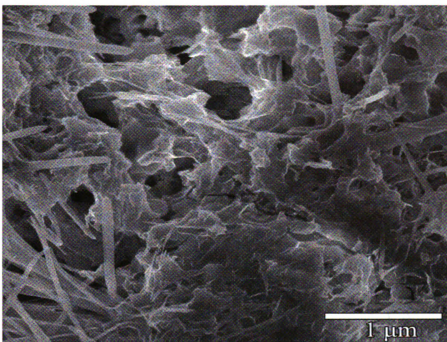


Figure 2. 30 SEM image of the fractured surface of cementitious paste incorporating milled waste glass as replacement for 20% of cement

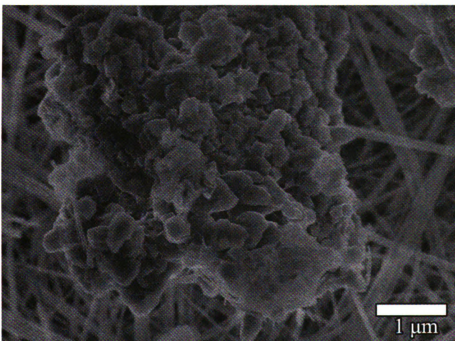


Figure 2. 31 SEM image of the fractured surface of cementitious paste incorporating milled waste glass as replacement for 40% of cement

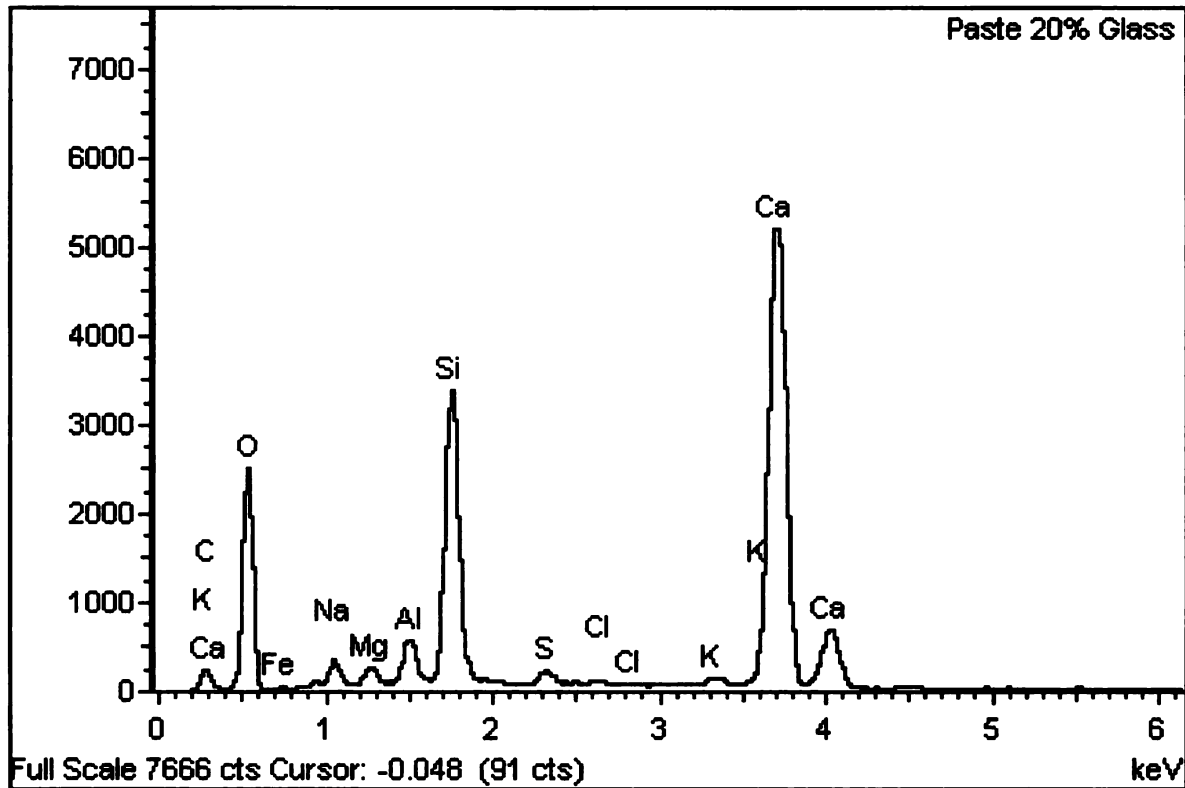


Figure 2. 32 EDX spectrum of the of the cement paste containing milled waste glass as replacement for 20% of cement at the location of Figure 2.30

### 2.6.3.2 SEM and EDX Analyses of Cementitious Mortars

Figure 2.33 shows an SEM image of the fractured surface of pure cement mortar made without milled waste glass (the SEM focuses on the cement paste constituent of the mortar). The SEM image of Figure 2.33 points at a heterogeneous structure. Figure 2.34 shows the microstructure of the cementitious mortar produced with milled waste glass as replacement for 20% of cement. As was the case in cementitious paste, the pozzolanic reaction of milled waste glass with cement hydrates forms a dense, homogeneous structure. The honeycombed or reticular network structure of the hydrated cement compounds indicate the presence of Type-II C-S-H [56]. Figure 2.35 shows an SEM image of the cement paste constituent of the mortar made without milled waste glass, and Figure 2.36 shows the EDX spectrum produced at the location of Figure 2.35. Figure

2.37 shows an SEM image of the cement paste constituent of the mortar made with milled waste glass used as replacement for 40% of cement, and Figure 2.38 shows the EDX spectrum produced at the location of Figure 2.37. The inclusion of milled waste glass is observed to produce an EDX spectrum pointing at a silica-rich structure (pointing at the occurrence of pozzolanic reactions).

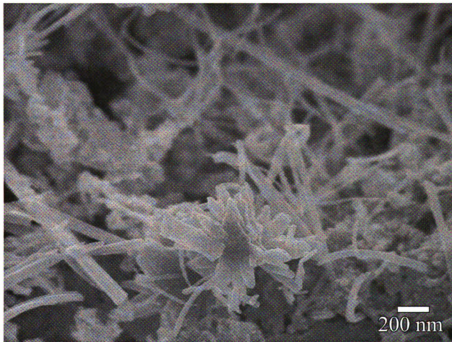


Figure 2. 33 SEM image showing heterogeneous microstructure of the cement paste constituent in mortar made without milled waste glass

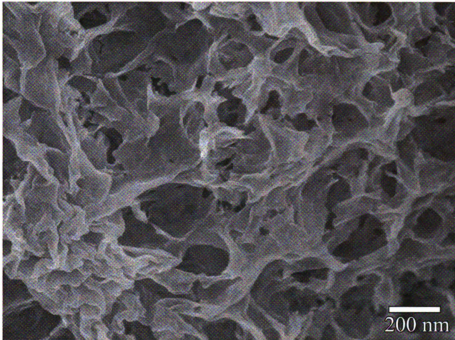


Figure 2. 34 SEM image showing homogeneous structure of the cementitious paste constituent in mortar made with milled waste glass as replacement for 20% of cement

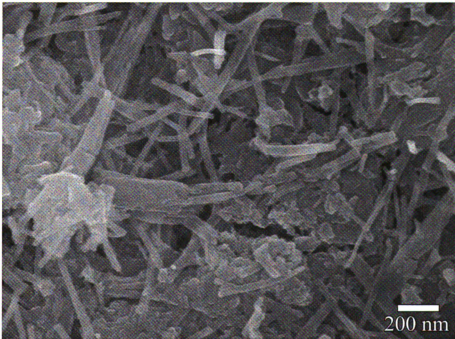


Figure 2. 35 SEM image of the cement paste constituent of mortar made without milled waste glass

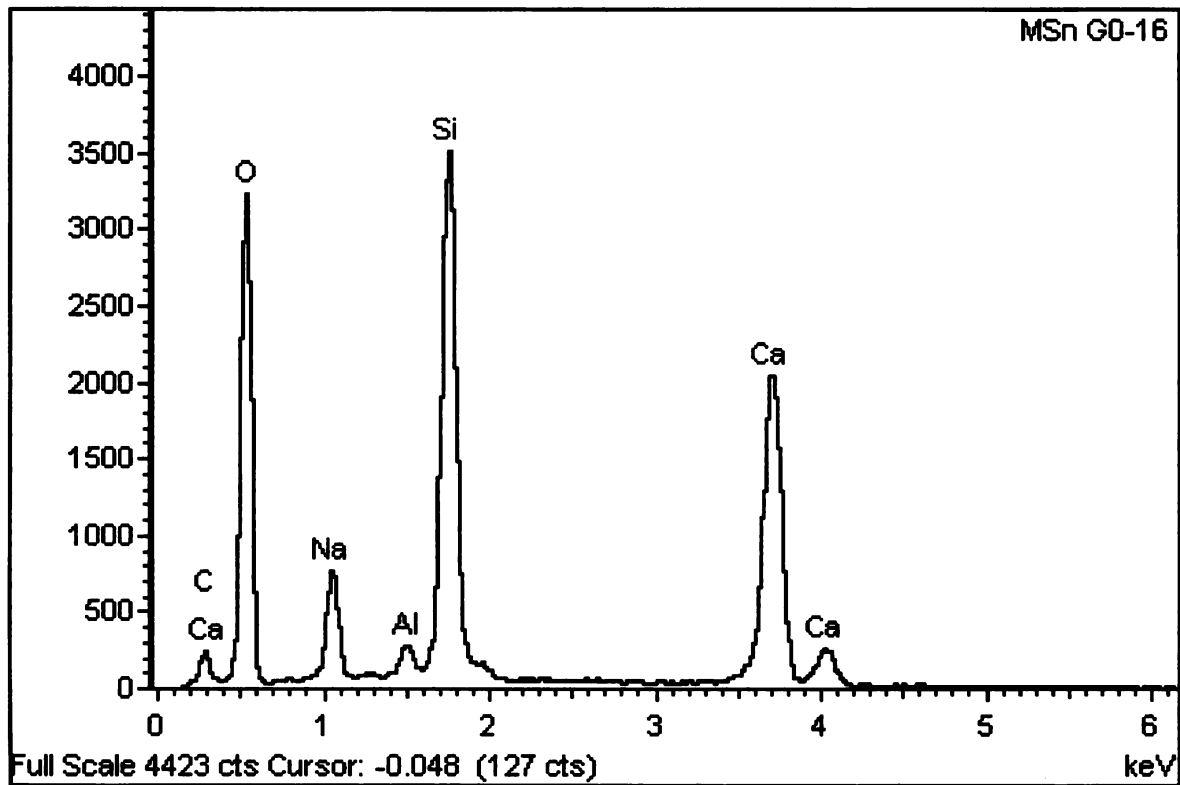


Figure 2. 36 EDX spectrum at the location of Figure 2.35 for the cement paste in mortar made without milled waste glass

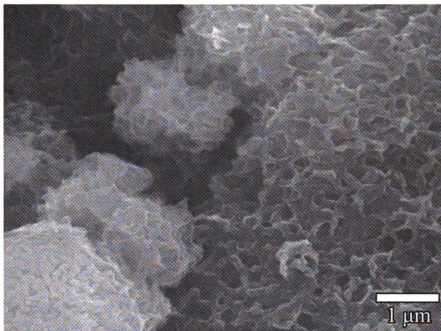


Figure 2. 37 SEM image of the cementitious paste constituent of mortar made with milled waste glass replacing 40% of cement

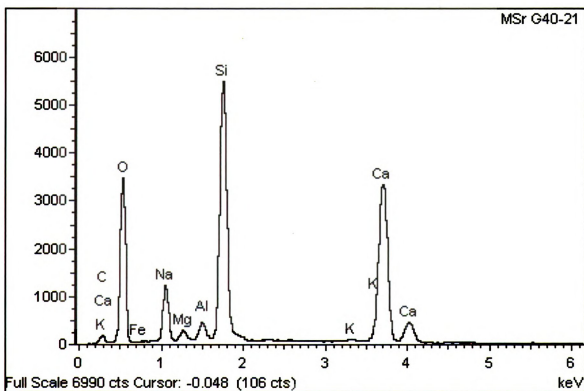


Figure 2. 38 EDX spectrum at the location of Figure 2.37 for the cementitious paste in mortar made with milled waste glass replacing 40% of cement

### 2.6.3.3 SEM Analysis of Concrete Specimens

Figure 2.39 shows an SEM image of the ITZ region of the fractured surface of a recycled aggregate concrete specimen (without milled waste glass). This image points at strong presence of large plate-like crystals of CH as well as some ettringite needles; the structure seems to be quite porous and heterogeneous. Figure 2.40 shows an SEM image of the ITZ region on the fractured surface of a recycled aggregate concrete specimen with milled waste glass replacing 20% of cement. In this case, the microstructure appears to be rich in type-I C-S-H, which point at the occurrence of pozzolanic reactions between CH and milled waste glass. Typical C-S-H fibrils appear to be 2 to 3  $\mu\text{m}$  long, and form a relatively dense structure.

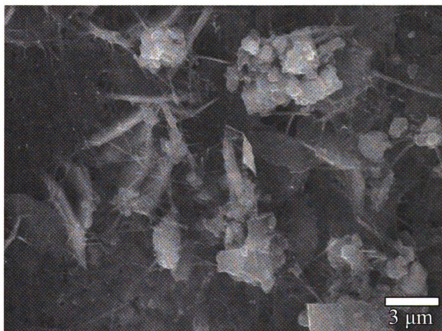


Figure 2. 39 SEM image of the ITZ region of a fractured surface of a recycled aggregate concrete specimen without milled waste glass

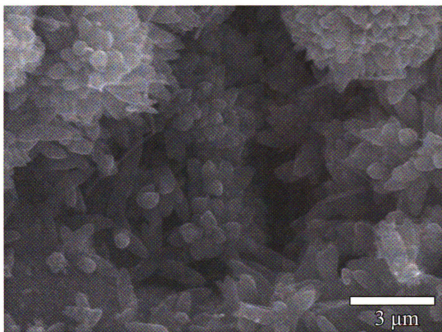


Figure 2.40 SEM image of the ITZ region of a fractured surface of a recycled aggregate concrete specimen with milled waste glass replacing 20% of cement, showing the prevalence of Type-I C-S-H

## REFERENCES

1. Richards, L.A., *Capillary conduction of liquids through porous mediums*. Physics (American Institute of Physics; American Physical Society; Society of Rheology), 1931. **1**(5): p. 318-333.
2. KLUTE, A., *A Numerical Method for Solving the Flow Equation for Water in Unsaturated Materials*. Soil Science, 1952. **73**(2): p. 105-116.
3. PHILIP, J.R., *The Theory of Infiltration: 1. the Infiltration Equation and Its Solution*. Soil Science, 1957. **83**(5): p. 345-358.
4. PHILIP, J.R., *The Theory of Infiltration: 2. the Profile of Infinity*. Soil Science, 1957. **83**(6): p. 435-448.
5. Hall, W.D.H.a.C., *Water transport in brick, stone and concrete*. 2002, London: Spon Press.
6. Padday, J.F., *Wetting, Spreading and Adhesion*. 1975, New York: Academic Press.
7. Hall, C., *Water movement in porous building materials--I. Unsaturated flow theory and its applications*. Building and Environment, 1977. **12**(2): p. 117-125.
8. Dhir, R.K., et al. , *Near-Surface characteristics of concrete: assessment and development of in-situ test methods* Magazine of Concrete Research, 1987. **39**(141): p. 183-195.
9. Janz, M., *Methods of measuring the moisture diffusivity at high moisture levels*. 1997, Lund Institute of Technology.
10. Kropp, J.a.H., H. K. , ed. *Performance Criteria for Concrete Durability*. 1995, E & FN Spon: London.
11. Sabir, B., S. Wild, and M. O'Farrell, *A water sorptivity test for martar and concrete*. Materials and Structures, 1998. **31**(8): p. 568-574.
12. Neithalath, N., *Analysis of moisture transport in mortars and concrete using sorption-diffusion approach*. ACI Materials Journal, 2006. **103**(Compendex): p. 209-217.
13. Hall, C., *Barrier performance of concrete: A review of fluid transport theory*. Materials and Structures, 1994. **27**(5): p. 291-306.

14. Hall, C., *Water sorptivity of mortars and concretes: A review* Magazine of Concrete Research, 1989. **41**(147): p. 51-61.
15. Martys, N.S. and C.F. Ferraris, *Capillary transport in mortars and concrete*. Cement and Concrete Research, 1997. **27**(5): p. 747-760.
16. Kunzel, M.H., *Simultaneous Heat and Moisture Transport in Building Components*. 1995, Fraunhofer Institute of Building Physics: Stuttgart.
17. Gummerson, R.J., C. Hall, and W.D. Hoff, *Water movement in porous building materials--II. Hydraulic suction and sorptivity of brick and other masonry materials*. Building and Environment, 1980. **15**(2): p. 101-108.
18. Hall, C. and M.H. Raymond Yau, *Water movement in porous building materials--IX. The water absorption and sorptivity of concretes*. Building and Environment, 1987. **22**(1): p. 77-82.
19. PHILIP, J.R., *The Theory of Infiltration: 4. Sorptivity and Algebraic Infiltration Equations*. Soil Science, 1957. **84**(3): p. 257-264.
20. Xi, Y., et al., *Moisture diffusion in cementitious materials Moisture capacity and diffusivity*. Advanced Cement Based Materials, 1994. **1**(6): p. 258-266.
21. Martys, N.S., *Survey of Concrete Transport Properties and their Measurement*, N. U.S. Department of Commerce, Editor. 1995: Gaithersburg, MD.
22. Černý R., R.P., *Transport processes in concrete 2002*, London: Spon Press.
23. Garboczi, E.J., ed. *Microstructure and transport properties of concrete*. Performance Criteria for Concrete Durability, ed. J.a.H. Kropp, H. K. . 1995, E & FN Spon: London.
24. Young, J.F., ed. *A review of the pore structure of cement paste and concrete and its influence on permeability*. Permeability of Concrete, ed. D.a.W. Whiting, A. Vol. SP-108. 1988, American Concrete Institute.
25. Hearn, N., Hooton, R. D., and Nokken, M. R., ed. *Pore Structure, Permeability, and Penetration Resistance Characteristics of Concrete* in Significance of Tests and Properties of Concrete and Concrete-Making Materials, ed. J.F.a.P. Lamond, J. H. Vol. STP 169D. 2006, ASTM International: West Conshohocken.
26. Mehta P. K., M.P.J.M., *Concrete: Microstructure, Properties and Materials*. 2006: McGraw-Hill New York.
27. Ollivier, e.a., ed. *Parameters influencing transport characteristics*. Performance Criteria for Concrete Durability, ed. H. Kropp J., H. K. 1995, E & FN Spon.

28. Neville, A.M., *Properties of Concrete*. 4th ed. 2000: Pearson Education.
29. Young, J.F., Mindess, S., Gray, R. J., and Bentur, A., *The Science and Technology of Civil Engineering Materials*. 1998: Prentice Hall.
30. Scrivener, K.L., ed. *The Microstructure of Concrete*. Materials Science of Concrete ed. J. Skalny. Vol. I. 1989, The American Ceramic Society: Westerville, OH.
31. Roy, D.M., Idorn, G. M., , *Concrete Microstructure*, in *SHRP-C-340*. 1993, Strategic Highway Research Program, National Research Council: Washington, DC.
32. Roy, D.M., Brown, P. W., Shi, D., Scheetz, B. E. , and May, W., *Concrete Microstructure Porosity and Permeability*. 1993, Strategic Highway Research Program: Washington, DC.
33. Powers, T.C., *Some Physical Aspects of the Hydration of Portland Cement*. PCA Research and Development Laboratories, 1961. 3(1): p. 47-56.
34. Hall, C. and T.K.-M. Tse, *Water movement in porous building materials--VII. The sorptivity of mortars*. *Building and Environment*, 1986. 21(2): p. 113-118.
35. Koopal, L.K., *Definitions, Terminology and Symbols in Colloid and Surface Chemistry*, in *Manual of Symbols and Terminology for Physicochemical Quantities and Units* 2001, International Union of Pure and Applied Chemistry: Washington DC.
36. Mindess S., Y.J.F., and Darwin D., *Concrete*. Second ed. 2003: Prentice Hall.
37. Scrivener, K.L. and K.M. Nematı, *The percolation of pore space in the cement paste/aggregate interfacial zone of concrete*. *Cement and Concrete Research*, 1996. 26(1): p. 35-40.
38. Maso, J.C., ed. *The Interfacial Transition Zone in Concrete*. 1996, E & FN Spon: London.
39. Winslow, D. and D. Liu, *Pore structure of paste in concrete*. *Cement and Concrete Research*, 1990. 20(Compendex): p. 227-235.
40. Ryu, J.S., *Improvement on strength and impermeability of recycled concrete made from crushed concrete coarse aggregate*. *Journal of Materials Science Letters*, 2002. 21(20): p. 1565-1567.
41. Otsuki, N., S.-I. Miyazato, and W. Yodsudjai, *Influence of recycled aggregate on interfacial transition zone, strength, chloride penetration and carbonation of*

- concrete. *Journal of Materials in Civil Engineering*, 2003. **15**(Compendex): p. 443-451.
42. Etxeberria, M., E. Vazquez, and A. Mari, *Microstructure analysis of hardened recycled aggregate concrete*. *Magazine of Concrete Research*, 2006. **58**(Compendex): p. 683-690.
  43. Malhotra V. M., M.P.K., *High-performance high-volume fly ash concrete: materials, mixtures incorporating properties, construction practice, and case histories*. 2002.
  44. Ann, K.Y., et al., *Durability of recycled aggregate concrete using pozzolanic materials*. *Waste Management*, 2008. **28**(Compendex): p. 993-999.
  45. Berndt, M.L., *Properties of sustainable concrete containing fly ash, slag and recycled concrete aggregate*. *Construction and Building Materials*, 2009. **23**(7): p. 2606-2613.
  46. Kou, S.C., C.S. Poon, and D. Chan, *Influence of fly ash as a cement addition on the hardened properties of recycled aggregate concrete*. *Materials and Structures/Materiaux et Constructions*, 2008. **41**(Compendex): p. 1191-1201.
  47. Kou, S.C., et al. *Hardened properties of recycled aggregate concrete prepared with fly ash*. in *International Conference on Sustainable Waste Management and Recycling, September 14, 2005 - September 15, 2005*. 2004. London, United Kingdom: Thomas Telford Services Ltd.
  48. Malhotra V. M., M.P.K., *Pozzolanic and Cementitious Materials*. *Advances in Concrete Technology*. Vol. 1. 1996, Amsterdam: Gordon and Breach Publishers.
  49. Kumar, B., G.K. Tike, and P.K. Nanda, *Evaluation of properties of high-volume fly-ash concrete for pavements*. *Journal of Materials in Civil Engineering*, 2007. **19**(Compendex): p. 906-911.
  50. Jerath, S. and N. Hanson, *Effect of Fly Ash Content and Aggregate Gradation on the Durability of Concrete Pavements*. *Journal of Materials in Civil Engineering*, 2007. **19**(5): p. 367-375.
  51. Manmohan, D., Mehta, P. K., *Influence of pozzolanic, slag, and chemical admixtures on pore size distribution and permeability of hardened cement pastes*. *Cement, Concrete, and Aggregates*, 1981. **3**(1): p. 63-67.
  52. Feldman, R.F., *Pore structure formation during hydration of fly-ash and slag cement blends*, in *Effects of Fly-Ash Incorporation in Cement and Concrete*, S. Diamond, Editor. 1981, Material Research Society: Pittsburgh, PA. p. 124-133.

53. *ASTM C 192-07 Standard Practice for Making and Curing Concrete Test Specimens in the Laboratory*. 2007, American Society for Testing and Materials.
54. McCarter, W.J., *Influence of Surface Finish on Sorptivity on Concrete*. *Journal of Materials in Civil Engineering*, 1993. 5(1): p. 130-136.
55. *ASTM C1585 - 04 Standard Test Method for Measurement of Rate of Absorption of Water by Hydraulic-Cement Concretes*. 2006, American Society for Testing and Materials.
56. Taylor, H.F.W., *Cement Chemistry*. 1990, London: Academic Press Limited.
57. Diamond, S. and M.E. Leeman. *Pore size distributions in hardened cement paste by SEM image analysis*. in *Proceedings of the 1994 MRS Fall Meeting, November 28, 1994 - November 30, 1994*. 1995. Boston, MA, USA: Materials Research Society.
58. Igarashi, S., M. Kawamura, and A. Watanabe, *Analysis of cement pastes and mortars by a combination of backscatter-based SEM image analysis and calculations based on the Powers model*. *Cement and Concrete Composites*, 2004. 26(Compendex): p. 977-985.
59. Mouret, M., E. Ringot, and A. Bascoul, *Image analysis: A tool for the characterisation of hydration of cement in concrete - Metrological aspects of magnification on measurement*. *Cement and Concrete Composites*, 2001. 23(Compendex): p. 201-206.

## **CHAPTER 3**

### **Effects of Partially Replacing Cement with Milled Waste Glass on the Fresh Mix Properties, and the Physical and Mechanical Performance of Normal and Recycled Aggregate Concrete**

#### **3.1 Background Investigations of the Fresh Mix Properties and Mechanical Performance of Recycled Aggregate Concrete**

Depending on the qualities of recycled and virgin aggregates, about 5% more free water is reportedly needed to produce a recycled aggregate concrete mix using coarse recycled aggregate and natural sand for achieving similar workability as that of normal concrete [1-4]. Some researchers [5] have, on the contrast, found that the workability of recycled aggregate concretes produced with coarse recycled aggregate and virgin sand could improve over that of normal concrete (prepared with virgin coarse aggregate). Ravindrarajah et al. [6] and Hansen and Narud [3] found that concrete produced with coarse recycled aggregate and natural sand loses workability and sets faster than the corresponding normal concrete. In their recent work, Fathifazl et al. [7] concluded, based on their “equivalent mortar volume” method of recycled aggregate concrete mixture proportioning, that fresh and hardened concrete properties of recycled aggregate can be improved and made comparable to that of normal concrete.

Mechanical properties of recycled aggregate concrete have been studied extensively by different researchers [3, 5, 8-25]. Most investigators have used laboratory-produced original concrete towards production of recycled aggregate, while others have used field-demolished concrete in their research [26-28]. Several researchers [3, 8, 16, 29] have concluded that the mechanical properties of recycled aggregate

concrete depends strongly on the quality of the original concrete from which the recycled aggregate has been produced. Rasheeduzzafar and Khan [5] found that when the strength of the recycled aggregate concrete was above the strength of the old concrete (from which recycled aggregate is produced), the strength of the new mortar and the new mortar-aggregate bond in recycled aggregate concrete was higher than the strength of the recycled aggregate or the bond between the old mortar and the original aggregate, thereby making the recycled aggregate the weaker and, therefore, the strength-controlling link. On the other hand, when the strength of the recycled aggregate concrete was below that of the old concrete, the inferior quality of the new mortar (or its bond to recycled aggregate) in recycled aggregate concrete formed the weaker link which controlled the failure mechanism. Hansen and Narud [3] concluded that the compressive strength of recycled aggregate concrete was dependent upon the strength of the original concrete, and that it was largely controlled by a combination of the water/cement ratios of the original concrete and the recycled aggregate concrete (when other factors were similar).

As stated earlier (Section 1.7) various mechanical properties of concrete produced with recycled aggregate are inferior to those of concrete produced with virgin aggregate. Some investigations [8] have concluded that the compressive strength of recycled aggregate concrete produced with coarse recycled aggregates and natural sand could be between 14% and 32% lower than that of normal concrete. Malhotra [4], Buck [2] and Frondistou-Yannas [30] concluded that recycled aggregate concrete had 10% lower strength than normal concrete. Ravindrarajah [31] has found that recycled aggregate concrete provides between 8% and 24% lower compressive strength when compared with normal concrete. Limbachiya et al. [23], Katz [19], Tavakoli and Soroushian [16], and

Kou et al. [28] concluded that the flexural and split tensile strengths of recycled aggregate concretes are inferior to those of concrete produced with virgin aggregate. Ravindrarajah [6] reported that the flexural and split tensile strengths of recycled aggregate concrete are consistently 10% below those of concrete produced with virgin aggregate. Frondistou-Yannas [30] reported that recycled aggregate concrete has up to 33% lower modulus of elasticity than normal concrete, whereas Rasheeduzzafar and Khan [5] reported that recycled aggregate concrete has up to 18% lower static modulus when compared with normal concrete. Tavakoli and Soroushian [26], Limbachiya et al. [23], Kou et al. [32], Hasaba et al. [33], Hansen and Boegh [34], Crentsil et al. [35] and Ravindrarajah [6] have concluded that the drying shrinkage of recycled aggregate concrete is significantly higher than that of normal concrete. It has been concluded that the drying shrinkage of recycled aggregate concrete made with coarse recycled aggregate and natural sand is about 50% higher than that of normal concrete [29]. This is one major drawback of recycled aggregate concrete, which makes it susceptible to restrained shrinkage cracking.

### **3.2 Background Information on the Effects of Milled Waste Glass on the Mechanical Performance of Normal Concrete**

Besides the beneficial effects of pozzolanic reaction of milled waste glass with cement hydrates improving the moisture barrier qualities of concrete (see Sections 1.4 and 2.4), the mechanical properties of concrete can also benefit from introduction of milled waste glass as partial replacement for cement [36-45]. These benefits are realized through timely pozzolanic reactions of the finely divided particles of milled waste glass which

form secondary C-S-H gel. Dyer and Dhir [36] observed more extensive C-S-H formation in concrete mixtures containing glass powder. Shayan and Xu [38] concluded that up to 30% of glass powder can be incorporated as cement replacement in concrete without any long-term detrimental effects. They further concluded that glass powder can be used as replacement for other pozzolanic materials such as silica fume and fly ash. In another investigation, Dyer and Dhir [45] concluded that cullet from container glass undergoes pozzolanic reaction with Portland cement, and up to 30% replacement of cement with powdered cullet benefits the compressive strength of glass concrete that match or exceed that of control concrete. In an other investigation, Shayan and Xu [42] found that it is possible, with up to 30% replacement of cement with glass powder, to achieve the intended strength. They also found that the drying shrinkage of concrete mixtures containing glass powder as partial replacement for cement met normal drying shrinkage requirements. Schwarz et al. [41] observed that, with 10% replacement of cement with glass powder, the 28-day compressive strength of concrete was higher than that of corresponding fly ash concrete. They also observed that the low water absorption capacity of glass powder facilitates the enhancement of early age hydration of cement. Shao and Lehoux [46] found that the performance of ground glass in concrete is size-dependent, with glass powder of 38  $\mu\text{m}$  particle size producing higher reactivity with lime, higher compressive strength and lower expansion when compared with the glass powders of 75  $\mu\text{m}$  or 150  $\mu\text{m}$  particle size. Furthermore, glass concrete materials containing 38  $\mu\text{m}$  particles size glass powder offered higher 90-day compressive strength and strength activity index than the corresponding fly ash and control concrete materials.

### **3.3 The Innovative Aspect of Our Approach**

Various earlier researchers have investigated the effect of fly ash on the mechanical performance of recycled aggregate concrete [22, 28, 32, 47-48]. In one investigation [27], structural-grade recycled aggregate concrete was produced through surface treatment of recycled aggregate with sodium silicate, lime, and silica fume. The innovative aspect of our approach involves overcoming the drawbacks of recycled aggregate concrete (see Sections 1.6 and 1.7 through the use of milled waste glass as partial replacement for cement. As described earlier (see Sections 1.8 and 2.4), this approach takes advantage of the silica-rich and amorphous nature of glass, with proper milling (size reduction) enhancing the kinetics of its beneficial reaction with cement hydrates. Our research also provides further insight into the mechanisms of action and benefits of milled waste glass in normal concrete.

A comprehensive experimental work was conducted on concrete mixtures with 0 and 20 wt.% of cement replaced with milled waste glass, using 0% (control), 50% and 100% recycled coarse aggregate as replacement for virgin coarse aggregate. The effects of milled waste glass on the engineering properties of recycled aggregate and normal concrete materials were investigated. Comparisons were also made between the effects of milled waste glass and coal fly ash as partial replacement for cement.

### **3.4 Materials and Concrete Mix Designs**

Details of the materials and mix design have been presented in Section 2.5. Milled waste glass with physical properties given in Table 2.1, and virgin aggregate, recycled aggregate and sand with physical properties presented in Table 2.2 were used in the

experimental program. Table 2.3 shows the details of 12 different mix designs incorporating virgin, recycled and 50: 50 blend of the two, with and without milled waste glass as partial (20 wt.%) replacement for cement. Table 2.4 shows the mix designs incorporating class-F and class-C fly ash as partial (20 wt.%) replacement for cement, with virgin aggregate, recycled aggregate and 50: 50 blend of the two.

### **3.5 Experimental Methods, Test Results and Discussion**

#### **3.5.1 Fresh Mix Properties**

Slump of fresh concrete mixtures was measured according to ASTM C 143, Air Content was determined following ASTM C 213, unit weight was measured per ASTM C 138, and temperature of fresh concrete was measured using ASTM C 1064 procedures. Tables 3.1 and 3.2 shows the slump, air content, temperature, and unit weight test results for various mixtures used in this experimental program.

Table 3.1 indicates that the slump of fresh concrete mixtures increased with the addition of milled waste glass. This is true for both low and high water/cement ratios considered here. The increase in slump with the incorporation of milled waste glass may be attributed to the low water absorption of glass. In general, the slump of recycled aggregate concrete tends to be higher than that of normal concrete; this observation is in line with the findings of some other researchers. Unit weight of fresh concrete mixtures decreased slightly with the addition of milled waste glass as partial replacement for cement. This effect is more pronounced for low w/c ratio mixtures as compared to those with high w/c ratio. The slightly reduced unit weight with milled waste glass partially replacing cement may be attributed to the low specific gravity of milled waste glass as

compared to Portland cement ( 2.46 Vs. 3.15) [49-50]. No appreciable changes in the entrained air content of fresh concrete mixtures was detected when milled waste glass replaced 20 wt.% of cement.

The test results presented in Table 3.2 point at drops in slump and entrained air content in the case of class-C fly ash mixtures when compared with the corresponding class-F fly ash mixtures. This may be attributed to high calcium oxide content of class-C fly ash, which is largely contained in a glassy fraction. Furthermore, class-C fly ash is known for high water demand and early stiffening (rapid-setting) effects when used as partial replacement for cement in concrete.

Table 3. 1 Fresh concrete properties for mixtures with and without milled waste glass

Mix Design	Slump cm (in.)	Unit Weight kg/m <sup>3</sup> (lb/ft <sup>3</sup> )	Temp °C (°F)	Air Content (%)
CIW	7 (2.75)	2299 (143.52)	24.5 (76)	4.5
RIW	8.25 (3.25)	2219 (138.50)	24.5 (76)	6
BIW	9.50 (3.75)	2231 (139.28)	20 (68)	5
CGIW	7.11 (2.80)	2290 (142.96)	22 (72)	4.25
RGIW	9.7 (3.80)	2193 (136.88)	22.7 (73)	5.75
BGIW	10.2 (4)	2209 (137.92)	19.4 (67)	5
ChW	19.7 (7.75)	2208 (137.84)	26 (79)	7
RhW	16.5 (6.5)	2084 (130.08)	25.5 (78)	8
BhW	17.8 (7)	2121 (132.40)	24.5 (76)	8
CGhW	20.32 (8)	2187 (136.56)	20.5 (69)	7
RGhW	19.7 (7.75)	2096 (130.88)	21.1 (70)	7.5
BGhW	21 (8.25)	2120 (132.32)	21.1 (70)	7

Table 3. 2 Fresh mix properties for fly ash concrete mixtures

Mix Design	Slump cm (in.)	Unit Weight kg/m <sup>3</sup> (lb/ft <sup>3</sup> )	Temp °C (°F)	Air Content (%)
CFIW	7 (2.75)	2299 (143.25)	23.3 (74)	4.5
RFIW	12.7 (5)	2129 (132.88)	23.9 (75)	7
BFIW	14 (5.5)	2146 (134)	24.5 (76)	7.5
CSIW	5.1 (2)	2253 (140.64)	22 (72)	3.5
RSIW	7.7 (3)	2159 (134.8)	22 (72)	4
BSIW	5.1 (2)	2214 (138.24)	22 (72)	3.75

### 3.5.2 Hardened Concrete Properties

#### 3.5.2.1 Density, Water Absorption and Porosity

The ASTM C 642 procedures were followed for measurement of the density, water absorption capacity and porosity of hardened concrete materials. Water absorption and porosity are important indicators of the durability of hardened concrete. As discussed earlier (Sections 2.2 and 2.4), reduction of water absorption and porosity can greatly enhance the long-term performance and service life of concrete in aggressive service environments. Decreased porosity also benefits the compressive and flexural strengths of concrete. Table 3.3 shows the results of the bulk density (dry), bulk density (after immersion) and volume of voids test results for hardened concretes with and without milled waste glass at 56 days of age. Partial replacement of cement with milled waste glass is observed to produce an increase in the bulk density (dry) and the bulk density (after immersion) of concrete. This could be attributed to the conversion of CH to C-S-H by the pozzolanic reaction of milled waste glass in concrete, noting that the specific gravity of the resulting C-S-H (that falls on the lower end of the 2.3-2.6 range) is

somewhat higher than that of CH (2.24) [49]. Water absorption of concrete is observed in Table 3.3 to be significantly reduced with introduction of milled waste glass as partial replacement for cement in both low and high water/cement ratio mixtures. Statistical analysis (of variance) at 95% confidence level, followed by pair-wise comparisons, pointed at the statistical significance of the milled waste glass effects towards reduction of water absorption. Statistical analyses also confirmed the (expected) significant effects of decreasing w/c ratio towards reduction of water absorption. Use of milled waste glass as partial replacement for cement also results lowered the volume of voids in concrete. Statistical analysis (of variance) at 95% confidence level indicated that the effect of milled waste glass towards reduction of the volume of voids is statistically insignificant. It should be noted that the void content test used here measures the volumes of both continuous and discontinuous pores in concrete. Unlike continuous pores, the presence of discontinuous pores in hydrated cement paste is not detrimental to the water absorption and thus durability of concrete. Such pores, however, results in reduction of concrete strength. Table 3.4 shows the results of subject tests for class-C and class-F fly ash concrete mixes. Improvements in water absorption of concrete resulting from the use of class-F fly ash as partial replacement of cement are similar to those obtained with milled waste glass.

Table 3. 3 Density, water absorption, and volume of voids for concrete materials with and without milled waste glass at 56 days of age

Mix Design	Bulk Density (Dry) Mg/m <sup>3</sup> (lb/ft <sup>3</sup> )	Bulk Density (After Immersion) Mg/m <sup>3</sup> (lb/ft <sup>3</sup> )	Absorption %	Volume of Voids %
CIW	2.22	2.36	5.93	13
RIW	2.07	2.22	7.50	15.50
BIW	2.19	2.32	6.26	14.25
CGIW	2.25	2.38	4.85	12.25
RGIW	2.10	2.26	5.85	13.15
BGIW	2.12	2.33	5.15	13.10
ChW	2.11	2.24	6.48	13.68
RhW	1.99	2.14	8.15	15.75
BhW	2.05	2.20	6.95	14.65
CGhW	2.15	2.29	5.50	13.49
RGhW	2.01	2.18	6.52	13.75
BGhW	2.07	2.22	6.12	13.70

Table 3. 4 Density, water absorption, and volume of voids for fly ash concrete materials at 56 days of age

Mix Design	Bulk Density (Dry) Mg/m <sup>3</sup> (lb/ft <sup>3</sup> )	Bulk Density after Immersion Mg/m <sup>3</sup> (lb/ft <sup>3</sup> )	Absorption %	Volume of Voids %
CFIW	2.25	2.37	4.93	12.28
RFIW	2.08	2.21	5.83	13.20
BFIW	2.09	2.22	5.23	13.15
CSIW	2.19	2.34	5.69	12.79
RSIW	2.11	2.27	6.27	14.02
BSIW	2.13	2.29	5.98	13.32

Statistical analysis (of variance) at 95% confidence level indicated the differences between the water absorption capacity of milled waste glass and Class-F fly concrete materials are statistically insignificant. The contributions of Class-C fly ash towards reduction of the water absorption capacity of concrete was inferior to that of milled waste glass in low as well as high w/c ratio concrete mixtures. Statistical analyses pointed at the statistical significance (at 95% confidence level) of this difference (in favor of milled waste glass). The effects of class-F and class-C fly ash towards reduction of the volume of voids were statistically comparable (at 95% level of confidence) when compared with that of milled waste glass.

### **3.5.2.2 Compressive Strength**

Concrete cylinders with 203 mm (8 in.) height and 102 mm (4 in.) diameter were produced and cured in lime-saturated water until different testing ages in accordance with ASTM C 192 for each of the mix designs presented in Tables 2.3 and 2.4. Each mix design was replicated three times, with three specimens tested for each replicate. These cylindrical specimens were tested in compression following the ASTM C39 procedures at concrete ages of 3, 7, 28, 90, 156 and 300 days. Figure 3.1 shows the compressive strength test results at different ages for low w/c ratio mixtures incorporating virgin, recycled and blended aggregates, with and without milled waste glass. Figure 3.2 shows the compressive strength test results of the corresponding high w/c ration mixtures. The compressive strength test results for fly ash concrete mixtures are presented in Figure 3.3. Comparisons between the compressive strengths of milled waste glass and class-F fly ash concrete mixtures are presented in Figure 3.4

Among the low w/c ratio mixtures, the compressive strengths of concrete materials with milled waste glass used as partial replacement for cement were lower than those of the corresponding concrete materials without milled waste glass at 3, 7 and 28 days of age. This trend reversed at 90, 156 and 300 days of age when partial replacement of cement with milled waste glass benefited the compressive strength of concrete. Statistical analysis (of variance) of test results indicated the 28-day compressive strengths of concrete materials with and without milled waste glass were statistically comparable (at 95% level of confidence). At 90, 156 and 300 days of age, however, statistical analyses pointed at the statistically significant benefits (at 95% level of confidence) of milled waste glass (as partial replacement for cement) to the compressive strength of concrete.

The compressive strength test results for the high w/c ratio mixtures (Figure 3.2) follow trends similar to those for the low w/c ratio mixtures. The strength of concrete high w/c ration concrete materials with milled waste glass partially replacing cement surpasses that of normal concrete materials (without milled waste glass) at the age of 90 days and onward. Statistical analysis (of variance) of test results indicated that the differences between the 28-day compressive strengths of concrete materials with and without milled waste glass were statistically insignificant (at 95% level of confidence). The beneficial effects of milled waste glass on the compressive strength of concrete at 90, 156 and 300 days of age were found to be statistically significant (at 95% level of confidence). Statistical analyses also confirmed that the expected gains in compressive strength with reduction of w/c ratio were statistically significant (at 95% confidence level).

Compressive strength test results of class-F and class-C fly ash concrete materials (Figure 3.3) pointed at the higher strength of class-F fly ash concrete when compared with that of class-C fly ash concrete at all ages. Comparisons between the compressive strengths of mixes with milled waste glass versus fly ash (Figure 3.4) pointed at the higher strength of milled waste glass mixes at 90, 156 and 300 days of age. Statistical analyses (of variance) of test results indicated that the differences between the compressive strengths of low w/c ratio concrete materials containing milled waste glass versus class-F fly ash were not statistically significant (at 95% level of confidence) at 3, 7 and 28 days of age. At ages of 90, 156 and 300 days, however, the benefits of milled waste glass to compressive strength were found to be superior to those of Class-F fly ash at 95% confidence level. Statistical analysis (of variance) of the differences between the compressive strengths of class-C fly ash and milled waste glass concrete materials pointed at the statistical significance (at 95% level of confidence) of the greater benefits of milled waste glass to compressive strength at 90, 156 and 300 days of age when compared with those of Class-C fly ash.

The contributions of milled waste glass to the compressive strength of concrete at later ages can be attributed to the formation of secondary C-S-H as a result of pozzolanic reactions between milled waste glass and the CH produced during hydration of cement. The binding action of the secondary C-S-H and its effect on increasing the gel-space ratio (i.e., lowering porosity) benefit the compressive strength of concrete. These contributions of milled waste glass are statistically comparable to those of Class-F fly ash (at all ages) and superior to those of Class-C fly ash.

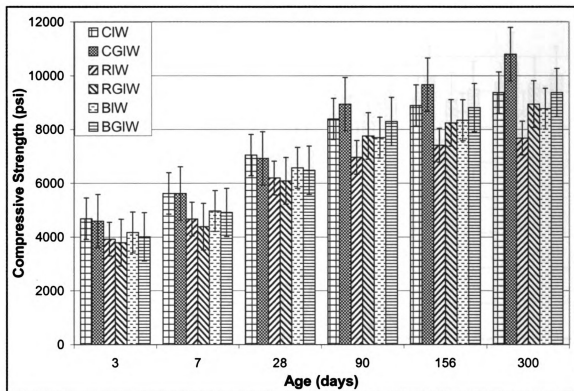


Figure 3. 1 Compressive strengths at different ages of low w/c ratio concrete materials with and without milled waste glass (means & standard errors)

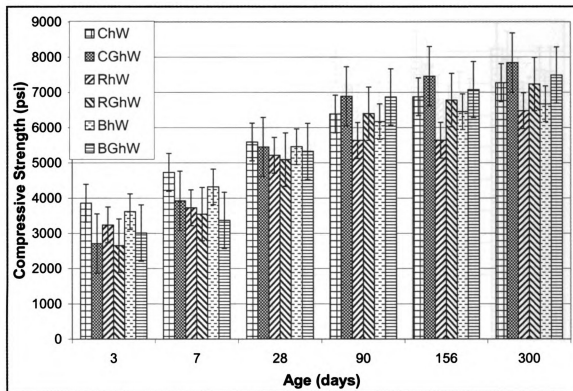


Figure 3. 2 Compressive strengths at different ages of high w/c ratio concrete materials with and without milled waste glass (means & standard errors)

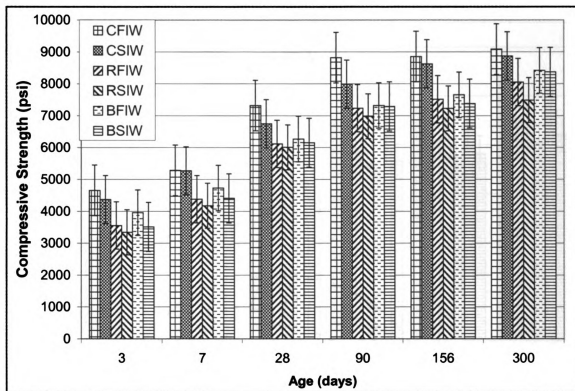


Figure 3.3 Compressive strengths at different ages of fly ash concrete materials (means & standard errors)

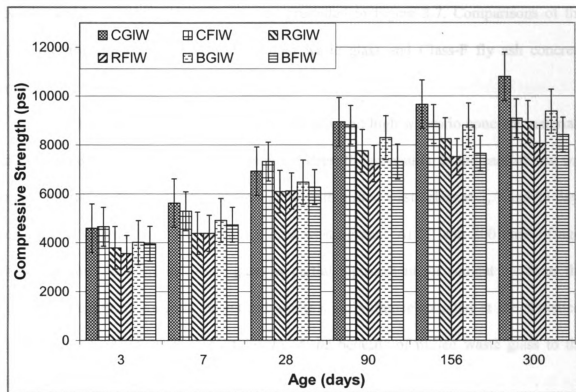


Figure 3. 4 Compressive strengths at different ages of milled waste glass and class-F fly ash concrete materials (means & standard errors)

### 3.5.2.3 Flexural Strength

Prismatic beam specimens with 102 mm (4 in.) x 102 mm (4 in.) cross-section and length of 356 mm (14 in.) were produced and cured in lime-saturated water until different test ages in accordance with ASTM C 192 for all the mix designs of Tables 2.3 and 2.4. Each mix design was prepared in three replications, with three specimens prepared and tested for each replicate. Beam specimens were tested in flexure following the ASTM C 78 procedures at 3, 7, 28, 90, and 200 days of age. Figure 3.5 shows the flexural strength test results at different ages for low w/c ratio concrete materials incorporating virgin, recycled and blended aggregates with and without milled waste glass. Figure 3.6 presents the corresponding test results for the high w/c ratio concrete materials. Flexural strength test

results for fly ash concrete materials are presented in Figure 3.7. Comparisons of the flexural strength test results for the milled waste glass and Class-F fly ash concrete materials are presented in Figure 3.8

Flexural strength test results of the low and high w/c ratio concrete materials follow trends similar to those of compressive strength test results. In the case of low w/c ratio concrete materials, the flexural strengths with milled waste glass at 3, 7 and 28 days of age are lower than those without milled waste glass. At 90 and 200 days of age, however, the use of milled waste glass as partial replacement for cement increases the flexural strength of concrete. Statistical analysis (of variance) pointed at the statistical significance (at 95% level of confidence) of the benefits of milled waste glass to the later age flexural strength of concrete.

The flexural strength of high w/c ratio concrete materials followed trends similar to those of low w/c ratio concrete materials. At 3, 7 and 28 days of age, the mean flexural strengths of high w/c ratio concrete materials incorporating milled waste glass were less than those of the corresponding concrete materials without milled waste glass. At 90 and 200 days of age, high w/c ratio concrete materials with milled waste glass provided a higher flexural strength than the corresponding concrete materials without milled waste glass. Statistical analysis (of variance) of test results indicated that the effects of milled waste glass on the flexural strengths of high w/c ratio concrete materials was statistically insignificant (at 95 % confidence level) at 28 days of age, whereas milled waste glass made statistically significant contribution (at 95% level of confidence) to the flexural strength of high w/c ratio concrete materials at 90 and 200 days of age.

Milled waste glass benefited the flexural strength of high w/c ratio concrete materials more than that of low w/c ratio materials.

The flexural strength test results for fly ash concrete materials (Figure 3.7) indicate that Class-C fly ash produced slightly higher flexural strengths when compared with Class-F fly ash at early ages of 3, 7 and 28 days. This trend is, however, reversed at later ages of 90 and 200 days. Comparisons of the mean flexural strengths of milled waste glass and Class-F fly ash concrete materials (Figure 3.8) point at higher flexural strengths of milled waste glass concrete materials at 90 and 200 days of age. Statistical analysis (of variance) of test results indicated that differences between the flexural strengths of low w/c ratio concrete materials incorporating milled waste glass versus class-F and class-C fly ashes were not statistically significant at 3, 7 and 28 days of age (at 95% confidence level). However, at 90 and 200 days of age, the benefits of milled waste glass to flexural strength were superior to those of Class-C and Class-F fly ash (at 95% level of confidence).

The significant increase in the later-age flexural strength of concrete materials with incorporation of milled waste glass as partial replacement for cement can be attributed to the improvements in the interfacial transition zone (ITZ) and the cementitious paste in concrete realized by the pozzolanic reactions of milled waste glass with cement hydrates (CH). The higher CH content of low w/c ratio concrete mixtures could explain the improved effects of milled waste glass in higher w/c ratio concrete materials.

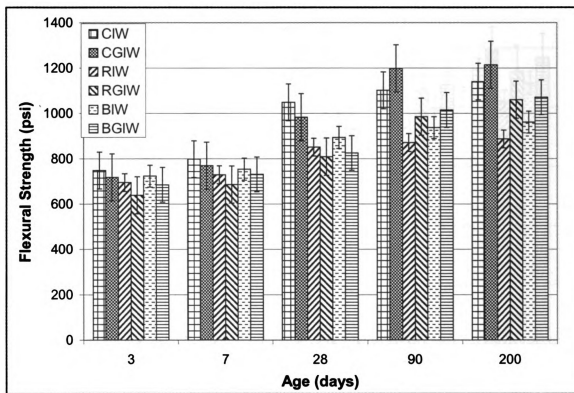


Figure 3. 5 Flexural strengths at different ages of low w/c ratio concrete materials with and without milled waste glass (means & standard errors)

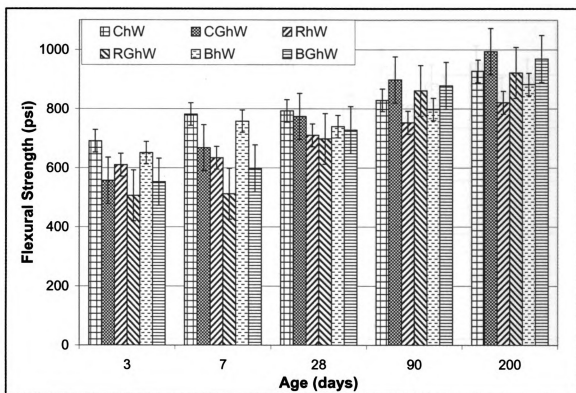


Figure 3. 6 Flexural strengths at different ages of high w/c ratio concrete materials with and without milled waste glass (means & standard errors)

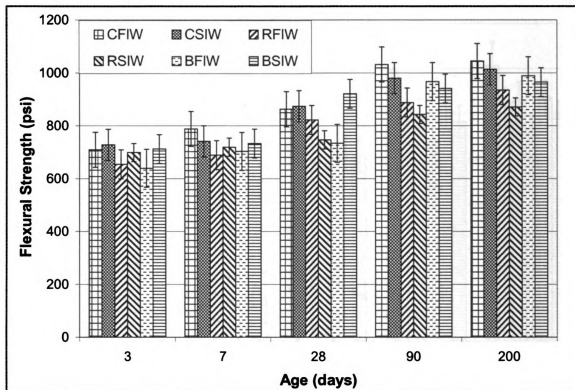


Figure 3. 7 Flexural strengths at different ages of fly ash concrete materials (means & standard errors)

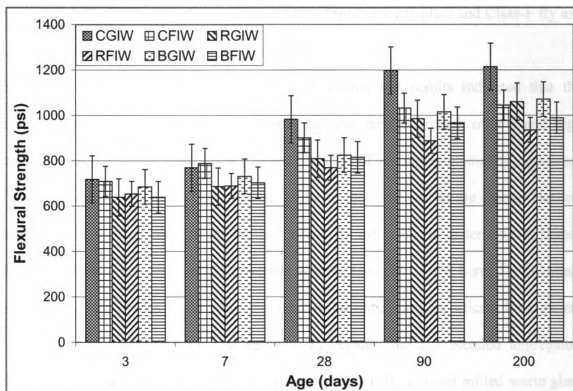


Figure 3. 8 Flexural strengths at different ages of milled waste glass and Class-F fly ash concrete materials (means & standard errors)

#### 3.5.2.4 Split Tensile Strength

Split tensile strength tests were carried out on cylindrical concrete specimens similar to those used in compression tests (see Section 3.5.2). For each of the mix designs presented in Tables 2.3 and 2.4, split tensile strength tests were carried out for two replicated mixes, with three specimens tested for each replicate. Split tension tests were performed at 120 and 200 days of age following ASTM C 496 procedures. Figure 3.9 shows the split tension test results for low w/c ratio concrete materials incorporating virgin, recycled and blended aggregates, with and without milled waste glass. Figure 3.10 shows the split tensile strength test results for the corresponding concrete materials with high w/c ratio. Figure 3.11 shows the split tensile strength test results for fly ash concrete materials.

Comparisons between the split tensile strengths of milled waste glass and Class-F fly ash concrete materials are presented in Figure 3.12.

Statistical analysis (of variance) and of split tension test results indicated that the contributions of milled waste glass towards the split tensile strength of low and high water w/c ratio concrete materials at 120 and 200 days of age were statistically significant (at 95% confidence level). This trend is similar to that observed in the case of flexural strength. The split tensile strength of the Class-F fly ash concrete materials was higher than the Class-C fly ash concrete materials at both ages considered here. This contrast between the two classes of fly ash were found to be statistically significant for concrete materials incorporating virgin and recycled aggregates, but not blended aggregates. Statistical comparison of concrete materials with Class-F fly ash and milled waste glass (Figure 3.12) indicated that their split tensile strengths were statistically comparable in the case of normal aggregate concrete materials; the effect of milled waste glass on split tensile strength was, however, superior to that of Class-F fly ash in the case of recycled aggregate concrete materials. This important finding points at the particularly high effectiveness of milled waste glass in recycled aggregate concrete, which can be attributed to the presence of two interfacial transition zones of relatively high porosity and CH content in recycled aggregate concrete, where the pozzolanic reactions of milled waste glass yield particular benefits. When compared with Class-C fly ash, milled waste glass produced enhanced benefits to split tensile strength (at 95% level of confidence) at both ages considered (120 and 200 days).

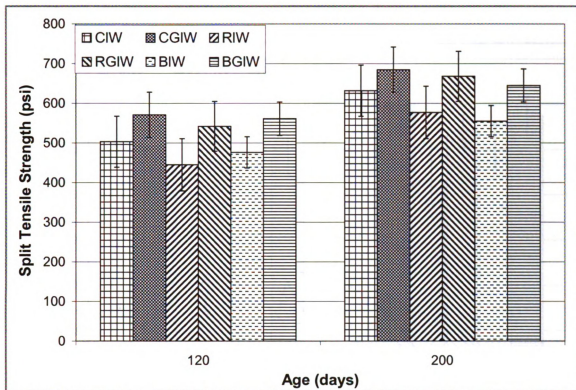


Figure 3.9 Split tensile strengths at different ages of low w/c ratio concrete materials with and without milled waste glass (means & standard errors)

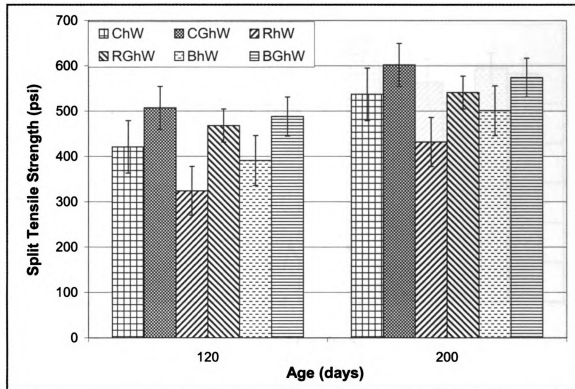


Figure 3. 10 Split tensile strengths at different ages of high w/c ratio concrete materials with and without milled waste glass (means & standard errors)

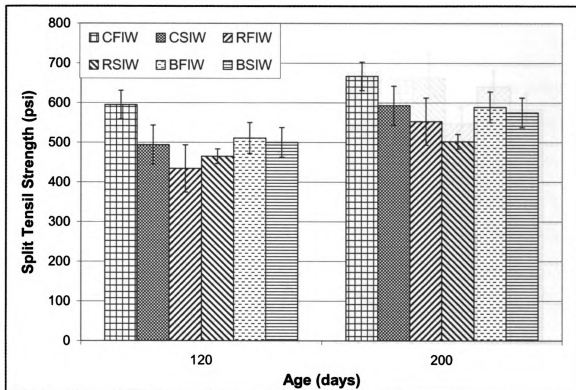


Figure 3. 11 Split tensile strengths at different ages of fly ash concrete materials (means & standard errors)

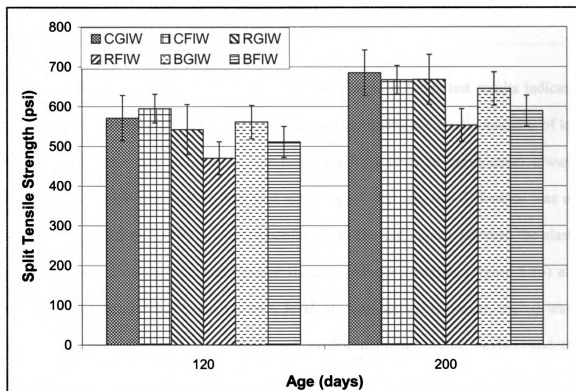


Figure 3. 12 Split tensile strengths at different ages of milled waste glass and Class-F fly ash concrete materials (means & standard errors)

### 3.5.2.5 Modulus of Elasticity

For each of the mix designs given in Tables 2.3 and 2.4, the concrete static modulus of elasticity (chord modulus) was measured using cylindrical specimens with 203 mm (8 in.) height and 102 mm (4 in.) diameter at 90 days of age. This test was carried out following the provisions of ASTM C 469. Figure 3.13 shows the elastic modulus test results for low w/c ratio concrete materials with and without milled waste glass. Figure 3.14 shows the results of elastic modulus tests for the corresponding high w/c ratio concrete materials with and without milled waste glass. The elastic modulus test results for fly ash concrete materials are given in Figure 3.15, and Figure 3.16 presents a

comparison between elastic moduli of milled waste glass and Class-F fly concrete materials.

Statistical analysis (of variance) of the elastic modulus test results indicated that the contributions of milled waste glass towards increasing the elastic modulus of low w/c ratio concrete was statistically significant (at 95% level of confidence) towards increase in stiffness was higher than that with Class-C fly ash, this difference was not statistically significant (at 95% level of confidence). The differences between the elastic moduli of milled waste glass and Class-F fly ash concrete materials (Figure 3.16) also were not statistically significant (at 95% level of confidence). However, milled waste glass, when compared with Class-C fly ash produced higher elastic moduli, and this effect was statistically significant (at 95% level of confidence).

The gains in elastic modulus of concrete with partial replacement of cement with milled waste glass can be attributed to the improvements of the interfacial transition zone and the hydrated cement paste structure due to the pozzolanic reactions of glass. It is worth mentioning that the elastic modulus of concrete is strongly influenced by the interfacial transition zone. The pozzolanic reactions tend to increase the density of hardened concrete (Table 3.3) due to the lowered porosity of hydrated cement paste and interfacial transition zone, noting that an inverse relationship exists between the porosity and elastic modulus.

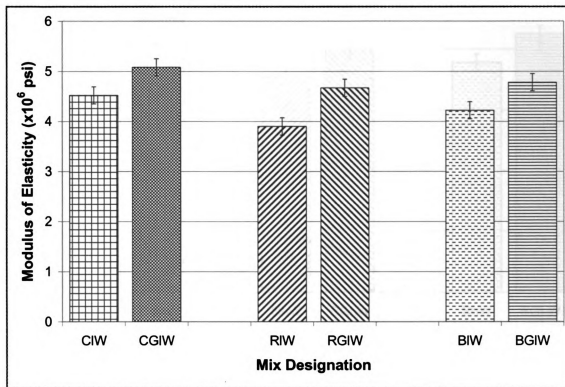


Figure 3. 13 Elastic moduli of low w/c ratio concrete materials with and without milled waste at 90 days of age (means & standard errors)

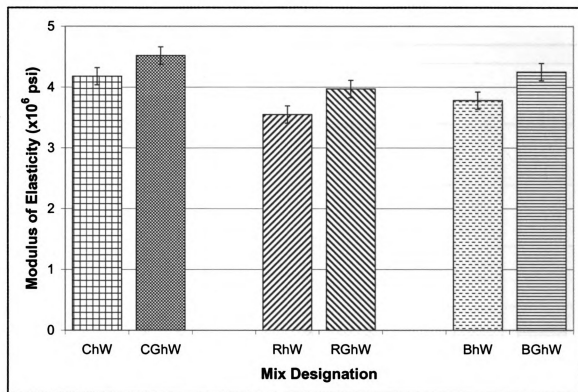


Figure 3. 14 Elastic moduli of high w/c ratio concrete materials with and without milled waste glass at 90 days of age (means & standard errors)

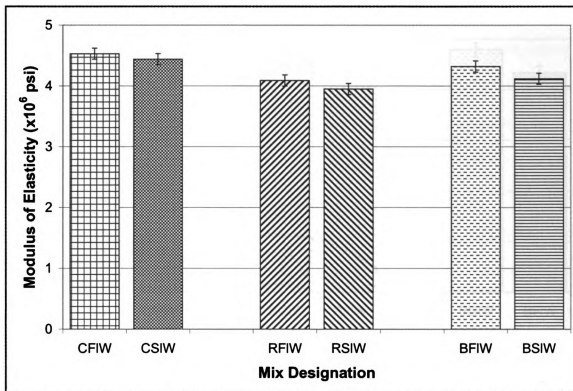


Figure 3. 15 Elastic moduli of fly ash concrete materials at 90 days of age (means & standard errors)

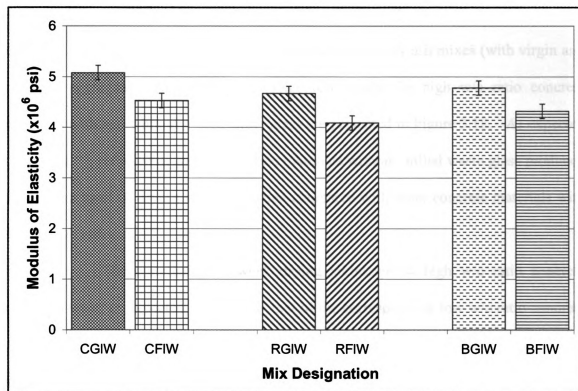


Figure 3. 16 Elastic moduli of milled waste glass versus Class-F fly ash concrete materials at 90 days of age (means & standard errors)

### 3.5.2.6 Drying Shrinkage

Concrete prisms with 76 mm (3 in.) square cross-section and 286 mm (11.25 in.) length were prepared in accordance with the practice described in ASTM C 192 for all the mix designs presented in Tables 2.3, and some mixes of Table 2.4. Specimens were subsequently cured in lime-saturated water at  $23 \pm 0.5$  °C ( $73 \pm 1$  °F) after taking an initial comparator reading at the age of 24 hrs. Drying shrinkage tests were carried out in accordance with the ASTM C 157 and C 490 procedures on a weekly basis up to the age of 20 weeks. For each concrete mix, three specimens were prepared, and each reading represents the average of three readings.

Figure 3.17 shows the drying shrinkage test results for low w/c ratio concrete materials with and without milled waste glass and Class-F fly ash mixes (with virgin and recycled aggregates). The drying shrinkage test results for high w/c ratio concrete materials with and without milled waste glass are presented in Figure 3.18. As expected (Section 1.7), recycled aggregate concrete materials without milled waste glass produced the highest level of drying shrinkage when compared with other concrete materials with similar w/c ratio.

The cumulative 20-week drying shrinkage of high w/c ratio concrete materials were, as expected, higher than that of the corresponding low w/c ratio concrete materials. The use of milled waste glass as partial replacement for cement resulted in significant reduction of the drying shrinkage concrete materials with virgin, recycled and blended aggregates.

Figures 3.19 and 3.20 show the reductions in 20-week cumulative drying shrinkage of concrete materials with low and high w/c ratios, respectively, resulting from partial replacement of cement with milled waste glass. Statistical analysis (of variance) of the (cumulative) drying shrinkage test results indicated that the control of drying shrinkage movements of low and high w/c ratio concrete materials with milled waste glass as partial replacement for cement was statistically significant (at 95% level of confidence). The use of milled waste glass as partial replacement for cement lowers the drying shrinkage of recycled aggregate concrete below that of normal aggregate concrete without milled waste glass (and this effect was statistically significant at 95% level of confidence). Milled waste glass can thus effectively overcome the problems with large drying shrinkage movements of recycled aggregate concrete. The differences between

drying shrinkage movements of milled waste glass and Class-F fly ash concrete materials (Figure 3.17) were not statistically significant at 95% level of confidence.

The reduced drying shrinkage of concrete materials incorporating milled waste glass as partial replacement for cement can be attributed to the enhanced impermeability of concrete due to reduced porosity and discontinuity of the capillary pore system brought about by the pozzolanic reactions of milled waste glass (Section 2.4). This drop in moisture movement prevents the loss of moisture from mesopores and micropores, including the loss of physically adsorbed water from the cement hydrates which is thought to be the leading cause of drying shrinkage in concrete. The use of milled waste glass also lowers the cement content of concrete mix, which consequently reduces the drying shrinkage of concrete (noting that an inverse relationship exists between cement content and drying shrinkage). The rise in the elastic modulus of concrete with the use of milled waste glass as partial replacement of cement (Section 3.5.2.5) is another contributing factor towards the reduction of drying shrinkage with introduction of milled waste glass, noting that drying shrinkage reportedly decreases as the elastic deformations of concrete decrease.

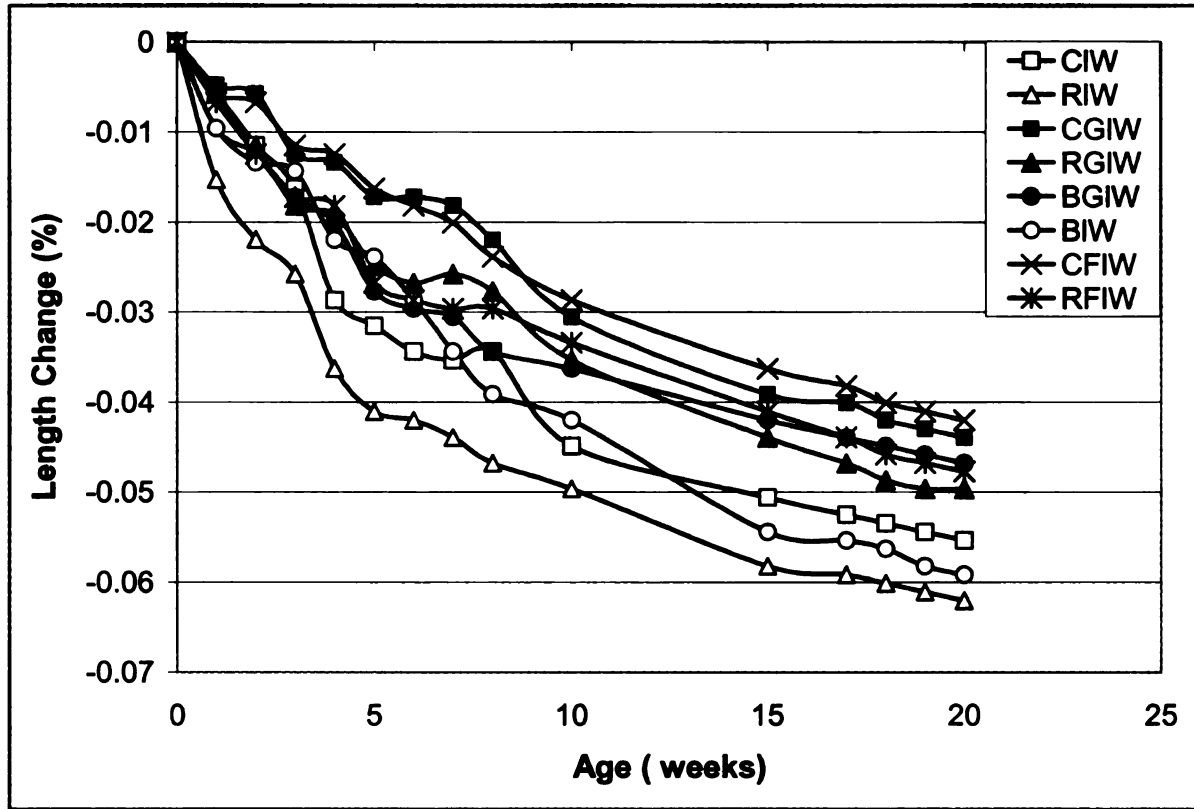


Figure 3. 17 Drying shrinkage versus time of low w/c ratio concrete materials with and without milled waste and Class-F fly ash

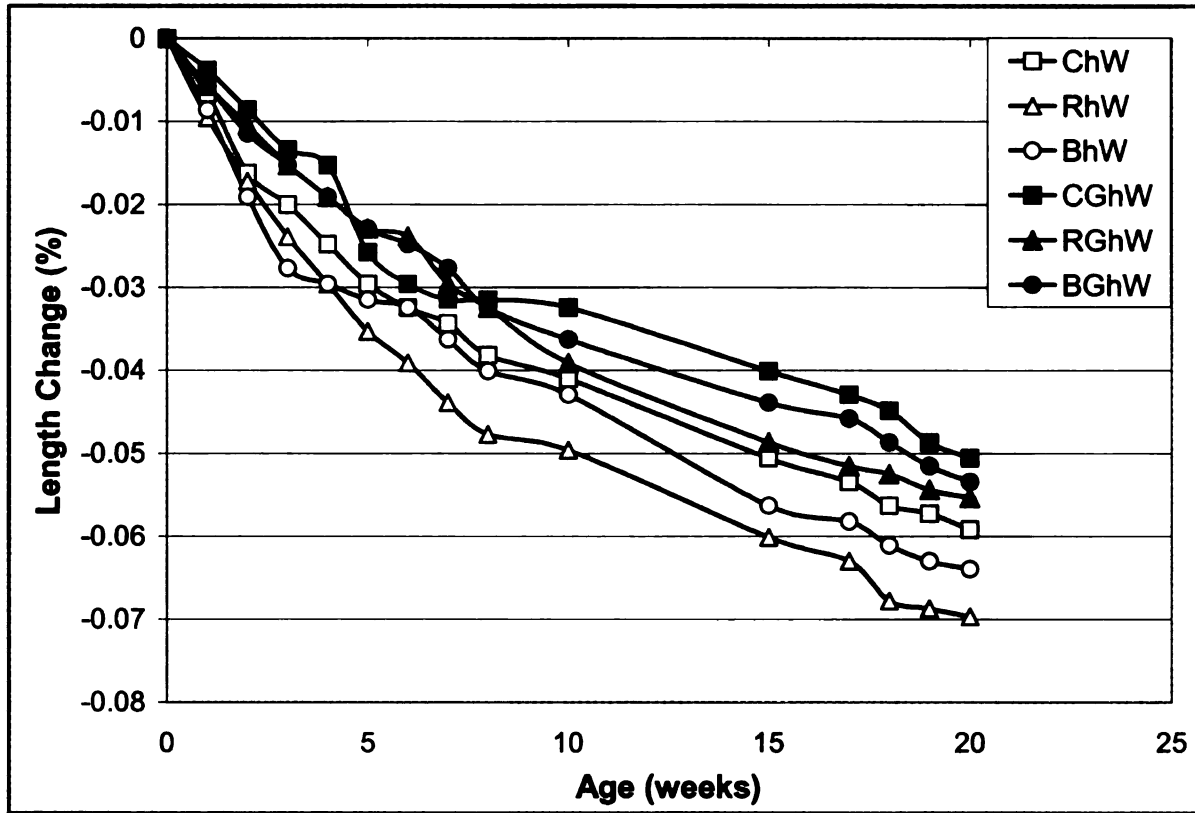


Figure 3. 18 Drying shrinkage versus time of high w/c ratio concrete materials with and without milled waste glass

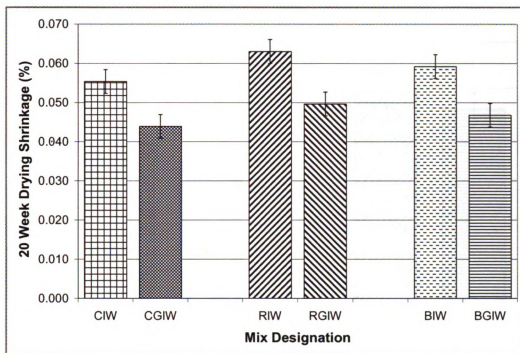


Figure 3. 19 Cumulative 20-week drying shrinkage of low w/c ratio concrete materials with and without milled waste glass (means & standard errors)

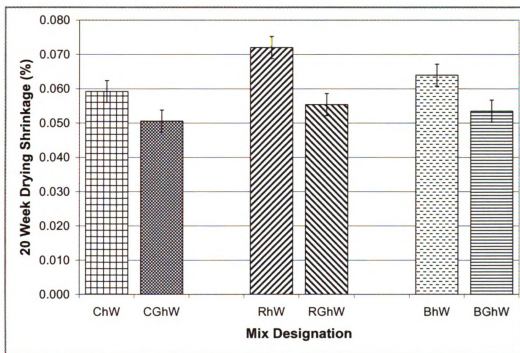


Figure 3. 20 Cumulative 20-week drying shrinkage of high w/c ratio concrete materials with and without milled waste glass (means & standard errors)

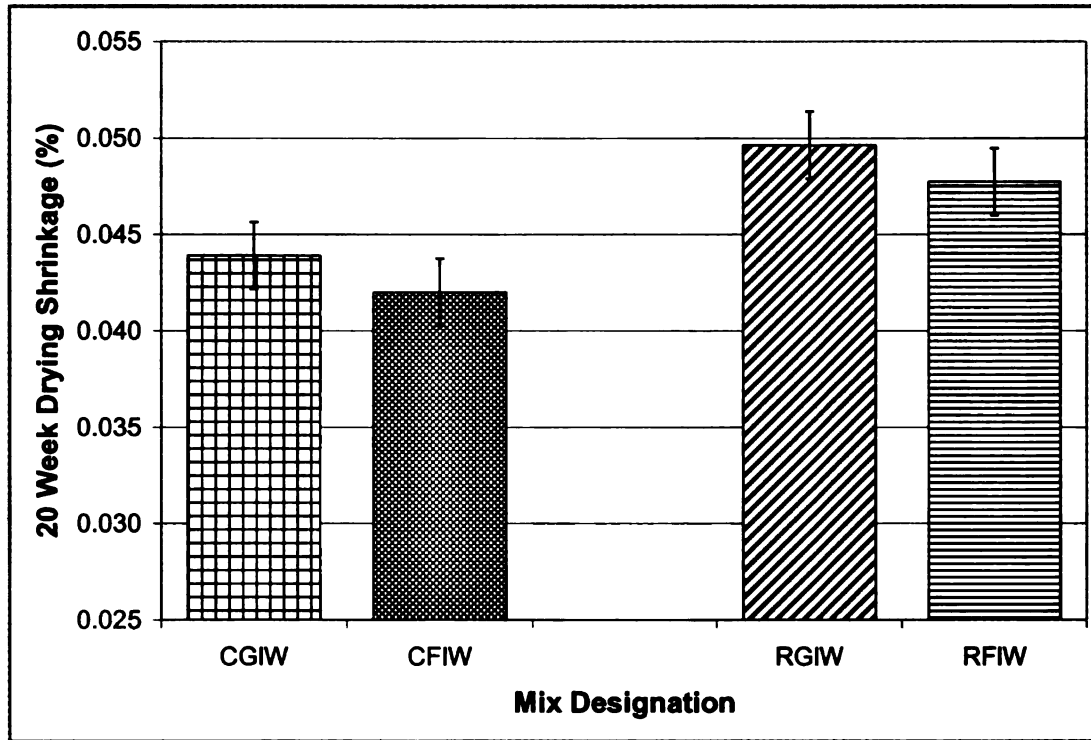


Figure 3. 21 Cumulative 20-week drying shrinkage of milled waste glass and class-F fly ash concrete materials (means & standard errors)

## REFERENCES

1. Mukai, T., Kikuchi, M., and Ishikawa, N., *Fundamental study on bond properties between recycled aggregate concrete and steel bars* 1978, Cement Association of Japan.
2. Buck, A.D., *Recycled concrete as source of aggregate*. ACI Materials Journal, 1977: p. 212-219.
3. Hansen, T.C. and H. Narud, *STRENGTH OF RECYCLED CONCRETE MADE FROM CRUSHED CONCRETE COARSE AGGREGATE*. Concrete International, 1983. 5(Compendex): p. 79-83.
4. Malhotra, V.M. *Use of recycled concrete as new aggregate*. in *Energy and Resource Conservation in the Cement and Concrete Industry*. 1978. Ottawa.
5. Rasheeduzzafar and Khan, A., *Recycled Concrete- A source of new aggregate*. Journal of Cement, Concrete and Aggregates 1984. 6(1): p. 17-27.
6. Ravindrarajah Sri, R., Y.H. Loo, and C.T. Tam, *RECYCLED CONCRETE AS FINE AND COARSE AGGREGATES IN CONCRETE*. Magazine of Concrete Research, 1987. 39(Compendex): p. 214-220.
7. Fathifazl, G., et al., *Proportioning Concrete Mixtures with Recycled Concrete Aggregate: A novel method*. Concrete International, 2010: p. 37.
8. B.C.S.J, *Study on recycled aggregate and recycled aggregate concrete*. Concrete Journal, Japan, 1978. 16(7): p. 18-31.
9. Cuttell, G.D., et al., *Performance of rigid pavements containing recycled concrete aggregates*. Transportation Research Record, 1996(Compendex): p. 89-98.
10. Hansen, T.C., *RECYCLED AGGREGATES AND RECYCLED AGGREGATE CONCRETE SECOND STATE-OF-THE-ART REPORT DEVELOPMENTS 1945-1985*. Materials and Structures/Materiaux et Constructions, 1986(Compendex): p. 201-246.
11. Hansen, T.C., *Recycled concrete aggregate and fly ash produce concrete without portland cement*. Cement and Concrete Research, 1990. 20(Compendex): p. 355-356.
12. Hansen, T.C. and S.E. Hedegard, *PROPERTIES OF RECYCLED AGGREGATE CONCRETES AS AFFECTED BY ADMIXTURES IN ORIGINAL CONCRETES*. Journal of the American Concrete Institute, 1984. 81(Compendex): p. 21-26.

13. Nixon, P., *Recycled concrete as an aggregate for concrete—a review*. Materials and Structures, 1978. **11**(5): p. 371-378.
14. Ravindrajah Sri, R., Y.H. Loo, and C.T. Tam, *STRENGTH EVALUATION OF RECYCLED-AGGREGATE CONCRETE BY IN-SITU TESTS*. Materials and Structures/Materiaux et Constructions, 1988. **21**(Compendex): p. 289-295.
15. Ravindrarahaj, R.S., *Utilization of waste concrete for new construction*. Conservation and Recycling, 1987. **10**(Compendex): p. 69-74.
16. Tavakoli, M. and P. Soroushian, *Strengths of recycled aggregate concrete made using field-demolished concrete as aggregate*. ACI Materials Journal, 1996. **93**(Compendex): p. 182-190.
17. Topçu, I.B., *Physical and mechanical properties of concretes produced with waste concrete*. Cement and Concrete Research, 1997. **27**(12): p. 1817-1823.
18. Torii, K., et al., *APPLICABILITY OF RECYCLED CONCRETE AGGREGATE AS AN AGGREGATE FOR CONCRETE PAVEMENT*. 1985. **6**(Compendex): p. 133-140.
19. Katz, A., *Properties of concrete made with recycled aggregate from partially hydrated old concrete*. Cement and Concrete Research, 2003. **33**(5): p. 703-711.
20. Kheder, G.F. and S.A. Al-Windawi, *Variation in mechanical properties of natural and recycled aggregate concrete as related to the strength of their binding mortar*. Materials and Structures/Materiaux et Constructions, 2005. **38**(Compendex): p. 701-709.
21. Kou, S.C. and C.S. Poon, *Mechanical properties of 5-year-old concrete prepared with recycled aggregates obtained from three different sources*. Magazine of Concrete Research, 2008. **60**(Compendex): p. 57-64.
22. Kou, S.C., et al. *Hardened properties of recycled aggregate concrete prepared with fly ash*. in *International Conference on Sustainable Waste Management and Recycling, September 14, 2005 - September 15, 2005*. 2004. London, United kingdom: Thomas Telford Services Ltd.
23. Limbachiya, M., T. Leelawat, and R. Dhir, *Use of recycled concrete aggregate in high-strength concrete*. Materials and Structures, 2000. **33**(9): p. 574-580.
24. Dhir, R.K., K.A. Paine, and S. O'Leary. *Use of recycled concrete aggregate in concrete pavement construction: A case study*. in *Sustainable Waste Management, Proceedings of the International Symposium, September 9, 2003 - September 11, 2003*. 2003. Dundee, United kingdom: Thomas Telford Services Ltd.

25. Anon, *Recycled concrete aggregate*. Concrete 2005. **39**(5).
26. Tavakoli, M. and P. Soroushian, *Drying shrinkage behavior of recycled aggregate concrete*. Concrete International, 1996. **18**(Compendex): p. 58-61.
27. Shayan, A. and A. Xu, *Performance and Properties of Structural Concrete made with Recycled Concrete Aggregate*. ACI Materials Journal, 2003. **100**(Compendex): p. 371-380.
28. Kou, S.C., C.S. Poon, and C. Dixon, *Influence of fly ash as cement replacement on the properties of recycled aggregate concrete*. Journal of Materials in Civil Engineering, 2007. **19**(Compendex): p. 709-717.
29. Hansen, T.C., ed. *Recycling of demolished concrete and masonry* 1992, Taylor & Francis. 336.
30. Frondistou -Yannas, S., *Waste concrete as aggregate for new concrete*. ACI Materials Journal, 1977. **373-376**.
31. Ravindrarajah Sri, R., *Properties of concrete made with crushed concrete as coarse aggregate*. Magazine of Concrete Research, 1985. **37**(130).
32. Kou, S.C., C.S. Poon, and D. Chan, *Influence of fly ash as a cement addition on the hardened properties of recycled aggregate concrete*. Materials and Structures/Materiaux et Constructions, 2008. **41**(Compendex): p. 1191-1201.
33. Hasaba, S., Kawamura, M., and Toriik, K. et al *Drying shrinkage and durability of concrete made of recycled concrete aggregates*. Japan Concrete Institute, 1981. **3**: p. 55-60.
34. Hansen, T.C. and E. Boegh, *ELASTICITY AND DRYING SHRINKAGE OF RECYCLED-AGGREGATE CONCRETE*. Journal of the American Concrete Institute, 1985. **82**(Compendex): p. 648-652.
35. Sagoe-Crentsil, K.K., T. Brown, and A.H. Taylor, *Performance of concrete made with commercially produced coarse recycled concrete aggregate*. Cement and Concrete Research, 2001. **31**(Compendex): p. 707-712.
36. Dyer, T.D. and R.K. Dhir, *Chemical reactions of glass cullet used as cement component*. Journal of Materials in Civil Engineering, 2001. **13**(Compendex): p. 412-417.
37. Dhir, R.K.a.D., T. D. , *Maximising Opportunities for Recycling Glass, in Sustainable Waste Management and Recycling: Glass Waste*, M.C.L.a.J.J. Roberts, Editor. 2004, Thomas Telford: London.

38. Shayan, A. and A. Xu, *Value-added utilisation of waste glass in concrete*. Cement and Concrete Research, 2004. **34**(Compendex): p. 81-89.
39. Shi, C., et al., *Characteristics and pozzolanic reactivity of glass powders*. Cement and Concrete Research, 2005. **35**(Compendex): p. 987-993.
40. Polley, C., S.M. Cramer, and R.V. de la Cruz, *Potential for using waste glass in Portland cement concrete*. Journal of Materials in Civil Engineering, 1998. **10**(Compendex): p. 210-219.
41. Schwarz, N., H. Cam, and N. Neithalath, *Influence of a fine glass powder on the durability characteristics of concrete and its comparison to fly ash*. Cement and Concrete Composites, 2008. **30**(6): p. 486-496.
42. Shayan, A. and A. Xu, *Performance of glass powder as a pozzolanic material in concrete: A field trial on concrete slabs*. Cement and Concrete Research, 2006. **36**(Compendex): p. 457-468.
43. Zhu, H. and E. Byars, *Potential for use of waste glass in concrete*. Concrete (London), 2005. **39**(Compendex): p. 41-45.
44. Zhu, H. and E. Byars. *Post-consumer glass in concrete: Alkali-silica reaction and case studies*. in *International Conference on Sustainable Waste Management and Recycling, September 14, 2005 - September 15, 2005*. 2004. London, United kingdom: Thomas Telford Services Ltd.
45. Dyer, T.D.a.D., R. K. *Use of glass cullet as a cement replacement*. in *Recycling and Reuse of Glass Cullet*. 2001. Dundee, Scotland: Thomas Telford.
46. Shao, P.L.a.Y., *Feasibility of using ground waste glass as cementitious material*, in *Recycling and Reuse of Glass Cullet*. 2001, Thomas Telford: Dundee, Scotland.
47. Salem, R.M. and E.G. Burdette, *Role of chemical and mineral admixtures on physical properties and frost-resistance of recycled aggregate concrete*. ACI Materials Journal, 1998. **95**(Compendex): p. 558-563.
48. Salem, R.M., E.G. Burdette, and N.M. Jackson, *Resistance to freezing and thawing of recycled aggregate concrete*. ACI Materials Journal, 2003. **100**(Compendex): p. 216-221.
49. Mindess S., Y.J.F., and Darwin D., *Concrete*. Second ed. 2003: Prentice Hall.
50. Neville, A.M., *Properties of Concrete*. 4th ed. 2000: Pearson Education.

## **CHAPTER 4**

### **Effects of Milled Waste Glass As Partial Replacement for Cement on the Durability Characteristics of Normal and Recycled Aggregate Concrete**

It is essential that a concrete-based infrastructure system continue to perform their intended functions over a relatively long service life. Such desired long-term performance can be ensured if concrete is able to withstand the deteriorating processes to which it is expected to be exposed during its life. The ACI Committee 201 defines the durability of Portland cement concrete as its ability to resist weathering action, chemical attack, abrasion, and any other relevant deteriorating conditions. Until recently, the developments in cement and concrete technology concentrated on producing stronger concrete, assuming that a stronger concrete is also more durable [1-3]. Given the growing emphasis on the life-cycle economy and the sustainability of infrastructure systems, the durability characteristics of concrete are receiving more careful considerations. Through durable construction, the increasing repair and replacement costs of infrastructure systems can be avoided, noting that up to 40% of total construction resources in industrially developed countries are devoted to repair and replacement activities (in lieu of new construction) [2]. Conservation of natural resources through durable construction is also an ecological step forward. Generally, a properly proportioned, well placed, and cured concrete can perform reasonably well in most natural environments. However, there have been instances of premature deterioration of concrete-based infrastructure systems that have led to a growing emphasis on controlling the factors responsible for concrete durability.

Lack of durability can be caused by external factors or by internal phenomena within concrete. Causes of concrete deterioration over time can be physical, chemical, mechanical or a combination thereof. The physical effects that influence the durability of concrete include surface wear, cracking due to crystallization of salts in pores, and exposure to extreme temperatures such as frost and fire. The difference in thermal expansion of aggregate and hydrated cement paste is also a physical cause of concrete deterioration. Chemical reactions of deleterious nature include sulfate attack, alkali-aggregate reaction, carbonation, and corrosion of steel in concrete. Furthermore, the attack by acidic solutions on hydrated cement paste and concrete involves leaching of soluble reaction products from concrete. In general, moisture transport characteristic of concrete is central to most durability problems.

#### **4.1 Durability of Recycled Aggregate Concrete**

As discussed earlier (Sections 1.6, 1.7 and 2.3), due to attachment of old porous mortar/hydrated cement paste, the microstructure of recycled aggregate concrete is in general inferior when compared with that of similar normal concrete. The higher porosity of recycled aggregate and the resulting concrete, and the increased moisture movement in recycled aggregate concrete make it more vulnerable than normal concrete to various causes of deterioration. Durability of recycled aggregate concrete also depends upon the durability characteristics of the original concrete from which recycled aggregates have been obtained [4].

Past researchers have reported diverse findings with regards to the frost resistance of recycled aggregate concrete. Hasaba et al. [5] reported that the freeze-thaw resistance

of air entrained recycled aggregate concrete was always inferior to that of normal concrete. Contrary to the findings of Hasaba et al., Malhotra [6] and Buck [7] did not find significant differences between the freeze-thaw resistance of recycled aggregate concrete when compared with that of normal concrete. Kawamura et al. [8] found lower freeze-thaw resistance for air entrained recycled aggregate concrete than the corresponding normal concrete. Visual inspection of the fracture surfaces of recycled aggregate concrete revealed that deterioration under repeated freeze-thaw cycles took place along the interface between cement mortars and original aggregate particles or within the cement mortar stuck on original aggregate grains. More recent studies of Salem et al. [9] and Salem and Burdette [10] pointed at the relatively low freeze-thaw resistance of recycled aggregate concrete when compared with conventional concrete. They concluded that the inferior freeze-thaw performance of recycled aggregate concrete is due to the higher water absorption of recycled aggregates. They also concluded that, while lowering of w/c ratio was helpful towards resistance against freeze-thaw attack in recycled aggregate concrete, the use of higher fly ash content and air-entrainment was far more beneficial.

The Building Contractor Society of Japan (BCSJ) [11] reports that the rate of carbonation of recycled aggregate concrete made with recycled aggregates that had already suffered carbonation was 65% higher than that of control concrete made with virgin aggregates. BCSJ also concluded that the reinforcement embedded in recycled aggregate concrete may corrode earlier than that in normal concrete. This risk of accelerated corrosion could be offset by producing recycled aggregate concrete with lower w/c ratios. Rasheeduzzafar and Khan [12] studied corrosion of reinforcing steel in concrete slabs made of recycled aggregate concrete versus normal concrete. They found

that, for the same w/c ratio, corrosion of reinforcement was greater in recycled aggregate concrete versus the corresponding normal concrete. Nobuaki et al. [13] also found that recycled aggregate concrete produced with higher w/c ratios had inferior resistance to carbonation when compared with normal concrete materials of similar w/c ratios.

Based on the results of a detailed investigation carried out at Portland Cement Association (PCA) [4], it was concluded that the recycled aggregate used as coarse aggregate in new concrete possesses the potential for Alkali-Silica Reaction (ASR) if the original concrete contained aggregates that were susceptible to ASR. The alkali content of cement hydrates in the new concrete containing recycled aggregate as coarse aggregate was found to have a significant effect on subsequent expansions due to ASR; the use of class-F fly ash in new concrete containing coarse recycled aggregate greatly reduced expansions due to ASR. The alkali content of cement hydrates in original concrete where expansions due to ASR occurred were found to have little bearing on expansions due to ASR in new concrete containing the recycled aggregate from original concrete as coarse aggregate. Shayan and Xu [14] concluded that the ASR performance of recycled aggregates should be tested based on evaluation of the individual sources of recycled aggregates.

Olorunsogo and Padayachee [15] found that the chloride permeability of recycled aggregate concrete increased with increasing replacement level of virgin aggregate with recycled aggregate. Otsuki et al. [13] found that the chloride penetration resistance of recycled aggregate concrete was slightly inferior to that of normal concrete due to the presence of old ITZ and the porous mortar clinging to recycled aggregates. In a more recent work reported by Kou et al. [16-17], chloride ion penetration into recycled

aggregate concrete increased with increasing content of recycled aggregate; the resistance of recycled aggregate concrete against chloride permeation was improved by lowering the w/c ratio and the use of fly ash.

Ravindrarajah and Tam [18] found that the abrasion resistance of recycled aggregate concrete was lower than that of normal concrete. Contrary to their findings, Limbachiya and Mukesh [19] found that the abrasion resistance of recycled aggregate concrete produced with 100% recycled aggregate as coarse aggregate was comparable to that of normal concrete of equivalent 28-day strength. Poon and Chan [20] studied the abrasion and skid resistance of paving blocks prepared with recycled aggregate concrete. These two properties of recycled aggregate concrete paving blocks produced with recycled aggregate (contaminated with broken bricks, ceramic tiles, glass cullet and wood chips) were found to be slightly less than, but still comparable with, those of control concrete.

#### **4.2 Effects of Milled Waste Glass on Durability of Normal and Recycled Aggregate Concrete**

The effects of milled waste glass, as partial replacement for cement, on the durability characteristics of normal and recycled aggregate concrete were evaluated. The effects of milled waste glass on concrete durability were also compared against those of Class-F and Class-C fly ash as partial replacement for cement.

Concrete materials made with three categories of aggregate (virgin, recycled, and blended), with and without milled waste glass (Table 2.3), as well as fly ash concrete materials (Table 2.4) were subjected to chloride permeability, freeze-thaw durability,

abrasion and alkali-silica reaction tests. The experimental methods and test results are presented in the following.

#### **4.2.1 Chloride Permeability**

For the concrete mix designs presented in Tables 2.3 and 2.4, disc specimens with thickness (height) of 50 mm (2 in.) were cut from the mid-height of cylindrical specimens having 100 mm (4 in.) diameter cured for 28 days in lime-saturated water to avoid any peculiarities related to top and bottom surfaces. Chloride permeability tests were carried out in accordance with ASTM C 1202. In this test, the specimens are sandwiched between NaOH (Sodium Hydroxide) and NaCl (Sodium chloride) solutions (Figure 4.1). The driving force for permeation of chloride ions was a 60-V potential applied between the opposite surfaces of the disc specimen. The conductivity of saturated specimens was measured through monitoring of current over the six-hour test period, with the total charge passed at the end of the recorded as the primary test result.

Figure 4.2 shows the rapid chloride permeability test results (charge passed through specimens) for concrete materials of low w/c ratio with and without milled waste glass as partial replacement of cement. Figure 4.3 shows the corresponding chloride permeability test results for concrete materials of high w/c ratio with and with milled waste glass as partial replacement of cement. The chloride permeability values for Class-F and Class-C fly ash concrete materials are shown in Figure 4.4.

In the case of low and high w/c ratio concrete materials, the inclusion of milled waste glass enhances the resistance of concrete to chloride permeation; the number of coulombs passed through the concrete specimens containing milled waste glass is thus

reduced significantly. Statistical analysis (of variance) at 98% confidence level confirmed the significant effect of milled waste glass towards enhancement of concrete resistance to chloride permeation. Statistical analysis (of variance) of the differences in number of coulombs passed through the milled waste glass concrete materials of low w/c ratio and the corresponding Class-F and Class-C fly ash concrete materials were found significant (at 95% confidence level) in favor of milled waste glass concrete materials. According to ASTM C 1202, if the number of coulombs passed lies between 2000 and 4000, the chloride permeability of concrete is considered low, and it is considered very low for the 100 to 1000 range. All low w/c ratio concrete materials (with the exception of recycled aggregate concrete) provided low chloride permeability levels. The recycled aggregate concrete mix containing milled waste glass had the number of coulombs passed slightly over 2000. Nevertheless, inclusion of milled waste glass resulted in 54% reduction of the number of coulombs passed through recycled aggregate concrete specimens when compared with corresponding concrete specimens without milled waste glass. Similar reductions in the charge passed through normal and blended aggregate concrete materials with introduction of milled waste glass were 52% and 53%, respectively. By comparison, the inclusion of Class-F fly ash resulted in 35%, 38%, and 36% reduction of charge passed in normal, recycled aggregate and blended aggregate concretes, respectively.

The enhanced resistance to chloride ion permeation (number of coulombs passed) is brought about by the pore refinement and pore blocking effects of milled waste glass pozzolanic reactions (Section 2.4), noting that the current flow through concrete is a function of pore fluid conductivity. The high resistance to chloride ion permeation

offered by concrete materials incorporating milled waste glass as partial replacement for cement makes them an ideal choice for construction of bridge decks, pavements and parking lots which are frequently exposed to the deleterious effects of deicer salts.

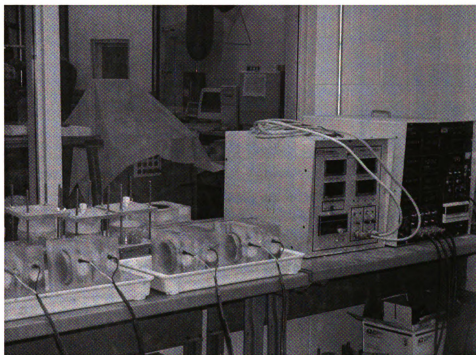


Figure 4. 1 The rapid chloride permeability test setup

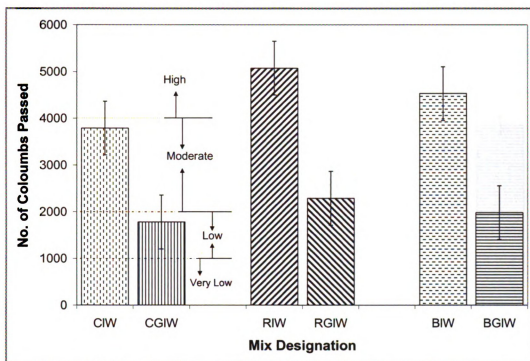


Figure 4.2 Rapid chloride permeability test results for low w/c ratio concrete materials with and without milled waste glass (means & standard errors)

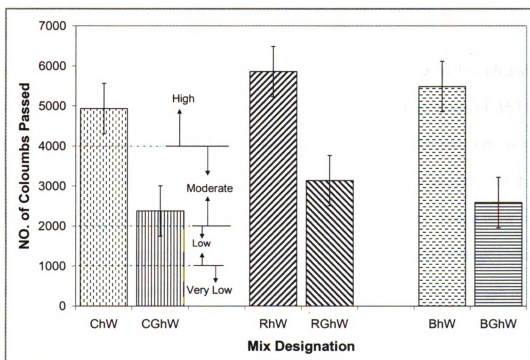


Figure 4.3 Rapid chloride permeability test results for high w/c ratio concrete materials with and without milled waste glass (means & standard errors)

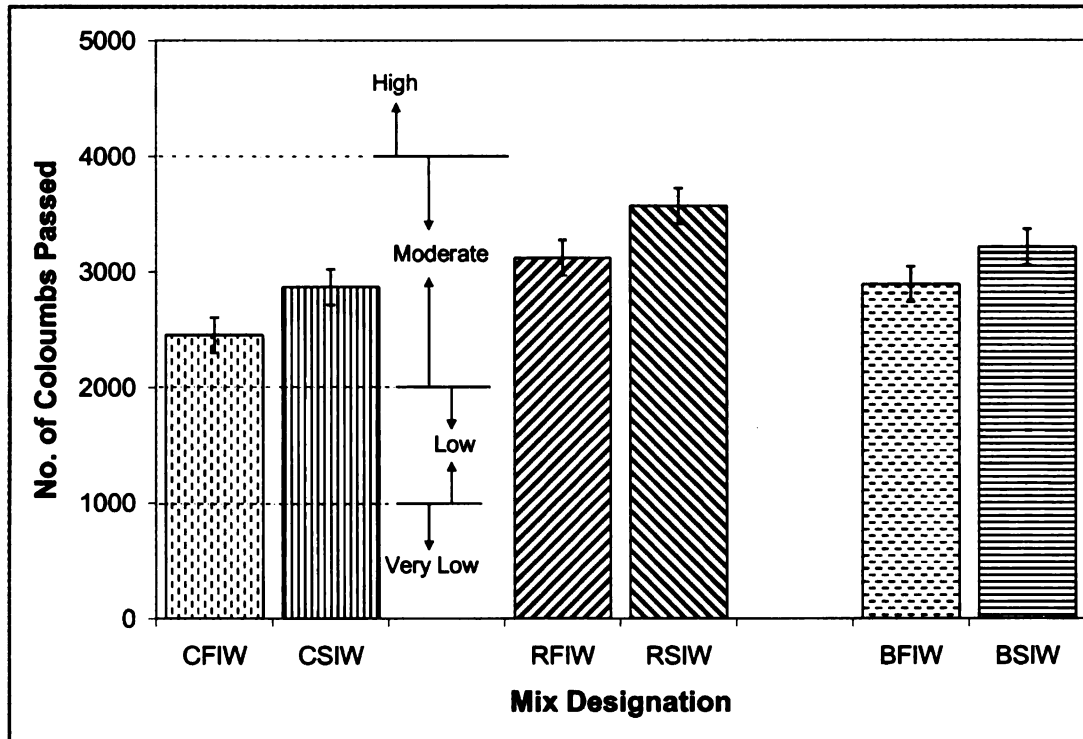


Figure 4. 4 Rapid chloride permeability test results for Class-F and class-C fly ash concrete materials (means & standard errors)

#### 4.2.2 Freeze-Thaw Durability

Freeze-thaw test results carried out on high w/c ratio concrete materials with and without milled waste glass are presented in Table 2.3. Following the provisions of ASTM C 666 (Procedure B), after 42 days of curing, three specimens from each mix were subjected to 310 freeze-thaw cycles. Figure 4.5 shows the plot of time vs. temperature for the freeze-thaw cycle to which the specimens were exposed inside the freeze-thaw chamber. Specimens were weighed before the start of the test, and the weight change under freeze-thaw cycles was recorded at the end of the test. The residual flexural strength of the aged specimens was also measured at the conclusion of the test following the provisions of ASTM C 78.

Increase in weight due to water absorption is an indication of the extent of deterioration of concrete due to cracking under freeze-thaw cycles. Table 4.1 shows the recorded values of weight gain for concrete materials with and without milled waste glass. There is a 52% decrease in cumulative weight gain after 310 freeze-thaw cycles in recycled aggregate concrete (compare the cumulative weight gains of RhW and RGhW) as a result of introducing milled waste glass. The corresponding drops in cumulative weight gain for virgin and blended aggregate concrete mixes were 28% and 45%, respectively.

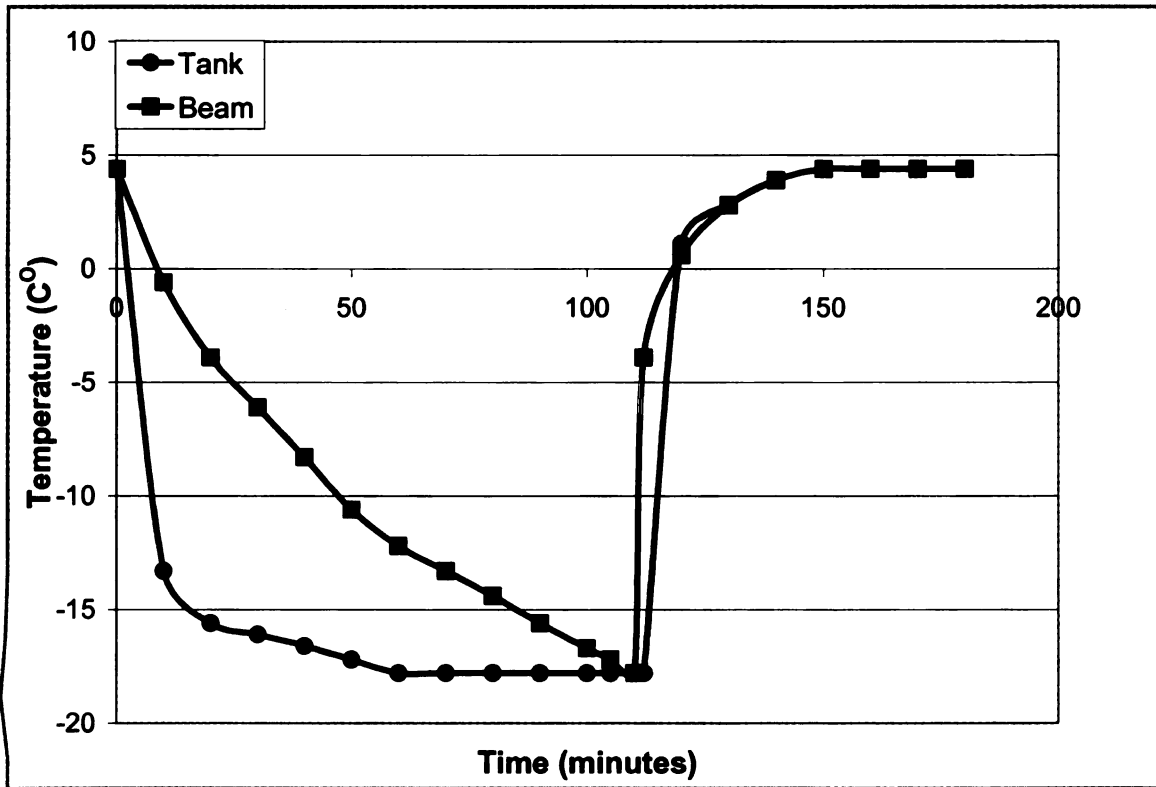


Figure 4. 5 The time-temperature plot of a freeze-thaw cycle

**Table 4. 1 Cumulative percent weight gains for concrete materials with and without glass after 310 freeze-thaw cycles**

Weight gain (%)					
ChW	CGhW	RhW	RGhW	BhW	BGhW
0.40	0.29	0.52	0.25	0.47	0.26

Table 4.2 shows the damage index values of concrete materials with and without milled waste. A damage index value of ‘1’ corresponds to very little damage, whereas a value of ‘5’ represents the worst damage caused due to the freeze-thaw cycles. A damage index value was assigned to each concrete mix based on the extent of visually observed surface damage (cracks, surface flaking, aggregate pop outs and corner chipping) and cumulative weight increase at the end of 310 freeze-thaw cycles.

Figure 4.6 shows the flexural strength test results of the aged and unaged concrete materials with and without milled waste glass. The introduction of milled waste glass is observed to produce a significant increase in residual flexural strength (aged flexural strength) of concrete materials made with virgin, recycled and blended aggregates. Statistical analysis (of variance) of the test results indicated that the differences in flexural strengths of aged specimens with and without milled waste glass were statistically significant (at 98% level of confidence) in favor of concrete materials incorporating milled waste glass.

Table 4. 2 Damage index values for concrete materials with and without milled waste glass

Mix Designs	ChW	CGhW	RhW	RGhW	BhW	BGhW
Damage Index	4	1	5	1	4	2

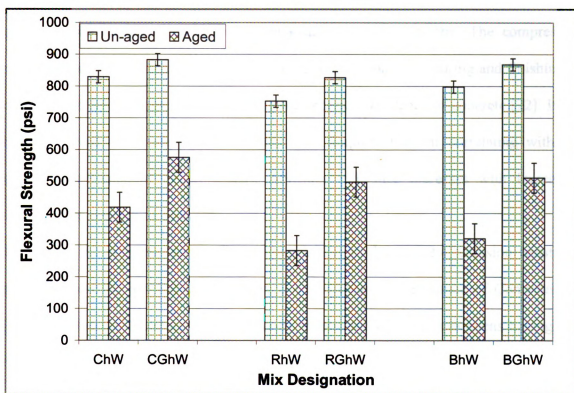


Figure 4. 6 Flexural strength of aged and unaged concrete materials with and without milled waste glass (means & standard errors)

The superior freeze-thaw resistance of concrete materials incorporating milled waste glass is brought about the improvements in the microstructure resulting from the pozzolanic reactions of milled waste glass. The beneficial effects of pore size refinement

and pore discontinuity (Section 2.4) associated with such reactions enhance the freeze-thaw durability of concrete (Sections 5.2 and 5.7).

#### **4.2.3 Abrasion Resistance**

ACI committee 116 defines abrasion as “the ability of a surface to resist being worn away by rubbing and friction” [21]. Wear on above-ground concrete structures can be a result of the wear of concrete floors subjected to movement of heavy loads, the wear of concrete road surfaces due to heavy truck and automobile traffic. The compressive strength of concrete, the quality of aggregates, and the quality of curing and finishing of concrete are the leading factors affecting the abrasion resistance of concrete [22]. It has been observed that compressive strength is an important factor correlating with the abrasion resistance of concrete [23]. Abrasion resistance increases with increasing compressive strength of concrete.

For the concrete mix designs shown in Tables 2.3 and 2.4, abrasion resistance tests were carried out following ASTM C 944 (Abrasion Resistance of Concrete and Mortar Surface by Rotating-Cutter Method). Replicated concrete specimens having 100 mm (4 in.) square cross-sections and 50 mm (2 in.) thickness (height) were subjected to rotating cutters in a drill press that applied a load of 98 N (22 lbf). Tests performed on concrete materials at age of 90 days. Each reading of weight loss due to abrasion was taken after 2 minutes of abrasion, with one set of readings comprising three measurements. Figure 4.7 shows abrasion test results for the low w/c ratio mixes with and without milled waste glass. Figure 4.8 shows the corresponding weight loss

measurements for high w/c ratio mixes with and without milled waste glass. Abrasion test results for the fly ash concrete mixes are shown in Figure 4.9.

The abrasion test results indicate that significant improvements in the abrasion resistance of concrete materials have been realized by the use of milled waste glass as partial replacement of cement. Statistical analysis (of variance) showed the effect of milled waste glass towards enhancement of abrasion resistance was statistically significant (at 95% level of confidence) for low w/c ratio concrete materials. This contribution of milled waste glass was also statistically significant for high w/c ratio concrete materials made with recycled aggregate. Statistical comparison between the abrasion weight loss of Class-F and Class-C fly ash concrete materials indicated the contributions of Class-F fly ash to abrasion resistance were more favorable when compared with those of Class-C fly ash in the case of normal aggregate concrete, but not recycled and blended aggregate concrete materials (at 95% confidence level). Statistically, the differences between the abrasion resistances of milled waste glass concrete and Class-F fly ash concrete were not significant (at 95% level of confidence). The contributions of milled waste glass to abrasion resistance were statistically more significant than those of Class-C fly ash (at 95% level of confidence).

The increase in abrasion resistance of concrete materials incorporating milled waste glass as partial replacement with cement is brought about by the improvements in structure and strength of concrete due to the timely pozzolanic reactions of milled waste glass with cement hydrates.

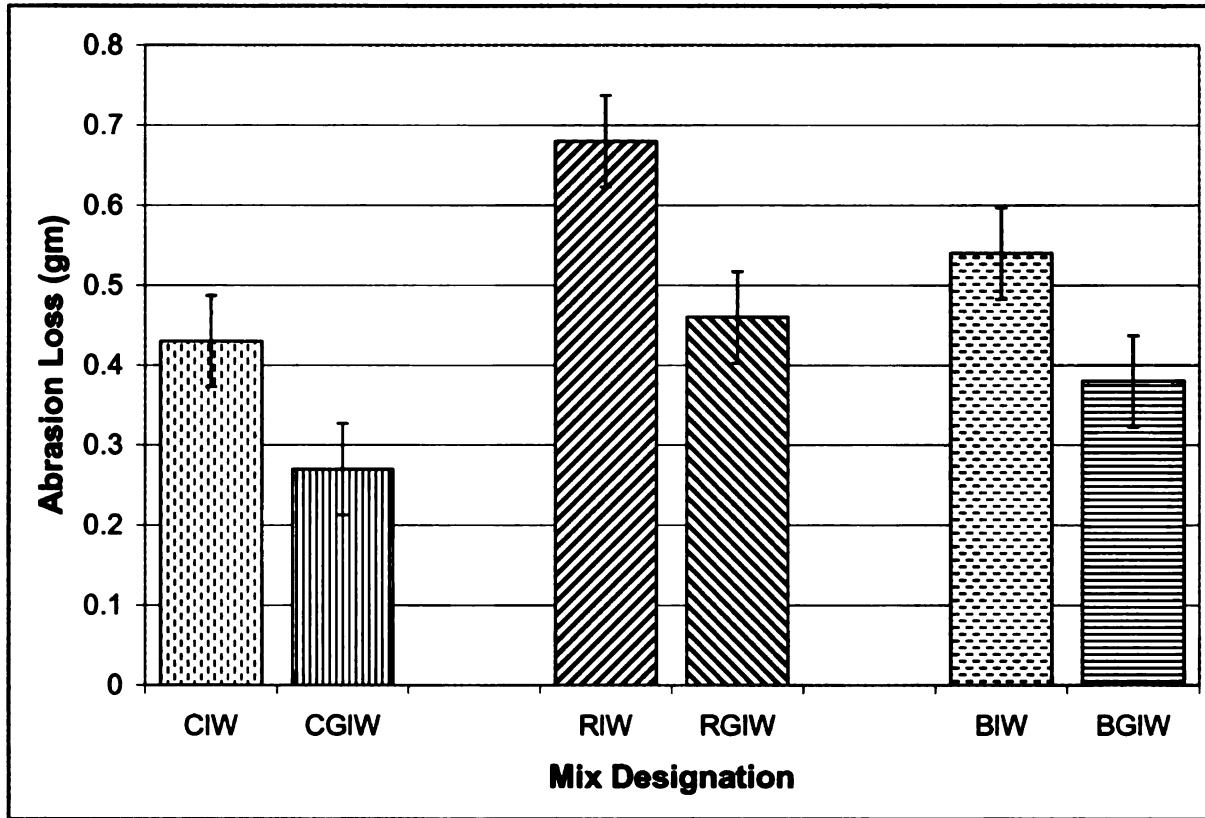


Figure 4. 7 Abrasion weight losses of low w/c ratio concrete materials with and without milled waste glass (means & standard errors)

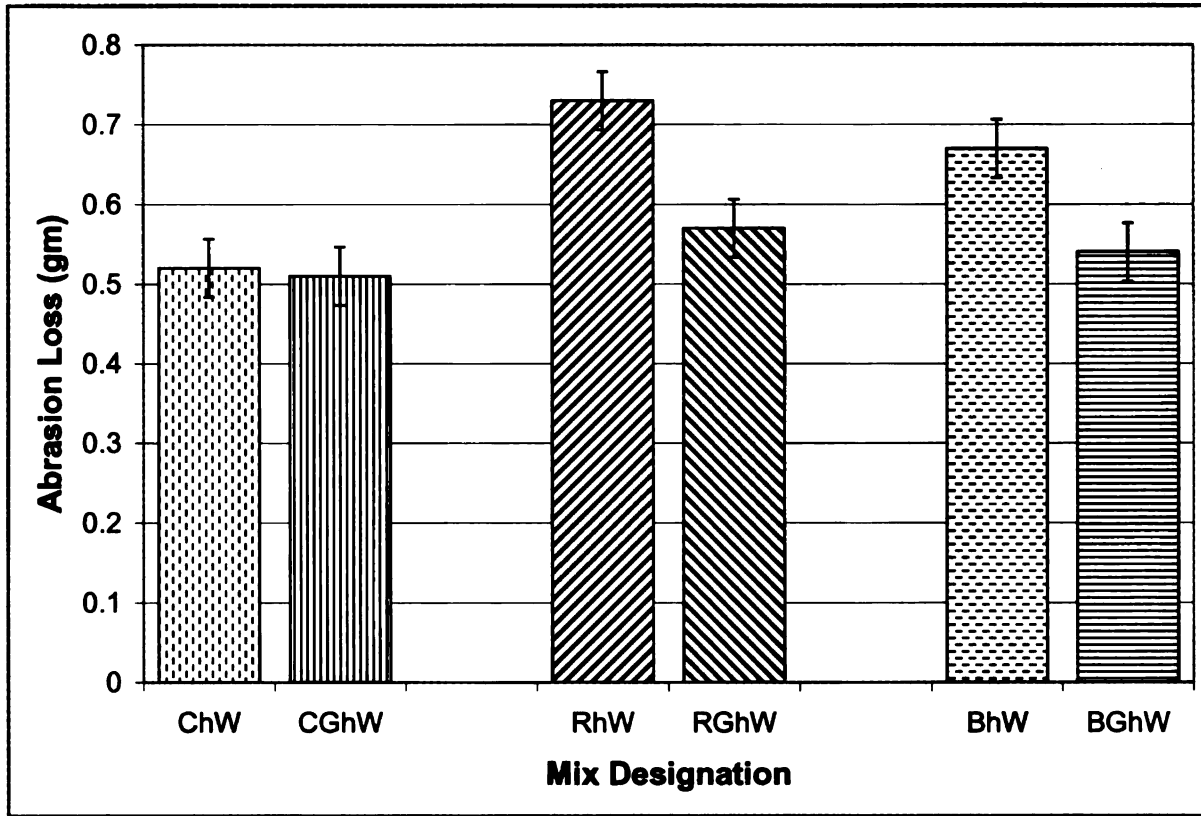


Figure 4. 8 Abrasion weight losses of high w/c ratio concrete materials with and without milled waste glass (means & standard errors)

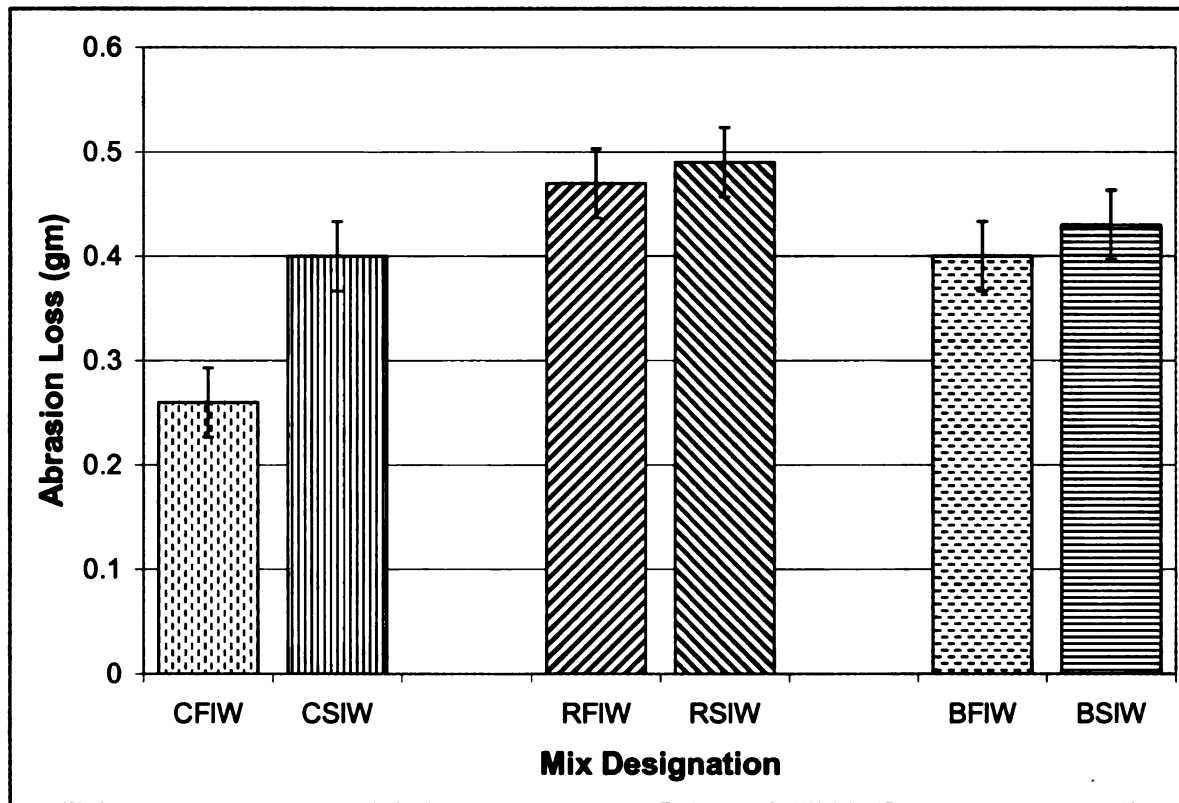


Figure 4. 9 Abrasion weight losses of fly ash concrete materials (means & standard errors)

#### 4.2.4 Alkali-Silica Reactions

Due to the presence of amorphous silica in glass also the alkaline nature of glass ( $\text{Na}_2\text{O} > 13\%$  by mass), the idea of using glass in concrete has traditionally risen concerns regarding the deleterious Alkali-Silica Reactions (ASR) between the highly alkaline pore solution of cement paste and glass [24-30].

The chemical nature of ASR and its subsequent damage in concrete involves a number of steps described as [27]:

- Dissolution of silica and formation of ASR gel
- Swelling of ASR gel through water imbibition
- Expansion and microcracking of concrete

The basic structural unit of silicate glasses is the silicon-oxygen tetrahedron in which a silicon atom is tetrahedrally coordinated to four surrounding oxygen atoms. When silica ( $\text{SiO}_2$ ) is quenched rapidly from molten state, it results in formation of vitreous (glassy) silica with a disordered three-dimensional network. In ASR, the Si-O-Si bond is attacked by the hydroxyl ion ( $\text{OH}^-$ ) present in basic solution. This results in formation of Si-OH bonds with more open “gel-like” structure [27, 31]. This reaction eventually turns into network dissolution. Others [32] have provided a similar account of ASR, according to which, the dissolution of glass in contact with an aqueous solution having a  $\text{pH} > 7$  starts when hydroxyl groups break the siloxane bonds in glass. This process, which strongly depends upon the concentration of alkalis in the aqueous solution, leads to the breakdown of glass structure [33]. Alkali ions, such as  $\text{Na}^+$  and  $\text{K}^+$ , subsequently occupy the available site in the  $\equiv\text{Si-O}^-$  structure [32-33]. This mechanism results in a damaged framework and open gel-like structure that is open to ingress of water, causing subsequent swelling of the leached layer by about 5% [34]. The damaged framework is quite deformable and cannot provide the binding and structural qualities of the key cement hydrate, C-S-H, which has a relatively rigid structure based on Ca-O layers [31].

According to Taylor [31], the chemistry of ASR is similar to that of pozzolanic reaction. Taylor further notes that different effect of ASR vs. pozzolanic reaction in concrete arises mainly from the difference in particle size of the siliceous material. In pozzolanic reaction, the alkali silicate gel is formed in an environment rich in  $\text{Ca}^{2+}$  and, except in a narrow zone close to the reacting surface, is quickly converted into C-S-H. On the contrary, in ASR, it is formed in an environment poor in  $\text{Ca}^{2+}$ , and massive outflows

of gel may result. The cement paste cannot supply  $\text{Ca}^{2+}$  fast enough to prevent much of this gel from persisting for long periods. Essentially, the difference between the deleterious ASR and the beneficial pozzolanic reactions is in the kinetics of the reaction (rapid for pozzolanic and slower for ASR). Both reactions, however, involve the invasion of Si-O-Si structure by the  $\text{OH}^-$  ions and formation of amorphous gel [31].

The fact that glass is capable of undergoing ASR means that it contains a reactive form of silica, implying that it will also undergo pozzolanic reaction with lime produced from the hydration of cement to form cementitious gel products referred to as C-S-H gel [35]. It is to be noted that most of the earlier reported glass-related ASR problems in concrete were associated with the use of coarse glass particles (as replacement of coarse or fine aggregate) in concrete [24-25, 28, 36-37]. Some researchers have determined the pessimum level of fineness (1.18 mm) below which the ASR-related expansion declines significantly. Similarly, others have concluded that the ASR expansion due to the use of glass decreases as the size of glass particle is reduced [38-39]. The color of waste glass has been reported by some researchers to affect the ASR-related expansion (when glass was used as replacement for fine aggregate), with green soda-lime glass causing the least expansion due to the presence of  $\text{Cr}_2\text{O}_3$  [27]. Others have found an opposite trend with green glass causing the maximum expansion due to ASR [34]. The effect of color on ASR expansion therefore remains inconclusive. When used in powder form (80% < 30  $\mu\text{m}$ ) as type-II addition, mixed-color the ASR-related expansion of concrete was reduced below that of control concrete two years of age, and was almost equal to that of control at three years of age. Mixed-color glass powder produced comparable ASR expansion when compared with single-color glass powder [34]. Milling glass to powder size (similar to

cement particle size) increases its surface area that is available for reaction in an environment where much calcium is still available in the solution. Dyer et al. [39] have also stated that the greater space available for gel formation in immature concrete and the resultant uniform distribution of gel probably assist in preventing the deleterious effects encountered in more mature concrete.

In this research, a major ASR experimental program was undertaken on mortar and concrete specimens. Prismatic specimens having 76 mm (3 in.) square cross-section and 286 mm (11.25 in.) length were prepared in accordance with ASTM C 109 for the mortar mixes shown in Table 4.3 and Table 4.4. These mortar mixes were prepared with 0, 10, 20 and 40% replacement of cement with milled waste glass using normal sand (Table 4.3) and reactive sand (Table 4.4). Pure cement paste mixes with 0, 20 and 40% replacement of cement with milled waste glass were also produced.

Table 4.3 Cement paste and mortar mixes with normal sand

Mix Designation	Cement kg (lb)	Milled glass kg (lb)	% Replacement of cement with glass	Sand kg (lb)	W/cm ratio
PG0	4.5 (10)	-	0	-	0.47
PG20	3.63 (8)	0.91 (2)	20	-	0.47
PG40	2.72 (6)	1.81 (4)	40	-	0.47
MSnG0	4.5 (10)	-	0	22.5 (49.59)	0.47
MSnG10	4 (9)	0.45 (1)	10	22.5 (49.59)	0.47
MSnG20	3.63 (8)	0.91 (2)	20	22.5 (49.59)	0.47
MSnG40	2.72 (6)	1.81 (4)	40	22.5 (49.59)	0.47

P = paste, G = glass, M = mortar, Sn = normal sand, W/cm = water to cement ratio

Table 4. 4 Mortar mixes with reactive sand

Mix Designation	Cement kg (lb)	Milled glass kg (lb)	Class-F fly ash kg (lb)	% Replacement of cement with glass	Sand kg (lb)	W/cm ratio
MSrG0	4.5 (10)	-	-	0	22.5 (49.59)	0.47
MSrG10	4 (9)	0.45 (1)	-	10	22.5 (49.59)	0.47
MSrG20	3.63 (8)	0.91 (2)	-	20	22.5 (49.59)	0.47
MSrF20	3.63 (8)	-	0.91 (2)	20	22.5 (49.59)	0.47
MSrG40	2.72 (6)	1.81 (4)	-	40	22.5 (49.59)	0.47

Sr = reactive sand, F = class-F fly ash

#### 4.2.4.1 Mortar Specimens

Prismatic specimens were tested in accordance with the provision of ASTM C 1260 by aging them in a sodium hydroxide (NaOH) solution at 80°C (176°F) continuously for 28 days with intermittent readings of the length change of bars taken during the course of the test. These experiments were prolonged for 28 days (exceeding the standard test period) in order to investigate the ASR-related expansions over longer time periods. Figures 4.10, 4.11, and 4.12 show the results of compressive strength tests carried out (parallel with ASR tests) according to ASTM C 109 for the cementitious paste and mortar materials introduced in Tables 4.3 and 4.4.

The test results presented in Figures 4.10, 4.11 and 4.12 indicate that the compressive strengths of paste and mortar materials incorporating milled waste tend to be less than that of corresponding mixes without milled waste glass. Compressive strength of Class-F fly ash mix is also observed to be less than that of normal mortar mix at both ages. Statistical analysis (of variance) indicated that the difference between the compressive strength of pure cement paste and that with 20% cement replacement with milled waste glass is not statistically significant at 28 and 70 days of age (at 95%

confidence level). With 40% milled waste glass paste, this difference was statistically significant (at 95% confidence level) at both ages. Among mortar materials, the statistical differences between the compressive strengths of normal mortar and those with 10 and 20% milled waste glass were not statistically significant at 70 days of age (at 95% level of confidence). This difference was, however, significant at 40% cement replacement with milled waste glass at 70 days of age. Mortar materials prepared with reactive sand exhibited similar trends in compressive strength when compared with normal sand mortar materials.

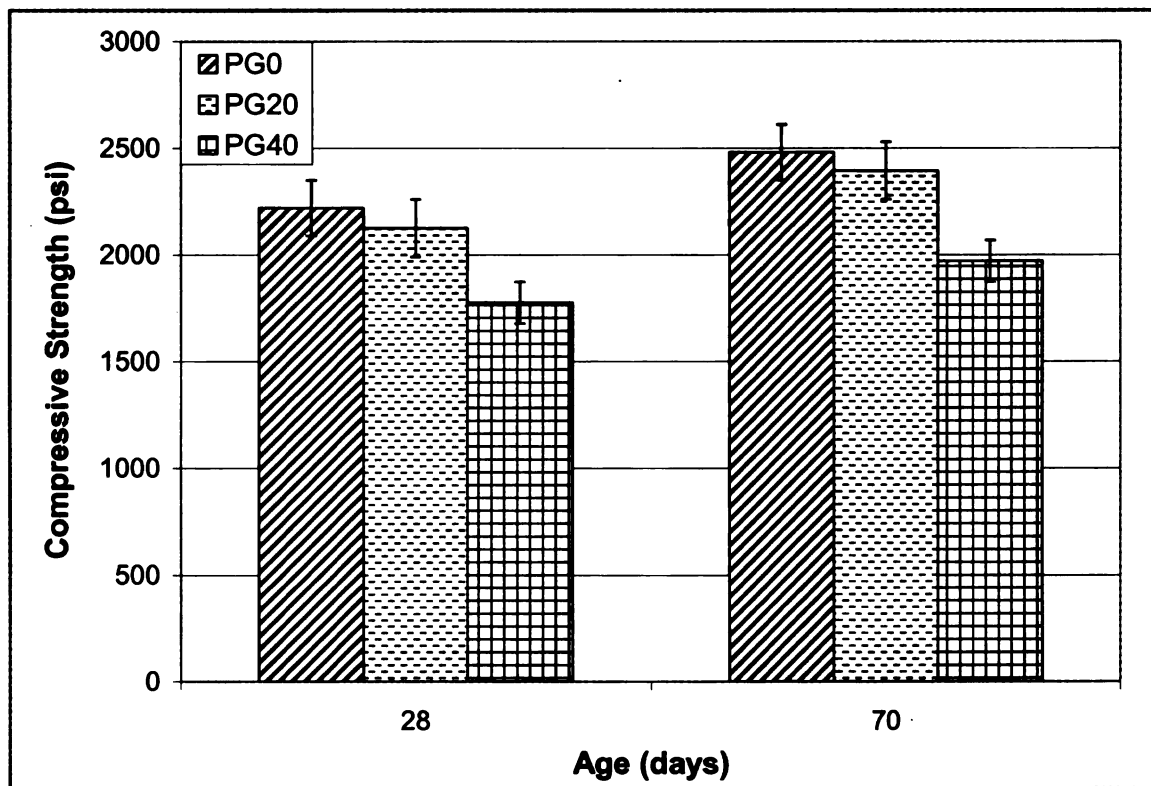


Figure 4. 10 Compressive strength test results at different ages for cement pastes with and without milled waste glass (means & standard errors)

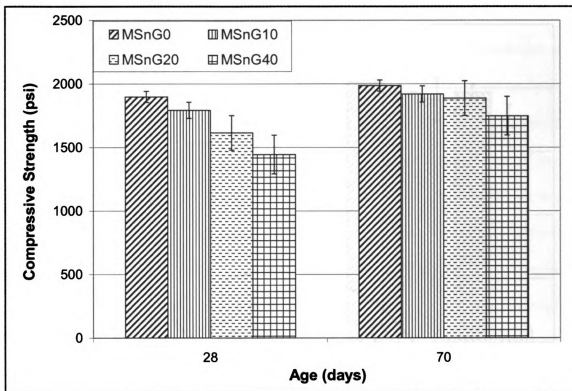


Figure 4. 11 Compressive strength test results at different ages for normal sand mortar mixes with and without milled waste glass (means & standard errors)

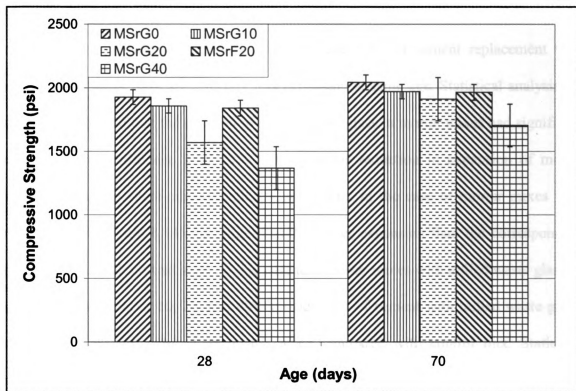


Figure 4.12 Compressive strength test results at different ages for reactive sand mortar mixes with and without milled waste glass (means & standard errors)

Figure 4.13 shows the results of ASR tests performed on mortar materials incorporating normal sand with and without milled waste glass. Similar results for mortar materials prepared with reactive sand are presented in Figure 4.14. According to ASTM C 1260, expansions less than 0.10% at 16 days after casting are indicative of innocuous behavior, while those between 0.10 and 0.20% at the same age are indicative of both innocuous and deleterious behavior in field performance, and expansions more than 0.20% at 16 days of age are indicative of potentially deleterious expansion.

The cumulative length change (expansion) in milled waste glass mortars is significantly less than that of control mortar (with no milled waste glass as partial replacement of cement). Among the normal sand mortars (Figure 4.13), the control

mortar exhibits distinctly higher expansions (although still slightly below 0.10% at 16 days); the corresponding mortars with 10, 20, and 40% of cement replacement with milled waste glass, have significantly less expansion at same age. Statistical analysis (of variance) indicated that the addition of milled waste glass in mortar mixes had significant effect at 98% confidence level ( $p = 0.02$ ) towards reduction in expansion of mortar specimens due to alkali-silica reaction. Control mix in the case of mortar mixes with reactive sand (Figure 4.14), had significantly higher expansion than the corresponding mix produced with normal sand. In this case too, mortar mixes with milled waste glass as cement replacement at 10, 20, and 40% replacement of cement with milled waste glass, exhibit substantially reduced expansion when compared with control mix. Statistical analysis (of variance) indicated, at 98% confidence level ( $p = 0.02$ ), that the inclusion of milled waste glass as partial replacement for cement had significant effect towards reduction of ASR-related expansion. Figures 4.13 & 4.14 suggest that milled waste glass has a suppressing effect on alkali-silica expansion. This effect is brought about by the pozzolanic reaction of milled waste glass with the cement hydrates. The high surface area of milled waste glass controls the kinetics of the reaction in favor of pozzolanic reaction, and utilizes the available alkalis in pore solution prior to their potential utilization towards formation of deleterious alkali-silica gel. Fly ash mortar materials had expansions at 16 days which were similar to those obtained with 20% cement replacement with milled waste glass; at the age of 28 days, however, the fly ash mix had slightly less expansion.

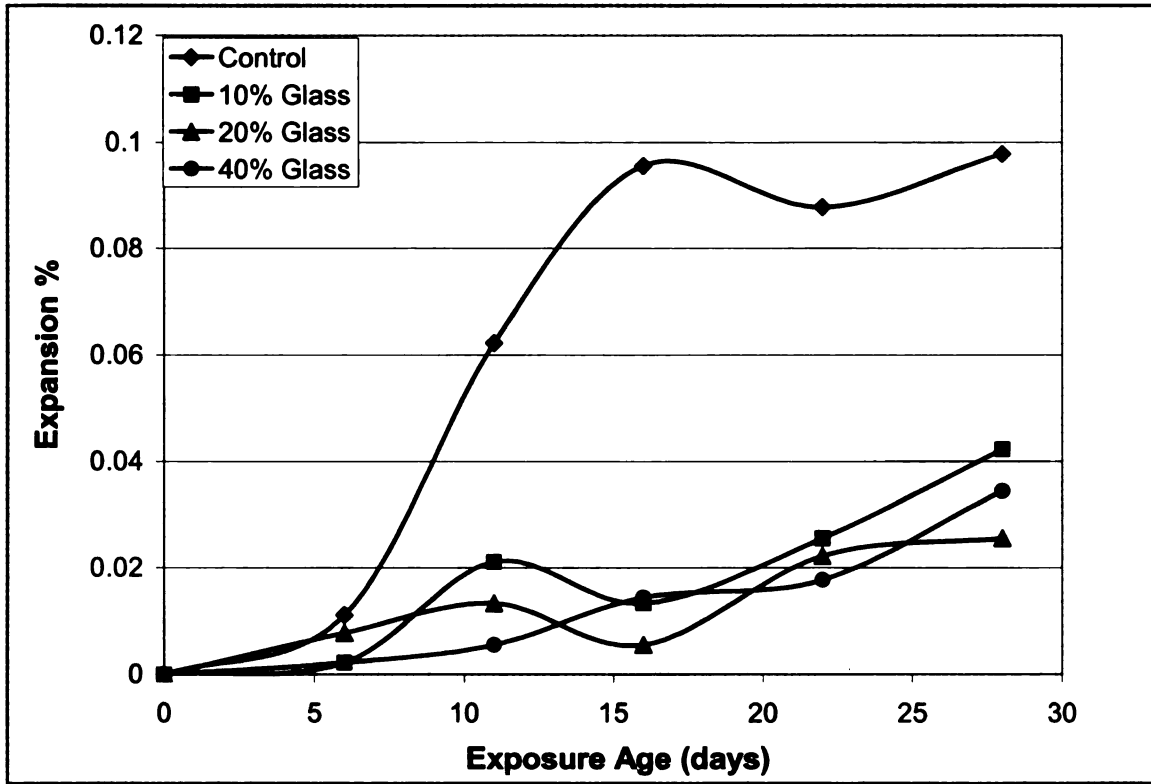


Figure 4. 13 ASR test results for normal sand mortars with and without milled waste glass

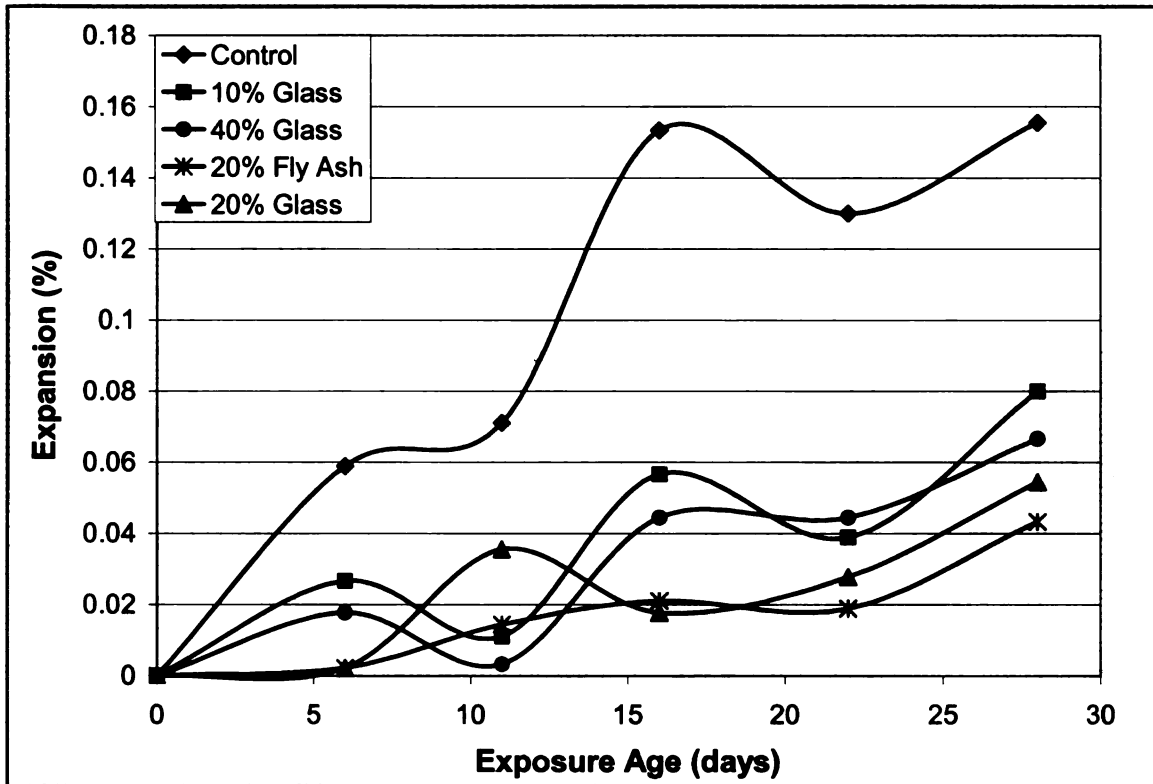


Figure 4. 14 ASR test results for reactive sand mortars with and without milled waste glass

#### 4.2.4.2 Concrete Specimens

ASR tests were also carried out on test specimens prepared from the concrete mixes introduced in Table 2.3. Figure 4.15 shows the ASR test results for the low w/c ratio concrete materials with and without milled waste glass. Test results for the corresponding high w/c ratio concrete materials are presented in Figure 4.16.

At 16 days, all materials had ASR expansions well below the threshold level of 0.10%, indicating innocuous behavior. Even at 28 days, the ASR expansions of these mixes were less than 0.10%. Concrete materials incorporating milled waste glass as partial replacement of cement exhibited smaller expansion than the corresponding

concrete materials without milled waste glass. This is again due to the ASR-suppressing pozzolanic reactions of milled waste glass in concrete.

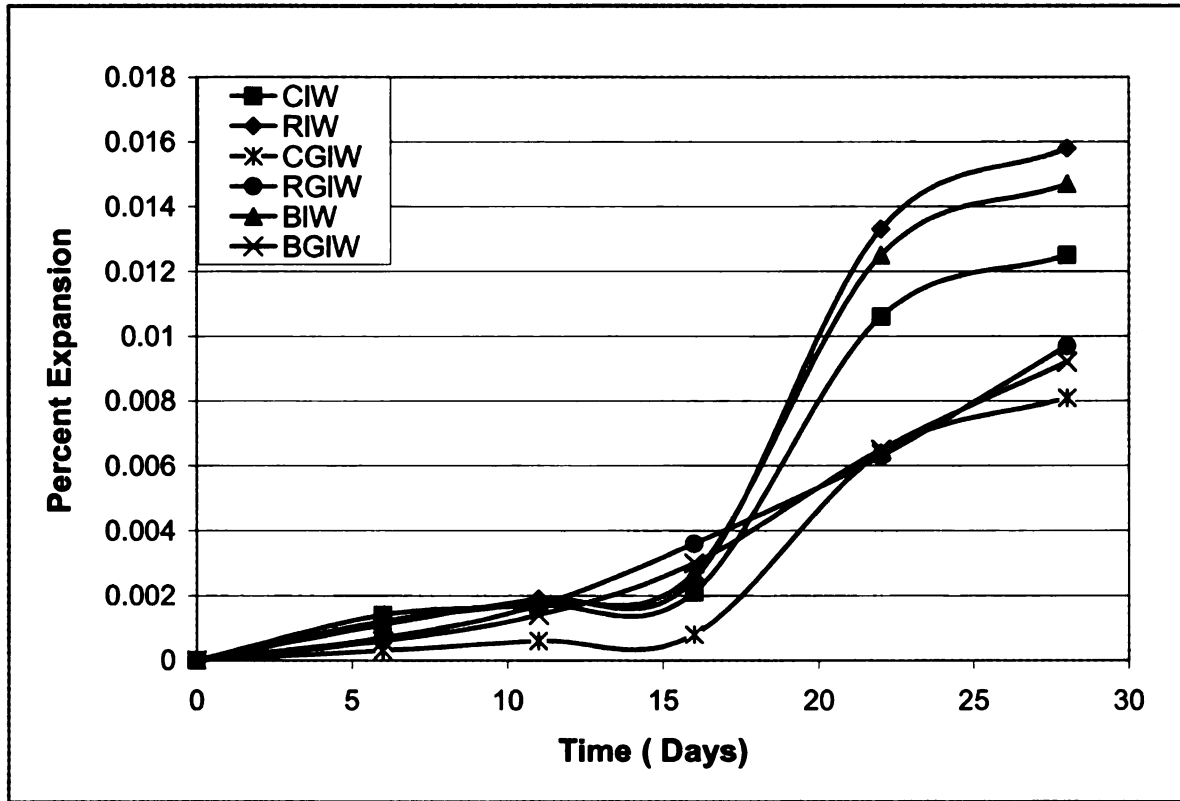


Figure 4. 15 ASR test results for low w/c ratio concrete materials with and without milled waste glass

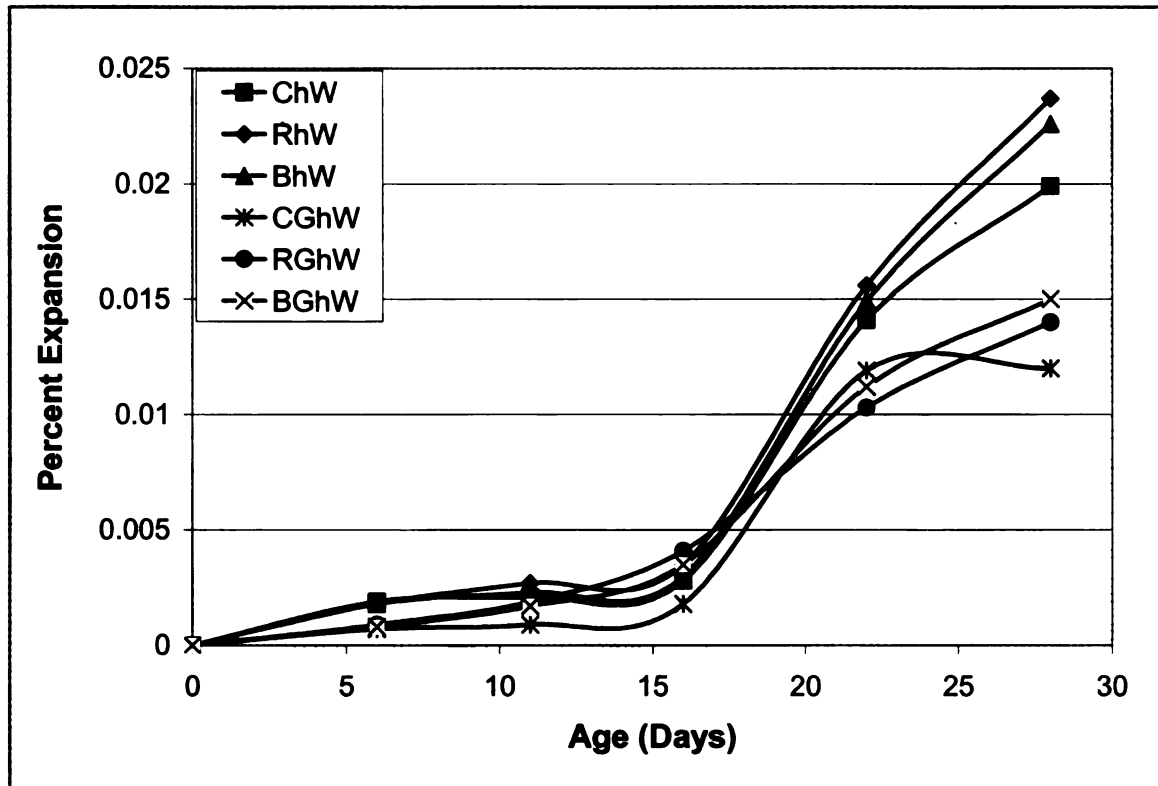


Figure 4. 16 ASR test results for high w/c ratio concrete materials with and without milled waste glass

#### 4.2.4.3 pH Analysis

The environment of cement paste and mortar is highly alkaline ( $\text{pH} > 12.5$ ). With a well-hydrated Portland cement paste, the solid phase exists in a state of stable equilibrium with a high-pH pore fluid. Theoretically, any environment with less than 12.5 pH may be regarded aggressive because reduction of the alkalinity of the pore fluid would, eventually, lead to destabilization of the cement hydration products. The pH of the pore solution in hydrated cement paste depends upon the alkali content of cement and any other source of alkalis. The addition of glass as a partial replacement of cement should generally result in increased pH of the cement paste and mortar, given the relatively high alkali content of glass in the form of sodium oxide. The pozzolanic reactions of glass

with cement hydrates, however, consume calcium hydroxide (CH) to form calcium silicate hydrate (C-S-H), producing some reduction of pH.

Cementitious pastes and mortars introduced in Tables 4.3 and 4.4 were ground to average particles size of  $< 50 \mu\text{m}$  for carrying out pH analyses of the solid phase in the mixes. Distilled water was used as solvent to prepare solutions of each mix at 50:50 ratio of solvent and solid. Mixing was carried out in a slow cell mixer at 35 rpm for a period of 15 min. Before the test, electrodes of the pH meter were calibrated in aqueous solutions with known pH values.

Figure 4.17 shows the results of the pH tests on cementitious paste materials with various levels of cement replacement with milled waste glass. The addition of milled waste glass is observed to produce an increase in the pH of the paste. Statistical analysis (of variance) indicated that 40% cement replacement with milled waste glass had a statistically significant effect (at 95% level of confidence) towards increasing the pH of the respective solution. Similar analysis of the effect of 20% cement replacement with milled waste glass showed statistically insignificant effects towards increasing the pH of the respective solution.

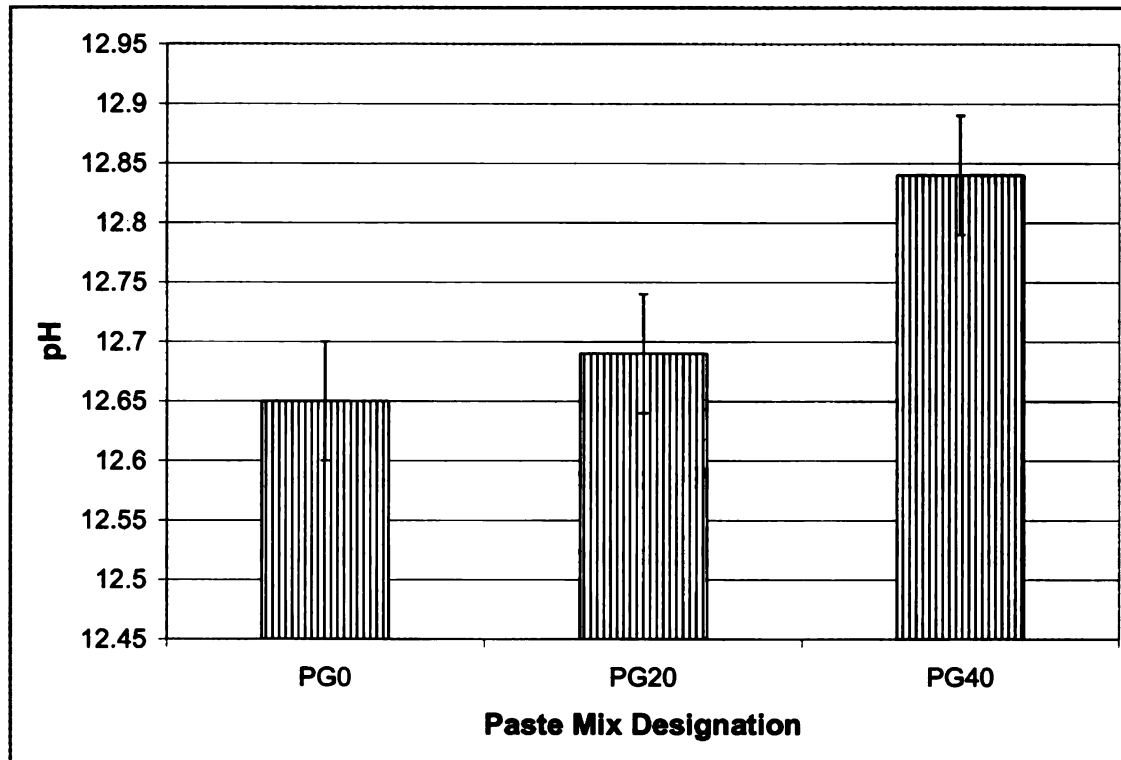


Figure 4. 17 Results of pH tests on cement paste mixes with and without milled waste glass (means & standard errors)

Figures 4.18 and 4.19 show the plots of pH vs. percent replacement of cement with milled waste glass for normal and reactive sand mortar mixes, respectively. Increased replacement levels of cement with milled waste glass are observed to produce increased pH levels. This trend is observed for mortar mixes with normal as well as reactive sands. The rate of increase is, however, higher up to 20% replacement, beyond which the rate of increase in pH slows down. This could be attributed to the reduced production of CH at higher dosages of milled waste glass as a result of the availability of less cement for hydration, noting that the pozzolanic reaction of milled waste glass with lime ( $\text{Ca(OH)}_2$ ) points at the lime-consuming nature of milled waste glass.

Contrary to the effects of traditional pozzolans (fly ash and silica fume) which result in reduction of the pH of concrete, milled waste glass increases the pH of the

concrete pore solution. This is actually a positive attribute of glass towards enhancing the stability of cement hydrates (by retaining the high-pH environment of concrete, which tends to be reduced over time due to carbonation and any potential reactions in acidic environments), and improved protection of reinforcing steel in concrete against corrosion (noting that reduced alkalinity of concrete compromises the stability of the protective iron oxide layer on steel). The fact that partial replacement of cement with milled waste glass (unlike traditional pozzolans) results in increased pH levels points at the contributions of glass alkalis which surpass any pH reduction due to the pozzolanic reactions of milled waste glass.

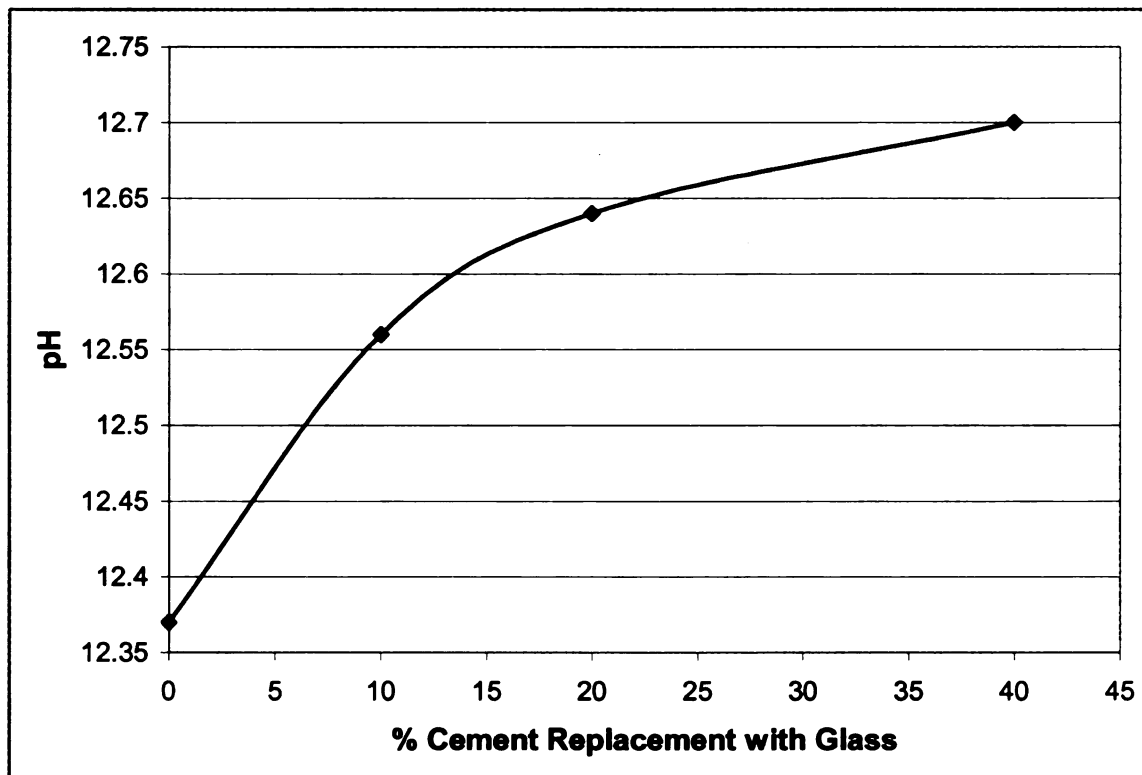


Figure 4. 18 Plot of pH vs. % replacement level of cement with milled waste glass in normal sand mortar

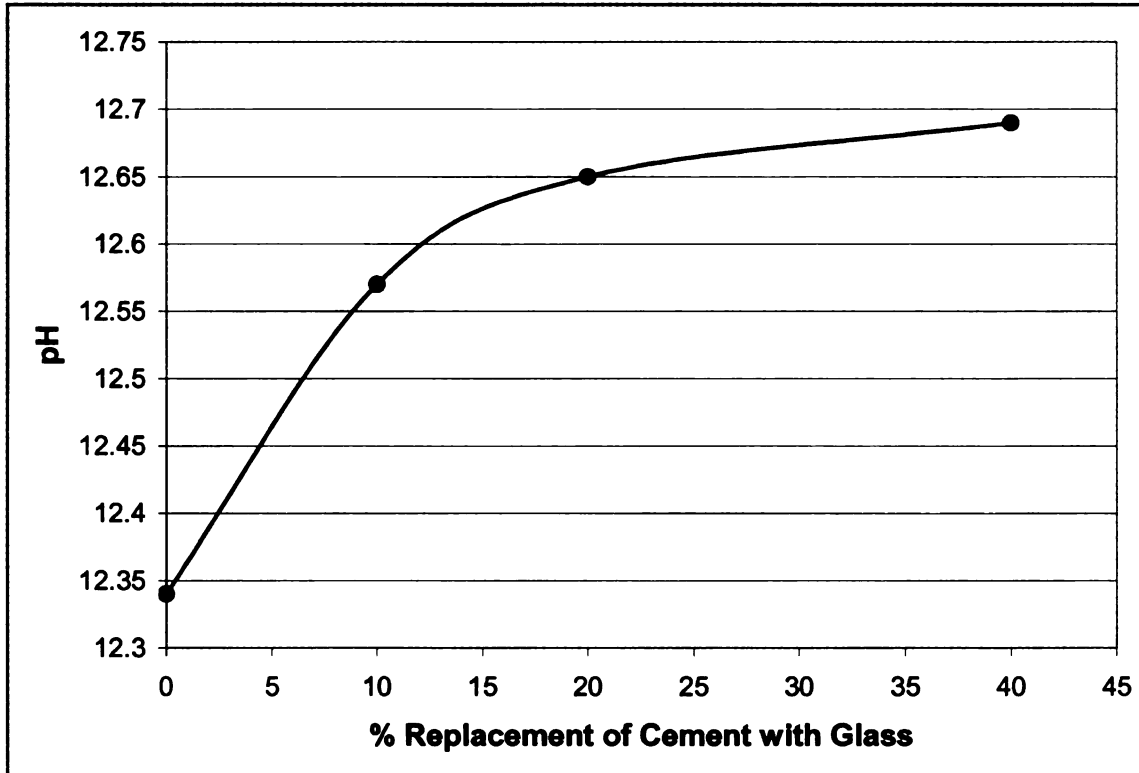


Figure 4. 19 Plot of pH vs. % replacement level of cement with milled waste glass in reactive sand mortar

#### 4.2.4.4 SEM Analysis of Specimens Exposed to ASR Test

This section presents the scanning electron microscopy (SEM) analysis of the mortar specimens exposed to ASR conducive environment (kept in NaOH solution at 80°C) described by ASTM C 1260 in an attempt to capture the microstructural developments indicative of the ASR manifestation.

Figure 4.20 shows the SEM micrograph of the fractured surface of mortar specimen without milled waste glass, whereas Figure 4.21 shows the SEM micrograph of fractured mortar specimen incorporating 40% of milled waste glass as replacement for cement after 20 days continuous aging in alkali silica test environment. As can be seen the mortar specimen with milled waste glass did not show signs (development of rosette

or lamellar crystalline structure) of ASR reaction after 20 days of continuous exposure to highly ASR conducive environment. Microstructure of mortar specimens containing 40% of milled waste glass is homogeneous even after 20 days of exposure to severe ASR conducive environment.

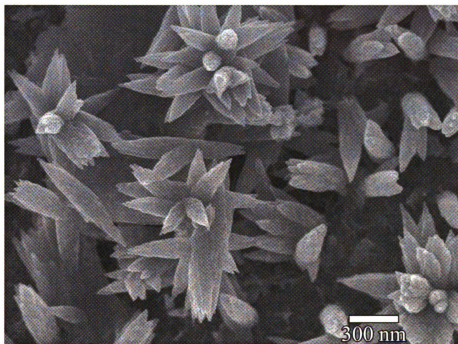


Figure 4. 20 SEM micrograph of fractured surface of mortar without milled waste glass after 20 days after exposure to ASR environment

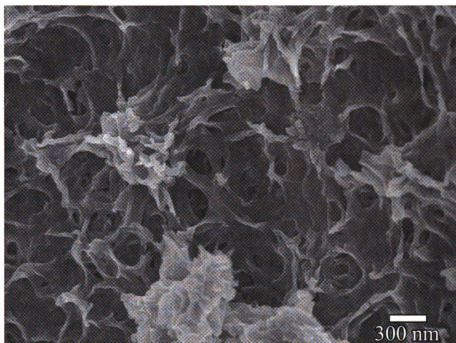


Figure 4. 21 SEM micrograph of fractured surface of mortar with 40% milled waste glass after 20 days after exposure to ASR environment

## REFERENCES

1. Neville, A.M., *Properties of Concrete*. 4th ed. 2000: Pearson Education.
2. Mehta P. K., M.P.J.M., *Concrete: Microstructure, Properties and Materials*. 2006: McGraw-Hill New York.
3. Alexander, M.G., Ballim, Y., *Experiences with durability testing of concrete: A suggested framework incorporating index parameters and results from accelerated durability tests*, in *Third Canadian Symposium on Cement and Concrete (CSCC 93)*. 1993, National Research Council Canada: Ottawa, Ontario.
4. Stark, D., *The Use of Recycled -Concrete Aggregate from Concrete Exhibiting Alkali-Silica Reactivity*. 1996, Research and Development Bulletin RD114, Portland Cement Association: Skokie, Illinois.
5. Hasaba, S., Kawamura, M., and Toriik, K. et al *Drying shrinkage and durability of concrete made of recycled concrete aggregates*. Japan Concrete Institute, 1981. 3: p. 55-60.
6. Malhotra, V.M. *Use of recycled concrete as new aggregate*. in *Energy and Resource Conservation in the Cement and Concrete Industry*. 1978. Ottawa.
7. Buck, A.D., *Recycled concrete as source of aggregate*. ACI Materials Journal, 1977: p. 212-219.
8. Kawamura, M., Toriik, K., Takemoto, K., *Properties of recycled aggregate concrete made with aggregate obtained from demolished pavement*. Journal of the Society of Materials Science, Japan 1983. 32(353).
9. Salem, R.M., E.G. Burdette, and N.M. Jackson, *Resistance to freezing and thawing of recycled aggregate concrete*. ACI Materials Journal, 2003. 100(Compendex): p. 216-221.
10. Salem, R.M. and E.G. Burdette, *Role of chemical and mineral admixtures on physical properties and frost-resistance of recycled aggregate concrete*. ACI Materials Journal, 1998. 95(Compendex): p. 558-563.
11. B.C.S.J, *Study on recycled aggregate and recycled aggregate concrete*. Concrete Journal, Japan, 1978. 16(7): p. 18-31.
12. Rasheeduzzafar and Khan, A., *Recycled Concrete- A source of new aggregate*. Journal of Cement, Concrete and Aggregates 1984. 6(1): p. 17-27.
13. Otsuki, N., S.-I. Miyazato, and W. Yodsudjai, *Influence of recycled aggregate on interfacial transition zone, strength, chloride penetration and carbonation of*

- concrete*. Journal of Materials in Civil Engineering, 2003. **15**(Compendex): p. 443-451.
14. Shayan, A. and A. Xu, *Performance and Properties of Structural Concrete made with Recycled Concrete Aggregate*. ACI Materials Journal, 2003. **100**(Compendex): p. 371-380.
  15. Olorunsogo, F.T. and N. Padayachee, *Performance of recycled aggregate concrete monitored by durability indexes*. Cement and Concrete Research, 2002. **32**(Compendex): p. 179-185.
  16. Kou, S.C., C.S. Poon, and C. Dixon, *Influence of fly ash as cement replacement on the properties of recycled aggregate concrete*. Journal of Materials in Civil Engineering, 2007. **19**(Compendex): p. 709-717.
  17. Kou, S.C., C.S. Poon, and D. Chan, *Influence of fly ash as a cement addition on the hardened properties of recycled aggregate concrete*. Materials and Structures/Materiaux et Constructions, 2008. **41**(Compendex): p. 1191-1201.
  18. Ravindrarajah Sri, R., *Properties of concrete made with crushed concrete as coarse aggregate*. Magazine of Concrete Research, 1985. **37**(130).
  19. Limbachiya, M.C., *Coarse recycled aggregates for use in new concrete*. Proceedings of the Institute of Civil Engineers: Engineering Sustainability, 2004. **157**(Compendex): p. 99-106.
  20. Poon, C.-S. and D. Chan, *Effects of contaminants on the properties of concrete paving blocks prepared with recycled concrete aggregates*. Construction and Building Materials, 2007. **21**(1): p. 164-175.
  21. ACI 116R, *Cement and Concrete Terminology in ACI Manual of Concrete Practice Part 1*. 2001: Farmington Hills, MI.
  22. Bakke, K.J., ed. *Abrasion Resistance*. Significance of Tests and Properties of Concrete and Concrete-Making Materials ed. J.H.P. Joseph F. Lamond. 2006, ASTM International.
  23. Witte, L.P., Backstrom J. E., *Some properties affecting abrasion resistance of air-entrained concrete*, in *Proceedings of the ASTM International*, vol. 51 1951: West Conshohocken, PA. p. 1141.
  24. Johnston, C.D., *Waste Glass as Coarse Aggregate for Concrete* Journal of Testing and Evaluation 1974. **2**(5): p. 344-350.

25. Dhir, R.K.a.D., T. D. , *Maximising Opportunities for Recycling Glass*, in *Sustainable Waste Management and Recycling: Glass Waste*, M.C.L.a.J.J. Roberts, Editor. 2004, Thomas Telford: London.
26. Jin, W., C. Meyer, and S. Baxter, "*Glascrete*"-concrete with class aggregate. *ACI Materials Journal*, 2000. **97**(Compendex): p. 208-213.
27. Jin, W., *Alkali-silica reaction in concrete with glass aggregate: A chemo-physico-mechanical approach*. 1998, Columbia University: United States -- New York. p. 109.
28. Meyer, C., Baxter, S., and Jin, W. *Alkali-silica reaction in concrete with waste glass as aggregate*. in *Materials for a New Millennium, Proceedings of the Fourth Materials Engineering Conference* 1996. Washington, D.C.
29. Shao, P.L.a.Y., *Feasibility of using ground waste glass as cementitious material*, in *Recycling and Reuse of Glass Cullet*. 2001, Thomas Telford: Dundee, Scotland.
30. Zhu, H. and E. Byars, *Potential for use of waste glass in concrete*. *Concrete (London)*, 2005. **39**(Compendex): p. 41-45.
31. Taylor, H.F.W., *Cement Chemistry*. 1990, London: Academic Press Limited.
32. Scholze, H., *CHEMICAL DURABILITY OF GLASSES*. *Journal of Non-Crystalline Solids*, 1981. **52**(Compendex): p. 91-103.
33. Douglas, R.W. and M.M. El-Shamy, *Reactions of glasses with aqueous solutions*. *American Ceramic Society -- Journal*, 1967. **50**(1): p. 1-8.
34. Dhir, R.K., T.D. Dyer, and M.C. Tang, *Alkali-silica reaction in concrete containing glass*. *Materials and Structures/Materiaux et Constructions*, 2009. **42**(Compendex): p. 1451-1462.
35. Dyer, T.D.a.D., R. K. *Use of glass cullet as a cement replacement*. in *Recycling and Reuse of Glass Cullet*. 2001. Dundee, Scotland: Thomas Telford.
36. Meyer C., E.N., and Andela C., *Concrete with waste glass as aggregate*, in *Recycling and Re-use of Glass Cullet*. 2001: Dundee, U.K.
37. Byars, E.A., B. Morales-Hernandez, and Z. HuiYing, *Waste glass as concrete aggregate and pozzolan Laboratory and industrial projects*. *Concrete (London)*, 2004. **38**(Compendex): p. 41-44.
38. Meyer, C. and Y. Xi, *Use of Recycled Glass and Fly Ash for Precast Concrete*. *Journal of Materials in Civil Engineering*, 1999. **11**(2): p. 89-90.

39. Dyer, T.D. and R.K. Dhir, *Chemical reactions of glass cullet used as cement component*. Journal of Materials in Civil Engineering, 2001. 13(Compendex): p. 412-417.

## **CHAPTER 5**

### **Prediction of the Recycled Aggregate and / or Milled Waste Glass Effects on Concrete Performance**

#### **5.1 Introduction and Background**

The growing emphasis on the life-cycle economy and the sustainability of infrastructure systems has increased the demands for durable concrete materials. Strength is no longer the only criterion for acceptance of concrete, nor is it the sole benchmark for comparison of different concrete mixtures [1]. The moisture barrier qualities of concrete are key factors governing their durability [2]. Degradation of large concrete structures such as pavements, bridge decks and retaining walls are often controlled by the ingress into concrete of deleterious species (e.g., chloride or sulfate ions) dissolved in water or (in the case of frost action) water by itself [1, 3] . Sorption is the prevalent transport mechanism of water (and aggressive ions) into the concrete-based infrastructure.

To proceed from concrete durability to prediction of the service life of a concrete-based infrastructure system, it is required to postulate a degradation mechanism and a quantitative degradation model that depends on measured material and environmental characteristics. The prediction of service life would require defining: (1) material's transport and mechanical properties; (2) adequate characterization of the exposure environment; and (3) development of quantitative relationships between transport characteristic and the degree of concrete deterioration [1, 4]. In this research, we focused on concrete pavement and bridge deck deterioration mechanisms involving freeze-thaw or sulfate attack, which are governed by the sorption of water and deleterious solutions (comprising sulfate ions) into concrete. Numerical analyses were conducted to compare

the service life of normal and recycled aggregate concretes with and without the use of milled waste glass as partial replacement for cement.

## **5.2 Freeze-Thaw Attack**

In cold climates, damage to concrete in the presence of moisture may occur due to repeated cycles of freezing and thawing. The damage caused by freeze-thaw attack on concrete includes cracking and spalling, caused by progressive expansion of the cement paste under repeated freezing and thawing cycles [3, 5-6]. Concrete slabs (e.g., pavements) exposed to freeze-thaw cycles in presence of moisture and deicing salts are susceptible to scaling (surface flaking/peel-off). Cracking in coarse aggregates under freeze-thaw attack may produce damage in concrete resembling capital letter 'D' at corners of concrete slabs (referred to as D-cracking).

Frost action in hardened cement paste is caused by internal pressures produced by the movement of water away from finer pores towards coarser pores where they can freeze to realize a lower-energy state [7], and also (to a lesser extent) by the expansion of water upon freezing. The magnitude of pressure depends upon the availability of "escape boundaries" (e.g., entrained air voids), the permeability of cement paste, and the rate of ice formation [8].

Water is physically present in cement paste in three forms (in order of decreasing mobility): capillary water in small capillaries (10 to 50 nm), adsorbed water in gel pores, and the interlayer water held in the C-S-H structure. As the water in gel pores does not freeze above  $-78^{\circ}\text{C}$  ( $-172^{\circ}\text{F}$ ), it is mostly the capillary water that turns into ice at reasonably reduced temperatures, with the water in gel pores staying liquid in a

supercooled state. Thermodynamically, the frozen water has a lower-energy state when compared with the liquid water in gel pores. The resulting thermodynamic disequilibrium forces migration of the gel water to capillary pores where it can assume the lower-energy frozen state. This movement of water produces a hydraulic pressure, and also increases the moisture content of capillary pores where the expansive effects of ice formation can produce additional pressure within the cement paste [3].

Air entrainment of cement paste is an effective defensive mechanism against frost attack. The air voids (which are discontinuous, and thus difficult to fully saturate) are spaced closely within the paste, and provide escape boundaries for reducing the hydraulic pressure formed under frost attack. The fact that the entrained air voids are only partially filled with water eliminates the potential for pressure buildup upon ice formation within entrained air voids. (Figure 5.1a & b) This process actually induces shrinkage within the cement paste. Figure 5.1c shows formation of ice crystals inside an air void; this figure indicates that the air void provides an open space for pressure-free formation of ice crystals. On the contrary, the formation of ice crystals in cement paste with no air void system would have produced pressure which could cause dilation and cracking of the cement paste and concrete [8].

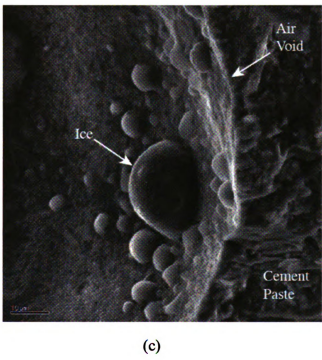
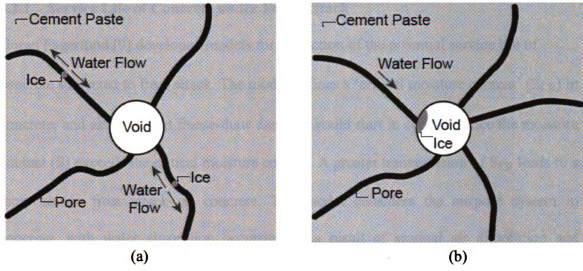


Figure 5. 1 (a) Schematic diagram of ice formation in capillary voids; (b) Ice formation in an air void; and (c) SEM micrograph of ice formation inside an air void [3]

### 5.2.1 Service Life of Concrete under Frost Attack

Goran Fagerlund [9] developed models for prediction of the potential service life of concrete subjected to frost attack. The model defines a 'critical moisture content' ( $S_{CR}$ ) in concrete, and assumes that freeze-thaw damage would start in concrete once the moisture content ( $S$ ) exceeds the critical moisture content. A greater transgression of  $S_{CR}$  leads to a more severe frost attack on concrete. The model considers the air/pore system in concrete, with water absorption occurring as a result of gradual air dissolution and replacement with water. The rate and amount of water uptake in the air/pore system is an important factor governing the service life of concrete; this highlights the importance of the sorption attribute of concrete as a factor determining its resistance to critical saturation and thus freeze-thaw damage.

Thermodynamic criteria favor filling of small pores with water first, where water assumes a lower-energy state due to interactions with the larger specific surface area of finer pores, after which the larger pores (voids) start to fill with water. The predominance of coarser pores (voids) is thus favorable to the service life of hydrated cement paste and concrete. Both frost damage mechanisms (hydraulic pressure formation by movement of ice and pressure formation by the expansion associated with ice formation) are correlated with the critical distance ( $L_{CR}$ ) between air-filled pores. As a result of air dissolution, the total surface area ( $A_T$ ) of all air-filled air pores (given in  $m^2/m^3$  of concrete) will gradually decrease. The ratio of  $A_T$  to residual air content ( $a_T$ ) is called the specific surface of a pore ( $\alpha_T$ ),  $m^2/m^3$  of pore, defining the "average" pore in the air-filled part of the air/pore system. Frost damage in concrete occurs when the water-filling effect is so

prevalent that the residual spacing factor exceeds the critical spacing factor. Accordingly, the residual air content corresponds to a critical air content ( $a_{CR}$ ), and the residual specific surface corresponds to a critical surface specific surface ( $\alpha_{CR}$ ). The conditions for frost damage are:

$$L_r > L_{CR} \quad (5.1)$$

$$a_r < a_{CR} \quad (5.2)$$

$$\alpha_r < \alpha_{CR} \quad (5.3)$$

The criteria governing service life can be expressed as:

$$S_{ACT}(t_{life}) = S_{CR}(t_{life}) \quad (5.4)$$

$$Sa_{ACT}(t_{life}) = Sa_{CR}(t_{life}) \quad (5.5)$$

Where,

$S_{ACT}$  = actual degree of saturation of concrete as a whole

$Sa_{ACT}$  = degree of saturation of air/pore system

$Sa_{CR}$  = critical degree of saturation of air/pore system

Given the challenges in prediction of the time required for conditions of Equations 5.4 and 5.5 to be met for the first time, a stochastic approach is used where the condition for frost damage is described by:

$$P\{S_{CR} < S_{ACT}\} = \int_0^1 F(S_{CR}(t)) \cdot f(S_{ACT}(t)) \cdot ds \quad (5.6)$$

where,

$P\{S_{CR} < S_{ACT}\}$	=	probability of fracture, $0 \leq P \leq 1$
$F(S_{CR}(t))$	=	distribution function of $S_{CR}$ at time 't'
$f(S_{ACT}(t))$	=	frequency function of $S_{ACT}$ at time 't'
$ds$	=	an interval in the degree of saturation 'S'

This implies that, if the variations of  $S_{CR}$  and  $S_{ACT}$  as a function of time can be expressed quantitatively, Equation 5.6 can be used to calculate the risk of frost damage at a certain point of time.

Fagerlund's model estimates the service life by also considering the 'capillary degree of saturation' ( $S_{CAP}$ ). This definition comes from the sorption test of a concrete specimen as described in Section 2.5. The change in slope between the initial sorption and the secondary sorption, called the "nick-point" in the sorption plot of 'water uptake' vs.  $t^{1/2}$ , is an indication of the filling of capillary pores and gel pores. Beyond the nick-point, water absorption continues more slowly which, according to Fagerlund, involves only slow absorption in air/pore system. The water content reached at the end of experiment is called the 'capillary degree of saturation'. Based on the  $S_{CAP}$  approach, the potential service life ( $t_{p,life}$ ) can be calculated, as the time it takes for the critical water absorption to be reached, using the following equation:

$$S_{CAP}(t_{p,life}) = S_{CR}(t) \quad (5.7)$$

The long-term absorption in air/pore system can be expressed as:

$$S_{CAP}(t) = C + D.t^E \quad (5.8)$$

where,

- C = coefficient corresponding to rapid absorption
- D = coefficient that depends upon diffusivity of dissolved air in pore water
- E = coefficient that depends on the shape of the air-pore system

Coefficient 'C' is defined by the volume of the capillary and gel pres as well as some of the finest air voids that are filled at a very early stage of the sorption process.

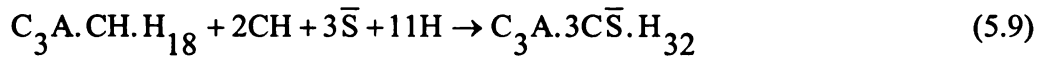
Based on the above discussion, Fagerlund concluded that frost resistance is strongly influenced by moisture sorption. The capillary saturation approach suggests that the water impermeability of concrete benefits its resistance to capillary saturation and thus frost attack. Therefore, improvements in microstructure and pore size distribution which benefit resistance to water sorption benefit the frost resistance of concrete.

### **5.3 Sulfate Attack**

Degradation of concrete as a result of chemical reactions between cement hydrates and sulfate ions, called sulfate attack, is marked by expansion and cracking of concrete. Sulfate attack causes progressive loss of strength and mass due to the loss of cohesiveness of cement hydrates [3, 5]. Cracking of concrete in this damage process increases its porosity and permeability, thus facilitating the transport of aggressive species and water into the interior of concrete, and accelerating the process of deterioration. The formation of ettringite is thought to be the cause of expansion under sulfate attack. Exertion of pressure by the growth of ettringite crystals and by the

swelling due to adsorption of water in poorly crystalline ettringite, results in disruption of concrete [3, 6].

The hydration products of Portland cement contain alumina in the form of monosulfate hydrate ( $C_3A.C\bar{S}.H_{18}$ ). If cement is rich in  $C_3A$  (more than 8 percent), the hydration products will also contain  $C_3A.CH.H_{18}$ . When cement paste comes in contact with sulfate ions, in presence of calcium hydroxide (CH) among cement hydrates, the alumina-containing hydrates get converted into ettringite. The chemical reactions can be summarized as [3]:



The formation of ettringite after the active period of cement hydration (during the service life of concrete), due to the presence of an internal source of sulfate ions, is called delayed ettringite formation. The source of sulfate ions is either a gypsum-contaminated aggregate or the use of cements containing unusually high sulfate contents. The phenomenon happens to be the cause of decomposition of ettringite, which is unstable at temperatures exceeding  $65^\circ\text{C}$  ( $149^\circ\text{F}$ ). If temperature is high enough (e.g., in case of steam curing of concrete), ettringite decomposes due to absorption of sulfate ions and reforms due to desorption of sulfate ions later in service. The re-formation of ettringite is accompanied by cracking and expansion. Figure 5.2 shows the ettringite lining expansion rims at the paste-aggregate interface and Figure 5.3 shows a  $20\ \mu\text{m}$  thick ettringite rim which forms under sulfate attack and causes expansion.

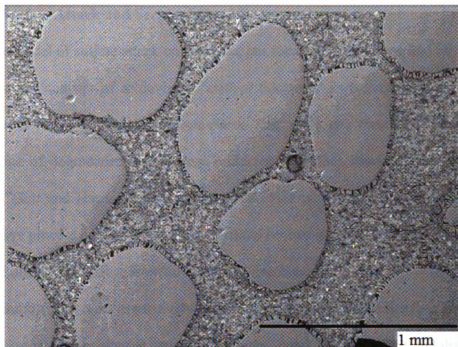


Figure 5.2 Ettringite lining rims around aggregates

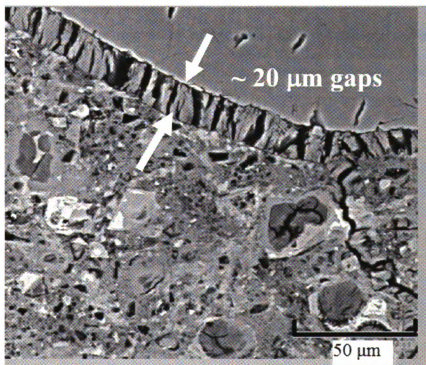


Figure 5.3 SEM micrograph showing 20 μm wide ettringite rim resulting in about 2.8% expansion

### 5.3.1 Sulfate Attack and Service Life of Concrete

A viable model of sulfate attack on concrete, put forward by Atkinson and Hearne [10], is based on the concept of achieving a 'critical thickness' in the reaction zone of sulfate attack, after which spalling of concrete starts. This model provides a mechanistic account of the rate of degradation of concrete subjected to sulfate attack. Based on the earlier work of Gutt and Harrison [11], Atkinson and Hearne [11] identified three steps in the destructive process of sulfate attack on Portland cement paste, mortar and concrete:

- i) Sulfate ions diffuse from environment into concrete;
- ii) Sulfate ions react expansively with aluminum-bearing phases in concrete; and
- iii) The resulting internal expansion causes stress, cracking and exfoliation of the reacted material from concrete surface.

In their model, Atkinson and Hearne hypothesized the formation of a reaction zone as a result of the ingress of sulfate ions into concrete and subsequent chemical reactions. Ettringite is thus formed in the reaction zone. The thickness of the reaction zone is given by:

$$\frac{X^2}{t} = 2D_i \frac{c_o}{C_E} \quad (5.11)$$

where,

- |       |   |  |
|-------|---|--|
| $X$   | = | thickness of reaction zone (m)                     |
| $t$   | = | time (sec)   |
| $D_i$ | = | intrinsic diffusion coefficient ( $m^2 / s$ )      |
| $c_o$ | = | external sulfate concentration                     |
| $C_E$ | = | concentration of the reacted sulfate as ettringite |

Equation 5.11 in Atkinson and Hearne's model shows the dependence of sulfate attack on the moisture transport attribute of concrete. The model further defines the critical thickness of the reaction zone (Equation 5.12) and the required spalling time (Equation 5.13):

$$X_{spall} = \frac{2\alpha\gamma(1-\nu)}{\{E(\beta C_E)^2\}} \quad (5.12)$$

$$t_{spall} = \frac{X_{spall}^2 C_E}{(2D_i c_o)} \quad (5.13)$$

where,

- $\alpha$  = roughness factor for fracture path
- $\gamma$  = fracture surface energy of concrete (taken equal to  $10 \text{ J/m}^2$ )
- $\nu$  = Poisson's ratio (taken equal to 0.3)
- $\beta$  = linear strain caused by one mole of sulfate reacted in  $1 \text{ m}^3$   
(taken equal to  $1.8 \times 10^{-6} \text{ m}^3/\text{mol}$ )

The degradation rate due to sulfate attack is given by:

$$R = \frac{X_{spall}}{t_{spall}}$$

$$R = \frac{E\beta^2 c_o C_E D_i}{\{\alpha\gamma(1-\nu)\}} \quad (5.14)$$

Equation 5.14 indicates that the rate of degradation of concrete increases with increase in diffusivity of concrete. The model also accounts for the mechanical properties

of concrete through the term  $E/\gamma$ ; since both these parameters increase with an improvement in concrete quality, however, the degradation caused by sulfate attack is likely to be insensitive to the mechanical properties of concrete. The main influence of concrete will come through its transport characteristics (diffusivity). Since penetration of sulfate ions into concrete is through transport of water carrying dissolved sulfate ions, the sorption characteristics of concrete is a key factor affecting the service life of concrete exposed to sulfate attack. Therefore, as is the case of freeze-thaw attack, improvements in the moisture barrier (sorption resistance) attributes of concrete can improve the service life of concrete under sulfate attack.

#### **5.4 Prediction of Concrete Pavement and Bridge Deck Service Life: Effects of Milled Waste Glass and/or Recycled Aggregate**

The previous sections reviewed the significance of the moisture sorption characteristics of concrete in determining the service life of concrete-based infrastructure systems subjected to freeze-thaw and sulfate attacks. The improvements in the sorption resistance of normal and recycled aggregate concrete brought about by the use of milled waste glass as partial replacement of cement can thus increase the service life of concrete-based infrastructure systems in aggressive environments. Numerical analyses were undertaken to quantify these improvements. The software package CONCLIFE [12], developed at the National Institute of Standards and Technology (NIST), was used for estimating the expected service lives of concrete pavements and bridge decks under freeze-thaw and sulfate attack. The experimental data produced in the project on the effects of milled waste glass and/or recycled aggregate on the moisture sorption resistance of concrete to

evaluate the service life of different environmentally friendly concrete formulations in aggressive environments.

ConcLife uses three concrete models and user-specified data on concrete properties and the external environment to estimate the time at which concrete spalls beyond a user-specified limit. Transport of sulfate ions and water through sorption into the partially saturated concrete is a key factor governing concrete degradation. The software calculates the end of service life of concrete pavements and bridge decks as the time it takes for the limit on concrete spall depth to be reached as a result of either freeze-thaw or sulfate attack. To predict service life, ConcLife considers concrete sorptivity (the initial and secondary sorption rates), mechanical properties and entrained air content. The three models used by ConcLife towards prediction of the service life of concrete pavements and bridge decks are reviewed in the following sections.

#### **5.4.1 Surface Temperature and Time-of-Wetness Prediction Model**

A one-dimensional finite difference scheme heat transfer model is used for estimating the surface temperature and time-of-wetness (and time-of-freezing) of the concrete in a user-specified climate [13]. Time-of-wetness events can be due to precipitation or due to condensation when concrete temperature falls below the current dew-point temperature. Time-of-wetness data for specified locations has been obtained from National Renewable Energy Laboratory (NREL) [14]. For other user-specified stations, separate weather input files can be generated for use by the software.

The surface temperature and time-of-wetness model considers heat transfer by conduction, convection and radiation. Figure 5.4 shows the basic configuration of the one-dimensional heat transfer model for use with concrete pavements, and Figure 5.5

shows a similar configuration for use with bridge decks. Environmental conditions are varied by using the typical meteorological data files from NREL. Figure 5.6 shows a typical plot of a wetting event from ConcLife. The top surface boundary conditions and the lower surface boundary conditions (for bridge decks) are established based on the weather data file. The model outputs include the variation of concrete surface temperature during the course of a year, all time-of-wetness events (start time, duration, concrete surface temperature and exterior relative humidity prior to event), and all time-of-freezing events (start time, duration, and minimum surface temperature during freezing).

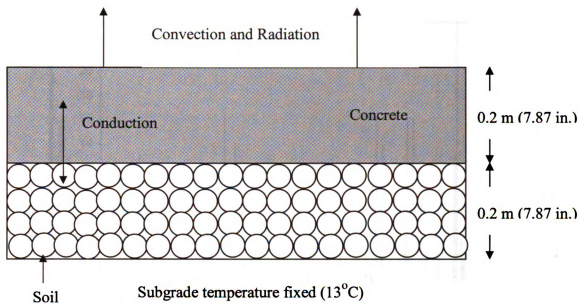


Figure 5.4 Cross-section of concrete pavement

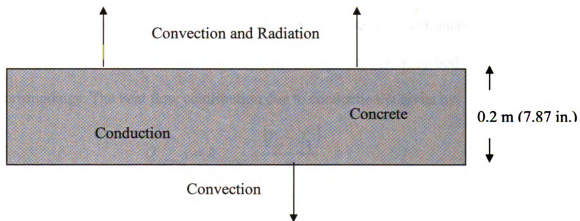


Figure 5.5 Cross-section of bridge deck

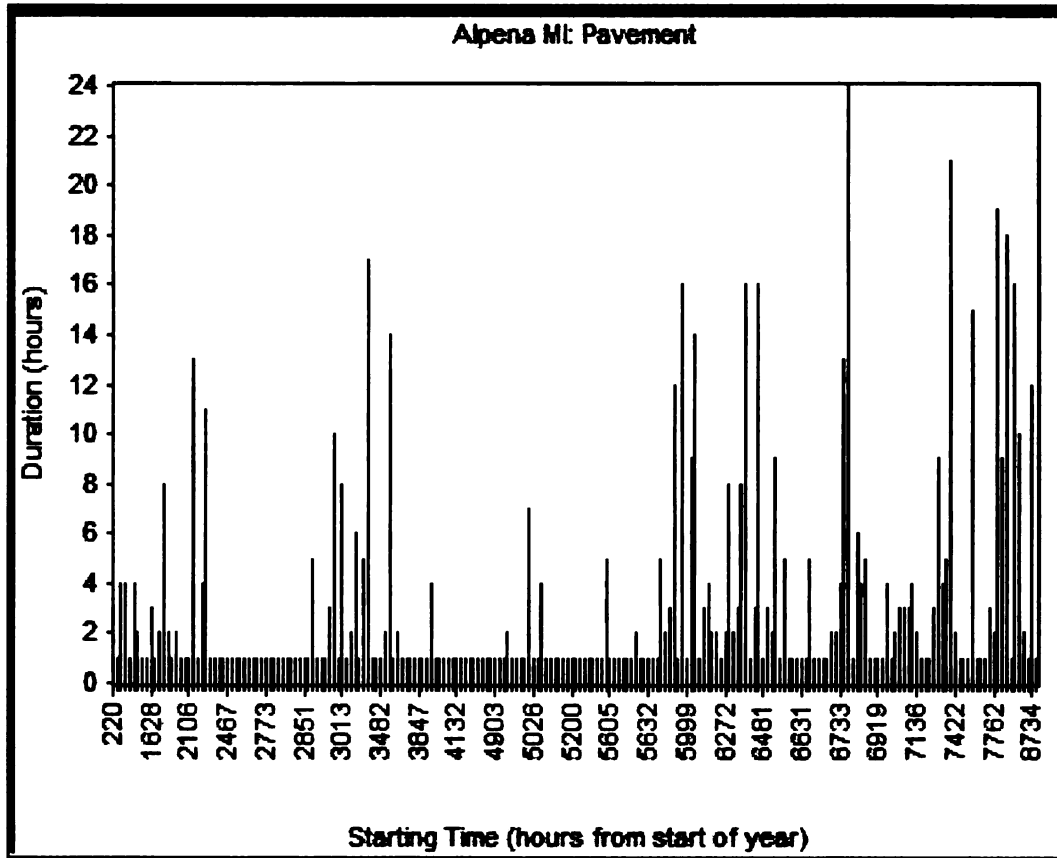


Figure 5. 6 Time-of-wetness plot for Alpena, MI (from Conclife)

At the top of pavement / bridge deck surface, four modes of heat transfer are considered: conduction into concrete, convection, solar absorption, and grey-body radiation to the surroundings. The heat flow contribution due to conduction is given by:

$$Q_{cond} = k_{conc} \times \frac{(T_o - T_1)}{\Delta x} \quad (5.15)$$

where,

- $Q_{cond}$  = heat flow due to conduction ( $\text{W/m}^2$ )
- $k_{conc}$  = thermal conductivity of concrete ( $\text{W/m } ^\circ\text{C}$ )
- $T_o$  = surface temperature at the first internal node

$T_1$  = internal temperature at the first internal node

$\Delta x$  = node spacing (20 mm)

Heat transfer due to convection is given by:

$$Q_{conv} = h_{conv} \times (T_o - T_{ambient}) \quad (5.16)$$

where,

$Q_{conv}$  = heat transfer due to convection

$h_{conv}$  = convection coefficient ( $W/m^2 \text{ } ^\circ C$ )

$T_{ambient}$  = ambient temperature

Convection coefficient is calculated using the wind speed available in the weather data file. Heat transfer through radiation at the top of concrete surface is considered from two points of view: radiation absorbed from incoming sunlight, and radiation from warm concrete to night sky, given by Equations 5.17 and 5.18, respectively:

$$Q_{sun} = \gamma_{abs} \times Q_{inc} \quad (5.17)$$

$$Q_{sky} = \sigma \varepsilon \times (T_{oK}^4 - T_{sky}^4) \quad (5.18)$$

where,

$Q_{sun}$  = radiation absorbed from incoming sunlight

$Q_{inc}$  = incident solar radiation ( $W/ m^2$ )

$\gamma_{abs}$  = solar absorptivity of concrete (taken as 0.65)

$\sigma$  = Boltzmann constant ( $5.669 \times 10^{-8} W/(m^2 \text{ } ^\circ C^4)$ )

$\varepsilon$	=	emissivity of concrete
$T_{oK}$	=	concrete surface temperature ( $^{\circ}\text{K}$ )
$T_{sky}$	=	calculated sky temp ( $^{\circ}\text{K}$ )

#### **5.4.2 Freeze-Thaw Attack Model**

The freeze-thaw model used by ConcLife is based on the principles described in Section 5.2.1. This model estimates the service life of a concrete pavement or bridge deck when freeze-thaw attack is the primary mechanism of concrete degradation. The basic assumption is the progressive filling of air voids by water when concrete is exposed to a humid environment and water ingresses through sorption. When a critical fraction of the air void system gets saturated with water, the next freeze-thaw cycle will cause the damage. A failure criterion in this case is the time required to achieve the critical degree of saturation. Figure 5.7 shows a typical service life plot based on freeze-thaw duration produced by ConcLife.

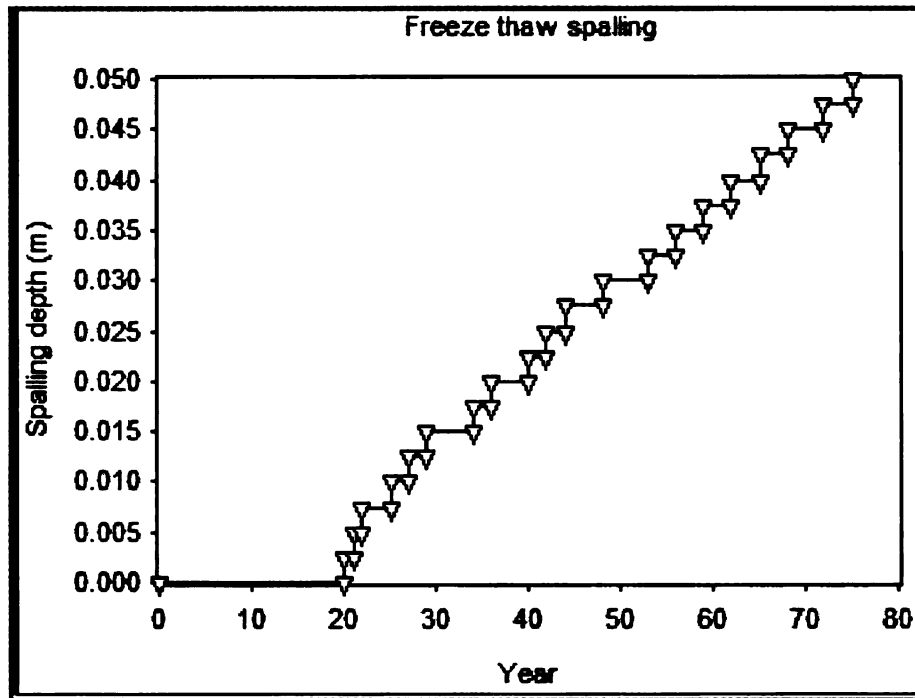


Figure 5.7 A typical ConLife plot for prediction of concrete service life under freeze-thaw attack

### 5.4.3 Sulfate Attack Model

The service life model under sulfate attack is based on the principles reviewed in Section 5.3.1. While the basic model considers transport of sulfate ions through diffusion, ConLife considers sorption to be the main mode of sulfate transport into concrete. According to this model, concrete failure occurs when the strain produced by the growing ettringite crystals exceeds the fracture energy of concrete. Failure of concrete occurs by spalling of a layer when its thickness reaches to a critical value as described in Section 5.3.1. Figure 5.8 shows a typical ConLife service life plot based on sulfate attack damage. As ConLife considers the sorption mode of ingress of ions within a solution, it requires the concentration of sulfate ions in the external solution (e.g., rainwater or groundwater) as well as the concrete sorptivity (initial and secondary sorption rates).

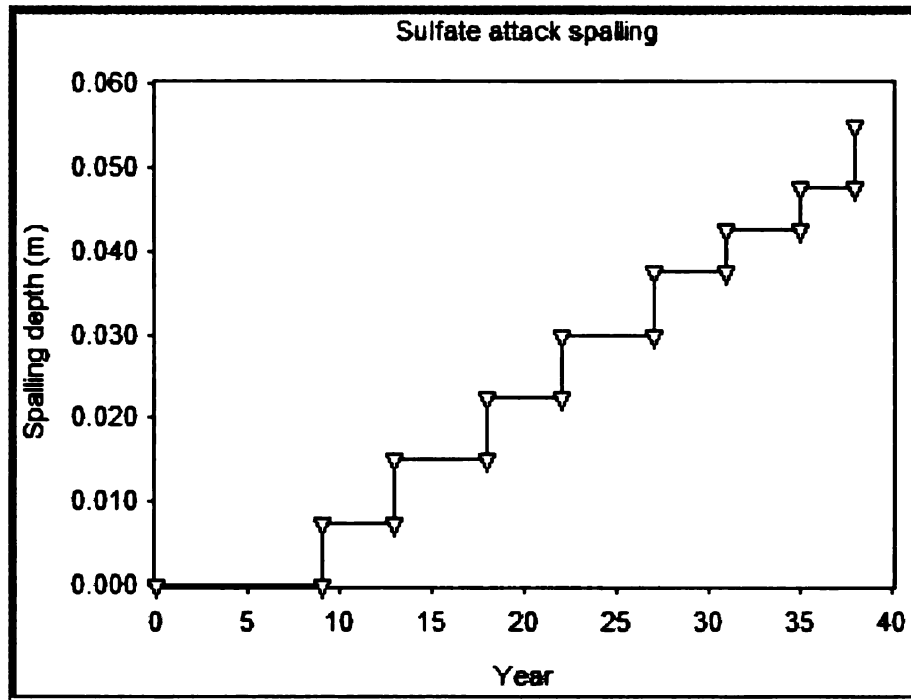


Figure 5. 8 A typical ConcLife plot for prediction of concrete service life under sulfate attack

## 5.5 Input Material Properties and Pavement / Bridge Deck Section

### Characteristics

Normal and recycled aggregate concretes with and without milled waste glass as partial replacement for cement were considered in numerical analyses. The (typical) cross-sections of concrete pavement and bridge deck considered here are shown in Figures 5.4 and 5.5, respectively. The experimental values of the (initial and secondary) sorption rates of concretes were taken from Section 2.5. The experimental values of the physical and mechanical properties of concretes (porosity, modulus of elasticity, density and air content) were taken from Section 3.3. The value of fracture energy was approximated at  $10 \text{ J/m}^2$  ( $8.8 \times 10^{-4} \text{ Btu/ft}^2$ ) for normal concrete and  $8 \text{ J/m}^2$  ( $7.04 \times 10^{-4} \text{ Btu/ft}^2$ ) for recycled aggregate concrete without milled waste glass. The fracture energies for normal and

recycled aggregate concretes incorporating milled waste glass (as partial replacement for cement) were approximated, based on measurements made on fly ash concretes, at 12 ( $10.56 \times 10^{-4}$  Btu/ft<sup>2</sup>) for normal concrete and 11 J/m<sup>2</sup> ( $9.68 \times 10^{-4}$  Btu/ft<sup>2</sup>) for recycled aggregate concrete [10]. Some other material properties used for numerical analyses are presented in Table 5.1.

Table 5.1 Some material properties used in numerical analyses

Material	Heat Capacity $C_p$ (J/kg °C)	Thermal Conductivity $k$ (W/m °C)	Density $\rho$ (kg/m <sup>3</sup> )
Concrete	1000	1.5	varies
Soil	800	0.3	1600

## 5.6 Meteorological Regions Considered for Analyses

Table 5.2 summarizes the weather information for ten geographic locations with different climatic conditions across the U.S. which were considered in numerical analyses (using ConcLife). Tucson, AZ is the driest location considered where concrete pavement gets wet for only 128 hrs per year. Conversely, Seattle, WA is the wettest climate considered where the pavement gets wet 1698 hrs per year. Concrete pavements and bridge decks located in Tampa, FL will experience the fewest freeze-thaw cycles, whereas in Cheyenne, WY, they will experience 125 freeze-thaw cycles per year. In the moderate winter climate of Baltimore, MD, there is a considerable difference between the numbers of freeze-thaw cycles experienced by bridge decks versus pavements. This is due to the

fact that, at 0 °C, bridge decks freeze while nearby pavements will be just above freezing point due to the insulation provided by their subgrade soil.

Table 5.2 Weather information of different geographical locations of the U.S. considered for analysis

Station	Cold days below freezing	Warm days (>32 °C)	Annual precipitation days (≥ 0.01 in.)	Min temp (°C)	Snow fall (in.)	Annual ave. temp (°C)	Annual ave. rain fall (in.)	Ave. R.H.
Alpena, MI	177	6	29	-8	83.5	6	28.8	78
Tucson, AZ	17	143	53	12.6	1.2	20.2	12	43.5
Providence, RI	117	10	125	-7.2	35.9	10.2	45.5	66.5
Fresno, CA	20	108	45	7.4	0.1	17.4	10.6	73.5
Tampa, FL	3	87	107	10	0	22.4	43.9	74
Baltimore, MD	97	31	114	-4.8	21.1	12.8	40.8	67.5
Waterloo, IA	156	16	104	-3.9	32.5	8.1	33.7	78
Cheyenne, WY	172	9	101	-9.3	55.4	7.6	14.4	59
Lubbock, TX	93	80	63	-4.1	9.9	15.6	18.6	61.5
Seattle, WA	19	1	151	2.4	7.3	11.6	38	43

## **5.7 Results of Numerical Analysis**

For the four concrete types (normal and recycled aggregate concretes with and without milled waste glass), numerical analyses were carried out using ConcLife for the ten geographical regions shown in Table 5.2. The numerical analyses included service life prediction of concrete pavement and bridge deck constructed with the four concrete types. It is to be noted that the maximum service life that ConcLife predicts is 99 years.

Table 5.3 and Figure 5.9 show the predicted service lives of concrete pavements and bridge decks when the damage mechanism is freeze-thaw attack and the concrete type is recycled aggregate concrete with and without recycled glass. Table 5.4 and Figure 5.10 show the predicted service lives for the recycled aggregate concrete with and without recycled glass when deterioration is caused by sulfate attack. The use of milled waste glass as partial replacement of cement is observed to enhance the service life of recycled aggregate concrete pavement under freeze-thaw as well as sulfate attack.

Table 5.5 and Figure 5.11 show the concrete pavement and bridge deck predicted service lives when the damage mechanism is freeze-thaw attack and the concrete type is normal with or without recycled glass. Table 5.6 and Figure 5.12 show the pavement and bridge deck predicted service lives for normal concrete with and without glass when deterioration is caused by sulfate attack. The use of milled waste glass as partial replacement for cement is observed to increase the service life of concrete pavements and bridge decks under freeze-thaw and surface attack.

The enhancement in service life of concrete pavement and bridge deck made with recycled aggregate and normal concrete materials can be attributed to the beneficial effects of recycled glass on the initial and secondary sorption rates of concretes as

Table 5.3 Predicted service life of concrete pavement and bridge deck based on freeze-thaw deterioration for recycled aggregate concrete with and without milled waste glass

Station	Weather	Service life based on freeze-thaw deterioration (years)					
		Recycled aggregate concrete		Recycled aggregate concrete with glass			
		Pavement	Bridge deck	Pavement	Bridge deck	Pavement	Bridge deck
Alpena, MI	Wettest -colder	58	55	84		81	
Tucson, AZ	Dry-warmest	82	79	> 99		> 99	
Providence, RI	Wet-colder	56	51	74		71	
Fresno, CA	Wetter-warm	69	67	> 99		> 99	
Tampa, FL	Wet-warmer	> 99	> 99	> 99		> 99	
Baltimore, MD	Wet-cold	66	59	87		75	
Waterloo, IA	Wet-cold	61	56	75		73	
Cheyenne, WY	Wet-coldest	38	35	54		49	
Lubbock, TX	Wet-cold	72	68	> 99		> 99	
Seattle, WA	Wettest-warmest	79	77	> 99		> 99	

discussed in section 2.5. The benefits of milled waste glass to service life tends to be more pronounced in the case of recycled aggregate concrete when compared with normal concrete.

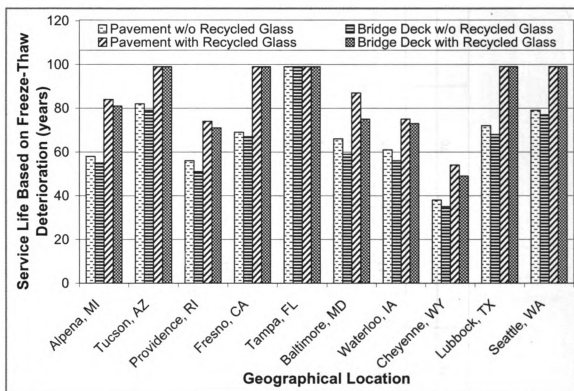


Figure 5.9 Predicted service lives of recycled aggregate concrete pavement and bridge deck with and without milled waste glass when damage is due to freeze-thaw attack

Table 5.4 Predicted service life of concrete pavement and bridge deck based on sulfate attack deterioration for recycled aggregate concrete with and without milled waste glass

Station	Weather	Service life based on sulfate attack deterioration (years)					
		Recycled aggregate concrete		Recycled aggregate concrete with glass			
		Pavement	Bridge deck	Pavement	Bridge deck	Pavement	Bridge deck
Alpena, MI	Wettest -colder	43	39	62	55		
Tucson, AZ	Dry-warmest	82	81	> 99	> 99		
Providence, RI	Wet-colder	67	64	88	88		
Fresno, CA	Wetter-warm	82	79	> 99	> 99		
Tampa, FL	Wet-warmer	77	76	> 99	> 99		
Baltimore, MD	Wet-cold	45	42	61	57		
Waterloo, IA	Wet-cold	69	68	> 99	> 99		
Cheyenne, WY	Wet-coldest	45	43	59	56		
Lubbock, TX	Wet-cold	73	71	> 99	> 99		
Seattle, WA	Wettest-warmest	51	50	70	69		

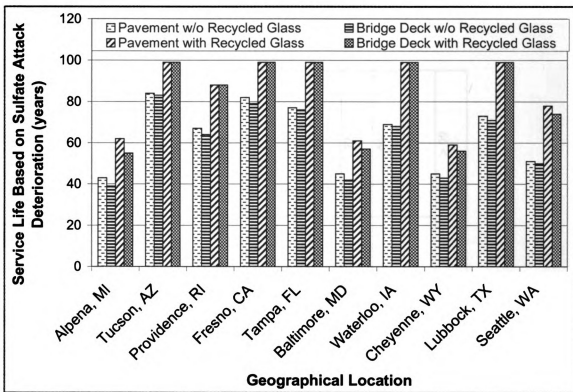


Figure 5.10 Predicted service lives of recycled aggregate concrete pavement and bridge deck with and without milled waste glass when damage is due to sulfate attack

Table 5. 5 Predicted service life of concrete pavement and bridge deck based on freeze-thaw deterioration for normal concrete with and without milled waste glass

Station	Weather	Service life based on freeze-thaw deterioration (years)					
		Normal concrete		Normal concrete with glass			
		Pavement	Bridge deck	Pavement	Bridge deck	Pavement	Bridge deck
Alpena, MI	Wettest -colder	69	67	89	87		
Tucson, AZ	Dry-warmest	88	85	> 99	> 99		
Providence, RI	Wet-colder	69	68	91	88		
Fresno, CA	Wetter-warm	73	71	> 99	> 99		
Tampa, FL	Wet-warmer	> 99	> 99	> 99	> 99		
Baltimore, MD	Wet-cold	76	67	> 99	87		
Waterloo, IA	Wet-cold	68	66	79	77		
Cheyenne, WY	Wet-coldest	51	48	68	64		
Lubbock, TX	Wet-cold	77	76	> 99	> 99		
Seattle, WA	Wettest-warmest	87	86	> 99	> 99		

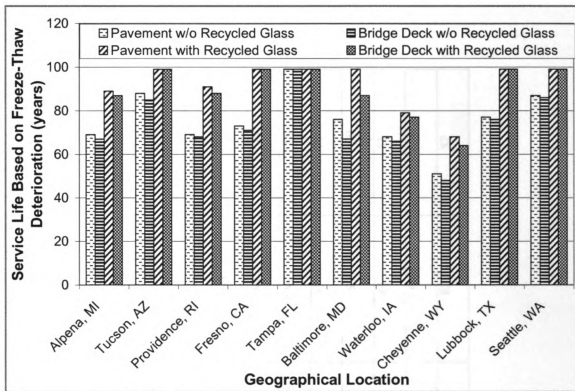


Figure 5. 11 Predicted service lives of normal concrete pavement and bridge deck with and without milled waste glass when damage is due to freeze-thaw attack

**Table 5.6 Predicted service life of concrete pavement and bridge deck based on sulfate attack deterioration for normal concrete with and without milled waste glass**

Station	Weather	Service life based on sulfate attack deterioration (years)					
		Normal concrete		Normal concrete with glass		Normal concrete with glass	
		Pavement	Bridge deck	Pavement	Bridge deck	Pavement	Bridge deck
Alpena, MI	Wettest -colder	58	55	80	76		
Tucson, AZ	Dry-warmest	84	83	> 99	> 99		
Providence, RI	Wet-colder	74	73	> 99	> 99		
Fresno, CA	Wetter-warm	88	88	> 99	> 99		
Tampa, FL	Wet-warmer	85	83	> 99	> 99		
Baltimore, MD	Wet-cold	61	60	81	79		
Waterloo, IA	Wet-cold	74	73	> 99	> 99		
Cheyenne, WY	Wet-coldest	62	60	84	81		
Lubbock, TX	Wet-cold	78	77	> 99	> 99		
Seattle, WA	Wettest-warmest	59	57	82	82		

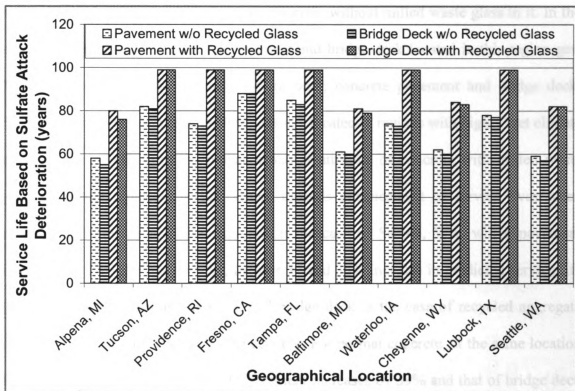


Figure 5.12 Predicted service lives of normal concrete pavement and bridge deck with and without milled waste glass when damage is due to sulfate attack

Figure 5.13 shows the percent gain in predicted service life of concrete pavement and bridge deck exposed to freeze-thaw or sulfate attack with the inclusion of milled waste glass as partial replacement for cement in recycled aggregate concrete. While Figure 5.14 shows the percent gain in predicted service life for the two structures constructed with normal concrete and exposed to freeze-thaw or sulfate attack. As can be seen concrete pavements and bridge decks located in geographical regions with large number of freeze-thaw cycles, significantly benefit in terms of service life gain with the introduction of milled waste glass as partial replacement for cement. For example, Cheyenne, WY, with 125 freeze-thaw cycles per year gets 42 and 40% increase in service life (Figure 5.13) for concrete pavement and bridge deck, respectively in the case of recycled aggregate concrete when compared with the predicted service lives of similar

structures made with recycled aggregate concrete without milled waste glass in it. In the case of normal concrete, concrete pavement and bridge deck located in this region gets 33% gain in service life (Figure 5.14) of both; concrete pavement and bridge deck. Similarly, concrete pavement and bridge decks located in regions with highly wet climate significantly benefit from the moisture barrier attribute of concrete with milled waste glass as partial replacement for cement towards enhancement of service lives when exposed to sulfate attack. For example in the case of Seattle, WA, where pavement remains wet for 1698 hrs per year, there is 37 and 38% increase in predicted service life (Figure 5.13) for concrete pavement and bridge deck in the case of recycled aggregate concrete with milled waste glass, respectively. For normal concrete, at the same location the predicted service life of concrete pavement increases by 39% and that of bridge deck increases by 44% (Figure 5.14) when compared with predicted service lives of similar structures made with normal concrete but without milled waste glass in it. Geographical locations with dry climatic conditions in the case of sulfate attack and freeze-thaw (e.g., Tucson, AZ) and locations with warm weather conditions (e.g., Tampa, FL) do not show significant increase in predicted service life of concrete pavement and bridge deck as the concrete in the two structures located in such regions is not exposed to severe weathering conditions (freeze-thaw and sulfate attack in this case). On average the predicted service lives of concrete pavement and bridge deck located in severe weather conditions (conducive to freeze-thaw or sulfate attack deterioration) are increased by 35% with the incorporation of milled waste glass, in the case of recycled aggregate concrete when compared with predicted service lives of similar structures made with recycled aggregate concrete without milled waste glass. In the case of concrete pavement and bridge deck

made with normal concrete the average increase in predicted service lives of the two structures is 30% when compared with similar structures made with normal concrete but without the incorporation of milled waste glass. The comparison of percent gain in predicted service lives of concrete pavement and bridge deck shows that the predicted service life increase is higher in recycled aggregate concrete than that of normal concrete as stated earlier.

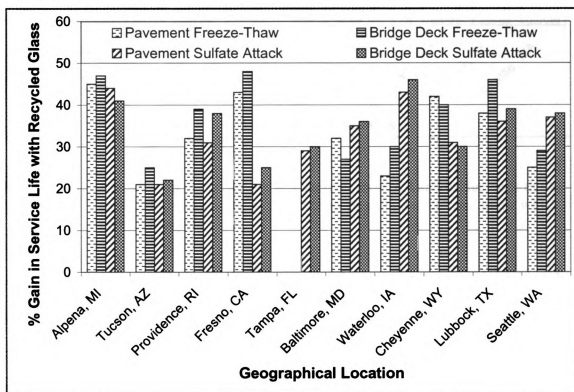


Figure 5. 13 Percent gain in service life of concrete pavement and bridge deck due to recycled glass exposed to freeze-thaw or sulfate attack and made with recycled aggregate concrete

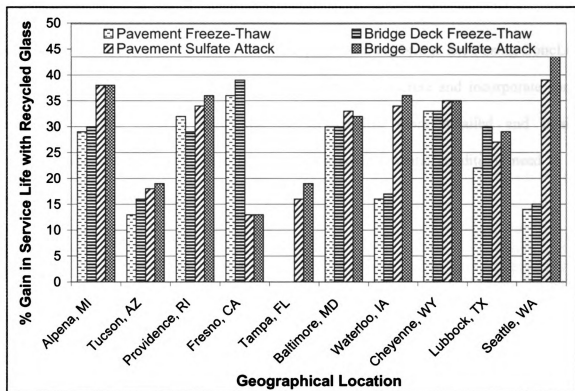


Figure 5. 14 Percent gain in service life of concrete pavement and bridge deck due to recycled glass exposed to freeze-thaw or sulfate attack and made with normal concrete

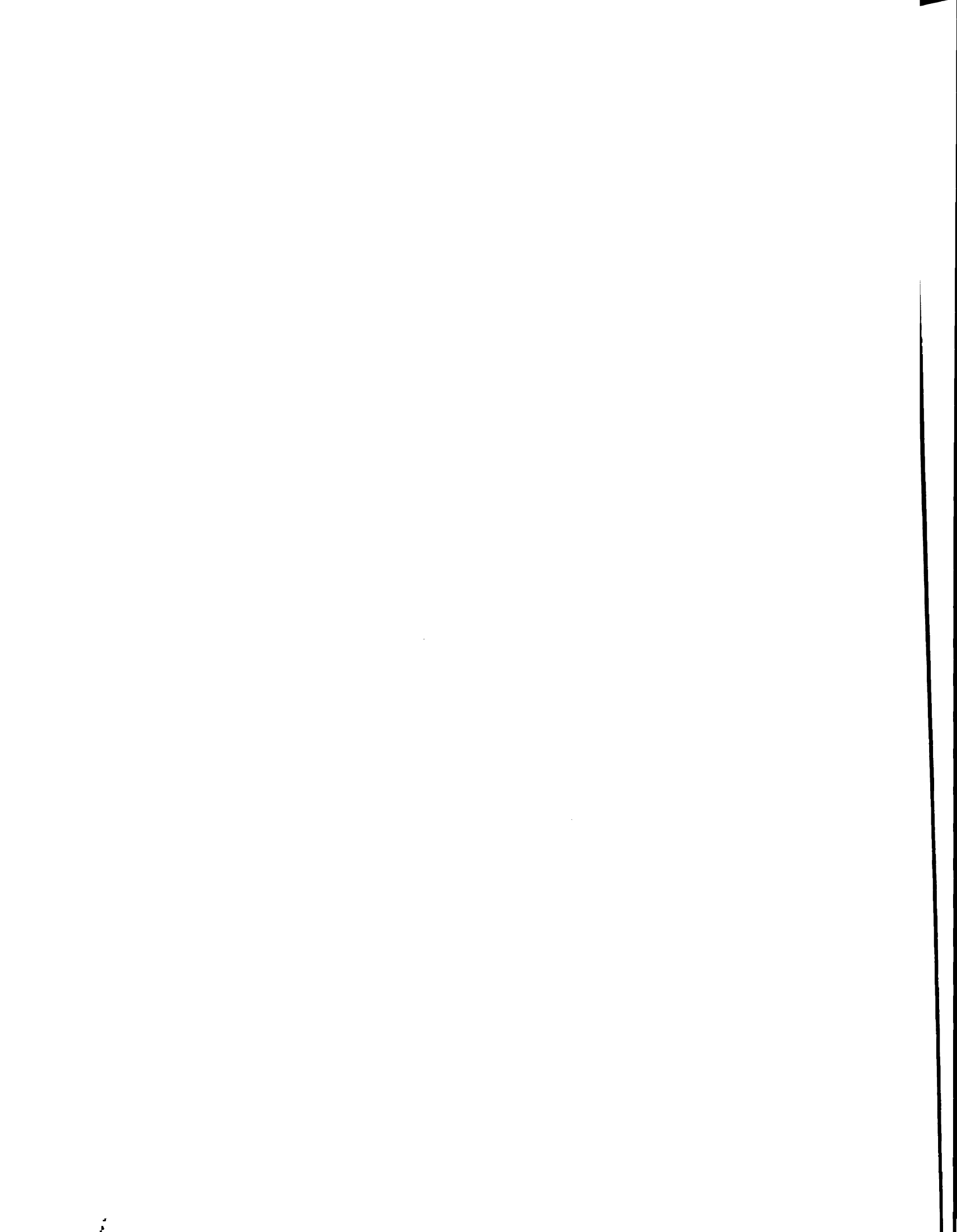
It is to be noted that service life analysis of concrete pavement and bridge deck using ConcLife has certain limitations. The analyses given above, only address the degradation caused due to freeze-thaw and sulfate attack and no effect of mechanical loads on concrete structures has been considered. Furthermore the service life analyses using ConcLife are based on the physical properties of various concrete mixes measured in the laboratory during the course of experimental work of this research, any such application to actual structures would require field measurements of the respective concrete physical properties. Service life prediction of concrete pavement and bridge deck are strictly based on one dimensional water sorption, such prediction might not be

valid if water sorption in concrete is considered in 2-d or 3-d. The analyses and subsequent service life prediction of concrete pavement and bridge deck using ConcLife are based on fundamental deterioration mechanisms of concrete and incorporate some assumptions. For accurate prediction of service life more detailed and in-situ measurement of concrete physical properties and environmental conditions need to be incorporated in the analyses.

## REFERENCES

1. Bentz, P., Ehlen, M., Ferraris, C. F., Garboczi, E. J., *Sorptivity-Based Service Life Predictions for Concrete Pavements*, in *7th International Conference on Concrete Pavements*. 2001: Orlando, FL.
2. Kropp, J.a.H., H. K., ed. *Performance criteria for concrete durability*. 1995, E & FN Spon: London.
3. Mehta P. K., M.P.J.M., *Concrete: Microstructure, Properties and Materials*. 2006: McGraw-Hill New York.
4. Alexander, M.G., Ballim, Y., *Experiences with durability testing of concrete: A suggested framework incorporating index parameters and results from accelerated durability tests*, in *Third Canadian Symposium on Cement and Concrete (CSCC 93)*. 1993, National Research Council Canada: Ottawa, Ontario.
5. Neville, A.M., *Properties of Concrete*. 4th ed. 2000: Pearson Education.
6. Mindess S., Y.J.F., and Darwin D., *Concrete*. Second ed. 2003: Prentice Hall.
7. Meier, U.G. and A.B. Harnik, *Das gefrieren von wasser in zementstein bei verhoinderter verdunstung*. *Cement and Concrete Research*, 1978. 8(5): p. 545-551.
8. Power, T.C., *The Physical Structure and Engineering Properties of concrete*, in *PCA Bulletin 90*. 1958, Portland Cement Association Skokie, IL.
9. Fagerlund, G., *Modeling the service life of concrete exposed to frost*, in *International Conference on Ion and Mass Transport in Cement-Based Materials* 1999: Toronto, Canada. p. 195-217.
10. Atkinson, A., Hearne, J. A. . *Mechanistic Model for the Durability of Concrete Barriers Exposed to Sulphate-Bearing Groundwaters*. in *Scientific Basis for Nuclear Waste Management XIII*. 1989. Boston, Mass: Materials Research Society.
11. Gutt, W.H., Harrison, W. H. , *Chemical resistance of concrete*. *Concrete*, 1977. 11(5): p. 35-37.
12. Bentz, D.P., Ehlen, M. A., Ferraris, C. F., Garboczi, E. J., *Sorptivity- Based Service Life Predictions for Concrete Pavements*, in *7th International Conference on Concrete Pavements*. 2001: Orlando, FL.
13. Bentz, D.P., *A computer model to predict the surface temperature and time-of-wetness of concrete pavements and bridge decks*, in *NISTIR 6551*. 2000, National Institute of Standards and Technology: Gaithersburg, MD.

14. *National Renewable Energy Laboratory*. Available from: <http://www.nrel.gov/>.



## **CHAPTER 6**

### **Field Projects**

#### **6.1 Introduction**

Based on the promising results obtained through laboratory experimental studies, two field projects were implemented on the campus of Michigan State University in order to evaluate the performance of recycled glass concrete under field construction and service conditions. The two field projects involved construction of: (i) sidewalk/maintenance vehicle pavement sections (constructed in May 2008); and (ii) external concrete work (driveway, sidewalk, curb) of the MSU recycling center (constructed in May 2009). These projects evaluated commercial production (in ready-mixed plants) of concrete incorporating milled waste glass as partial replacement for cement, and its large-scale use in concrete pavement (and curb) construction. The field performance of recycled glass concrete is subject of long-term evaluation in field conditions. Recycled glass concrete has performed satisfactorily in all field studies, which also helped introduce the concept to concrete producers and contractors.

In the field project, milled waste glass with 25  $\mu\text{m}$  average particle size was used as replacement for 15%, 20% and 23% of Type I Portland cement in concrete. Cores were taken from sections of concrete pavements at different ages, and were tested for evaluation of the compressive strength, water sorption, chloride permeability, and abrasion resistance of field recycled glass concrete versus normal concrete. Compression and flexure tests were also performed on recycled glass and control concrete specimens prepared from field concrete during construction.

## 6.2 Materials, Mix Designs and Construction Methods

Table 6.1 shows the chemical composition of the milled waste glass and ordinary Portland cement used in field projects. Table 6.2 presents some physical properties of the milled waste glass used here, and Figure 6.1 shows the micrograph of the milled waste glass.

Table 6.1 Typical chemical compositions of waste glass and Portland cement

Chemical	Glass	Cement
SiO <sub>2</sub>	73.5%	20.2%
Al <sub>2</sub> O <sub>3</sub>	0.4%	4.7%
CaO	9.2%	61.9%
Fe <sub>2</sub> O <sub>3</sub>	0.2%	3.0%
MgO	3.3%	2.6%
Na <sub>2</sub> O	13.2%	0.19%
K <sub>2</sub> O	0.1%	0.82%
SO <sub>3</sub>	-	3.9%
Loss on ignition	-	1.9%

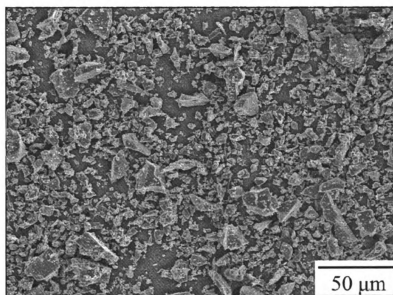


Figure 6.1 SEM micrograph of milled waste glass

**Table 6.2 Physical properties of milled glass**

<b>% Passing # 325 Mesh</b>	<b>93%</b>
<b>Specific Gravity</b>	<b>2.46 gm/cc</b>
<b>Median Particle Size</b>	<b>25 <math>\mu\text{m}</math></b>
<b>Moisture content</b>	<b>0.1%</b>
<b>Brightness</b>	<b>80%</b>
<b>Specific Surface Area</b>	<b>4280 <math>\text{cm}^2/\text{gm}</math></b>

Three mix designs containing milled waste glass replacing 15%, 20% and 23% of cement were prepared at ready-mix concrete plants for use in the two field projects. Pavement and driveway sections using control concrete were also constructed for comparative evaluation of recycled glass concrete. Table 6.3, shows the mix designs and fresh concrete properties of recycled glass and control concrete mixtures used in these projects.

Crushed limestone coarse aggregate with maximum size of 19 mm ( $\frac{3}{4}$  in) and non-reactive river sand were used in all mixes. All batches of concrete were manufactured in ready-mix concrete plants. Representative concrete cylinders with 6 in. (152 mm) diameter and 12 in (350 mm) height were prepared and tested following ASTM C 39 procedures after 7, 14, 28, 90 and 270 days of moist curing (in lime-saturated water). Similarly, concrete beams were prepared from all mixes, and were tested following ASTM C 78 procedures at 7, 28, 90 and 270 days of moist curing. In addition, 90 days and 450 days after construction of the recycling center and the sidewalk/maintenance vehicle projects, respectively, cores were drilled from the constructed pavement sections and tested for compressive strength, water sorption

(ASTM C1585), chloride permeability (ASTM C 1202), and abrasion resistance (ASTM C 944).

The slump test results presented in Table 6.3 indicate that, at equal water/cement ratios, the recycled glass concrete mixtures have slightly lower fresh workability (with the exception of the concrete mix with 15% replacement of cement with milled waste glass). This trend may be attributed to the non-spherical and rough geometry of the milled glass particles (see Figure 6.1). Unlike fly ash, the introduction of milled waste glass did not significantly affect the entrained air content of concrete mixtures prepared with similar dosages of air entraining agent.

Table 6. 3 Concrete Mix Designs and fresh concrete properties

Ingredient	Mix Designs			
	Control	15% Glass	20% Glass	23% Glass
Cement Type I, kg/m <sup>3</sup> (lb/yd <sup>3</sup> )	312 (526)	265 (447)	250 (421)	240 (405)
Milled Glass, kg/m <sup>3</sup> (lb/yd <sup>3</sup> )	-	47 (79)	62 (105)	72 (121)
Fine aggregate, kg/m <sup>3</sup> (lb/yd <sup>3</sup> )	799(1347)	799 (1347)	799 (1347)	799 (1347)
Coarse aggregate, kg/m <sup>3</sup> (lb/yd <sup>3</sup> )	1063 (1792)	1063 (1792)	1063 (1792)	1063 (1792)
Water content, kg/m <sup>3</sup> (lb/yd <sup>3</sup> )	141 (237)	141 (237)	141 (237)	141 (237)
Air entraining agent (ml/100 lb of cement)	60	60	60	60
Water/Cement ratio	0.45	0.45	0.45	0.45
Slump, cm (inch)	9 (3.5)	9 (3.5)	7.5 (3)	7.5 (3)
Air content (%)	4.5	4.5	4.0	4.0

### **6.2.1 Construction of Sidewalk / Maintenance Vehicle Pavement Sections**

Concrete pavement sections 2.4 m (8 ft) in width x 3 m (10 ft) in length (between construction joints) with 0.18 m (7 in.) thickness were constructed in May 2008 over compacted base using three recycled glass and one control concrete mixtures. Two pavement slabs were constructed using each concrete mix. Figure 6.2 shows pictures taken during construction of the pavement slabs. During pouring, compaction, and finishing operations, recycled glass concretes performed similar to control concrete. The pavement sections have so far performed satisfactorily over two years of exposure to mid-Michigan climate and light maintenance vehicle traffic.

### **6.2.2 Construction of the Recycling Center External Concrete Pavements and Curbs**

This project involved construction of driveways, heated pavement slabs, sidewalks, gutters, curbs, and parking stands at the MSU Recycling Center in May 2009 using recycled glass concrete with 20% of cement replaced with milled waste glass. Mix designs were slightly different in the case of heated pavement and curbs in comparison to other components. Pump-grade flowing recycled glass concrete was produced for the heated pavement, and low-slump concrete was produced for curb construction by the extrusion method. Other components were made using more conventional concrete mixtures (with partial milled waste glass replacement of cement). A control concrete was also used in construction of an approach driveway. Figure 6.3 presents pictures taken during construction of the driveway and curb in this project.



Figure 6.2 Construction of the sidewalk/maintenance vehicle pavement with recycled glass concrete (a) pouring of concrete; (b) finishing of concrete

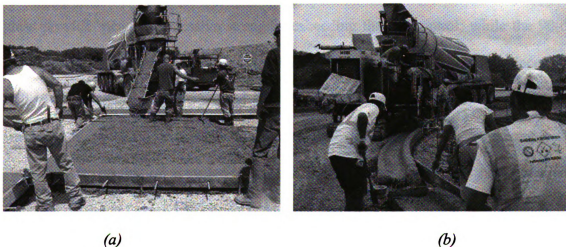


Figure 6.3 Construction with recycled glass concrete at the MSU Recycling Center (a) concrete driveway (b) concrete curb

### 6.3 Test Results and Discussion

This section presents the combined test results produced in the two field projects. Various test results at different ages were generated for the three recycled glass concrete mix and one of the control mixtures. Tests were performed on concrete specimens prepared at the time of pouring the field concrete, and also on cores drilled at different ages from field concrete sections.

### **6.3.1 Compressive and Flexural Strength of Concrete Specimens**

Figures 6.4 and 6.5 show the compressive and flexural strength tests results, respectively, for representative concrete specimens at various ages. Recycled glass concretes are observed in Figure 6.4 to offer lower mean compressive strengths at 7, 14 and 28 days of age when compared with the control concrete. Statistical analysis (of variance) followed by pairwise comparison of results indicated that only the recycled glass concrete mix with 23% cement replacement with milled waste glass produced compressive strengths that were lower than that of control concrete (at 95% confidence level). At the age of 90 days, recycled glass concretes with 15% and 20% of cement replaced with milled waste glass provide mean compressive strengths exceeding that of control; while the 90-day compressive strength of the recycled glass concrete with 23% of cement replaced with milled waste glass was lower than that of control concrete. Statistical analysis (of variance) of the 90-day test results indicated that the differences between the compressive strength test results of recycled glass and normal concretes were not statistically significant (at 95% confidence level). At 270 days, recycled glass concretes with 15% and 20% of cement replaced with milled waste glass provided higher mean compressive strengths when compared with control concrete; the mean compressive strength with 23% of cement replaced with milled waste glass was comparable to that of concrete. Statistical analysis (of variance) of the 270-day compressive strength test results indicated that, at 95% level of confidence, the recycled glass and normal concrete materials provided 270-day compressive strengths which were statistically comparable (at 95% level of confidence).

Flexural strength test results shown in Figure 6.5 follow the trend of compressive strength. Mean flexural strength of recycled glass concrete at 7 and 28 days of age is less than that of control concrete. Statistical analysis (of variance) indicated that the mean flexural strength of recycled glass concrete with 23% of cement replacement with milled glass was lower than that of control concrete at all ages. At the age of 90-day, the difference between mean flexural strengths of recycled glass concretes (with the exception of 23% glass mix) and control concrete were not statistically significant (at 95% confidence level). At the age of 270-day, recycled glass concrete mixes with 15 and 20% replacement of cement with milled glass surpassed the mean flexural strengths of control concrete. However, statistical analysis (of variance) showed that strengths of recycled glass concrete having 15 and 20% cement replacement with milled glass had mean flexural strengths that were statistically comparable (at 95% confidence level) with the mean flexural strength of control concrete at the same age.

The above test results indicated that strength gain in recycled glass concrete occurs at a somewhat lower rate than in normal concrete, but recycled glass concrete has the potential to offer compressive strengths surpassing those of normal concrete over time. The slower rate of strength gain in the case of recycled glass concrete can be attributed to the rate of pozzolanic reactions of glass with the calcium hydroxide in cement hydrates. The long-term advantages of recycled glass concrete over normal concrete can be attributed to the enhanced binding qualities of the calcium silicate hydrate which results from pozzolanic reaction of glass with calcium hydroxide, and also to the reduced porosity of the cementitious binder undergoing such pozzolanic reactions involving milled waste glass. These test results also suggest that there is an upper limit on the

cement replacement level with milled waste glass if one desires to produce recycled glass concretes with long-term strengths that are equivalent to or more than those of normal concrete.

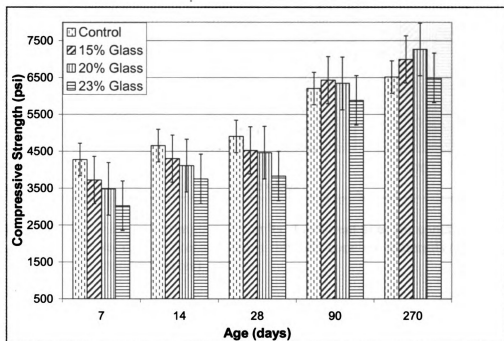


Figure 6.4 Compressive strength test results at different ages for concrete specimens prepared using the field concrete materials (means and standard errors)

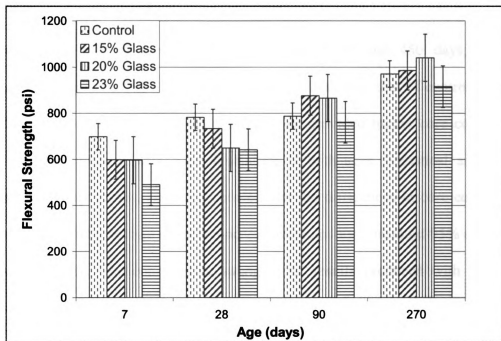


Figure 6. 5 Flexural strength test results at different ages for concrete specimens prepared using the field concrete materials (means and standard errors)

### 6.3.2 Compressive Strength of Concrete Cores

Cores with 102 mm (4 in.) diameter and heights varying from 178 to 203 mm (7 to 8 in.) were drilled from the recycled glass and normal concrete pavements produced in the project at the ages of 90 and 450 days. Figure 6.6 shows the compressive strength test results produced using these cores. Generally, the strengths of cores exposed to field environment are less than those obtained using continuously moist-cured cylindrical specimens produced using the same concrete (see Figure 6.4). This finding was statistically significant at 95% level of confidence. The lower strength of specimens cored from field concrete is due to the improved curing and probably the better preparation quality of cylindrical samples when compared with the field construction of relatively large concrete sections.

The strength gain with time for cores follows trends which are similar to those observed with cylindrical specimens. At the ages of 90 and 450 days, the core compressive strength with 23% milled waste glass is less than that of control. With 15 and 20% recycled glass content, concrete materials provided higher core compressive strengths when compared with control concrete at both ages. Statistical analysis (of variance) of the test results, however, showed that the differences in core compressive strengths of recycled glass and control concretes were not significant (at 95% confidence level) at both ages. The compressive strength test results produced with cores and cylindrical concrete specimens provide strong evidence for the occurrence of pozzolanic reactions between milled waste glass and cement hydrates. These pozzolanic reactions seem to continue to contribute to the concrete quality up to 450 days of age.

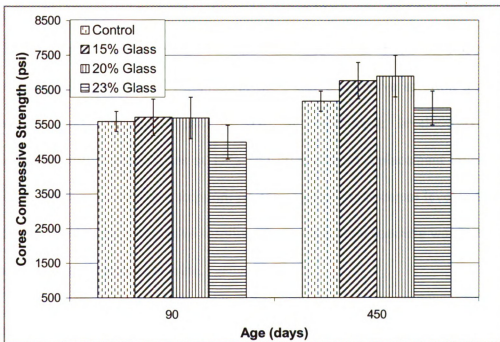


Figure 6. 6 Compressive strength of concrete cores at different ages (means and standard errors)

### **6.3.3 Water Sorption of Concrete Cores**

Moisture transport is a fundamental characteristic of concrete that governs its long-term durability [1-3]. Many durability problems in concrete are caused by water transporting dissolved deleterious species into concrete. Moisture itself can play damaging roles under freeze-thaw attack; moisture movements (e.g., drying) of concrete also cause cracking by generating restrained shrinkage stresses. The moisture barrier qualities of concrete can be improved through refinement of the pore size, partial blocking of the continuous capillary pores, and reduction of the pore volume [4]. Milled waste glass, through pozzolanic reactions, brings about these desired changes in the pore structure of hydrated cement paste. Figure 6.7 shows the results of moisture sorption tests (ASTM C 1585) on 51 mm (2 in.) thick concrete discs prepared from drilled cores at the age of 450 days. The sorbed water versus time plot shows significant improvements in the moisture sorption attributes of recycled glass concrete materials when compared with control concrete. Figure 6.8 shows the cumulative water sorption of concrete disc specimens after 9 days of exposure to water. Statistical analysis (of variance) of the 9-day cumulative sorption test results indicated the statistical significance ( $p=0.02$  or confidence level=98%) of the contributions of milled waste glass at 15% and 20% cement replacement levels to the resistance of concrete to moisture sorption. At 23% cement replacement level with milled waste glass, however, the cumulative sorption of recycled glass concrete was statistically comparable to that of normal concrete.

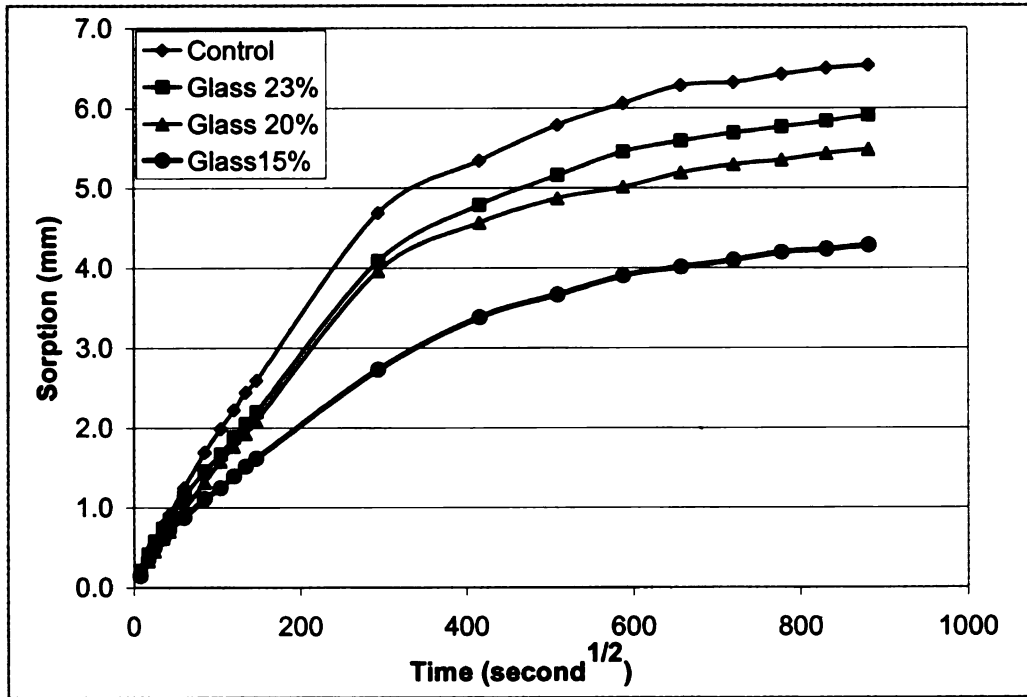


Figure 6. 7 Water sorption versus time of concrete cores

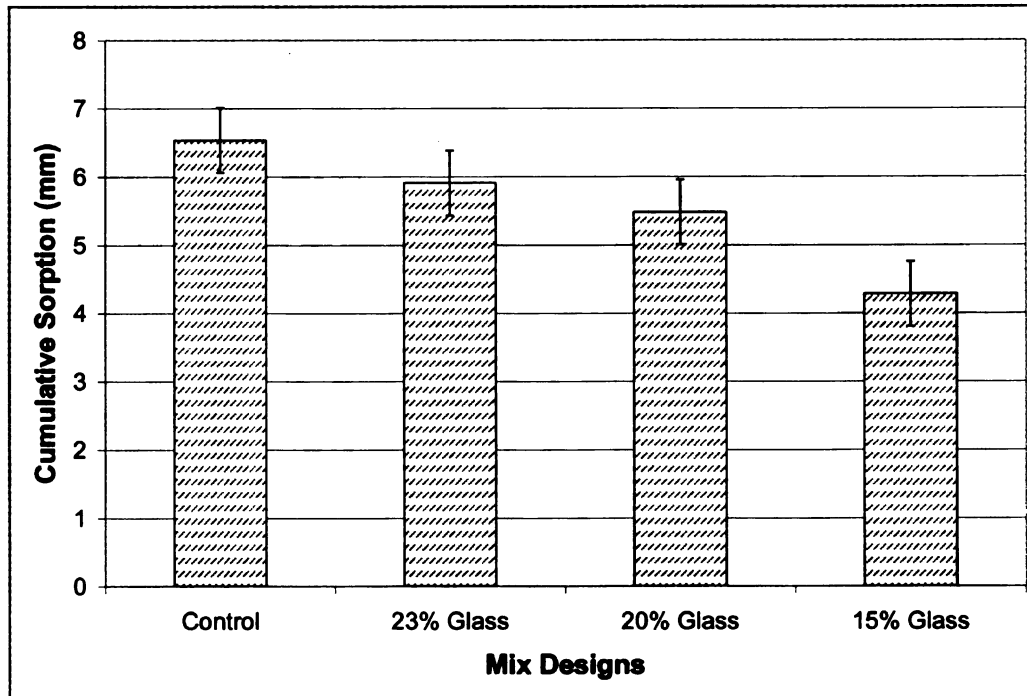


Figure 6. 8 Cumulative water sorption of concrete cores after 9 days of exposure to water (means and standard errors)

### 6.3.4 Chloride permeability of concrete cores

Resistance offered by concrete to chloride ion permeation gives an indication of the barrier qualities of concrete against salt solution, which critically influence its long-term durability. As can be seen in Figure 6.9, the chloride permeability of the three recycled glass concretes (at the age of 450 days) is on the average reduced (pointing at improved barrier qualities) by up to 40% when compared with the control concrete. The significant improvements in resistance to chloride permeation are brought about by the blocking of pores in hydrated cement paste with the products of pozzolanic reactions involving milled waste glass.

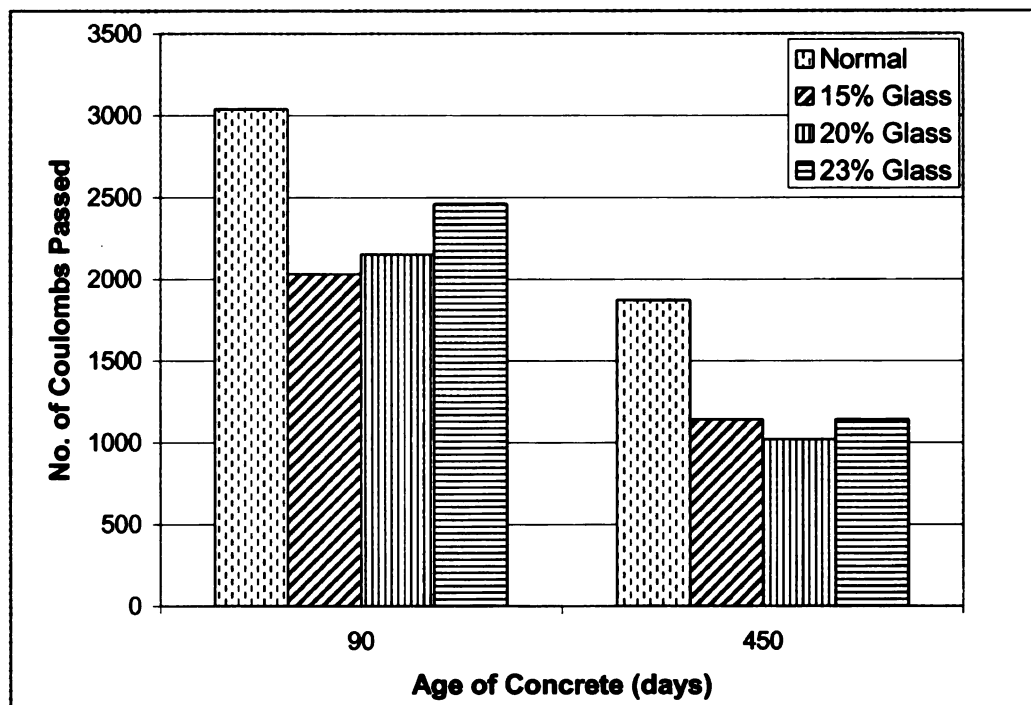


Figure 6.9 Chloride permeability of concrete cores

### **6.3.5 Abrasion resistance**

Abrasion resistance of concrete is an important property influencing the performance of concrete pavements and floors subjected to abrasive action of traffic [5-8]. Figure 6.10 summarizes the abrasion resistance test results produced using cores obtained from the recycled glass and control concrete pavements at 450 days of age. The abrasive weight losses of recycled glass concretes with 15% and 20% cement replacement with milled waste glass are less than that of control, which points at the positive contributions of the pozzolanic reactions of milled waste glass with cement hydrates to abrasion resistance. The abrasive weight loss of recycled glass concrete with higher (23%) cement replacement level was comparable to that of concrete. Statistical analysis (of variance), followed by pairwise comparison of the abrasion test results indicated that the contributions of milled waste glass to abrasion resistance of concrete was statistically significant ( $p=0.05$ ) at 15% cement replacement with milled waste glass. Other recycled glass concretes produced abrasion resistances which were statistically comparable to that of control concrete.

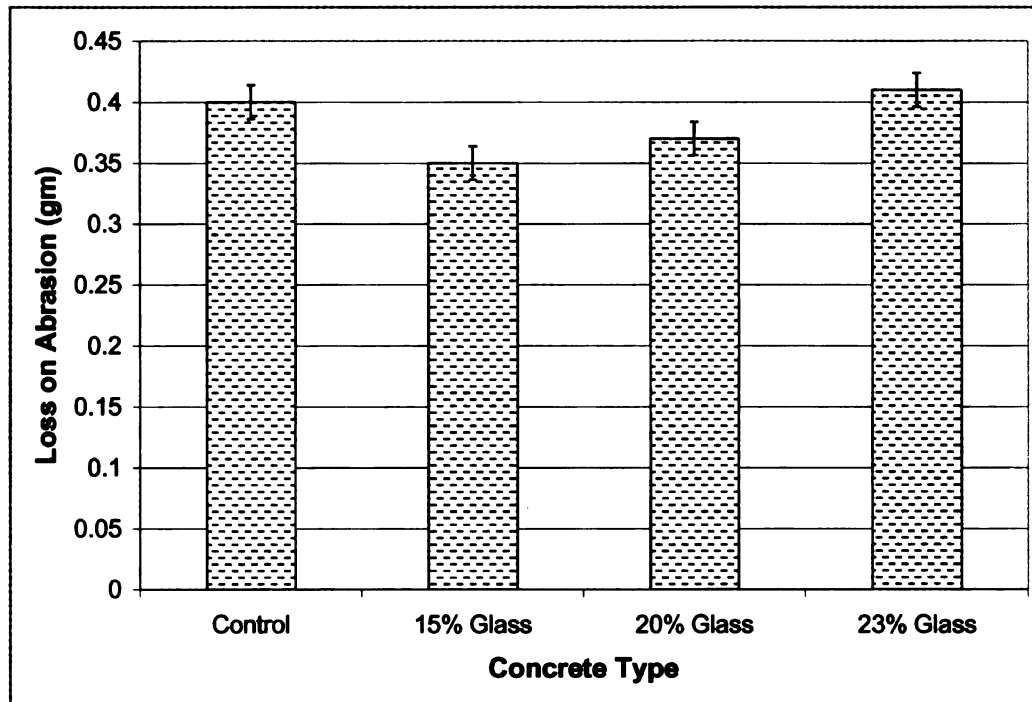


Figure 6. 10 Abrasion resistance of recycled glass and control concretes (means and standard errors)

## REFERENCES

1. Mehta, P.K., *Concrete Technology at the Crossroads--Problems and Opportunities*, in *Concrete technology - past, present and future*. 1994, ACI, SP 144.
2. Basheer, P.A.M., S.E. Chidiac, and A.E. Long, *Predictive models for deterioration of concrete structures*. *Construction and Building Materials*, 1996. **10**(Compendex): p. 27-37.
3. Basheer, L., J. Kropp, and D.J. Cleland, *Assessment of the durability of concrete from its permeation properties: a review*. *Construction and Building Materials*, 2001. **15**(2-3): p. 93-103.
4. Mehta P. K., M.P.J.M., *Concrete: Microstructure, Properties and Materials*. 2006: McGraw-Hill New York.
5. Fwa, T.F. and P. Paramasivam. *Surface-deterioration resistance of concrete pavement materials*. in *First International Symposium on Surface Characteristics, June 8, 1988 - June 9, 1988*. 1990. State College, PA, USA: Publ by ASTM.
6. Kumar, B., G.K. Tike, and P.K. Nanda, *Evaluation of properties of high-volume fly-ash concrete for pavements*. *Journal of Materials in Civil Engineering*, 2007. **19**(Compendex): p. 906-911.
7. Li, H., M.-h. Zhang, and J.-p. Ou, *Abrasion resistance of concrete containing nano-particles for pavement*. *Wear*, 2006. **260**(Compendex): p. 1262-1266.
8. Nanni, A., *Abrasion resistance of roller compacted concrete*. *ACI Materials Journal*, 1989. **86**(Compendex): p. 559-565.

## **CHAPTER 7**

### **Conclusions and Recommendations**

#### **7.1 Summary and Conclusions**

Manufacturing of cement, a key ingredient for the production of concrete, is responsible for 5-8% of the anthropogenic CO<sub>2</sub> emissions, with production of each ton of cement resulting in emission of one ton of CO<sub>2</sub> to the atmosphere. Besides, cement production is an energy-intensive process accounting for about 5% of the global industrial energy consumption.

Each year, about 50% of the total construction and demolition (C&D) waste produced (300 million tons), and about 77% of the total waste glass produced (12.2 million tons) are landfilled in the U.S. Growing environmental concerns, rising energy costs and increasing tipping fees coupled with shortage of quality aggregates near construction sites encourage value-added recycling of the waste glass and concrete.

The recycled aggregate obtained from demolished concrete exhibits higher moisture absorption due to the old (porous) mortar clinging to its surface. This hampers effective use of recycled aggregate in new concrete which would have relatively high moisture absorption and thus drying shrinkage. The waste glass found in the solid waste stream has limited market value owing to its mixed color, increased degree of contamination and higher breakage percentage that limit its use towards production of new glass. Waste glass, on the other hand, has favorable chemical composition for use as partial replacement for cement in concrete. The favorable chemistry of waste glass can be used effectively towards production of concrete as far as the waste glass is milled to

about the particle size of cement; the reactions of milled waste glass with cement hydrates occur largely during the active period of cement hydration. The resulting calcium silicate hydrate improves the pore system and the structure of hydrated cement paste as well as the interfacial transition zones in recycled aggregates and new concrete. The use of milled waste glass as partial replacement for about 20 wt.% of cement in recycled aggregate concrete leads to effective reduction of moisture sorption and thus improvement of the dimensional stability, durability and mechanical properties of the resulting concrete. Similar benefits can be realized by using milled waste glass as partial replacement for cement in normal concrete. Major environmental, energy and economic benefits can be realized by diverting landfill-bound (mixed-color) waste glass for use as partial replacement for cement in recycled aggregate and normal concrete. The enabling role of waste glass towards value-added use of recycled aggregate in concrete adds to the environmental, energy and cost benefits of the practice.

A comprehensive experimental program was undertaken to study the effects of milled waste glass on the structure and properties of cement paste, mortar and concrete. The aggregates considered in concrete mixtures included recycled, virgin, and (50:50), blends of recycled and virgin aggregates. Field investigations were also undertaken to verify the scalability of the practice and the concrete performance under natural weathering. Numerical studies were also conducted in order to assess the effects of recycled aggregate and milled waste glass on the service life of concrete-based infrastructure systems. Major findings and conclusions of this research are as follows:

1. Replacement of about 20 wt.% of cement with milled waste glass results in significant improvement of the structure of hydrated cement paste and

interfacial transition zone. Pozzolanic reactions of milled waste glass with cement hydrates convert calcium hydroxide to calcium silicate hydrate, thereby producing a more stable chemical structure and a refined (and less continuous) capillary pore system.

2. Milled waste glass, as replacement for about 20 wt.% of cement, as significantly benefits the resistance of normal and especially recycled aggregate concrete to moisture sorption, which reflects on the refined and less continuous pore system in the presence of milled waste glass. The rate of water sorption and the cumulative sorption were reduced to about half by introduction of milled waste glass as partial replacement for cement. Milled waste glass proved to be more effective than Class-F and Class-C fly ash in these regards.
3. An increase in workability (slump) of fresh concrete mixtures was observed when about 20 wt.% of cement was replaced with milled waste glass. This effect was attributed to the relatively low moisture sorption of milled waste glass when compared with cement.
4. Partial replacement of cement with milled waste glass lowered the volume of voids in hardened concrete. This reduction, which can be attributed to the pozzolanic reactions of milled waste glass, were comparable to those obtained with partial replacement of cement with Class-F fly ash, and better than those obtained using Class-C fly ash as partial replacement for cement.
5. Mean compressive strengths of concrete materials incorporating milled waste glass as replacement for about 20 wt.% of cement were comparable to those of

control concrete materials (without milled waste glass) at 28 days of age. At 90, 156, and 300 days of age, the strengths of recycled glass concrete materials were higher than those of the corresponding control concrete materials at different water/cement ratios. The long-term gains in compressive strength is a typical feature of the pozzolanic reactions which tend to occur when adequate quantities  $\text{Ca(OH)}_2$  become available upon hydration of cement. The significant gains in the long-term compressive strength of recycled aggregate concrete upon introduction of milled waste glass as partial replacement for cement point at the synergy of milled waste glass with recycled aggregate. At 90, 156, and 300 days of age, partial replacement of cement with milled waste glass produced more gains in compressive strength than corresponding replacements of cement with Class-F and Class-C fly ashes.

6. Beyond 28 days of age, replacement of about 20 wt.% of cement with milled waste glass benefited the flexural strength of normal and recycled aggregate concretes made with different water/cement ratios. These benefits of milled waste glass were superior to those obtained using Class-F and Class-C fly ash as partial replacement for cement.
7. The long-term split tensile strength of normal and recycled aggregate concretes benefited from the introduction of milled waste glass as replacement for about 20 wt.% of cement. Milled waste glass performed similar to Class-F fly ash in normal concrete; in recycled aggregate concrete, milled waste glass

produced superior gains in split tensile strength when compared with Class-F fly ash.

8. At 90 days of age, the modulus of elasticity (chord modulus) of concrete benefited from replacing 20 wt.% of cement with milled waste glass. Milled waste glass performed similar to Class-F fly ash and better than Class-C fly ash in this regard. The effects of pozzolanic reactions on the pore system characteristics of hydrated cement paste and the interfacial transition zone explain the benefits of milled waste glass to elastic modulus.
9. Significant reductions of drying shrinkage in normal and recycled aggregate concrete were realized by replacing 20 wt.% of cement with milled waste glass. This is a major achievement because excess drying shrinkage is a key hurdle against widespread use of recycled aggregate in concrete production. Milled waste glass reduce the drying shrinkage of concrete primarily through reduction of moisture sorption through capillary pores in hydrated cement paste and the interfacial transition zone.
10. Chloride permeability of normal and recycled aggregate concretes dropped to about half upon replacement of 20 wt.% of cement with milled waste glass. This effect of milled waste glass was superior to that of Class-F fly ash, which reduced chloride permeability by about one-third. The refined and discontinuous capillary pore system produced by the pozzolanic reactions of milled waste glass are key to the corresponding gains in resistance to chloride permeation.

11. The favorable effects of milled waste glass (as replacement for 20 wt.% of cement) on the resistance of concrete to moisture sorption benefited the durability of normal and recycled aggregate concretes under repeated freeze-thaw cycles.
12. Significant improvements in the abrasion resistance of normal and recycled aggregate concretes was realized by replacing 20 wt.% of cement with milled waste glass. These effects of milled waste glass were found to be comparable to those of Class-F fly ash.
13. A thorough investigation of alkali-silica reactions (ASR) pointed at significant benefits of milled waste glass, as partial replacement for cement, in reduction of alkali-silica reactions with different aggregate types. The milled waste glass exhibited an innocuous behavior with major suppressing effects on ASR-related expansions. The fine particle size of milled waste glass promotes rapid pozzolanic reactions with cement hydrates, and eliminate any potential deleterious long-term reactions involving glass. Scanning electron microscope investigations of ASR test specimens revealed a dense and uniform microstructure which did not exhibit any manifestations of ASR reactions.
14. Unlike other pozzolans, milled waste glass did not reduce the pH of hydrated cement paste. This benefits the chemical stability and the protective qualities of recycled glass concrete against corrosion of embedded (reinforcing) steel.
15. Numerical analysis of the service life of concrete pavements and bridge decks exposed to freeze-thaw and sulfate attack in different climatic conditions pointed at significant gains in service life of normal and recycled aggregate

concrete systems realized by replacing about 20 wt.% of cement with milled waste glass. These improvements result from the improved resistance of concrete to ingress of moisture and aggressive ions upon partial replacement of cement with milled waste glass.

16. Field investigations confirmed the compatibility of recycled glass concrete with industrial-scale concrete production and construction techniques. Partial replacement of cement with milled waste glass produced concrete pavement sections with excellent performance under weathering effects (after two years of performance).

## **7.2 Practical Implications of the Findings**

1. This research has shown that the use of milled waste glass as partial replacement for cement in normal and recycled aggregate concrete is a viable practice which makes value-added use of otherwise landfill-bound waste materials.
2. Use of milled waste glass in concrete would reduce the cement content of concrete, thereby reducing the environmental and energy implications of manufacturing cement.
3. Milled waste glass, as partial replacement for cement, is especially effective in overcoming the deficiencies of recycled aggregate concrete, enabling widespread use of recycled aggregate in concrete-based infrastructure systems, rendering major environmental, energy and cost benefits.

5. Pozzolanic reactions of milled waste glass with cement hydrates produce normal and recycled aggregate concretes with enhanced moisture barrier attributes, strength and durability as compared to equivalent concretes without milled waste glass. The resulting gains in service life render major benefits in terms of the life-cycle economy of concrete-based infrastructure systems.
6. The use of milled waste glass alone or in conjunction with recycled aggregates offers major contributions towards development of sustainable concrete-based infrastructure systems.

### **7.3 Recommendations for Future Research**

The following areas of research can build upon the findings this research project:

1. Unlike other pozzolans, the benefits of milled waste glass to the structure and pore system characteristics of cement hydrates are not accompanied with a corresponding reduction of the alkalinity of hydrated cement paste. This is expected to benefit the chemical stability of recycled glass concrete as well as its protective role against corrosion of the embedded reinforcing steel. These benefits of the technology need to be verified through experimental investigations and supportive theoretical studies.
2. Given the promise and commercial prospects of the technology, more fundamental investigations of the milled waste glass effects on the structure and chemistry of cement hydrates and the interfacial transition zones in normal and recycled aggregate concrete is worth pursuing for achieving

further insight into the mechanisms of action of milled waste glass in cement-based materials.

3. Investigations of the effects of milled waste glass on the creep behavior of normal and recycled aggregate concrete would have important practical implications, and would also reflect upon the effects of milled waste glass on pore system characteristics and moisture barrier qualities of normal and recycled aggregate concrete.
4. Investigations of the effects of variations in recycled glass composition on the performance of milled waste glass in concrete would facilitate market transition of the technology.
5. Implementation and long-term monitoring of field projects employing milled waste glass in normal and recycled aggregate concrete would be critical for demonstrating the value of the technology to the construction industry in order to facilitate its large-scale implementation.

MICHIGAN STATE UNIVERSITY LIBRARIES



3 1293 03063 5894